

**CORTICAL OSCILLATIONS AND
PLASTICITY INDUCED BY REPETITIVE
TRANSCRANIAL MAGNETIC STIMULATION**

Thesis submitted for the degree of

Doctor of Philosophy

at the University of Leicester

by

Nor Azila Noh

School of Psychology

University of Leicester

2012

Abstract

CORTICAL OSCILLATIONS AND PLASTICITY INDUCED BY REPETITIVE TRANSCRANIAL MAGNETIC STIMULATION

Nor Azila Noh

Repetitive transcranial magnetic stimulation (rTMS) is a non-invasive technique that is able to modulate cortical activity beyond the stimulation period. The residual aftereffects are akin to the plasticity mechanism of the brain and suggest the potential use of rTMS for therapy. In parallel, there is evidence that altered oscillatory brain rhythms and network dynamics may lead to symptoms of neuropsychiatric disorders. However, the rTMS interference upon cortical and network oscillatory activity remains relatively unknown. Despite this uncertainty, rTMS continues to be used to alleviate symptoms of neuropsychiatric disorders. By combining rTMS and electroencephalography (EEG), the thesis explored the local and network cortical plasticity in healthy humans through the characteristics of oscillatory brain rhythms. We investigated cortical and network oscillatory activity following simple rTMS protocols and continuous theta burst stimulation (cTBS) to the primary motor cortex. The measurements of rTMS-induced aftereffects were quantified by the direct electrophysiology index of EEG and the indirect behavioural measures of motor evoked potentials (MEPs). The results of the experiments showed that rTMS was able to transiently modulate cortical brain rhythms, especially low frequency theta oscillations. The significance of this finding is the possible involvement of independent cortical theta generators besides mu and beta generators over the motor network with different reactivity to rTMS protocols. However, long-term potentiation/depression (LTP-/LTD)-like mechanisms may not be the only mechanisms that drive the rTMS aftereffects as shown by the dissociation between EEG and MEPs cortical output. Here, we explore alternative explanations that drive the EEG oscillatory modulations post rTMS. The significance of this work is the ability of rTMS to transiently modify the internal state of the brain by altering brain oscillations particularly low-frequency brain rhythms. This finding offers exciting possibilities for future clinical trials to explore the use of non-invasive brain stimulation to reverse abnormal synchronisation in neuropsychiatric disorders.

Acknowledgements

To God Almighty for His blessings and providence;

to my supervisor Dr. Giorgio Fuggetta;

to my co-supervisor Dr. Douglas Barrett;

to my postgraduate tutor Dr Robin Holliday;

to my sponsors Ministry of Higher Education, Malaysia and Islamic Sciences
University of Malaysia;

to Prof. Paolo Manganotti and his staff at the Department of Neurological and
Visual Sciences, University of Verona, Italy;

to my friends, lecturers and staff at the School of Psychology, University of
Leicester;

to my friend Miss Victoria McGowan for revision of the language of the thesis;

to my friend Mr Abubaker Almabruk;

to my parents and siblings;

and finally, special acknowledgement to my loving husband, Adam Rizal Azwar
and our sons Amir Faisal and Amin Fahim.

Publications

Journals

1. Noh, N.A., & Fuggetta, G. (2011). Human cortical theta reactivity after repetitive transcranial magnetic stimulation. *Human Brain Mapping*. DOI:10.1002/hbm.21355.
2. Noh, N.A., Fuggetta, G., Manganotti, P., Fiaschi, A. (2012). Long-lasting modulation of cortical oscillations after continuous theta-burst transcranial magnetic stimulation. *PloSOne*. DOI:10.1371/pone.0035080.
3. Fuggetta, G., & Noh, N.A. A neurophysiological insight into the potential link between transcranial magnetic stimulation, thalamocortical dysrhythmia, and neuropsychiatric disorders. *Submitted*.
4. Fuggetta, G., Noh, N.A., Manganotti, P., Fiaschi, A. Long-lasting modulation of motor network oscillations after continuous theta-burst stimulation. *Submitted*.

Conferences

1. Noh, N.A., & Fuggetta, G. Modulation of cortical oscillatory activity induced by high-frequency repetitive transcranial magnetic stimulation. *First International Workshop on Synaptic Plasticity, Sicily, Italy*. May 2010.
2. Noh, N.A., & Fuggetta, G. Direct electrophysiological evidence of human cortical oscillations after continuous theta-burst stimulation. *Magstim TMS summer school, University of Oxford, UK*. June 2010.
3. Noh, N.A., & Fuggetta, G. Human cortical theta reactivity to transcranial magnetic stimulation. *Magstim TMS summer school, University of Oxford, UK*. May 2011.
4. Noh, N.A., & Fuggetta, G. Stimulating the brain non-invasively via TMS and EEG. *Postgraduate festival, University of Leicester, UK*. June 2011.
5. Noh, N.A., & Fuggetta, G. The link between transcranial magnetic stimulation and dysrhythmic thalamocortical interplay. *Psychology postgraduate conference, University of Leicester, UK*. December 2011.

Contents

Acknowledgements	iii
Publications	iv
Contents.....	v
List of Figures	x
Abbreviations	xiii
1. Introduction.....	1
1.1 Focus and motivation	5
1.2 Research aims	8
1.3 Thesis at a glance.....	9
2. rTMS-EEG: a window to the brain.....	12
2.1 Motor cortex	12
2.1.1 Primary motor cortex	13
2.1.2 Other cortical motor areas	16
2.1.3 Subcortical motor areas.....	16
2.2 Repetitive transcranial magnetic stimulation.....	21
2.2.1 Principles of magnetic stimulation	25
2.2.2 rTMS protocols	28
2.2.3 Safety of rTMS.....	37
2.2.4 Modulation of cortical oscillations by rTMS	38
2.2.5 Cortical plasticity induced by rTMS	44

2.3	Electroencephalography	55
2.3.1	Principles of EEG	55
2.3.2	Event-related potential.....	59
2.3.3	Cortical oscillations.....	61
2.4	Combining TMS and EEG.....	68
2.5	Alternative measurements of rTMS aftereffects.....	71
2.6	Summary.....	73
3.	Methods.....	75
3.1	Participants	75
3.2	Experimental paradigms	76
3.3	TMS procedure	78
3.4	MEP data acquisition	80
3.5	EEG data acquisition.....	82
3.6	EEG spectral analysis.....	89
3.6.1	Event-related desynchronisation/synchronisation	89
3.6.2	Event-related power	90
3.6.3	Event-related coherence	92
3.7	Statistical analysis.....	93
3.8	Summary.....	93
4.	The number of rTMS pulses and cortical oscillations	95
4.1	Introduction	95
4.2	Aims	98
4.3	Methods	99

4.3.1	Participants.....	100
4.3.2	Experimental design.....	100
4.3.3	TMS-EEG recording.....	102
4.3.4	EEG spectral analysis.....	103
4.3.5	Statistical analysis.....	104
4.4	Results.....	105
4.4.1	EEG Event-related power.....	106
4.4.2	EEG Event-related coherence.....	115
4.4.3	MEPs.....	119
4.5	Discussion.....	119
4.5.1	rTMS and regional oscillatory activity.....	119
4.5.2	rTMS and interregional functional connectivity.....	125
4.5.3	MEPs and cortical excitability.....	126
4.6	Summary.....	127
5.	The frequencies of rTMS and cortical oscillations.....	129
5.1	Introduction.....	129
5.2	Aim.....	131
5.3	Methods.....	132
5.3.1	Participants.....	132
5.3.2	Experimental design.....	132
5.3.3	TMS-EEG recording.....	133
5.3.4	EEG spectral analysis.....	134
5.3.5	Statistical analysis.....	135

5.4	Results	135
5.4.1	EEG Event-related power.....	135
5.4.2	EEG Event-related coherence.....	150
5.5	Discussion.....	155
5.5.1	rTMS and regional oscillatory activity	156
5.5.2	rTMS and interregional functional connectivity.....	160
5.6	Summary.....	162
6.	Theta-burst stimulation and cortical oscillations.....	164
6.1	Introduction	164
6.2	Aims	167
6.3	Methods	167
6.3.1	Participants.....	167
6.3.2	Experimental design.....	167
6.3.3	TBS procedure and MEP recording.....	169
6.3.4	Reaction time task.....	169
6.3.5	EEG recording and spectral analysis	171
6.3.6	Statistical analysis	172
6.4	Results	174
6.4.1	MEPs.....	174
6.4.2	Motor RT.....	175
6.4.3	EEG Event-related power.....	177
6.4.4	EEG Event-related coherence.....	186
6.5	Discussion.....	195

6.5.1	cTBS and MEPs	196
6.5.2	cTBS and reaction time	196
6.5.3	cTBS and regional oscillatory activity	198
6.5.4	cTBS and interregional functional connectivity	201
6.6	Summary	203
7.	Conclusion	205
7.1	Summary of the main experimental findings	205
7.2	Future directions	207
	References	213

List of Figures

- Figure 2-1 Primary motor cortex
- Figure 2-2 Cortical and subcortical motor areas
- Figure 2-3 Transcranial magnetic stimulator
- Figure 2-4 TMS circuit
- Figure 2-5 Low frequency rTMS 1Hz
- Figure 2-6 High frequency rTMS 5Hz and 10Hz
- Figure 2-7 Continuous Theta-burst stimulation
- Figure 2-8 EEG scalp potentials
- Figure 2-9 EEG brain rhythms
- Figure 3-1 EEG-recording cap of 10-20 and 10-10 systems
- Figure 4-1 Experimental paradigm: rTMS-EEG number of pulses
- Figure 4-2 ERPow θ for Condition x Epoch
- Figure 4-3 ERPow θ for Condition x Electrode
- Figure 4-4 ERPow θ for Condition x Epoch x Electrode
- Figure 4-5 ERPow μ for Condition x Epoch
- Figure 4-6 ERPow μ for Condition x Epoch x Electrode
- Figure 4-7 ERPow μ for Condition x Epoch x Part
- Figure 4-8 ERPow β for Condition x Epoch
- Figure 4-9 ERPow β for Condition x Epoch x Electrode
- Figure 4-10 ERCoh θ for Condition x Epoch x Pairs of Electrodes

- Figure 5-1 Experimental paradigm: rTMS-EEG frequencies
- Figure 5-2 ERPow 1-30 Hz
- Figure 5-3 ERPow δ for rTMS Frequency x Epoch
- Figure 5-4 ERPow δ for rTMS Frequency x Electrode
- Figure 5-5 ERPow δ for rTMS Frequency x Epoch x Electrode
- Figure 5-6 Topographic brain maps for ERPow δ
- Figure 5-7 ERPow θ for rTMS Frequency x Epoch
- Figure 5-8 ERPow θ for rTMS Frequency x Electrode
- Figure 5-9 ERPow θ for rTMS Frequency x Epoch x Electrode
- Figure 5-10 Topographic brain maps for ERPow θ
- Figure 5-11 ERPow μ for rTMS Frequency x Epoch
- Figure 5-12 ERPow β for rTMS Frequency x Epoch
- Figure 5-13 ERCoh θ for rTMS Frequency x Epoch x Pairs of Electrodes
- Figure 5-14 ERCoh μ for rTMS Frequency x Epoch x Pairs of Electrodes
- Figure 6-1 Experimental paradigm: cTBS-EEG
- Figure 6-2 Spatial compatibility RT task
- Figure 6-3 MEPs normalised amplitude
- Figure 6-4 Normalised RT
- Figure 6-5 ERPow θ “rest” for Group x Block x Electrode
- Figure 6-6 ERPow θ “active” for Group x Electrode
- Figure 6-7 ERPow low β “rest” for Group x Electrode
- Figure 6-8 ERPow low β “active” for Group x Electrode
- Figure 6-9 ERPow high β “rest” for Group x Electrode

Figure 6-10 ERPow high β “rest” for Group x Block x Electrode

Figure 6-11 ERCoh low β “rest” for Group x Pairs of Electrodes

Figure 6-12 ERCoh low β “rest” for Group x Block x Pairs of Electrodes

Figure 6-13 ERCoh high β “active” for Group x Pairs of Electrodes

Figure 6-14 ERCoh high β “active” for Group x Block x Pairs of Electrodes

Abbreviations

AD	Analog-to-digital
Ag/AgCl	Silver/Silver chloride
α	Alpha
AMPA-R	α -amino-3-hydroxy-5-methyl-4-isoxazolepropionic acid receptor
AMT	Active motor threshold
ANOVA	Analysis of variance
β	Beta
BDNF	Brain-derived neurotrophic factor
BOLD	Blood oxygen level dependent
Ca^{2+}	Calcium ions
Cl^-	Chloride ions
CaMK	Calcium-calmodulin protein kinase
cTBS	Continuous theta-burst stimulation
δ	Delta
DLPFC	Dorsolateral prefrontal cortex
ECG	Electrocardiography
EEG	Electroencephalography
EMG	Electromyography
EOG	Electrooculography
ERCoh	Event-related coherence
ERD	Event-related desynchronisation
ERP	Event-related potential
ERPow	Event-related power
ERS	Event-related synchronisation
FFT	Fast Fourier transforms
fMRI	Functional magnetic resonance imaging
γ	Gamma
GABA	γ -aminobutyric acid

GABA _A	γ-aminobutyric acid type A
GABA _B	γ-aminobutyric acid type B
HFS	High-frequency stimulation
Hz	Hertz
iEEG	Intracranial electroencephalography
IFSECN	International federation of societies for electroencephalography and clinical neurophysiology
ISI	Inter-stimulus interval
iTBS	Intermittent theta-burst stimulation
K ⁺	Potassium ions
LFO	Low-frequency oscillations
LFS	Low-frequency stimulation
LTD	Long-term depression
LTP	Long-term potentiation
M1	Primary motor cortex
min	Minutes
MEG	Magnetoencephalography
MEP	Motor-evoked potential
mGluR	Metabotropic glutamate receptor
ms	Milliseconds
μ	Mu
μV	Microvolt
NMDA-R	N-methyl-D-aspartate receptor
PET	Positron emission tomography
PMA	Premotor area
PMd	Dorsolateral premotor cortex
PMv	Ventrolateral premotor cortex
PSP	Postsynaptic potential
RMT	Resting motor threshold
RMP	Resting membrane potential

RN	Reticular nucleus neurons
rTMS	Repetitive transcranial magnetic stimulation
RT	Reaction time
s	Seconds
SMA	Supplementary motor area
SQUID	Superconducting quantum interference device
STP	Short-term potentiation
θ	Theta
TBS	Theta-burst stimulation
TC	Thalamocortical neurons
TCD	Thalamocortical dysrhythmia
TCR	Thalamocortical relay neurons
tDCS	Transcranial direct current stimulation
TE	Thenar eminence muscle
TEP	TMS-evoked potential
TES	Transcranial electrical stimulation
TMS	Transcranial magnetic stimulation
VEP	Visual evoked potential

1. Introduction

Neuroscience is the multidisciplinary approach of unravelling the mystery of how the brain works. Traditional research on the working of the brain primarily involved animal experimentation, non-alive human brains, or lesion studies involving patients with brain damage. However, the limitations of the previous approaches are the problems of inference in animal experiments and in the non-living human brain, the reorganisation process after brain damage, and the inability to use the same patients as both experimental subjects and controls (Hallett, 2000). Therefore, a tool that is able to interfere with the activity of the intact brain directly and non-invasively will greatly advance basic and clinical neuroscience research.

In 1985, Professor Anthony Barker and colleagues from the University of Sheffield, UK, introduced transcranial magnetic stimulation (TMS), an alternative to the conventional electrical stimulation. TMS is a non-invasive neurophysiologic method of delivering electrical stimuli by rapidly changing the magnetic field (Barker, Jalinous, & Freeston, 1985). The magnetic coil placed near the scalp will electrically excite the cortical axon directly underneath it, trigger nerve depolarisation, propagate action potentials, and release neurotransmitters into the postsynaptic neurons (Hallett & Rothwell, 2011; Siebner, 2000). However, what occurs afterward remains unclear (Hoogendam et al., 2010; Huerta & Volpe, 2009).

TMS can be applied as single pulse, or repetitive pulses. Using single pulse protocol, TMS can either excite or inhibit the brain depending on the parameters of stimulation, such as frequency, duration, intensity of stimulation, and the number of magnetic pulses (Fitzgerald, Fountain, & Daskalakis, 2006). The effects of single pulse or single-train can add up with repeated stimulation—the rTMS protocol—leading to the modulation of cortical activity beyond the stimulation period (Kobayashi & Pascual-Leone, 2003; Ridding & Rothwell, 2007; Siebner & Rothwell, 2003). This prolonged rTMS aftereffect emulates the pattern of synaptic plasticity in rodent hippocampus (Huerta & Volpe, 2009; Walsh & Cowey, 2000).

Plasticity is defined as the ability of the brain to reorganise itself in order to primarily improve the functioning of the brain networks (Cooke & Bliss, 2006; Pascual-Leone et al., 2011; Siebner & Rothwell, 2003). Plasticity enables the modification of neural interaction that outlasts the experimental manipulation (Hoogendam et al., 2010; Pascual-Leone et al., 2011). The hypotheses that suggest a link between the residual effects of rTMS and cortical plasticity are due to the ability of rTMS to induce changes that outlast the period of stimulation (Hoogendam et al., 2010). The plasticity-like effect of rTMS implies the potential use of this artificial non-invasive magnetic stimulation for basic neurophysiology research as well as for rehabilitation and therapy (Hallett & Rothwell, 2011; Ridding & Rothwell, 2007; Walsh & Cowey, 2000).

It was proposed that rTMS interferes with both neuronal and non-neuronal processes (Hoogendam et al., 2010; Huerta & Volpe, 2009). The neuronal mechanisms range from local cellular changes (Di Lazzaro, Ziemann, & Lemon, 2008; Siebner & Rothwell, 2003) to global-scale alteration of neuronal circuits such as network oscillations (Thut & Miniussi, 2009; Thut & Pascual-Leone, 2010a). The cellular changes consist of the local synaptic processes of synaptic excitation, synaptic inhibition, and synaptic plasticity, which are akin to the mechanisms of plasticity of long-term potentiation (LTP) and long-term depression (LTD) in animal studies (Chen et al., 1997; Di Lazzaro et al., 2008; Huerta & Volpe, 2009; Kujirai, Sato, Rothwell, & Cohen, 1993). Other neuronal changes involve neuromodulators such as dopamine (Khedr et al., 2007; Strafella, Paus, Fraraccio, & Dagher, 2003; Ziemann, Bruns, & Paulus, 1996), growth factors such as brain-derived neurotrophic factor (BDNF) (Cheeran et al., 2008; Wang et al., 2011), and early genes proteins (Aydin-Abidin et al., 2008). In addition to neuronal effects, rTMS also alters non-neuronal processes including cerebral blood flow by changes in blood oxygen level dependent (BOLD) (Bestmann et al., 2003; Hubl et al., 2008; Lee et al., 2003) and brain metabolic activity such as glucose metabolism (Allen, Pasley, Duong, & Freeman, 2007; Paus & Wolforth, 1998).

However, it has always been assumed that the mechanism underlying cortical plasticity is the driving force of sustained rTMS aftereffects (Pascual-Leone et al., 2011; Pell et al., 2011). Unfortunately, the precise mechanism of rTMS-induced cortical plasticity particularly in humans remains elusive

(Pascual-Leone et al., 2011). The ability of rTMS to emulate the patterns of synaptic plasticity in the hippocampus suggests that rTMS can affect synaptic efficacy in the neural network and modulate the cortical and network oscillatory activity (Huerta & Volpe, 2009). However, the cortical and network changes induced by rTMS are still relatively unknown (Shafi et al., 2012).

Cortical neurons are largely interconnected and consist of various neural networks ranging from the simple, micro-level interconnections, to the dynamic and complex macro-level networks (Steriade, 2001; Timofeev, 2011). The neural networks are widely implicated in the process of cortical information coding (Sauseng & Klimesch, 2008; Schyns, Thut, & Gross, 2011). Network oscillations through the balance of synchronisation and desynchronisation of neural assemblies are the important mechanisms involved during cortical information transfer (Basar, Basar-Eroglu, Karakas, & Schurmann, 1999; Houweling, van Dijk, Beek, & Daffertshofer, 2010; Pareti & De Palma, 2004). However, knowledge on the cortical and network oscillatory activity is still limited (Thut, Schyns, & Gross, 2011).

Artificial brain stimulation such as rTMS can perturb the cortical and network oscillations (Thut et al. 2011; Thut, Schyns, & Gross, 2011). The residual effects of rTMS are not confined to the stimulated cortex, but may spread across the functionally connected cortical circuits, such as the cortico-cortical and the cortico-thalamic networks (Shafi et al., 2012). This functional connectivity can be explored using electroencephalogram (EEG) through the modulation of brain oscillatory activity (Pascual-Leone et al., 2011; Shafi et al.,

2012). Moreover, rhythmic stimulation protocol such as rTMS has been shown to entrain the natural frequency of the brain to oscillate with the same cycle as rTMS (Thut, Schyns, & Gross, 2011). This means that rTMS has the potential to directly influence the brain oscillations in a control manner (Thut et al. 2011; Thut, Schyns, & Gross, 2011). The rTMS-EEG combined methods are able to provide in-depth insights into the significance of cortical oscillations and the dynamics of brain functions (Miniussi & Thut, 2010; Rogasch & Fitzgerald, 2012), as well as a potential therapeutic tool to reverse abnormal synchronisation (Thut et al. 2011; Thut, Schyns, & Gross, 2011).

1.1 Focus and motivation

The thesis will focus on the modulatory effect of rTMS on the motor cortical oscillatory brain rhythms in healthy humans. In the present thesis, the oscillatory activity was quantified using high-density surface EEG, a non-invasive electrophysiologic technique that measures electrical activity of the brain directly with excellent temporal resolution in the range of milliseconds (Maki & Ilmoniemi, 2010; Sauseng & Klimesch, 2008).

The importance of the current research is due to the increasing evidence that has demonstrated the link between abnormal electrophysiological properties of network oscillations and the generation of neurological and psychiatric disorders (Llinas & Ribary, 2001; Llinas, Ribary, Jeanmonod, Kronberg, & Mitra, 1999; Schulman et al., 2011; Walton, Dubois, & Llinas, 2010). Altered brain rhythms are seen in patients of Parkinson's disease, schizophrenia, neuropathic pain, tinnitus, migraines, major

depression, obsessive-compulsive disorder and psychosis (Jeanmonod et al., 2003; Jones, 2010; Langguth, Kleinjung, Landgrebe, de Ridder, & Hajak, 2010; Llinas et al., 1999; Schulman et al., 2011; Uhlhaas, Haenschel, Nikolic, & Singer, 2008; Uhlhaas & Singer, 2010; Walton et al., 2010). In 1999, the term “Thalamocortical dysrhythmia (TCD)” was introduced to describe abnormal prolonged low-frequency oscillations of delta and theta brain rhythms seen in patients of various neurological and psychiatric disorders (Llinas et al., 1999). Although low-frequency oscillations are normal during slow-wave sleep, prolonged slow oscillations, such as theta rhythms, during awake periods and at rest interrupt the complex dynamic flow of information between the thalamus and cortex, and therefore may produce symptoms of neuropsychiatric illnesses (Jeanmonod et al., 2003; Jones, 2002; Zhang, Llinas, & Lisman, 2009).

In parallel, there is the rise of research attempting to use rTMS to treat symptoms of neurological and psychiatric disorders, such as in patients with Parkinson’s disease, tinnitus, major depression, or schizophrenia, or in those who have suffered from a stroke (Feinsod, Kreinin, Chistyakov, & Klein, 1998; Hallett & Rothwell, 2011; Langguth et al., 2010; Lefaucheur et al., 2008; Londero et al., 2006; Mally & Stone, 1999; McClintock, Freitas, Oberman, Lisanby, & Pascual-Leone, 2011; Miniussi & Rossini, 2011; Pascual-Leone et al., 2000; Ziemann, 2011). Despite the rise in clinical research exploring the therapeutic potential of rTMS, and the evidence of altered brain rhythms in neuropsychiatric patients, knowledge of the precise mechanisms of cortical oscillatory activity after the full range of rTMS applications is still lacking

(Hoogendam et al., 2010; Pascual-Leone et al., 2011; Shafi et al., 2012; Thut et al., 2011; Ziemann, 2011). Therefore, a study exploring the rTMS aftereffects on the modulation of cortical oscillations, especially on low frequency brain rhythms, is timely.

Moreover, there is the limitation of studies investigating the global effects of cortical oscillations after rTMS (Miniussi & Thut, 2010; Thut & Pascual-Leone, 2010a). In 1997, Ilmoniemi and colleagues successfully measured the TMS-evoked brain responses using multichannel EEG (Ilmoniemi et al., 1997). Following that, most TMS-EEG co-registration studies focused on analysing the TMS-evoked responses in the time domain of Event-related potential (ERP) (Thut, Ives, Kampmann, Pastor, & Pascual-Leone, 2005). Only very few studies have explored the effect of rTMS interference upon oscillatory activity through multiple brain rhythms (Brignani, Manganotti, Rossini, & Miniussi, 2008; Fuggetta, Fiaschi, & Manganotti, 2005; Fuggetta, Pavone, Fiaschi, & Manganotti, 2008; Paus, Sipila, & Strafella, 2001; Veniero, Brignani, Thut, & Miniussi, 2011). However, these studies only concentrated on the alpha and beta bands, the brain rhythms that mostly associated with the sensorimotor cortex (Sauseng & Klimesch, 2008; Thut & Miniussi, 2009), but did not investigate the effects of rTMS on low frequency oscillations, such as theta band. Moreover, previous studies failed to differentiate the dichotomy of low and high frequency of stimulation as shown by motor evoked potentials (MEPs) (Brignani et al., 2008; Fuggetta et al., 2008; Veniero et al., 2011). In order to fill in the gap in the knowledge of rTMS modulation of low frequency oscillations,

our present investigations examined the EEG response patterns using a number of experimental manipulations that led to corresponding changes in brain excitability. We evaluated the effects of different rTMS frequencies on cortical oscillations—low frequency (1Hz) versus high frequency (5Hz and 10Hz) rTMS over M1—and the varying number of magnetic pulses, and extended the EEG frequency analysis to include low frequency oscillations of delta and theta, as well as mu and beta frequency bands.

In the present thesis, we examined the modulation of ongoing EEG oscillatory activity after rTMS. EEG oscillations are not used to measure cortical excitability; therefore, there is no measurement on TMS-evoked potentials. Instead, the modulation of brain oscillations is used as a correlate of network interactions in a resting brain, not as index of excitability.

1.2 Research aims

The present research was designed to gain an insight into the neurophysiological mechanisms of rTMS aftereffects on cortical and network oscillations in humans. Focusing on EEG as the direct index of cortical output, the goal was to develop a deeper understanding of the modulation of oscillatory activity through various brain rhythms after non-invasive magnetic stimulation. The thesis also explores the indirect behavioural measurements as well as the direct EEG oscillations as indices of cortical output. The research objectives can be summarised as follows:

1. To better understand the neuronal responses to TMS by simultaneously recording EEG.

2. To evaluate what EEG response patterns may emulate LTP-/LTD-like changes—as assessed by Motor evoked potentials (MEP)—using a number of experimental manipulations that have been shown to lead to corresponding changes in brain excitability.
3. To explore alternative response patterns that cannot be explained by LTP-/LTD-like changes.
4. Through 1-3, to provide information on versatile mechanisms of TMS actions, possibly exploitable in therapy.

1.3 Thesis at a glance

This thesis is arranged in the following manner:

Chapter 2 introduces the co-registration method of rTMS-EEG as a direct index of cortical output. The chapter begins with a brief introduction of the motor cortex, the site of stimulation in the present research. The subsequent section introduces transcranial magnetic stimulation. It explains the principles behind electromagnetic induction, protocols of rTMS, the mechanisms of rTMS aftereffects, and highlights the reason why the present thesis focuses on rTMS effects on the local and global circuit-level pattern of network oscillations. Next, the chapter presents a section on EEG—a neuroimaging technology based on the electrophysiological activity within the brain. It introduces the oscillatory brain rhythms, their generations, and their functional significance. The most important section performs a literature review on the rTMS-EEG co-registration studies. The importance of the current work in extending the understanding of the relationship between rTMS-induced EEG oscillations and cortical plasticity is emphasised. The subsection presents several rTMS studies that emulate LTP-/LTD-like mechanisms of synaptic plasticity. However, LTP-/LTD-like

mechanisms may not be the only mechanisms that drive the rTMS aftereffects. Here, we explore alternative hypothesis/explanations that reflect the EEG oscillatory modulations post rTMS.

Chapter 3 discusses the general method employed in the present thesis. The chapter presents details of the subjects, experimental paradigms, TMS procedure, EMG recording, EEG data acquisition and spectral analysis of event-related power and event-related coherence to quantify oscillatory brain rhythms. The main purpose of chapter 2 and 3 is to familiarise the reader with the terminology of rTMS and EEG characteristics that will be referred to in later chapters.

Chapter 4 presents the investigation of the acute modulation of human cortical oscillations after high frequency rTMS by manipulating the number of magnetic pulses while keeping other parameters constant. The comparison of cortical output post rTMS was made between behavioural measurements of MEPs and direct electrophysiological EEG at rest. The study described in this chapter forms the basis of the article “Human cortical theta reactivity after repetitive transcranial magnetic stimulation” published in the journal *Human Brain Mapping*.

Chapter 5 continues the rTMS-EEG experiments on short-term oscillatory modulation using simple rTMS protocols. Here, we manipulated different frequencies of magnetic stimulation (low rTMS frequency versus high rTMS frequency) while keeping other parameters of stimulation constant, and looked at the acute cortical plasticity effects in terms of oscillatory activities. The main

purpose was to explore the dichotomy between low and high frequency rTMS using the low frequency brain rhythms of delta and theta oscillations. A version of this chapter forms the basis of the paper “A neurophysiological insight into the potential link between transcranial magnetic stimulation, thalamocortical dysrhythmia, and neuropsychiatric disorders” submitted for publication.

Chapter 6 describes the experiment exploring the long-lasting modulation of cortical oscillations after pattern rTMS protocol of cTBS. The cTBS aftereffects were measured at rest and during a choice motor reaction time task, by EEG and behavioural measurements of MEPs and RT. The study described in this chapter form the basis of the article “Long-lasting modulation of cortical oscillations after theta-burst transcranial magnetic stimulation” published in the journal PloSONE. The findings on network connectivity after cTBS form the basis of another article “Long-lasting modulation of motor network oscillations after continuous theta-burst stimulation” submitted for publication.

Finally, chapter 7 discusses the main theme that emerged from the findings of the current research. Here, we emphasise the ability of rTMS to transiently modify brain function by altering brain oscillations particularly the low-frequency brain rhythms. We discuss the significant of an important negative finding in the present thesis, which is the dissociation between EEG oscillatory activity and MEPs cortical output. This chapter also highlights the possible areas of future research. The general conclusion for the significance of the present findings particularly on the modulation of low frequency oscillations by rTMS wraps up the thesis.

2. rTMS-EEG: a window to the brain

This chapter serves to introduce the combined method of rTMS and EEG as direct methods to study the modulation of cortical oscillatory activity, and the plasticity-like mechanisms induced by rTMS. It begins with a brief overview of the motor cortex, the chosen site of stimulation for the experiments in the present thesis. In the following section, the readers are introduced to rTMS with the presentation of the basic principles of magnetic stimulation, rTMS protocols of simple and pattern protocols, the safety issues, and the techniques to measure rTMS aftereffects. The subsequent part of the chapter describes EEG as a direct cortical read-out after magnetic stimulation. It discusses the principles of EEG and the oscillatory brain rhythms—both their generation and functional significance. Next, the subsection highlights the advantages of combining rTMS and EEG to facilitate the investigations of rTMS aftereffects. Having clarified the concept of rTMS-EEG co-registration approaches, the chapter moves on to review studies of the ongoing cortical oscillatory activity after rTMS and research exploring the plasticity-like mechanisms induced by rTMS. Finally, the chapter concludes with the presentation of the knowledge gaps that drive the subsequent rTMS-EEG investigations in the present thesis.

2.1 Motor cortex

The experiments in the present thesis explored the aftereffects of rTMS to the motor region of the cerebral cortex, as revealed by EEG and the behavioural

measurements. A brief overview of the anatomy and physiology of the motor cortex is presented in order to establish a framework for interpreting the results of the subsequent experiments.

The motor cortex is a region of the frontal lobe. It comprises of Brodmann's area 4, which is anterior to the central sulcus of the precentral gyrus, and Brodmann's area 6 that lies anterior to area 4 (Figure 2-1). The evidence that these areas constitute the motor cortex in humans came from the work of Canadian neurosurgeon Wilder Penfield. He electrically stimulated the cortical surface in patients who were undergoing surgery for epileptic seizures. The electrical stimulation of Brodmann's area 4 would produce a twitch of the muscles on the contralateral side, whereas stimulation of Brodmann's area 6 could elicit complex movements of either side of the body (Penfield & Welch, 1951). Area 4 is often referred to as the primary motor cortex (M1). It generates neural impulses through the corticospinal tract for movement of specific muscles or muscle groups. Area 6 consists of the premotor area (PMA) and the supplementary motor area (SMA). It is the "higher" motor area in humans and is involved in initiating and planning voluntary movement.

2.1.1 Primary motor cortex

The primary motor cortex, M1 is located on the anterior of the precentral gyrus of the agranular frontal lobe (Chouinard & Paus, 2006). It is characterised by the presence of giant pyramidal cells (Betz cells) in layer V, and a lack of granule cells in layer IV pyramidal cells (Chouinard & Paus, 2006; Meyer, 1987). The Betz cells and the other layer V pyramidal cells give rise to

excitatory cortical and spinal projections and have numerous local collateral branches with horizontal connection systems within M1 extending over 1cm (Porter & Sakamoto, 1988). The excitatory glutamatergic horizontal pathways are probably influenced by GABA-ergic inhibitory interneurons (Hess and Donoghue, 1994). The horizontal pathways are the basis for cortical plasticity (Boroojerdi, Ziemann, Chen, Butefisch, & Cohen, 2001; Ziemann, Hallett, & Cohen, 1998). This is shown by the reorganisation of the cortical maps that is confined to cortical areas with strong horizontal connections (Ziemann et al., 2008; Ziemann, Wittenberg, & Cohen, 2002). The horizontal pathways in M1 are involved in the mechanisms of synaptic plasticity—LTP and LTD—that may include cortico-cortical and thalamocortical pathways (Timofeev, 2011; Ziemann, 2004a; Ziemann, Ilic, & Jung, 2006).

The role of M1 is to produce the commands that control the execution of movement (Chouinard & Paus, 2006; Hari et al., 1998; Meyer, 1987). Neural impulses from M1 activate skeletal muscles on the contralateral side of the stimulated hemisphere. Every body part is represented somatotopically in M1 (Meyer, 1987). The amount of brain matter for a specific body part indicates the amount of control that M1 has over that body part (Meyer, 1987). For example, hands and fingers have larger representations in M1 than the trunk or legs, because more cortical space is required to control the complex movements of the hand and fingers. This motor map of the body in the motor cortex is called the motor homunculus. Figure 2-1 illustrates the primary motor cortex.

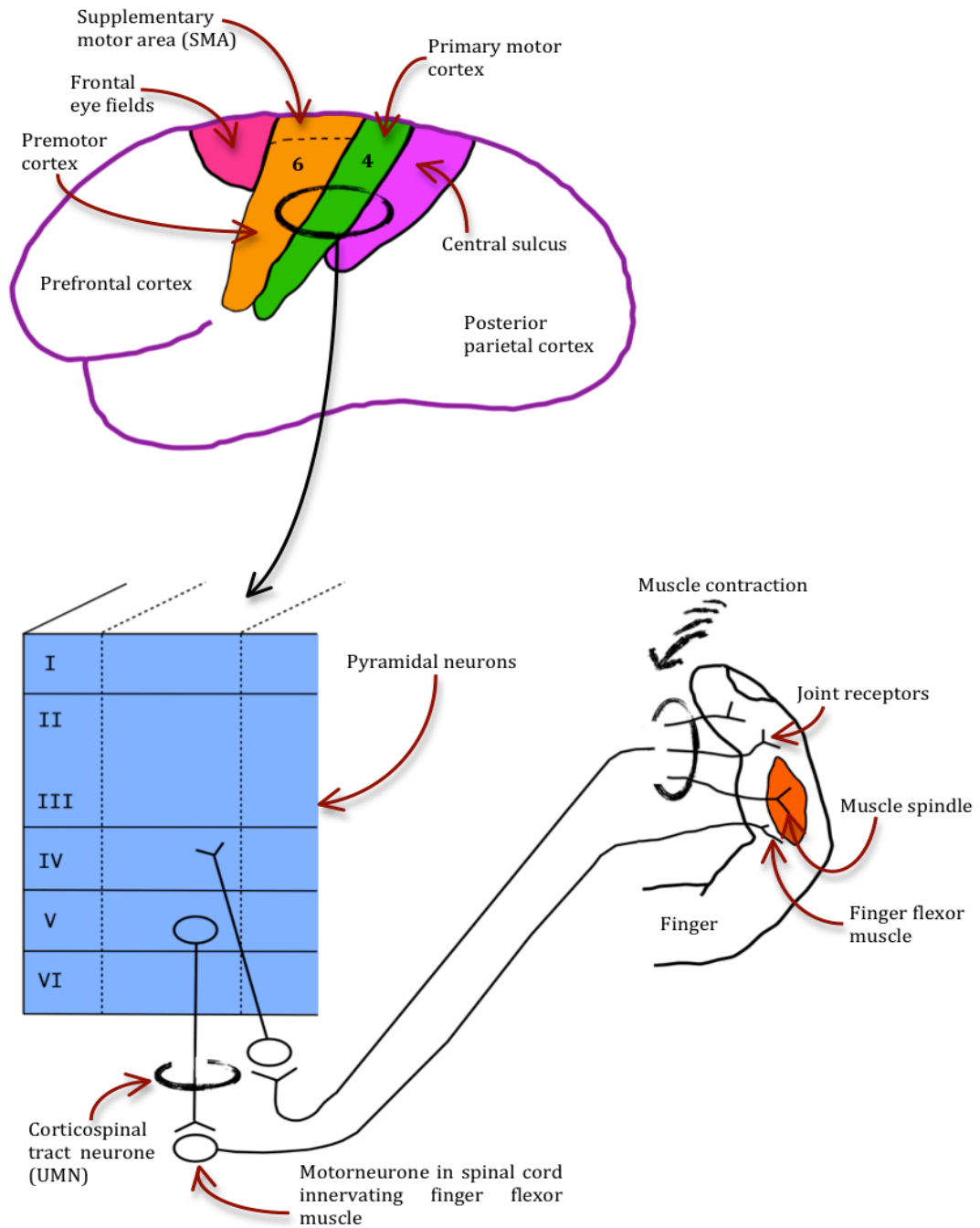


Figure 2-1 Primary motor cortex. Adapted with permission from Barker, R. A., Barasi, S., & Neal, J. M. (2008). *Neuroscience at a glance*: Blackwell Publishing.

2.1.2 Other cortical motor areas

The Brodmann's cytoarchitectonic map of the human cortex defines area 6 (PMA and SMA) as the extension of the precentral gyrus and the superior frontal gyrus on the lateral and medial surfaces of the brain (Chouinard & Paus, 2006). The lateral PMA in humans is divided into the dorsolateral premotor cortex (PMd), and the ventrolateral premotor cortex (PMv). The PMd is within the rostral precentral gyrus and the caudal superior frontal gyrus. It may be involved in action planning, response selection, movement preparation and visual guidance of motor responses (Chouinard & Paus, 2006). The PMv is located ventral to the frontal eye fields. Although not conclusive, neuroimaging studies in humans implicated the role of PMv in action observation and object manipulation tasks (Picard & Strick, 2001).

The SMA is divided into SMA proper (caudal SMA) and pre-SMA (rostral SMA) (Picard & Strick, 2001). It is implicated in simple motor tasks, movement initiation, motor preparation, and learnt sequences (Passingham, 1988, 1989; Thaler, Chen, Nixon, Stern, & Passingham, 1995). The pre-SMA is linked to the cognitive aspects of motor control, such as the processing of movement cues (Picard & Strick, 2001; Sadato, Ibanez, Deiber, & Hallett, 2000).

2.1.3 Subcortical motor areas

The thalamus is a subcortical area originated from the forebrain and is part of the limbic system. It transmits information from the basal ganglia, cerebellum, and somatosensory spinal cord to the cerebral cortex, and also between the cortical areas (Guillery & Sherman, 2002; Sherman & Guillery, 2002). It is

involved in the regulation of sensory perception and motor functions (Sherman, 2007; Steriade, 2001). It receives afferents inputs from the somatosensory, visual and auditory cortex, and relays sensory signals to the cerebral cortex (Sherman, 2007; Steriade, 2001). The thalamus, with its massive input to the cerebral cortex, can also act as a powerful pacemaker to coordinate rhythmic, synchronous activity of the brain (Sherman, 2001, 2007; Steriade, 2001; Timofeev, 2011).

The basal ganglia are comprised of the striatum (caudate nucleus and putamen), the subthalamic nucleus, the globus pallidus and the substantia nigra reticulata. The motor loop through the basal ganglia originates with excitatory connections from the somatosensory and motor cortex to the putamen (Levy et al., 1997; Parent & Hazrati, 1995b). The subthalamic nucleus receives input from M1, SMA, and PMd (Parent & Hazrati, 1995b). The striatum and subthalamic nucleus project to the globus pallidus and the substantia nigra, which in turn project to the thalamus and the brain stem. The thalamus and basal ganglia therefore form part of the cortico-basal ganglia-thalamocortical loop (Parent & Hazrati, 1995a). The role of basal ganglia is to initiate and regulate voluntary movements (Haber & Calzavara, 2009; Middleton & Strick, 2000). The basal ganglia, SMA, PMA, and the prefrontal cortex make up the highest level of motor control, which involve in the initiation of movement including planning and programming of movement (Barker, Barasi, & Neal, 2008). In the motor cortex, the net dopamine levels of the basal ganglia may

modulate synchronised neural oscillations at beta frequencies (Jenkinson & Brown, 2011).

The cerebellum, or the “little brain”, is a complex structure connected to the brainstem by three pairs of cerebellar peduncles (Barker, Barasi, & Neal, 2008). It receives afferent inputs from the spinocerebellar tracts conveying movement-related sensory information from muscle spindles, tendon organs, joint and cutaneous receptors, and spinal interneurons (Baillieux, De Smet, Paquier, De Deyn, & Marien, 2008; O'Halloran, Kinsella, & Storey, 2012). It also gets sensory inputs from the contralateral cerebral cortex via the pontine cerebellar nuclei (O'Halloran et al., 2012). Purkinje cells from the cerebellar cortex project to the cerebellar nuclei to the spinal cord and the ventrolateral thalamus to the primary, supplementary, and premotor cortices. The role of the cerebellum includes control of muscle tone, fine movement coordination, regulation of equilibrium, and motor learning (Baillieux et al., 2008).

The corticospinal tract is the major efferent of the motor cortex. It originates from the axons of layer V pyramidal cells that project via the internal capsule to the medullary pyramids, thus “pyramidal tract” is often used as a synonym for corticospinal tract (Martinez, Lamas, & Canedo, 1995). Near the junction between the medulla and the spinal cord, the pyramidal tract crosses from one side of the midline to the other side—known as pyramidal decussation (Martinez et al., 1995). The crossing of the axons in the medulla or the decussation explains why the cortex of one side of the brain hemisphere controls movement of the contralateral muscles of the body. Descending

corticospinal fibers terminate in the spinal cord, synapsing either on the interneurons, or directly on the motor neurons, and exit the spinal cord via the ventral horns to the skeletal muscles (Nathan, 1990; Canedo, 1997). Figure 2-2 illustrates the cortical and subcortical motor areas.

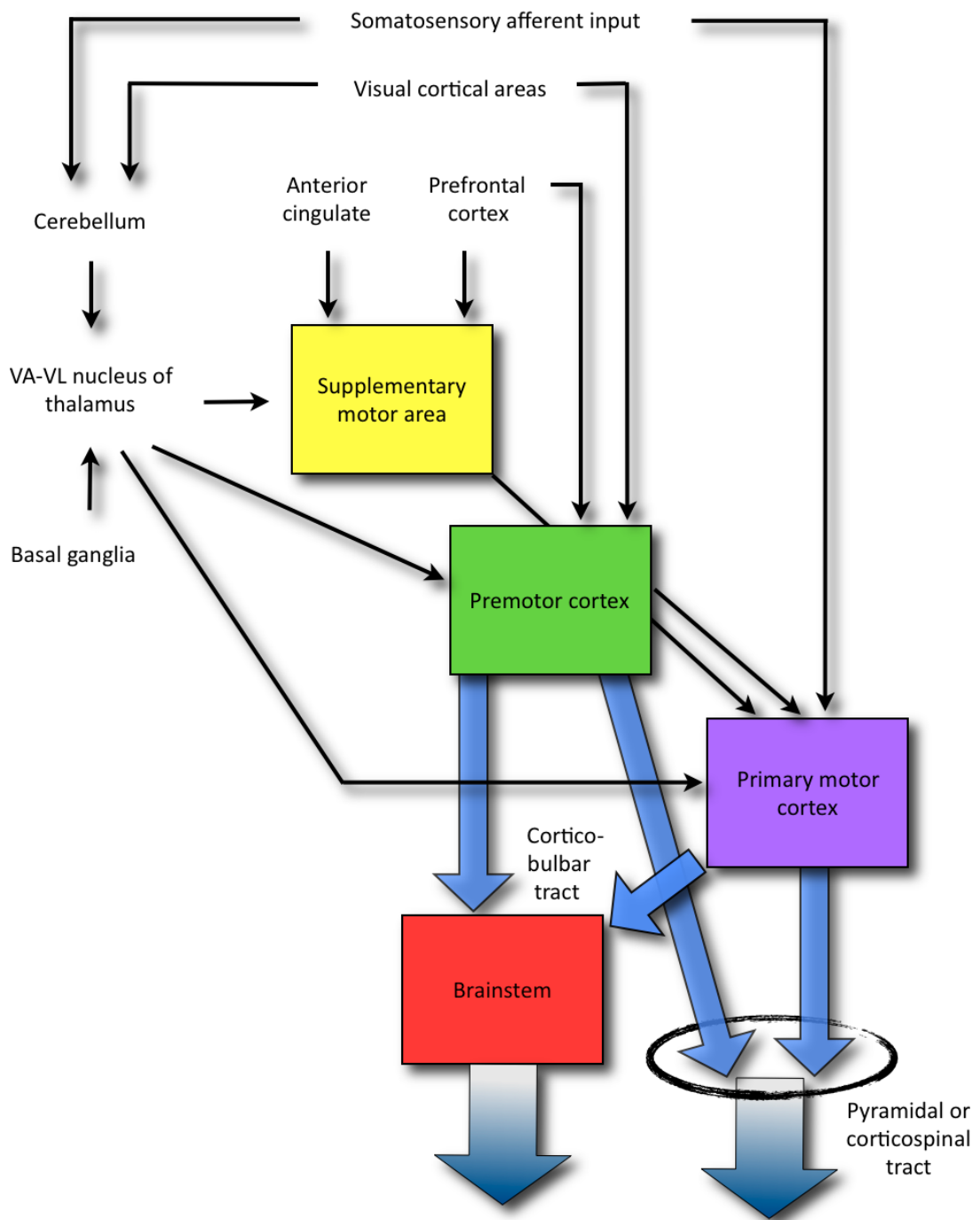


Figure 2-2 Cortical and subcortical motor areas. Adapted with permission from Barker, R. A., Barasi, S., & Neal, J. M. (2008). *Neuroscience at a glance*. Blackwell Publishing.

2.2 Repetitive transcranial magnetic stimulation

This section introduces transcranial magnetic stimulation, a neurophysiology technique that stimulates the brain non-invasively. It explains the principles of TMS, the rTMS protocols used to study the excitability of the motor cortex, and the safety issues of magnetic stimulation. The subsequent subsection presents the methods used to assess rTMS aftereffects on cortical excitability and highlights the advantages of using EEG as the direct index of cortical output after magnetic stimulation.

In 1980, Merton and Morton successfully invented Transcranial electrical stimulation (TES) that was able to stimulate the living human brain non-invasively (Merton & Morton, 1980). TES uses a brief, high-voltage electric shock from a low-output-resistance stimulator, delivered through electrodes on the intact scalp (Merton, Hill, Morton, & Marsden, 1982). By stimulating the motor cortex, TES produces a peripheral muscle response of motor evoked potentials of the contralateral body, whereas stimulation over the visual cortex produces a phosphene—the phenomenon of seeing light without light entering the eyes (Rothwell, 1991). The applications of TES in basic neuroscience and clinical research include electrophysiological measurement of motor central conduction time, the conduction velocity in the pyramidal tract, and the detection of neuropathy (Merton et al., 1982). Although effective and useful, the electrical stimulation has some drawbacks. The current is injected directly to the scalp electrode, and will stimulate the pain receptors located near the skin, thus producing pain and discomfort to the subject (Amassian, Cracco, & Maccabee,

1989; Rothwell, 1991). The other major problem with TES is that only a little of the induced current actually penetrates the brain due to the high electrical resistance of the skull, resulting in the attenuation of the aftereffects of stimulation (Amassian et al., 1989; Rothwell, 1991).

Five years later in 1985, Professor Anthony Barker and colleagues from the University of Sheffield, UK, introduced transcranial magnetic stimulation, an alternative to the conventional electrical stimulation. TMS is a non-invasive neurophysiologic method of delivering electrical stimuli by rapidly changing the magnetic field (Barker, Jalinous, & Freeston, 1985). Unlike TES, TMS induces current into the brain without physical contact, as there are no implanted or surface electrodes (Hallett, 2007). Instead, it works by placing an electromagnetic coil that carries pulses of current near the human scalp. The current from the TMS coil will generate an intense but brief magnetic field (up to 2 Tesla that lasts for 100 μ s) that passes through the scalp, skull, and meninges to the cortical region beneath the coil without attenuation (Anand & Hotson, 2002). Based on Faraday's law of electromagnetic induction—the process by which electrical energy is converted into magnetic fields—the rapidly changing magnetic field will induce an electrical current in the surrounding cortical tissue below the coil (Barker et al., 1985). As body tissue is electrically conductive, the ionic current will flow, eliciting nerve depolarisation and action potentials, and will subsequently stimulate the cortical neurons (Hallett, 2007). Figure 2-3 illustrates an example of a modern transcranial magnetic stimulator.



Figure 2-3 Example of a modern transcranial magnetic stimulator

There are several advantages of magnetic stimulation over electrical stimulation. Firstly, TMS does not generate strong pain whereas TES is painful due to the activation of pain fibres (Hallett, 2007; Rothwell, 1991). This is because the TMS coil is placed near the scalp with no actual physical contact. Therefore, the induced current of magnetic stimulation does not pass through the skin—the location of most pain nerve endings—resulting in minimal or no activation of the pain receptors (Barker et al., 1985; Rossini et al., 1994; Siebner, Hartwigsen, Kassuba, & Rothwell, 2009). Secondly, the current induced by magnetic stimulation does not attenuate because of the relatively low frequency magnetic fields that pass through the extra-cerebral layers—scalp, skull and meninges (Hallett & Rothwell, 2011; Pascual-Leone, Walsh, & Rothwell, 2000). Thirdly, magnetic stimulation is relatively safer than electrical stimulation provided strict safety guidelines are followed (Oberman, Edwards, Eldaief, & Pascual-Leone, 2011; Rossi, Hallett, Rossini, & Pascual-Leone, 2009; Wassermann et al., 1996). The current induced by magnetic stimulation is

more diffuse unlike the focal, high current intensities injected directly below the electrodes during electrical stimulation (Hallett, 2007; Rothwell 1997). All these advantages make TMS the method of choice by many neuroscientists in studying the physiology of the living human brain (Hallett & Rothwell, 2011; Hoogendam, Ramakers, & Di Lazzaro, 2010; Kobayashi & Pascual-Leone, 2003; Pascual-Leone et al., 2000).

Following the introduction of TMS, electrical stimulation was reintroduced in the late 1990s as transcranial direct current stimulation (tDCS) (Lefaucheur et al., 2008; Nitsche & Paulus, 2000, 2011). The tDCS consists of a battery-powered device and two electrodes—the anodal and cathodal electrodes (Nitsche & Paulus, 2000). It works by introducing weak direct current via the scalp electrodes, and modulates cortical excitability through membrane polarisation (Nitsche & Paulus, 2011). If the anode is placed near the motor cortex, it depolarises the resting membrane potential (RMP), and results in increased cortical excitability (Lang, Nitsche, Paulus, Rothwell, & Lemon, 2004). However, the cathodal stimulation will hyperpolarise the underlying neurons and decreases cortical excitability (Lang et al., 2004). Unlike TMS, which directly activates the cortical neurons, tDCS only stimulates spontaneous cell firing due to its lower current (Shafi, Westover, Fox, & Pascual-Leone, 2012). This results in weaker aftereffects for tDCS as compared to rTMS, thus makes tDCS less beneficial for therapy and neuroplasticity research (Shafi et al., 2012).

2.2.1 Principles of magnetic stimulation

The fundamental principle of magnetic stimulation is based on the law of electromagnetic induction introduced by Michael Faraday in 1831. In a nutshell, the Faraday's law of electromagnetic induction is the process by which electrical energy is converted into magnetic fields. An electric current, which flows through a coil of wire, will generate a magnetic field. Then, the rapidly changing magnetic field induces a flow of secondary electric current in adjacent conductors (Epstein, 2008; Hallett, 2000). Transcranial magnetic stimulation works by creating a changing magnetic field from a stimulation coil that will induce electric current in nearby conductors (Barker et al., 1985; Rothwell, 1991). As body tissue is electrically conductive, the ionic current will flow, triggering nerve depolarisation and above a certain threshold will result in action potentials that excite cortical neurons (Hallett, 2007).

There are only three elements that make up the circuitry of a TMS apparatus—the power capacitor as an energy storage element, the stimulation coil as an inductor, and a high-power switch that closes to connect the circuit (Barker et al., 1985; Epstein, 2008). Figure 2-4 illustrates the TMS circuit.

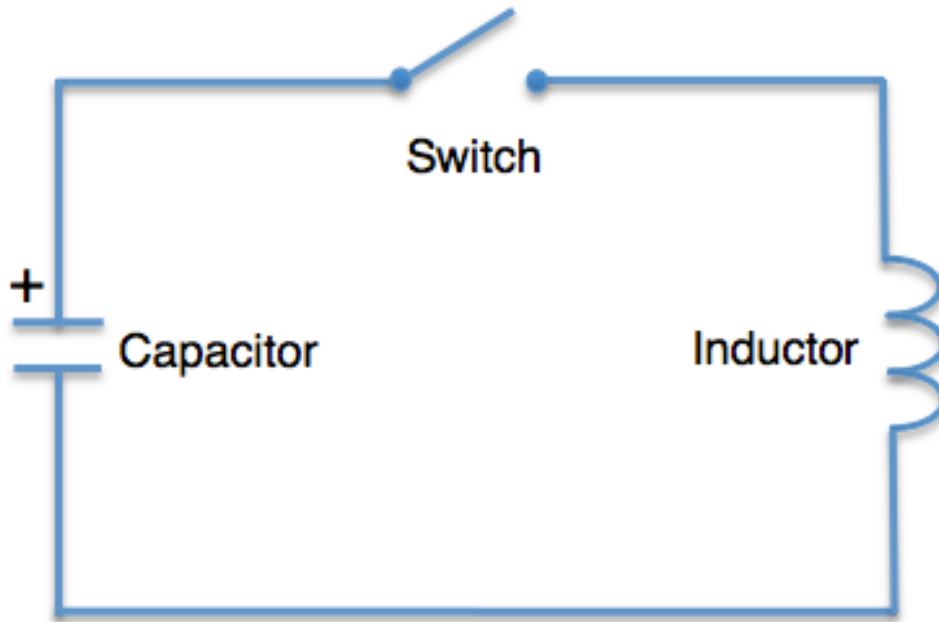


Figure 2-4 Basic TMS circuit showing the three elements of TMS apparatus—power capacitor, stimulation coil as inductor, and high-power switch.

The power capacitor is a large energy storage element of about 2000 joules of stored energy, and provides efficient energy transfer from capacitor to coil; approximately 500 joules transfer to the coil in less than $100\mu\text{s}$ (Taylor, Walsh, & Eimer, 2008; Walsh & Cowey, 2000). When the power capacitor is discharged through the coil, a very large current flows. A peak value of several thousand amps within $200\mu\text{s}$ is reached and the current declines to zero over duration of approximately 1ms (Taylor et al., 2008; Walsh & Cowey, 2000). This electric current will produce a magnetic field of up to 3 Tesla (Barker et al., 1985). Based on Faraday's law of electromagnetic induction, the high intensity but rapidly changing magnetic field induces a secondary electrical eddy current in the cortical tissue below the stimulation coil (Barker et al., 1985; Hallett & Rothwell, 2011; Ridding & Rothwell, 1999). The secondary current induced by

magnetic stimulation does not attenuate because of the low impedance to the magnetic fields that pass through the scalp (Walsh & Cowey, 2000; Walsh & Rushworth, 1999). However, the magnetic field declines rapidly with distance from the stimulation coil (Hallett, 2000). Therefore the effect of the stimulation is strongest at the superficial layers of the cerebral cortex and diminishes at the subcortical tissues, such as the basal ganglia and the thalamus (Hallett, 2000, 2007; Kobayashi & Pascual-Leone, 2003).

The stimulation coil consists of well-insulated coils of copper wire molded in a plastic cover, and is available in a variety of shapes and sizes. The types of coils that are commonly used in TMS research are circular and figure-8 coils. These two types of coils differ in the focality and the penetration of the induced current (Kobayashi & Pascual-Leone, 2003). The current density of the circular coil is strongest near the outer edge of the coil, but the magnetic field is maximal directly below the center of the coil (Amassian et al., 1989; Walsh & Pascual-Leone, 2003). Its relatively large diameter (8-15cm) also results in better penetration to the cerebral cortex. However, the main shortcoming of the circular coil is its lack of focality (Walsh & Pascual-Leone, 2003). This is because the circumference of the coil covers a large area of the brain and the radius of the greatest field is not precisely known (Walsh & Pascual-Leone, 2003). The figure-8 coils are two circular coils joined to each other. The induced current density is higher at the intersection of the two circular components of the figure-8 coils, and it allows better focality at a definable site (Conforto et al., 2004). Therefore, the figure-8 coil is used more than the circular coil in basic

and clinical neuroscience research (Hallett, 2007; Shafi et al., 2012). The disadvantage of the figure-8 coils is the limited penetration of the induced current because the diameter of the loops is relatively smaller than the circular coil (Conforto et al., 2004; Hallett, 2007).

2.2.2 rTMS protocols

TMS can be applied in a single pulse or in trains of several TMS pulses—repetitive TMS (Wassermann et al., 2008). A single TMS pulse is the application of one stimulus every 3s or more to a specific cortical area (Wassermann et al., 2008). It is usually used to explore the excitability of the central motor circuits by measuring the motor threshold or MEPs (Fitzpatrick & Rothman, 2000; Rothwell et al., 1999). Moreover, a single TMS pulse can be used as a tool to explore brain-behaviour functions by disrupting normal cognitive tasks (Chen, 2000; Chen et al., 2008). It can briefly (in approximately tens of milliseconds) disrupt normal brain functioning by introducing random neural activity into the targeted cortical region; if the stimulated area is essential for the given task, performance should be impaired (Walsh & Cowey, 2000). When applied to the motor cortex, a single TMS pulse of sufficient intensity is able to induce movement in a contralateral limb and can be used to investigate the time course of the execution of the motor programs (Chen, 2000). Applied to the visual cortex it can induce the perception of a flash of light—a phosphene—and can be used to investigate the time course of detection and perception of the visual stimuli (Walsh & Pascual-Leone, 2003).

The application of magnetic stimulation in repeated pulses or as trains of stimuli at various frequency delivered to the same cortical region for several seconds is known as repetitive TMS. The rTMS protocol has the potential to modulate cortical excitability lasting for several minutes (Chen & Udupa, 2009; Ziemann et al., 2008) in analogy to electrical stimulation in animal studies of hippocampal rat tissue (Bear & Malenka, 1994; Malenka, 1994). The modulatory effects of rTMS depend on the stimulation intensity, frequency of stimulation, intertrain-interval, the total number of magnetic pulses, coil position, current direction, and pulse waveform (Fitzgerald et al., 2006; Hoogendam et al., 2010).

The repetitive magnetic stimulation can be classified into simple/conventional, and pattern rTMS protocols. The protocol is defined “simple” if individual stimuli are spaced apart by identical inter-stimulus intervals (ISI), and the trains of stimuli are delivered at a fixed frequency, usually in the range of 1-20Hz (Wassermann et al., 2008) However, when there are different ISI involved, and the trains of stimuli are delivered at multiple frequencies, the protocol is known as pattern rTMS (Wassermann et al., 2008). The present subsection focuses on the protocols used in this thesis: the simple rTMS paradigms of low frequency and high frequency rTMS protocols, and the pattern protocol of theta-burst stimulation.

2.2.2.1 Low frequency rTMS

The distinction between high- and low-frequency magnetic stimulation has not been clearly defined (Feinsod et al., 1998). According to the convention

adopted at the International rTMS Safety Conference in Bethesda, MD (1996), it is currently accepted to distinguish low frequency and high frequency rTMS by the cut-off of 1Hz (Wassermann et al., 1996). Low frequency rTMS is defined as the application of repetitive magnetic pulses at slow frequency of one stimulus every second or less ($\leq 1\text{Hz}$) (Figure 2-5).

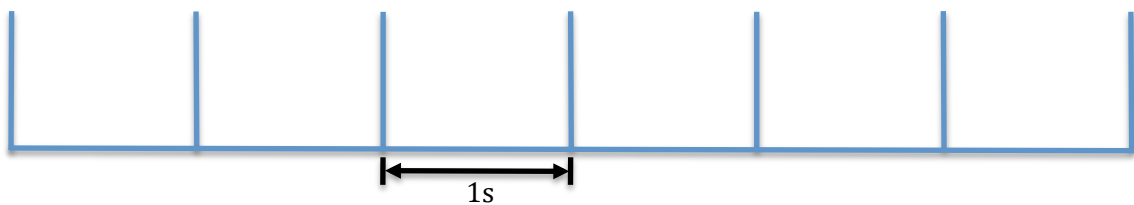


Figure 2-5 Low frequency rTMS 1Hz protocol showing one magnetic stimulus for every second.

The protocol of 1Hz rTMS is the most frequently used paradigm to establish structure-function relationships in the motor cortex and other cortical areas (Fitzgerald et al., 2006). However, studies investigating the residual effects of 1Hz rTMS on cortical excitability differ in stimulus intensity and the number of magnetic pulses (Hoogendam et al., 2010). An initial study by Chen and colleagues (1997) demonstrated that 0.9Hz rTMS with a stimulus intensity of 115% resting motor threshold (RMT) applied for 15-min resulted in a decrease in MEP amplitude lasting beyond the 15-min application (Chen et al., 1997). Subsequently, Muellbacher and colleagues (2000) using 1Hz rTMS showed a significant suppression of MEP amplitude that lasted for about 30-min. The group reported a spatially focused effect of rTMS; the effect was specific for the hand motor representation, which was the target of the rTMS,

not the adjacent muscle representations (Muellbacher, Ziemann, Boroojerdi, & Hallett, 2000). Since then, there have been many studies of 1Hz rTMS of varying intensities and number of pulses replicated the MEPs outcome (Chouinard, Van Der Werf, Leonard, & Paus, 2003; Heide, Witte, & Ziemann, 2006; O'Shea & Walsh, 2007; Siebner et al., 2004; Suppa, Bologna, et al., 2008).

In 2002, Fitzgerald and colleagues demonstrated that the suppressive effect of low frequency rTMS was dependent on the intensity of the magnetic stimulation (Fitzgerald, Brown, Daskalakis, Chen, & Kulkarni, 2002). They applied 1Hz rTMS for 15-min at the stimulus intensity of 85 and 115% RMT, showing that only suprathreshold stimulation (115% RMT) reduced the size of MEPs. In contrast, Romero *et al.* (2002) showed that even 10-min of subthreshold 1Hz rTMS at 90% of RMT led to a suppression of MEP amplitudes that lasted beyond the stimulation period (Romero, Ansel, Sparing, Gangitano, & Pascual-Leone, 2002). The suppression of MEPs might be due to the fact that corticospinal output neurons are activated at 90% of RMT; intensities lower than 90% RMT have not been reported to lead to lasting excitability changes (Fitzgerald et al., 2006). Other groups have demonstrated that besides intensity of stimulation, longer trains of 1Hz rTMS applied at 90% or 95% RMT led to longer lasting MEP suppression than shorter trains of stimulation (Maeda, Keenan, Tormos, Topka, & Pascual-Leone, 2000b; Touge, Gerschlager, Brown, & Rothwell, 2001).

2.2.2.2 High frequency rTMS

rTMS can also be applied at higher stimulation frequencies. High frequency rTMS is defined as the application of repetitive stimuli delivered more than one stimulus per second ($> 1\text{Hz}$). Figure 2-6 illustrates the rTMS 5Hz and rTMS 10Hz of high frequency protocols.

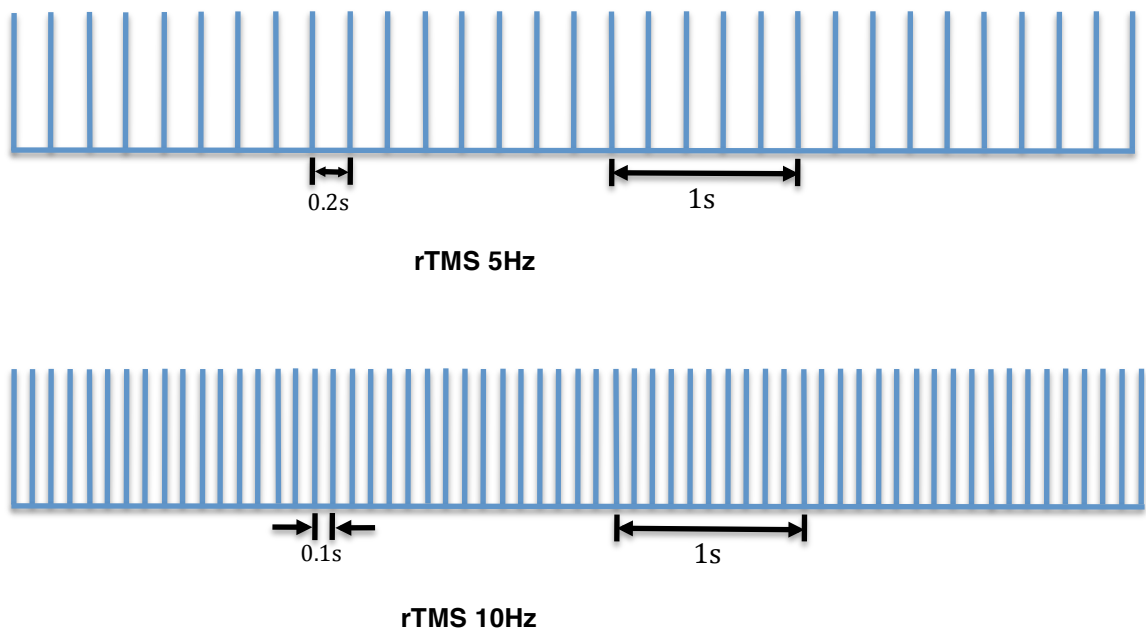


Figure 2-6 High frequency rTMS 5Hz and 10Hz protocols showing five stimuli per second in rTMS 5Hz and ten stimuli per second in rTMS 10Hz.

In a pioneering study by Pascual-Leone *et al.* (1994) using ten pulses of 20Hz rTMS at 150% motor threshold, high frequency rTMS led to an increase in the excitability of the motor cortical region for 3-4 minutes (Pascual-Leone, Valls-Sole, Wassermann, & Hallett, 1994). Subsequent studies of short trains of high frequency rTMS ($\geq 5\text{Hz}$) to the motor cortex also demonstrated an increase in MEP size (Maeda *et al.*, 2000b; Peinemann *et al.*, 2000). Studies on longer

trains of high frequency rTMS have also shown increased MEP amplitudes (Modugno et al., 2001; Quartarone et al., 2005).

However, studies that explored the interaction between frequency, intensity, and duration of rTMS have demonstrated that the alteration of cortical excitability by high frequency rTMS depends also on the intensity of stimulation. High frequency rTMS ($\geq 5\text{Hz}$) of subthreshold intensity tends to produce post-train MEPs suppression (Todd, Flavel, & Ridding, 2006), whereas suprathreshold stimuli tend to produce MEPs facilitation (Modugno et al., 2001). However, the cortical inhibitory effect of subthreshold high frequency rTMS is only applicable for short trains of magnetic pulses (<20), whereas longer trains produce MEPs facilitation. In a study by Modugno *et al.* (2001), it was demonstrated that a shorter train of 5Hz rTMS at 100% RMT produced MEPs suppression, whereas longer trains with an identical stimulus resulted in MEPs facilitation (Modugno et al., 2001). The authors speculated that gradual build up of inhibition and facilitation occurred during the course of a stimulus train, with inhibition reaching its maximum after a relatively shorter stimulus train (Modugno et al., 2001). In another study by Quartarone *et al.* (2005) using longer trains of stimulation (>900 pulses) of 5Hz rTMS at 90% RMT, MEPs facilitation was demonstrated in the relaxed and tonically contracted hand muscle. The authors suggested that prolonged 5Hz rTMS might enhance synaptic transmission of connections onto pyramidal cells in the motor cortex (Quartarone et al., 2005).

Although simple rTMS protocols are able to alter cortical excitability beyond the duration of magnetic stimulation, the aftereffects are usually short lasting, typically only lasting for several minutes (Hallett, 2000; Pell et al., 2011). Although this is enough for basic neuroscience research, this short-term “plasticity-like” effect is not enough for optimal clinical intervention (Hallett, 2000; Pell et al., 2011). A protocol that can induce a longer-lasting effect is thus needed. One such protocol is theta-burst stimulation.

2.2.2.3 Theta-burst stimulation

Apart from simple rTMS protocol, there is another protocol called pattern rTMS, which comprises of trains of magnetic pulses with different ISIs and intensities. One example of pattern rTMS protocol that is widely used in basic neuroscience and clinical research is theta-burst stimulation (TBS) (Huang, Edwards, Rounis, Bhatia, & Rothwell, 2005). The TBS paradigm was based on animal studies, where bursts of 3-5 pulses at 50-100Hz repeated at an interval of 200ms from each other, induced LTP—the mechanism responsible for synaptic plasticity—when applied to the motor cortex or hippocampus (Davies, Starkey, Pozza, & Collingridge, 1991; Hess, 2004; Hoogendam et al., 2010). The term theta is because 200ms is the main periodicity of the theta rhythm, an oscillatory rhythm that occurs during the periods of increased attention, such as when an animal explores a new environment (Huerta & Volpe, 2009; Kahana, Seelig, & Madsen, 2001).

In a theta-burst paradigm involving human subjects, brief trains of pulses are delivered at 5Hz—at theta frequency. There are two modalities of TBS,

continuous TBS that will induce long-lasting, reversible cortical inhibition, and intermittent TBS (iTBS) that will induce long-lasting cortical facilitation (Huang et al., 2005; Huang, Rothwell, Chen, Lu, & Chuang, 2011). The cTBS paradigm refers to bursts of three TMS pulses of 50Hz (20ms between each stimulus) repeated at intervals of 200ms (5Hz-theta rhythm) for the duration of either 20s (300 pulses), or 40s (600 pulses) at a stimulus intensity of 80% active motor threshold (AMT) (see Figure 2-7). In contrast, iTBS consists of a 2s train of TBS repeated every 10s for a total of 190s (600 pulses). However, there is still no consensus to the optimal stimulation parameters due to the fact that several study-groups have modified the original TBS protocols (Cardenas-Morales, Nowak, Kammer, Wolf, & Schonfeldt-Lecuona, 2010), changing the number of pulses, stimulation intensity, and current directions (Grossheinrich et al., 2009; Ishikawa et al., 2007; Nyffeler et al., 2006; Stefan, Gentner, Zeller, Dang, & Classen, 2008; Talelli, Greenwood, & Rothwell, 2007; Zafar, Paulus, & Sommer, 2008). The main difference between TBS and simple rTMS protocol is the ability of TBS to extend the aftereffects of the induced plasticity changes for up to an hour despite its lower stimulus intensity and shorter duration of stimulation (Huang et al., 2005; Paulus, 2005). This makes TBS particularly useful for neuroplasticity research due to its prolong residual effects and its relative safety efficacy (Cardenas-Morales, Gron, & Kammer, 2011).

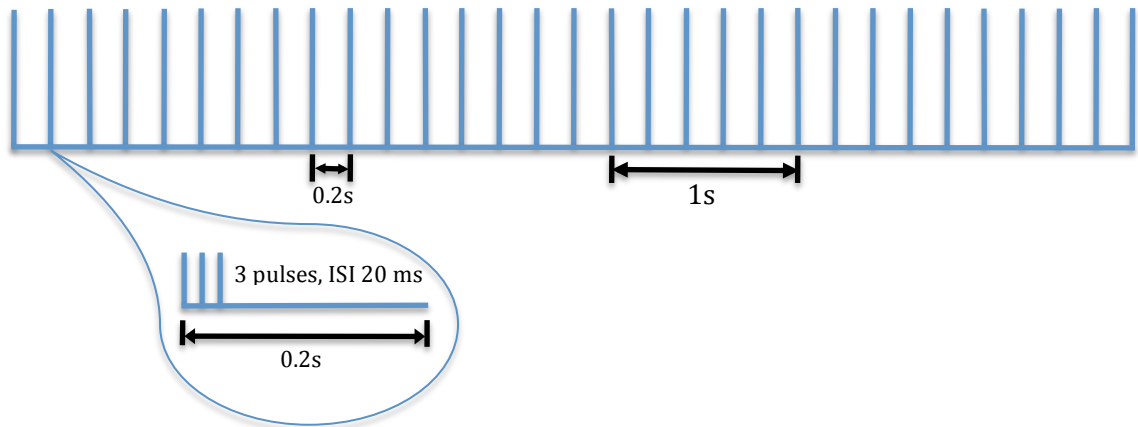


Figure 2-7 Continuous theta-burst stimulation showing bursts of three pulses of 50Hz (20ms) repeated at intervals of 5Hz (200ms) for the duration of either 20s or 40s.

The stimulation design of theta-burst protocol is analogous to the paradigms used to generate plasticity in the animal hippocampus (Cardenas-Morales et al., 2010; Hoogendam et al., 2010; Huerta & Volpe, 2009). This similarity suggests that the TBS-induced cortical excitability emulates the mechanisms of LTP and LTD of synaptic efficacy, the main mechanisms of memory in the brain (Cardenas-Morales et al., 2010; Huang et al., 2011; Huerta & Volpe, 2009). An important fact is that the stimulus intensity of TBS (80% AMT) is subthreshold for the activation of the descending pathways. This low intensity indicates that TBS-induced aftereffects are likely to be generated only at the cortical level (Paulus, 2005). This fact was verified by Di Lazzaro and colleagues (2005), who recorded the corticospinal volleys induced by single-pulse TMS over M1 before and after a 20s period of cTBS in patients of cervical spinal surgery (Di Lazzaro et al., 2005). The amplitude of the corticospinal I1-wave is decreased post cTBS, with approximately the same duration as the MEP size (Di Lazzaro et al., 2005). This result emphasises a cortical origin of

cTBS and LTD-like plasticity mechanism that drives the cTBS suppression of MEPs (Di Lazzaro et al., 2008; Di Lazzaro et al., 2005).

In the present thesis, simple rTMS protocols of low frequency (rTMS 1Hz), high frequency (rTMS 5Hz and 10Hz), and pattern protocol of cTBS were used to elicit the plasticity changes in cortical excitability.

2.2.3 Safety of rTMS

Single-pulse TMS is safe if used with precautions (Wassermann et al., 1996). However, the protocols of rTMS have been reported to induce side effects such as epileptic seizures, pain or headache (Rossi et al., 2009). In order to prevent the risk of induced seizures—a major adverse effect during rTMS experiments—safety guidelines have been established (Rossi et al., 2009; Wassermann et al., 1996). The guidelines specify the maximum limits of stimulation parameters such as frequency, intensity, and duration of stimulation; as well as contra-indications to rTMS such as implanted brain stimulators (Rossi et al., 2009; Wassermann et al., 1996). If followed strictly, the risk of inducing seizure in rTMS interventions is negligible (Oberman et al., 2011; Rossi et al., 2009).

At present there is only one reported case of TBS-induced seizure—the most serious adverse event after repetitive magnetic stimulation (Oberman & Pascual-Leone, 2009). The one reported case involved a 33-year-old healthy man with no risk factors for epilepsy. The seizure occurred after 50 trains (10s) of TBS to the M1 at an intensity of 100% RMT (Oberman & Pascual-Leone, 2009). In a recent meta-analysis of 4500 TBS sessions involving 776 healthy

participants and 225 clinical patients, seizure has only been reported once (Oberman et al., 2011). The risk of seizure after TBS is only 0.02% as compared to other high frequency rTMS protocols where seizures have been reported in approximately 0.1% of patients (Oberman et al., 2011). The lower stimulation intensity and the shorter duration of stimulation in TBS protocols may contribute to a reduced risk of seizure despite the delivery of high frequency bursts (Oberman et al., 2011; Oberman & Pascual-Leone, 2009). The most typically manifested side effects are transient headache and neck pain, similarly experienced in other rTMS protocols, and were reported in less than 3% of the TBS participants (Oberman et al., 2011) as compared to approximately 40% in other high frequency rTMS protocols (Rossi et al., 2009). The TBS single-pulse paradigm is also safe and well tolerated in children (Wu, Shahana, Huddleston, Lewis, & Gilbert, 2012).

2.2.4 Modulation of cortical oscillations by rTMS

The first study that demonstrated the ability of magnetic stimulation to modulate cortical oscillatory activity was by Paus *et al.* (2001). The authors delivered single-pulse TMS over the sensorimotor cortex at rest and showed increased synchronisation of β band (15-30 Hz) that lasted for several hundred milliseconds (Paus et al., 2001). They suggested that the magnetic pulse was able to stimulate the previously “idling” cortical neurons to begin to oscillate depending on the stimulus intensity (Paus et al., 2001). This brief increase of synchronisation reflects the ability of TMS to induce the resetting of oscillations in a “resting” brain (Paus et al., 2001).

A follow-up study by Fuggetta *et al.* (2005) showed that single-pulse TMS applied over M1 at rest induced synchronisation in the α and β band for 500ms post magnetic stimulation, and increased linearly with stimulus intensity (Fuggetta *et al.*, 2005). As Paus *et al.* (2001) previously, the authors concluded that the TMS-induced oscillations were linked to the resetting of the cortical oscillators (Fuggetta *et al.*, 2005; Paus *et al.*, 2001), instead of the “idling” state of the brain (Pfurtscheller, Stancak, & Neuper, 1996a, 1996b).

The resetting phenomenon might occur in cortical networks (Destexhe, Contreras, & Steriade, 1999) or may be propelled by the thalamic pacemaker (Steriade, 2006). In 2006, Van Der Werf and Paus investigated the oscillatory activity of patients with Parkinson’s disease who underwent partial thalamotomy—unilateral surgery of the ventrolateral nucleus of the thalamus (Van Der Werf, Sadikot, Strafella, & Paus, 2006). Applying TMS over the intact hemisphere, the authors observed higher synchronisation of β frequency band in the unoperated hemisphere (with the thalamus intact) than in the operated hemisphere (with thalamotomy) (Van Der Werf *et al.*, 2006). This result implies the role of the thalamus in generating cortical oscillatory activity through various cortico-cortical networks and cortico-thalamic feedback loops (Van Der Werf & Paus, 2006; Van Der Werf *et al.*, 2006). However, the oscillating properties depend on the connectivity of different pacemakers and the modulation of the reticular system, which is interconnected with all the thalamic nuclei (Llinas & Steriade, 2006).

Besides thalamus, basal ganglia have an important role in driving oscillatory activity in the human motor cortex during motor performance (Joundi et al., 2012). Using TMS, it has been shown that beta frequencies is prominent during tonic contraction but is attenuated prior to and during voluntary movement (Brown, 2003; Joundi et al., 2012). In Parkinson's disease, the alterations of basal ganglia physiology may involve the alteration in the pattern of neuronal synchronisation particularly involving beta brain rhythms (Brown, 2003). The level of beta synchronisation is in turn modulated by net dopamine levels at sites of cortical input to basal ganglia (Jenkinson & Brown, 2011). Dopamine deficiency as in the case of Parkinson's disease will disrupt the cortico-basal ganglia-thalamocortical circuits, leading to pathologically exaggerated beta oscillations (Moran et al., 2011).

In recent years there has been a growing interest in the cortical oscillatory activity at "rest" as an index of the internal state of the brain (Stamoulis, Oberman, Praeg, Bashir, & Pascual-Leone, 2011; Thut & Miniussi, 2009). The term "rest" represents the cortex during behaviourally silent states, with the absence of any sensory or motor output (Thut & Miniussi, 2009). The properties of neuronal oscillatory brain rhythms in a resting brain can provide the baseline for researchers and clinicians in distinguishing the oscillatory patterns that may be disrupted in patients of various neuropsychiatric disorders (Rogasch & Fitzgerald, 2012; Shafi et al., 2012; Ziemann, 2011).

However, only few studies have examined the potential use of rTMS to transiently modulate brain rhythms over M1 at "rest". These studies have shown

that the response of the EEG oscillatory state of the sensorimotor cortex at “rest” depends on TMS intensity, frequency of magnetic stimulation, and the total number of magnetic pulses (Fuggetta et al., 2005; Fuggetta et al., 2008; Sauseng et al., 2009; Van Der Werf & Paus, 2006). Strens *et al.* (2002) applied a train of 1500 pulses of 1Hz rTMS for 25 minutes over M1 at a subthreshold intensity (Strens et al., 2002). They demonstrated a decrease in EEG power of α frequency band of 6% and a focal increase of coherence during active task compared to resting condition ipsilateral to the site of stimulation (Strens et al., 2002). A follow up study by Oliviero *et al.* (2003) used a short train of 50 pulses of high frequency 5Hz rTMS over M1 at active motor threshold (Oliviero, Strens, Di Lazzaro, Tonali, & Brown, 2003). They showed a significant decrease in cortico-cortical interhemispheric coherence in the upper α frequency band (10.7-13.6Hz) between the motor and premotor cortex for a few minutes after magnetic stimulation (Oliviero et al., 2003).

In an online rTMS-EEG study, Fuggetta *et al.* (2008) used spectral analysis of event-related power (ERPow) and event-related coherence (ERCoh) to reveal how intermittent short trains of high frequency (5Hz) rTMS delivered over left M1 induced an ERPow increase in upper α (10-12Hz) and β (18-22Hz) frequency ranges for threshold (100% RMT) and subthreshold intensities (80% RMT) (Fuggetta et al., 2008). ERCoh showed a decrease in functional coupling for subthreshold rTMS in α and threshold rTMS for β band (Fuggetta et al., 2008). However, the aftereffect of rTMS in this experiment was short lasting—confined to 500ms after the magnetic stimulation—with no effect found 2s after

the train of magnetic pulses (Fuggetta et al., 2008). The topography of the brain rhythms was maximal over the stimulated cortex and spread to the parietal region (Fuggetta et al., 2008).

Another on-line rTMS-EEG study by Brignani *et al.* (2008) explored the immediate effects of low frequency 1Hz rTMS on the ongoing cortical oscillatory activity at “rest” (Brignani et al., 2008). They delivered 1Hz rTMS over M1 at 110% AMT of 600 stimuli divided into three blocks of stimulation (block I: 0-3.33-min, block II: 3.34-6.66-min, block III: 6.67-10.0-min). They showed a simultaneous increase of synchronisation of α (8-12Hz) more than β (12-30Hz) across all three stimulation blocks, which was inversely correlated with the progressive decrease of MEP amplitude (Brignani et al., 2008). The topography of β was focally restricted over central electrodes, but the topographical distribution of α differed, starting at the central region and then spreading to ipsilateral parietal sites (Brignani et al., 2008).

A recent study by Veniero *et al.* (2011) investigated the effects of the ongoing oscillatory activity of M1 at rest after high frequency 20Hz rTMS (Veniero et al., 2011). Using the same analysis approach of EEG ERPow and ERCoh with previous studies (Brignani et al., 2008; Fuggetta et al., 2008), they observed increased synchronisation in α (8-12Hz) more than β (13-30Hz), and α induction lasted for 5-min after magnetic stimulation (Veniero et al., 2011). They showed a dose dependent increase of synchronisation in both the α and β activities, spreading from the central region to the posterior, parietal sites (Veniero et al., 2011).

In most TMS studies involving humans, low and high stimulation frequencies often result in opposite physiological effects as index by MEPs, expressed as either an increase or decrease in the amplitude of MEPs (Chen, 2000; Fitzgerald et al., 2006). Low frequency (≤ 1 Hz) decreases cortical excitability (MEPs suppression) whereas high frequency stimulation (≥ 1 Hz) increases cortical excitability (MEPs enhancement) (Chen, 2000; Fitzgerald et al., 2006). However, rTMS-EEG studies of low and high frequency protocols (Brignani et al., 2008; Fuggetta et al., 2008; Veniero et al., 2011) were not able to emulate the classical dichotomy between low versus high frequency rTMS of MEPs measurements. Instead, they observed linear EEG synchronisation for both low and high frequency rTMS in both α and β frequency bands (Brignani et al., 2008; Fuggetta et al., 2008; Veniero et al., 2011).

The inability of rTMS-EEG to distinguish the opposite effect of low versus high frequency at the cortical level may be because α and β frequency bands are not the best index to reflect the dichotomy between low versus high frequency (Veniero et al., 2011). A differential effect of low-high frequency rTMS may be better demonstrated by the modulation of other brain rhythms such as θ or γ (Veniero et al., 2011). The reason why majority of rTMS-EEG studies of the motor cortex concentrated on the modulation of α and β brain rhythms is because these two frequencies are dominant over the motor cortex (Sauseng & Klimesch, 2008; Thut & Miniussi, 2009). However, explorations of other frequency brain rhythms are also important as shown by altered low frequency

brain rhythms such as θ oscillations in thalamocortical dysrhythmia syndrome (Llinas & Ribary, 2001; Llinas et al., 1999; Schulman et al., 2011).

In order to fill in the gap in the knowledge of rTMS modulation of low frequency oscillations, our present investigations evaluated the effects of different rTMS frequencies on cortical oscillations—low frequency (1Hz) versus high frequency (5Hz and 10Hz) rTMS over M1—and extended the EEG frequency analysis to include low frequency oscillations of δ and θ , as well as α and β frequency bands. We explored the possible changes of EEG oscillations between repetitive stimuli up to 20 seconds after each train of stimulation to verify the presence of short-term modulatory effect of cortical oscillations by short-train of rTMS. Besides looking at the differential effects of the frequencies of magnetic stimulation, investigations of the different effects of the total number of pulses during short (rTMS 20 pulses) and longer trains (rTMS 60 pulses) were made to observe the presence of cortical and network oscillatory activity associated with repetitive stimulation. On-line evaluation of EEG responses to cortical oscillatory activity by means of ERPow and ERCoh transformations, which reflect the regional neural activity and the inter-regional functional coupling between cortical areas were performed along with behavioural measurements of MEPs.

2.2.5 Cortical plasticity induced by rTMS

The hypotheses that suggest a link between the residual effects of rTMS and plasticity is due to the ability of rTMS to induce changes that outlast the period of stimulation (Chen & Udupa, 2009; Cohen et al., 1998; Hoogendam et al.,

2010; Pascual-Leone et al., 2011). This lasting modulation has been demonstrated in rTMS studies of the motor system using MEPs as index of cortical excitability (Fitzgerald et al., 2006; O'Shea & Walsh, 2007; Peinemann et al., 2000; Quartarone et al., 2005).

The residual effects of rTMS are thought to originate from synaptic plasticity because its effects tend to emulate the patterns of synaptic plasticity in the rodent hippocampus (Huerta & Volpe, 2009; Pell et al., 2011). The long-term changes in the strength of hippocampal synapses involve the mechanisms of LTP and LTD (Bear & Malenka, 1994; Malenka, 1994; Malenka & Bear, 2004). LTP and LTD describe the direction of a long-lasting change in synaptic strength (Malenka & Bear, 2004). LTP is an increase in the synaptic efficacy that could last for hours, days or weeks following brief high-frequency stimulation (HFS) protocols (Malenka & Bear, 2004). The HFS paradigm in animal experiments that can induce LTP in the hippocampus is a protocol that consists of a single train of 100Hz for 1s (100 pulses with 10ms intervals) (Cooke & Bliss, 2006; Huerta & Volpe, 2009). Another HFS protocol is theta-burst stimulation that consists of 10 bursts (each burst is 4 pulses at 100Hz) that are separated by an interval of 200ms (Larson, Wong, & Lynch, 1986). LTD is the long lasting weakening of the strength of hippocampal synapses following low-frequency stimulation (LFS) (Malenka & Bear, 2004). The most frequent LFS protocol is a single train of 1Hz for 10-min (600 pulses) or for 15-min (900 pulses) (Malenka & Bear, 2004).

The cellular basis of LTP and LTD originates from the hippocampal synapses of the axons of CA3 neurons and the dendritic spines of CA1 pyramidal neurons (Bear & Malenka, 1994; Crochet, Fuentealba, Cisse, Timofeev, & Steriade, 2006; Malenka, 1994). The CA3 axon terminals discharge glutamate while the CA1 neurons express three types of glutamatergic receptors: alpha-amino-3-hydroxy-5-methyl-4-isoxazolepropionic acid receptor (AMPA-R), N-methyl-D-aspartate receptor (NMDA-R), and metabotropic glutamate receptor (mGluR) (Cooke & Bliss, 2006). The induction of LTP depends on the influx of Ca^{2+} in the postsynaptic cell (Cooke & Bliss, 2006). It starts when glutamate binds to AMPA-R, allowing Na^+ to enter into the dendritic spine, resulting in membrane depolarisation (Cooke & Bliss, 2006). When the postsynaptic neuron is sufficiently depolarised, the Mg^{2+} ions that block the NMDA-R at resting membrane potential will be removed, thus opening the NMDA-R. As a result, Ca^{2+} enters the postsynaptic neuron, and activates calcium-sensitive signaling pathways such as calcium-calmodulin protein kinase II (CaMKII) that leads to phosphorylation and upregulation of the AMPA-R (Crochet et al., 2006; Duffau, 2006). HFS protocols during experimental stimulations are able to remove the Mg^{2+} block of the NMDA-R, probably because HFS activates many AMPA-R, thus eliciting a large depolarisation in the dendritic spine (Malenka, 2003).

The mechanism of LTD induction also depends on NMDA-R activation, which elevates Ca^{2+} concentration postsynaptically (Malenka & Bear, 2004). The element that determines whether LTP or LTD is induced is the nature of the

Ca^{2+} signal that activates specific pathways (Malenka & Bear, 2004). Large and fast elevation of Ca^{2+} concentration induces LTP by activating CaMKII, whereas small and slow rises of Ca^{2+} induce LTD by activating protein phosphatases that leads to dephosphorylation and down-regulation of the AMPA-R (Malenka & Bear, 2004). LTD can be induced by LFS protocols that will mildly stimulate NMDA-R and produce an intermediate elevation of Ca^{2+} concentration (Malenka & Bear, 2004).

Direct insight into the link between rTMS effects and synaptic plasticity has come from animal studies as cellular and molecular changes in synaptic plasticity can be investigated directly using brain slices of animals (Hoogendam et al., 2010). Ogiue-Ikeda *et al.* (2003) stimulated the rat hippocampus using HFS protocol of rTMS 25Hz at 0.75 Tesla and showed enhance LTP, whilst the same HFS at intensity of 1.25 Tesla depressed LTP for 10-60 minutes after stimulation (Ogiue-Ikeda, Kawato, & Ueno, 2003).

Several studies have attempted to extend the principles of synaptic plasticity in the animal investigations to the rTMS alterations of human cortical excitability (Di Lazzaro, Ziemann, et al., 2008; Hoogendam et al., 2010; Pascual-Leone et al., 2011). M1 has been the most investigated cortical region with regards to TMS-induced plasticity (Pascual-Leone et al., 2011). The studies highlight the success of rTMS protocols in emulating the induction paradigms for LTP and LTD by changes in MEP sizes that outlast the TMS application. One rTMS protocols that is able to produce long-term changes that emulate the protocols used for inducing LTP and LTD in rodent preparations is

TBS. Huang *et al.* (2005) showed that two TBS modalities have opposite effects on motor cortex excitability reminiscent of LTP and LTD (Huang *et al.*, 2005). The iTBS of 600 pulses at 80% AMT produce a facilitatory effect for 15-min, whereas cTBS of 300 or 600 pulses suppress MEP amplitude for 20 or 60-min, respectively (Huang *et al.*, 2005). Other studies of iTBS (Agostino *et al.*, 2008; Iezzi *et al.*, 2008; Zafar *et al.*, 2008) and cTBS (Huang, Chen, Rothwell, & Wen, 2007; Iezzi *et al.*, 2008; Suppa, Ortu, *et al.*, 2008; Trippe, Mix, Aydin-Abidin, Funke, & Benali, 2009; Zafar *et al.*, 2008) showed similar results.

The application of conventional 1Hz rTMS with a longer stimulation train was also shown to induce MEP suppression for a longer duration. Touge *et al.* (2001) demonstrated that rTMS 1Hz of 95% RMT applied for 25-min (1500 pulses) depressed MEP size for approximately 30-min (Touge *et al.*, 2001). Other rTMS 1Hz studies by O'Shea *et al.* (2007) of 900 pulses at 90% AMT and Suppa *et al.* (2008) of 1500 pulses suppressed MEP for 15 and 30-min, respectively (O'Shea & Walsh, 2007; Suppa, Bologna, *et al.*, 2008). These results are in line with the LTD studies in rodents. In contrast, HFS protocols of rTMS 5Hz and 10Hz increased MEP amplitude and emulated the pattern of LTP in rodent hippocampus. Peinemann *et al.* (2004) demonstrated that 5Hz rTMS of 1800 pulses at 90% RMT increased MEP for more than 40-min (Peinemann *et al.*, 2004). Using rTMS 10Hz at 80% RMT of 300 pulses, Jung *et al.* (2008) demonstrated an elevation of MEP amplitude for up to 120-min (Jung, Shin, Jeong, & Shin, 2008).

Several pharmacological studies of TBS in the human cortex revealed that NMDA receptors seem to have parallel roles in the plasticity of cortical synapses as in the hippocampus. In a double-blind placebo-control study, Huang *et al.* (2007) investigated the residual effects of TBS by prescribing the NMDA-R antagonist memantine and measuring the MEP size (Huang *et al.*, 2007). The authors discovered that memantine blocked both the facilitatory effect of iTBS and the suppressive effect of cTBS as shown in the difference of the MEP size compared to control (Huang *et al.*, 2007). Teo *et al.* (2007) showed that by giving NMDA-R coagonist D-cycloserine, the effect of iTBS was altered from facilitation to inhibition (Teo, Swayne, & Rothwell, 2007). Both pharmacological studies indicate that TBS influences NMDA receptor activity in humans and thus provide evidence of the involvement of rTMS in neuroplasticity (Huang *et al.*, 2007; Teo *et al.*, 2007).

Although the modulatory changes in cortical efficacy by rTMS seem to emulate the paradigms of synaptic plasticity, it is important to emphasize the difference between the plasticity studies of the animal hippocampus and rTMS studies of the cerebral cortex (Pell *et al.*, 2011). The excitation of neural tissue in animal studies of synaptic plasticity and rTMS studies in humans is fundamentally different (Hoogendam *et al.*, 2010). The stimulation of hippocampal slices in LTP/LTD studies is focal, whereas rTMS stimulation has a larger spatial resolution ranging from mm² to cm² (Hoogendam *et al.*, 2010). Moreover, the brain region stimulated by rTMS in human studies is the cerebral cortex, which has a structurally more complex network than the hippocampal

circuits. Cortical neurons are placed in multi-layered arrangements (the canonical six layers), with abundant synaptic connections. Cortical neurons receive massive inputs from the thalamus and, in turn, project heavily to the same structure (Steriade, 2001). Therefore, this suggests that rTMS may affect the vast recursive loops of excitation and inhibition between the cortex and the thalamus, between the different areas of the cortex, and including loops of both cerebral hemispheres (Hoogendam et al., 2010).

Moreover, the majority of rTMS-induced plasticity studies in humans used MEP amplitudes, which represent an indirect index of plasticity at the neuronal level (Pell et al., 2011). In addition, MEP is a polysynaptic read-out, separated by at least three synapses from the TMS source (Huerta & Volpe, 2009; Siebner & Rothwell, 2003), whereas LTP and LTD are monosynaptic events (Malenka & Bear, 2004). Therefore, in order to obtain a more accurate interpretation, it is important to combine rTMS with a recording technique that is also linked by a single synapse to the TMS pulse (Huerta & Volpe, 2009). One such technique is high-density EEG, which can provide a monosynaptic cortical readout during and after magnetic stimulation (Maki & Ilmoniemi, 2010). Taking this into account, the present thesis moves beyond MEPs and proposes another sensitive measure of EEG for finding evidence of plasticity-like mechanism induced by rTMS.

Previous studies of combined rTMS-EEG have demonstrated the ability of EEG to record cortical output even at subthreshold intensities, when there is no apparent muscular activity (Komssi & Kahkonen, 2006). At a subthreshold

intensity of 60% of individual motor threshold (MT), clear EEG waveforms are seen after magnetic stimulation (Komssi, Kahkonen, & Ilmoniemi, 2004). Even fMRI through BOLD could not detect any changes in brain activity when TMS was delivered at an intensity of 80% of MT (Bohning et al., 1999; Nahas et al., 2001). These findings indicate that EEG is a sensitive and robust method for the assessment of cortical excitability induced by rTMS (Thut & Pascual-Leone, 2010b). In one of the experiment in the present thesis, we assessed the long-lasting modulation of cortical excitability after cTBS—a long-lasting TBS protocol that mimics LTD—using both measurements of EEG and MEPs.

Studies that combined TBS and EEG to investigate the effect of cortical excitability induced by magnetic stimulation are lacking (Cardenas-Morales et al., 2010; Schindler et al., 2008). A study that examined EEG network oscillations post-cTBS of 600 pulses was performed on the frontal eye field of only four healthy subjects (Schindler et al., 2008). The study demonstrated higher neuronal synchronisation of the cerebral hemisphere ipsilateral to the stimulation site relative to the non-stimulated hemisphere up to one hour with synchronisation computed for broadband EEG and frequency bands of δ , θ , α , β , and γ (Schindler et al., 2008). The authors speculated that cTBS might interfere with information transfer through its effect on neuronal synchronisation (Schindler et al., 2008). However, in their study, there was no direct comparison between surface EEG and behavioural measurements during rest and active conditions to look at post-cTBS cortical plasticity effects. Moreover, the authors changed the site of stimulation (frontal eye field instead of motor cortex), the

stimulation intensity (80% RMT instead of 80% AMT), and modified the cTBS paradigm (30 Hz bursts repeated at 6 Hz) from the original cTBS protocol introduced by Huang *et al.* (2005), making direct comparison with the original protocol problematic.

Recently, McAllister *et al.* (2011) investigated the modulation of cortical oscillatory activity by cTBS of 600 pulses after a visuomotor training task using both MEP and EEG measurements (McAllister, Rothwell, & Ridding, 2011). The authors did not find any significant results for the baseline power of δ , θ , α or β , but found significant α power that was positively correlated with MEP after the visuomotor training (McAllister *et al.*, 2011). They concluded that EEG was not useful as an index of cortical output to plasticity-inducing paradigms such as cTBS (McAllister *et al.*, 2011). However, in that study, the EEG was recorded using a single electrode of C3 over the motor cortex, and was therefore unable to ascertain the possible cTBS effects on cortico-cortical coupling. An investigation using multi-channel EEG will provide a more thorough outlook on the effects of cTBS on the motor network excitability. Therefore, in the subsequent experiment, we addressed the lack of knowledge of cTBS effects on motor network oscillations and their correlation with behavioural measurements by applying the original cTBS protocol (Huang *et al.*, 2005) consisting of 100 bursts of three pulses (300 pulses) at 50Hz repeated every 200ms (5Hz) in 13 healthy subjects and measured the EEG oscillatory properties using high-density multi-channel EEG.

In order to demonstrate how the present work in the thesis relates to the literature, table 2.1 summarises the studies on rTMS and resting EEG that led to the present investigations.

Table 2.1 rTMS and EEG at rest

rTMS Protocol	Study	Site	Intensity	Number of pulses	EEG measures	Notes
rTMS 1Hz	Strens et al. 2002	M1	90% AMT	1500	ERCoh α	Increase corticocortical & interhemispheric coherence in α for 25-min
TMS 5Hz	Oliviero et al. 2003	M1	90% AMT	50	ERCoh α	Decrease ipsilateral corticocortical intrahemispheric coherence in upper α
rTMS 1Hz	Brignani et al. 2008	M1	110% RMT	600	ERD/ERS, ERPow for α and β	Increase ERPow α for 10-min, inversely correlated with MEPs
rTMS 5Hz	Fuggetta et al. 2008	M1	80% vs. 100% RMT	400	ERD/ERS, ERPow and ERCoh upper α and β	Increase ERPow $\alpha > \beta$, $>$ in threshold, Decrease ERCoh, effect $< 2s$
rTMS 20Hz	Veniero et al. 2011	M1	100% RMT	400	ERD/ERS, ERPow α and β	Dose dependent increase ERPow $\alpha > \beta$ for 5-min, inversely correlated with MEPs
rTMS 11Hz	Experiment 1	M1	100% RMT	400 vs. 1200	ERD/ERS, ERPow and ERCoh θ, μ and β	EEG at rest for 60s, MEPs at rest
rTMS 1Hz, 5Hz, 10Hz	Experiment 2	M1	100% RMT	400	ERD/ERS, ERPow and ERCoh δ, θ, μ and β	EEG at rest for 20s
cTBS	Schindler et al. 2008	FEF	80% AMT	600 (3 pulses at 30Hz, repeated every 100ms)	Spectral power δ , θ , α , β , γ for 60-min	EEG synchronisation for stimulated hemisphere relative to non-stimulated hemisphere for all frequency bands
cTBS	McAllister et al. 2011	M1	80% AMT	600 (3 pulses at 50Hz, repeated every 200ms) for 40s	Spectral power for baseline δ , θ , α , β and after visuo-training task	No increase EEG synchronisation at rest, MEPs suppression, increase EEG power α after visuomotor training task
cTBS	Experiment 3	M1	80% AMT	300 (3 pulses at 50Hz, repeated every 200ms) for 20s	ERD/ERS, ERPow and ERCoh θ, α, low β, high β at rest and active; MEPs at rest; RT active	EEG at rest, EEG active for 30-min, MEPs at rest, RT active

2.3 Electroencephalography

This section begins with a brief explanation of the principles of EEG, the classical method of recording brain rhythms. Next, it introduces the EEG brain rhythms, their generation and functional significance. The discussion on the EEG data acquisition and analysis will be presented in the following chapter on methods.

2.3.1 Principles of EEG

EEG helps us to understand the activity of the cerebral cortex by measuring the generalised electrical activity of a large population of cortical neurons (Schoffelen & Gross, 2009). In 1929, Hans Berger (1873-1941), a German neuropsychiatrist, measured the first EEG on the human scalp using ordinary radio equipment to amplify the brain's electrical activity. In the defining experiment, Berger demonstrated that weak electrical current generated in the cortex could be recorded non-invasively over the human scalp (Berger, 1969). He observed the transformation of the brain electrical activity as the functional states of the subject changes, such as from relaxation to alertness (Berger, 1969). Berger introduced the word "electroencephalogram" to describe the electrical activity of the brain recorded from the human scalp. However, in modern times, the term EEG also applies to the electrical activity generated by brain structures as measured directly from the cortical surface (electrocorticogram), or within the brain using depth electrodes both in humans and in animals (da Silva, Gomez, Velis, & Kalitzin, 2005; Niedermeyer, 2003). In this thesis, we refer only to the EEG recorded from the surface of the scalp.

In spite of the emergence of modern functional neuroimaging such as PET and fMRI, which are able to assess the functional states of the brain, the scalp EEG is still considered as an important research and diagnostic tool in neuroscience (Miniussi & Thut, 2010; Rogasch & Fitzgerald, 2012; Thut & Pascual-Leone, 2010a). The advantage of scalp EEG over functional neuroimaging is its high temporal resolution of less than a millisecond, which enables real-time brain behavioural analysis (Maki & Ilmoniemi, 2010; Niedermeyer, 2003; Taylor et al., 2008). Moreover, EEG can directly record brain electrical activity, it is relatively inexpensive, and is simple to record (Maki & Ilmoniemi, 2010; Niedermeyer, 2003; Taylor et al., 2008).

The ionic current (such as Na^+ , K^+ , Ca^{2+} , and Cl^-) in the neurons generates electric and magnetic fields recordable on the scalp surface by the EEG or MEG (da Silva et al., 2005; Harmony et al., 1999; Niedermeyer, 2003). The EEG signal does not come from action potentials of the cortical neurons but from the electrical potentials of the pyramidal dendrites of the cortex. The electrical potentials are generated by the summed inhibitory and excitatory postsynaptic potentials (PSP) from the pyramidal neurons of the cerebral cortex that produce electrical dipoles between the soma and the apical dendrites (Rogasch & Fitzgerald, 2012; Schoffelen & Gross, 2009). These PSP summate in the cortex and are recorded as the EEG on the scalp surface (Figure 2-8) (Freeman, 2005). The pyramidal neuron—the predominant neuron in the cortex—is responsible for most of the electrical activity measured by EEG. It has a long straight dendrite that lies right under the skull and makes up 80% of

the brain's mass. Therefore, most neurons in the cerebral cortex have parallel dendrites causing summation of PSP in one direction (Freeman, 2004a; Niedermeyer, 2003). Additionally, other interconnected neurons that share the same presynaptic sources will generate a synchrony of potentials that can form a macroscopic source of the EEG signal (Freeman, 2004a; Niedermeyer, 2003). The synchronous inputs of a large population of neurons make EEG a sensitive tool to study interaction between cortical areas and the functional connectivity of cortical networks (Sauseng & Klimesch, 2008; Shafi et al., 2012).

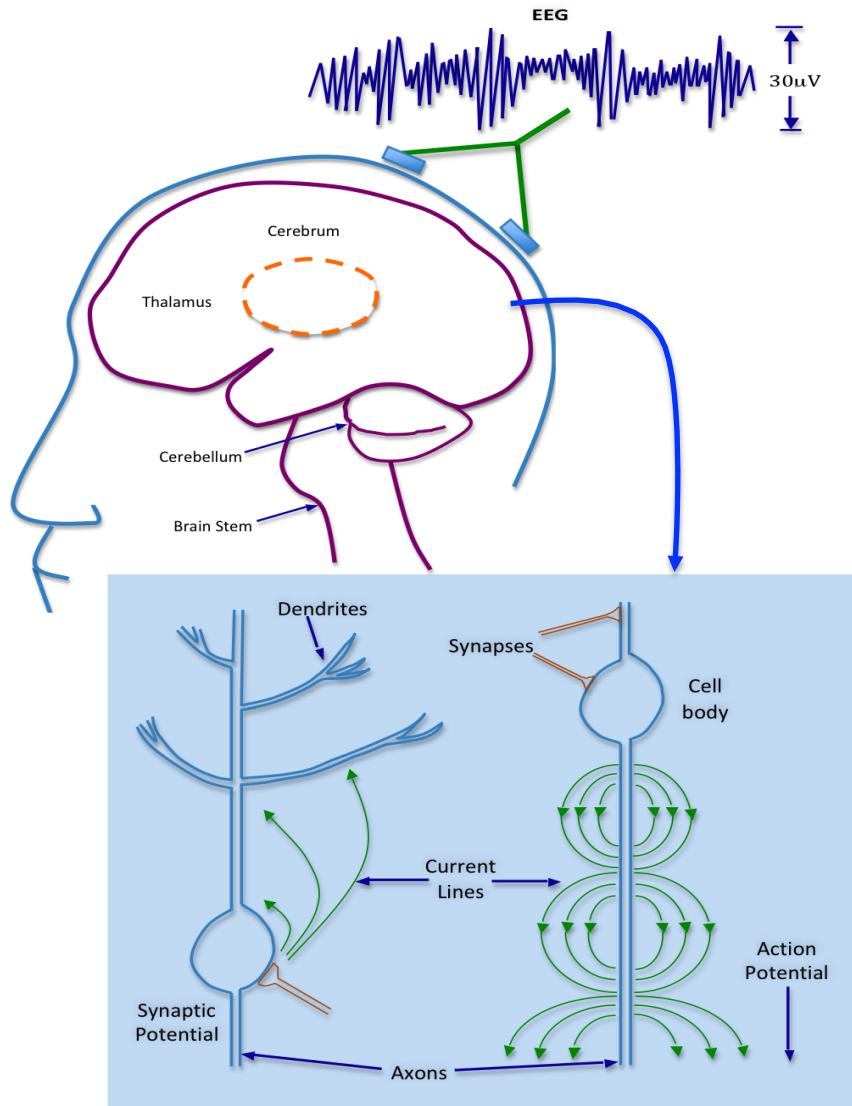


Figure 2-8 EEG scalp potentials. EEG signal is the sum of postsynaptic potentials from the pyramidal neurons of the cerebral cortex. Adapted with permission from Nunez, P. L., & Srinivasan, R. (2006). *Electric fields of the brain: The Neurophysics of EEG*: Oxford University Press.

The amplitude of the EEG signal depends largely on the synchronous activity of the underlying neurons (Freeman, 2004a). If a population of pyramidal neurons is stimulated within a narrow time window, the neurons are

synchronised, and the summed activity detected by the EEG is large (Sauseng & Klimesch, 2008). However, if the pyramidal neurons are stimulated at irregular intervals, the neurons are not synchronised, and the resulting EEG is small (Sauseng & Klimesch, 2008). The number of activated neurons and the amount of stimulation may be similar, but the timing of activity will determine the resulting amplitude of the EEG signal (Freeman, 2004a). Nevertheless, it is important to emphasise that it takes many thousands of interconnected neurons, activated together, to generate an EEG signal large enough to be recorded at the scalp (Rogasch & Fitzgerald, 2012).

In summary, to record the electrical activity of any populations of neurons, several characteristics of synaptic organisation of the local circuits and the synchrony of the incoming signals must be fulfilled; the neuronal dendrites should be aligned in parallels; the generation of the electrical potentials by the neurons must be oriented perpendicular to the scalp; the neurons are interconnected by feedback loops of excitatory and inhibitory synapses; and the neurons must fire in near synchrony (Basar, Basar-Eroglu, Karakas, & Schurmann, 1999). All these characteristics, in combination with the intrinsic oscillatory properties of the neuronal populations, are responsible for the generation of brain rhythms—the oscillatory phenomena of EEG (Sauseng & Klimesch, 2008).

2.3.2 Event-related potential

This subsection introduces the characteristics of EEG waveforms. ERP is one of the EEG signal properties that are widely used in neuroscience research.

Evoked or Event-related potential is the electrical response in the EEG to a specific “event” or stimulus (Gevins, Morgan, Bressler, Doyle, & Cutillo, 1986). It is time- locked and phase-locked (evoked) to the ongoing electrical activity of the cortex (Pfurtscheller & Lopes da Silva, 1999). The amplitude of ERP is low and cannot be distinguished during routine EEG recordings. However, the ERP components can be elicited with the use of computer signal-averaging techniques that average the time-locked EEG epochs to sensory, cognitive or motor stimuli (Nunez, 1989, 1996). Here, the ERP is assumed to have a fixed time delay to the stimulus, whereas the background EEG activity is random. By averaging out the random background EEG activity, the signal (ERP) -to-noise (background EEG activity) ratio is increased (Light et al., 2010). Therefore, the ERP reflects the changes of neural activity evoked by a stimulus, with high temporal resolution (Light et al., 2010). As a research tool, ERPs can provide the precise time course and cortical distribution of electrical potentials during cognitive processes, and can be used as a direct index of cortical excitability (Light et al., 2010). In the present thesis, analysis of the EEG data was performed in the frequency-domain, not in the time-domain. This is because in the present thesis the EEG oscillations are not used to measure cortical excitability, but as index of network interactions possibly correlating with excitability changes as measured by MEPs.

An averaged ERP waveform consists of several deflections. The TMS-evoked waveform produced by single-pulse TMS at M1 consists of positive waves peaking at 30ms (P30) and 60ms (P60), and negative waves peaking at

45ms (N45) and 100ms (N100) (Paus, Sipila, et al., 2001). The generations of these waveforms are triggered by different mechanisms (Paus, Sipila, et al., 2001). For example, the amplitude of the negative wave N45 correlates with the intensity of magnetic stimulation (Paus, Sipila, et al., 2001), and N100 reflects the inhibitory mechanisms in the cortex (Light et al., 2010).

2.3.3 Cortical oscillations

This subsection is an introduction to the concept of the synchronous oscillatory EEG activity of the brain rhythms. A population of neurons that are strongly interconnected will generate rhythmic, synchronised oscillations by either taking cues from a central clock, or pacemaker; or by the collective behaviour of the cortical neurons through exciting or inhibiting one another (Basar, Demiralp, Schurmann, Basar-Eroglu, & Ademoglu, 1999; Buzsaki & Draguhn, 2004; Sauseng & Klimesch, 2008).

The thalamus, with its complex excitatory and inhibitory feedback loops to the cerebral cortex, can be a powerful pacemaker (Sherman, 2007; Sherman & Guillery, 2002). It can generate rhythmic, self-sustaining action potential discharges even without external stimuli to the thalamic cell, and then becomes synchronised with other thalamic cells through collective, cooperative interactions (Sherman, 2007; Sherman & Guillery, 2002). The collective behaviour of the excitatory and inhibitory interconnections of the thalamic neurons will influence each other to conform to the rhythm of the group. The resulting rhythmic, synchronous pattern of activity will be carried by the thalamocortical axons to the cerebral cortex (Steriade, 2001; Timofeev, 2011).

Therefore, with this mechanism, a small number of thalamic cells are able to influence larger regions of the cortex (Steriade, 2001; Timofeev, 2011).

2.3.3.1 EEG brain rhythms

The EEG rhythmic, synchronous signals comprise of time series of neural oscillations ranging from low to high frequency bands (Harmony et al., 1999; Niedermeyer, 2003). The frequency bands of neural oscillations are named after Greek letters: δ (delta) 0.5-3.5Hz, θ (theta) = 4-7.5Hz, α (alpha) = 8-12 Hz, μ (mu) = 10-12 Hz, β (beta) = 13-30 Hz, and γ (gamma) > 30 Hz (Buzsaki & Draguhn, 2004). Figure 2-8 illustrates the EEG brain rhythms.

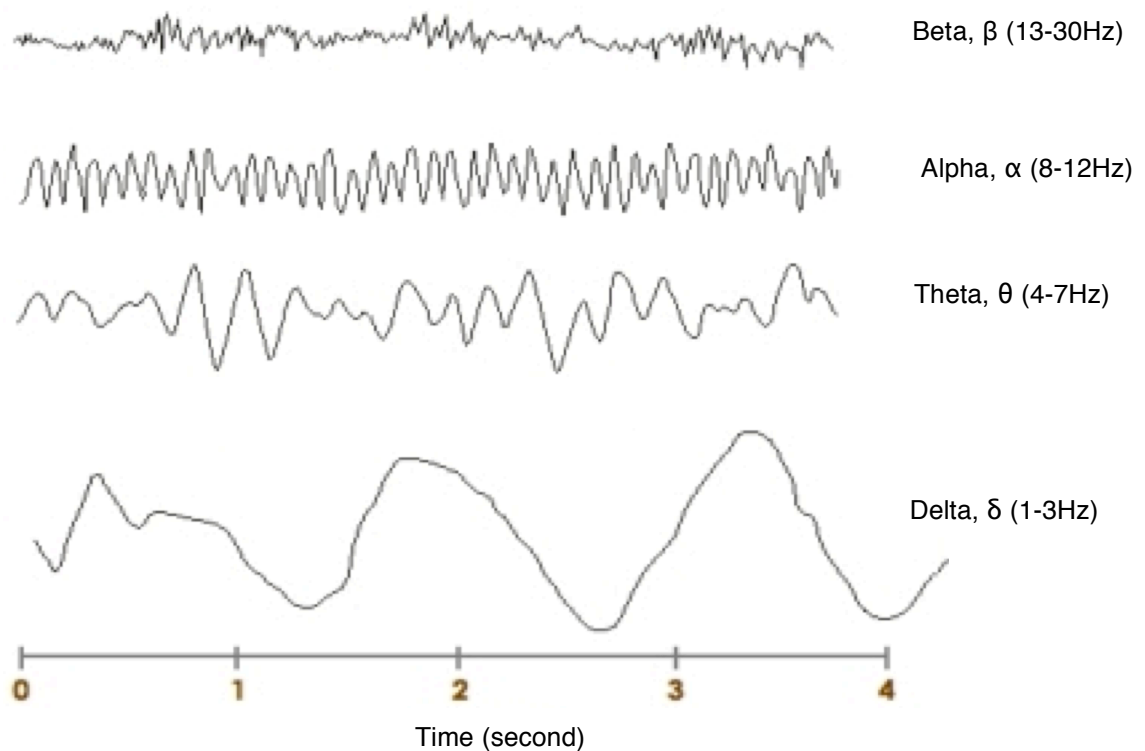


Figure 2-9 EEG brain rhythms of δ , θ , α , and β .

Table 2-2 presents the common EEG brain rhythms and their characteristics.

Table 2-2 EEG brain rhythms and their characteristics

Brain rhythms	Frequency (Hz) Amplitude (μV)	Location	Characteristics
Delta, δ	0.5 - 3.5Hz < 100 μV	Parietal lobes and central cerebrum	Dominant in infants. Deep stages of sleep in adult. Focal in brain pathologies. Occur after transactions of the brain stem separating the reticular activating system (RAS) from the cortex.
Theta, θ	4 - 7.5Hz < 100 μV	Frontal, parietal and temporal lobes	In children during awake periods. Drowsiness in adults. Increased theta activity at frontal midline region during learning and memory. Focal theta indicates focal pathology. Diffuse theta indicates generalised neurologic diseases.
Alpha, α	8 - 12 Hz 20-60 μV	Occipital and parietal lobes	Most prominent rhythm in normal adult brain. During alert, resting, eyes closed but awake. Attenuate by eye opening, mental activity and deep sleep.
Mu, μ	10 - 12 Hz < 50 μV	Central rolandic area, over motor and somatosensory cortex	A variant of the alpha rhythm. Topographically different to the alpha rhythm. Is not blocked by eye opening. Attenuated by contralateral movement of the limbs, or mental intention to perform a movement. Can be used to activate a brain-computer interface for controlling robotic device for paralysed patients.
Beta, β	13 – 30 Hz < 20 μV	Frontal, widespread cortical beta, and posterior regions	Functionally different between low beta and high beta frequencies: Low beta (13-19.5Hz) is attenuated during mental activity. High beta (20– up to 50Hz) appears during alert and intense mental activity. Frontal beta is blocked by movement Posterior beta reactive to eye opening.
Gamma, γ	> 30 Hz < 2 μV	Widespread over cortical regions	During intense mental activity, focused attention and sensory stimulation. Its low amplitude makes it difficult to isolate during EEG recording.

2.3.3.2 Functional significance of brain rhythms

The functional roles of brain rhythms in the cerebral cortex are largely undetermined. One hypothesis is that the brain rhythms are epiphenomenal, with no functional significance, and only the insignificant side effects of the interconnections of the various brain networks (Basar, Basar-Eroglu, et al., 1999; Hari & Salmelin, 1997). However, many studies suggest that the frequency of neural discharges are not merely epiphenomenal but may have functional significance (Buzsaki & Draguhn, 2004; Steriade, 2006; Timofeev, 2011).

Low frequency oscillations of δ is the dominant rhythm during deep sleep, and has been suggested to be involved in the process of memory consolidation, and large-scale cortical integration although the precise mechanisms are not known (Babiloni et al., 2006; Harmony et al., 1996). The neocortical and thalamo-cortical networks generate the δ oscillations (Steriade, 2006).

The θ rhythm has been studied extensively in the CA1 region of the rat hippocampus (Buzsaki, 2002, 2005). This “hippocampal theta” of a frequency range of 6-7 Hz in animals is thought to be important in the temporal coding and decoding of neural assemblies during memory processes, and also dominant during active motor behaviour such as virtual navigation (Buzsaki, 2002, 2005). Another type of theta rhythmicity is the “cortical theta”, with a frequency range of 4-7 Hz recorded from the human scalp EEG (Kahana et al., 2001). The human “cortical theta” does not appear to be restricted to the hippocampus, but

appears over widespread regions of the neocortex (Mitchell, McNaughton, Flanagan, & Kirk, 2008; Raghavachari et al., 2006). Studies using human intracranial EEG recordings have found θ scattered across multiple locations in the brain of the same subject with the absence of coupling between hippocampus and neocortical θ (Cantero et al., 2003; Jacobs, Hwang, Curran, & Kahana, 2006; Raghavachari et al., 2006; Rizzuto, Madsen, Bromfield, Schulze-Bonhage, & Kahana, 2006). External and internal stimuli can elicit θ oscillations in various sites of the cortex due to the parallel processing of the θ system in the brain (Basar et al., 1999). Many cognitive functions are associated with theta such as memory encoding, declarative memory, memory retention and episodic memory processing (Belluscio, Mizuseki, Schmidt, Kempter, & Buzsaki, 2012; Kahana et al., 2001; Klimesch, 1999; Raghavachari et al., 2001).

The α frequency range has several rhythms depending on the site and behavioural state of the cortex (Freeman, 2006; Sauseng, Klimesch, Gerloff, & Hummel, 2009). The posterior α rhythm—located in the occipital, parietal and posterior temporal areas—is the classical brain rhythm that occurs during wakeful relaxation with closed eyes (Freeman, 2006; Sauseng et al., 2009). The posterior α is attenuated or blocked during eye opening, and increase mental alertness (Freeman, 2006; Sauseng et al., 2009).

An α variant called μ can be found over the motor cortex, the central or the rolandic area of the cortex (Niedermeyer, Goldszmidt, & Ryan, 2004). Interestingly the μ rhythm does not attenuate during eye closure but is blocked

by contralateral movement or even the mental intention to perform a movement (Niedermeyer et al., 2004; Pfurtscheller, Brunner, Schlogl, & Lopes da Silva, 2006; Pineda, 2005). This property makes the μ rhythm useful to activate a brain-computer interface (BCI) for controlling robotic devices for paralysed patients (Niedermeyer et al., 2004; Pineda, 2005). Another variant of α frequency is the midtemporal α rhythm seen in the temporal lobe during MEG recordings, which is attenuated by sound stimuli (Sauseng & Klimesch, 2008).

The α rhythm, the most prominent rhythm in the normal adult brain was traditionally described as “idling rhythm” because both the μ and the posterior α rhythms represent “resting states” of the sensorimotor cortex and the visual cortex (Sauseng & Klimesch, 2008). It was speculated that in the absence of sensory inputs, α oscillations represent partial disengagement of the brain from the external stimuli or the internal mental processing (Sauseng & Klimesch, 2008). However, as the cortical rhythms parallel much human behaviour, many scientists argue that the functional significance of these rhythms has to be derived from basic neurophysiology (Buzsaki & Draguhn, 2004; Steriade, 2006; Timofeev, 2011). Studies have shown that the oscillations in the α rhythms are generated by the thalamocortical relay neurons (TCR) and the reticular nucleus neurons (RN) in the thalamus (Llinas & Steriade, 2006; Steriade, Timofeev, & Grenier, 2001). During oscillatory activity in the α range, the RN neurons are active, but the TCR neurons are inhibited (Steriade, 2001, 2006). Animal studies using EEG showed changes in hyperpolarisation-rebound sequences with progressive decreases in hyperpolarisation of thalamocortical (TC) cells

mediated by γ -Aminobutyric acid (GABA) receptors, GABA_B in response to thalamic stimulus at 1Hz and \sim 11Hz, and medium-term neuronal plasticity that lasted for 8 seconds (Grenier, Timofeev, Crochet, & Steriade, 2003; Steriade, 2006). The hyperpolarised membrane does not mean that the neuronal populations are idling; instead it shows an active inhibition role of the neurons in gating the transfer of information in neuronal networks (Llinas & Steriade, 2006; Sherman, 2007; Steriade, 2006).

The functional significance of β oscillations is mostly associated with motor activity (Hari & Salmelin, 1997; Pfurtscheller & Lopes da Silva, 1999). A significant decrease in β amplitudes (event-related desynchronisation or ERD) was observed at the motor cortex during movements, followed by an increase in β amplitudes (event-related synchronisation or ERS), a rebound phenomenon that occurs over the contralateral cortex after the completion of a finger or hand movement (Manganotti et al., 1998a). This β rebound signifies cortical disfacilitation that occurs when movements are stopped (Calmels et al., 2006). The β rhythm may also be involved in higher cognitive functions and attention (Hari & Salmelin, 1997; Sauseng & Klimesch, 2008).

The pioneering study by Gray and colleagues (1989) showed that γ oscillations are linked to visual awareness (Gray & Singer, 1989). At present, γ is associated with memory encoding, retention and retrieval, and maintenance in visual memory (de Lange, Jensen, Bauer, & Toni, 2008; Jensen, Kaiser, & Lachaux, 2007; Osipova et al., 2006). The high frequency range of γ oscillations (30-100Hz) means that the amplitude of γ is very small ($< 2\mu\text{V}$), and this makes

it very difficult to distinguish γ from electrical muscle activity in scalp EEG (Sauseng & Klimesch, 2008). The functional meaning of EEG synchronisation across different frequencies suggests specific neural activity for various cognitive functions of the brain (Sauseng & Klimesch, 2008).

2.4 Combining TMS and EEG

The emergence of an interest in brain rhythms has paralleled the development of non-invasive brain stimulation, such as TMS, and the advancement of computational tools for the time-frequency analysis of oscillatory dynamics (Rogasch & Fitzgerald, 2012; Thut & Miniussi, 2009). The simultaneous measurements of synchronised combinations of TMS and EEG enable the investigator to stimulate brain circuits while simultaneously monitoring changes in brain activity (Rogasch & Fitzgerald, 2012).

EEG has the temporal sensitivity that allows an investigation into the immediate effects of TMS and provides a means to study the instantaneous neuronal effects of TMS in the brain with a millisecond time scale, which is presently not possible with any functional imaging method, as blood flow responses usually take some seconds following changes in neuronal activity (Shafi et al., 2012). Such a simultaneous approach provides the opportunity to investigate the local responses to TMS at a neurophysiological level, thus helping to determine the brain areas that are either directly or transynaptically affected by magnetic stimulation (Sack, 2006; Sack & Linden, 2003).

In 1989, Cracco and colleagues performed the first measurements of TMS-evoked EEG (Cracco, Amassian, Maccabee, & Cracco, 1989). By

applying TMS in four subjects, they observed cortico-cortical responses with an onset latency of 8.8-12.2 ms from a single scalp electrode (Cracco et al., 1989). However, the EEG measurements were problematic due to the technical limitations of EEG at the time in removing large artifacts produced by the strong TMS pulses (Cracco et al., 1989). Another TMS-EEG study by the same group reported EEG responses with an onset latency of 8.8-13.8ms lasted for 17.4-29.0ms in the inter-aural line (C3, Cz, C4) and 3.5ms later in the frontal electrodes, after TMS over the cerebellar region (Amassian, Cracco, Maccabee, & Cracco, 1992). These pioneering studies (Amassian et al., 1992; Cracco et al., 1989) showed the potential of EEG to measure the aftereffects of TMS, but new EEG technology was needed to remove the large TMS-generated artifacts (Wassermann et al., 2008). It took almost a decade after these pioneering studies for the development of a TMS-compatible multichannel EEG that provided reliable measurements of the direct cortical effects of TMS (Ilmoniemi, Ruohonen, Virtanen, Aronen, & Karhu, 1999; Virtanen, Ruohonen, Naatanen, & Ilmoniemi, 1999).

The improved TMS-compatible EEG has many advantages (Rogasch & Fitzgerald, 2012); it allows direct and non-invasive measurement of cortical excitability induced by TMS (Komssi & Kahkonen, 2006); it can assess the functional connectivity between the cortical networks (Shafi et al., 2012); it allows detailed study of the instantaneous effects of TMS over the cortex in a millisecond time scale (Komssi & Kahkonen, 2006); it measures the modulation of cortical oscillatory activity after TMS (Thut, Ives, Kampmann, Pastor, &

Pascual-Leone, 2005; Thut & Pascual-Leone, 2010a); and it can monitor the safety of TMS by the epileptiform activity that may appear in the EEG waves (Rossi et al., 2009).

A review by Miniussi and Thut (2010) grouped the applications of TMS-EEG co-registration studies into three categories: inductive—using TMS-EEG as index of brain physiological state in behaviourally silent regions; interactive—using TMS-EEG to investigate the functional and dynamics of the brain; rhythmic—using TMS-EEG to study the generation and functional significance of brain rhythms (Miniussi & Thut, 2010). The inductive approach of TMS-EEG uses TMS-evoked potentials (TEP) recorded over the scalp as markers of the internal state of the brain in behaviourally silent areas (Miniussi & Thut, 2010). In other words, TEP is measured in brain regions that are unable to produce a peripheral marker of cortical excitability (Komssi & Kahkonen, 2006) such as MEPs or a phosphene in the visual cortex. The interactive approach of TMS-EEG investigations involves the application of these combined methods to explore the transient modulation of neuronal networks during task performance (Taylor et al., 2008). This approach is mainly used to identify the cortical area that is involved in a particular task (Fuggetta, Pavone, Walsh, Kiss, & Eimer, 2006; Fuggetta, Rizzo, Pobric, Lavidor, & Walsh, 2009; Taylor et al., 2008). The rhythmic approach uses TMS-EEG to examine the modulation of oscillatory brain activity by rTMS and the link between specific frequency bands and their functional role (Thut & Miniussi, 2009). The significance of this approach is the potential role of using TMS to transiently modify brain functions by altering brain

oscillations, and therefore, it may contribute to the therapeutic strategy of using TMS to reverse abnormal synchronisation in neuropsychiatric disorders (Thut & Miniussi, 2009).

2.5 Alternative measurements of rTMS aftereffects

The effects of rTMS on cortical excitability can be measured directly using EEG or MEG (Komssi & Kahkonen, 2006), and indirectly by measuring MEPs and assessments of motor behavior, such as reaction times, response accuracy, movement accuracy, and sequence learning (Kobayashi & Pascual-Leone, 2003; Walsh & Pascual-Leone, 2003). Functional neuroimaging such as PET and fMRI also indirectly measure rTMS effects on cortical excitability by assessing the metabolic activity of a given functional area (Bestmann et al., 2003; Hubl et al., 2008; Paus & Wolforth, 1998). Both methods of functional neuroimaging detect changes in regional blood flow and metabolism within the brain. Neurons that are active will need more glucose and oxygen, and more blood will flow to the active regions. Thus, by detecting changes in blood flow, PET and fMRI indirectly reveal the brain regions that are most active for a cognitive task (Shafi et al., 2012; Siebner, Bergmann, et al., 2009). Although functional neuroimaging such as PET and fMRI provide excellent spatial resolution (millimeters as compared to centimeters in EEG), their temporal resolutions are poor (seconds as compared to milliseconds in EEG) due to the relatively slow responses of brain metabolism (Formaggio et al., 2008; Pascual-Leone et al., 2011; Pell et al., 2011; Sack & Linden, 2003; Shafi et al., 2012).

Table 2-3 provides a summary of several neuroimaging techniques, their principles and applications with rTMS.

Table 2-3 rTMS and Neuroimaging techniques

Neuroimaging Techniques	Principles	Applications with rTMS
EMG	Detection of electrical activity produced by skeletal muscles. MEP is relatively easy to measure. Non invasive	Index of cortical excitability post rTMS
EEG	A macroscopic measurement of electrical activity of the brain and recorded from the scalp. High temporal resolution but low spatial resolution. Non invasive Relatively inexpensive	Assessment of the effects of rTMS on oscillatory activity. Index of cortical excitability post rTMS via TEP.
MEG	Detection of magnetic fields generated by intracellular electrical current in the neurons of the brain. MEG measurements are conducted using superconducting quantum interference device (SQUID). High temporal and spatial resolution. Non invasive Expensive	Direct index of brain rhythms altered by rTMS.
fMRI	Tracking of the difference in magnetic resonance of oxyhemoglobin to deoxyhemoglobin. High spatial but low spatial resolution. Non invasive	Detects the location of increased neural activity by measuring Blood oxygen level dependence (BOLD) after rTMS.
PET	Introduces a radioactive solution containing atoms that emit positrons into the bloodstream. High spatial but low temporal resolution.	Measures the level of neuronal metabolic activity by the number of positron emissions. Detect brain receptors that are activated by neurotransmitters or drugs.

The majority of previous TMS studies investigating M1 used MEP amplitudes and latencies to indirectly measure corticomotor excitability and to investigate TMS-induced plasticity (Fitzgerald et al., 2006; Pascual-Leone et al., 2000; Ridding & Ziemann, 2010; Rothwell et al., 1999). MEP is technically easy

to measure as even a weak, single TMS pulse applied over M1 can produce a muscle response contralateral to the site of stimulation (Rothwell et al., 1999). However, using MEP to quantify cortical excitability is problematic because it provides polysynaptic readout whereas synaptic plasticity mechanisms are monosynaptic events (Huerta & Volpe, 2009). MEPs are further from the TMS source; at least three synapses (synapses onto corticospinal neurons, synapses onto spinal motor neurons, and neuromuscular synapses) separate MEPs from TMS at the scalp (Huerta & Volpe, 2009; Siebner et al., 2009; Siebner & Rothwell, 2003). Thus, any correlation between MEP sizes and cortical excitability is indirect. It would be highly advantageous to monitor a cortical readout that is linked by a single synapse to the TMS pulse (Huerta & Volpe, 2009). A direct and more accurate monosynaptic cortical readout can be achieved by using EEG (Huerta & Volpe, 2009). In the present thesis, assessment of cortical excitability post rTMS was made with both behavioural measures (MEP and RT), and EEG.

2.6 Summary

In summary, this chapter presents the importance of rhythmic stimulation in extracting meaning from the on-going brain oscillations in the intact human brain. In particular, the chapter highlights the motivation of exploring the modulation of EEG oscillatory activity and the rTMS-induced cortical plasticity in the resting human cortex. Although rTMS is clinically used to improve symptoms of neuropsychiatric disorders and there is evidence that abnormal oscillatory brain rhythms results in neuropsychiatric illnesses, studies

investigating the mechanism of cortical and network oscillations induced by rTMS are still lacking. An improved understanding of the precise neurophysiological mechanism of rTMS involving oscillatory brain activity may enable better control of the sustained aftereffects, and will thus be beneficial for therapeutic applications.

3. Methods

This chapter serves as an introduction to the methods used in the subsequent experiments of the present thesis. It explains the rationale of using normal subjects in the present investigations. The chapter moves to present the experimental paradigms used to investigate the rTMS aftereffects on the cortical oscillatory activity and the plasticity-like mechanisms of the motor cortex. Here, it highlights the approaches of measuring the modulatory aftereffects of oscillatory activity using both direct measures (EEG) and indirect measures (MEP and RT) as indices of cortical excitability. Next, it introduces the TMS procedure and the EMG recording. The subsequent sections focus on the EEG data acquisitions and EEG spectral analysis of event-related power and event-related coherence to quantify the oscillatory activity post rTMS. The chapter concludes by describing the statistical analysis performed in the present experiments.

3.1 Participants

The participants of the current research were adult volunteers, mainly undergraduate and postgraduate university students, who volunteered to take part in the experiments. None of the participants had any contraindications to rTMS or any previous history of head trauma, neurological or psychiatric disorders, or other adverse medical conditions. Subjects were right-handed as assessed by the Edinburgh handedness inventory (Oldfield, 1971). Written

informed consent was obtained from all the subjects in accordance with the declaration of Helsinki. The actual TMS experiments were performed at the G.B Rossi Hospital “Borgo Roma” Verona Italy, and the local ethical committee approved the experimental procedures. The full EEG analysis of the current research was performed at the EEG lab, School of Psychology, University of Leicester.

3.2 Experimental paradigms

The present research aimed to explore the global and macro-level effects of rTMS on the neuronal processes of oscillatory brain rhythms of healthy human subjects in the hope of understanding the electrophysiological mechanisms underlying the aftereffects of rTMS. The research was designed to explore the short-term and long-term modulations of motor cortical oscillatory activity induced by rTMS. In the current research, we used different experimental paradigms of simple rTMS protocols and pattern rTMS protocol of continuous theta burst stimulation. EEG was measured immediately and after rTMS manipulations for several seconds to investigate the short-term potentiation effect of rTMS, and for up to 30 minutes in cTBS to explore the long-term plasticity mechanism induced by rTMS pattern protocol. Besides direct electrophysiological EEG measurements of cortical excitability, behavioural measures of MEP and RT were also quantified as indirect indices of cortical excitability post rTMS.

The first experiment aimed to investigate the acute modulation of EEG oscillatory brain rhythms in healthy human brains induced by different numbers

of magnetic pulses. The experiment involved the manipulation of the number of rTMS pulses after high frequency rTMS at individual mu-frequency, while holding other TMS parameters constant. Twenty, intermittent trains of 20 rTMS pulses (rTMS 20) versus twenty intermittent trains of 60 rTMS pulses (rTMS 60) were delivered at individual mu-frequency ($\sim 11\text{Hz}$) at 100% RMT over left M1. The EEG oscillatory activity was quantified for immediate responses up to 60s post rTMS for the θ , μ and β frequency bands. The detailed experimental paradigm, results and discussion are presented in Chapter 4.

The second experiment aimed to explore the dichotomy or differential effects between high frequency rTMS and low frequency rTMS at cortical level using EEG power and coherence modulations of brain rhythms. In the experiment, we used simple rTMS low frequency protocols of 1Hz rTMS versus high frequency protocols of 5Hz and 10Hz rTMS applied over the left M1. Here, we extended previous rTMS-EEG investigations (Brignani *et al.* 2008 of 1Hz rTMS, Fuggetta *et al.* 2008 of 5Hz rTMS, and Veniero *et al.* 2011 of 20Hz rTMS) by not only analysing the effects of rTMS on α and β , but also on the low frequency oscillations of δ and θ frequency bands. The detailed experimental paradigm, results and discussion are presented in Chapter 5.

The third experiment aimed to examine the long-lasting modulation of cortical oscillatory activity and the plasticity-like mechanisms induced by the pattern protocol of continuous theta burst stimulation. In the experiment, we delivered subthreshold high frequency cTBS over the left M1 and compared the temporal dynamics of cortical excitability after cTBS using direct

electrophysiological measurements of EEG and indirect behavioural responses of MEP and RT during “rest” and during an active motor task. Evaluation of EEG oscillatory phenomenon to cTBS was quantified by spectral analysis of the frequency ranges of θ , low α , μ , low β , and high β frequency bands. The detailed experimental paradigm, results and discussion are presented in Chapter 6.

3.3 TMS procedure

In the present thesis, TMS was carried out with a Magstim Super Rapid stimulator (Magstim, Whitland, Dyfed, UK). The magnetic stimulus had a biphasic waveform with a pulse width of about $300\mu\text{s}$. TMS was delivered through a figure-8 coil (70 mm standard coil, Magstim Co., Whitland, Dyfed, UK), oriented so that the induced electric current flowed in a posterior-anterior direction over the left M1. The coil was placed tangentially with respect to the scalp with the handle pointing backwards and laterally at a 45° angle away from the midline, approximately perpendicular to the line of the central sulcus. This orientation was chosen based on the finding that the lowest motor threshold is achieved when the induced electrical current in the brain flows approximately perpendicular to the line of the central sulcus (Brasil-Neto et al., 1992).

The motor threshold refers to the lowest stimulus intensity to produce minimum five MEP of at least $50\mu\text{V}$ in ten successive stimuli (Rossini et al., 1994). It reflects the neuronal membrane excitability (Ziemann, 2004b) and can be measured in resting muscles (RMT) or activated muscles (AMT). The TMS threshold depends on the excitability of the corticospinal axons, and the

membrane potential of cortical and spinal motor neurons (Di Lazzaro et al., 1999). Therefore the RMT has a higher TMS threshold compared to the AMT of any given muscle (Rothwell, 1997). The RMT illustrates the stimulus intensity that is able to stimulate the corticospinal neurons; therefore the magnetic stimulation at or above RMT might activate the cortico-cortical pathways (Rothwell, 1997). In the present thesis, stimulus intensities are expressed as the percentage of the subject's RMT. Subthreshold stimulation refers to magnetic stimulation below RMT, whilst suprathreshold stimulation refers to magnetic stimulation above RMT.

The participants of the subsequent experiments were naive to the differences between active rTMS and sham rTMS (control condition) prior to the study. In the present thesis, the sham condition was performed with an intensity of 100% RMT with the coil tilted at 90° to the skull in order to avoid real stimulation to the motor cortex. Using a valid sham condition in rTMS research is vital in order to produce valid outcomes (Arana et al., 2008; Herwig, Cardenas-Morales, Connemann, Kammer, & Schonfeldt-Lecuona, 2010). Better devices that can provide sensory artifacts by electrical stimulation and can emulate the effects of magnetic stimulation are not yet available (Rossi et al., 2009). A study by Herwig *et al.* (2010) demonstrated that using a "real" TMS coil with a modified stimulation condition such as angling and dislocating the coil and reducing the stimulation intensity can be used for a reliable sham condition in randomised rTMS trials (Herwig et al., 2010).

3.4 MEP data acquisition

MEP is defined as the electrical muscular response produced by artificial stimulation of the motor cortex (Rothwell et al., 1999). In the first experiment of TMS applied over the human motor cortex, twitching of the contralateral peripheral hand muscles to the site of stimulation was observed (Barker et al., 1985). Since then, subsequent studies have demonstrated the reliability of MEP as a non-invasive quantitative measure of cortical excitability after TMS (Di Lazzaro et al., 1999). Moreover, MEP is also widely used as a clinical tool to assess the integrity of the central motor pathway, and in diagnosing the abnormalities of the corticospinal pathways in various neurological disorders (Di Lazzaro, Ziemann, et al., 2008).

In TMS studies, the magnetic stimulator is connected to a TMS-compatible EMG machine to synchronise the recording of the peripheral muscular responses (i.e. MEP) with the TMS pulse (Di Lazzaro, Ziemann, et al., 2008). A period of 50-100ms is needed to measure MEPs after magnetic stimulation for post-stimulus analysis of the peripheral limbs (Di Lazzaro, Ziemann, et al., 2008). A brief pre-stimulus recording to assess EMG activity prior to TMS is required for baseline MEP, and to assure muscle inactivity in TMS studies at “rest” (Di Lazzaro et al., 2011; Di Lazzaro et al., 2010). MEPs are recorded using surface electrodes attached to the skin of the hand muscles in a belly-tendon montage (Di Lazzaro et al., 2011; Di Lazzaro et al., 2010). A low-pass or band-pass filter is essential in order to minimise the technical

artifacts during the magnetic stimulus (Di Lazzaro et al., 2011; Di Lazzaro et al., 2010).

During MEP recordings, the subjects should be comfortably seated in a relaxed position with their eyes open. Then, the optimal magnetic stimulation for the activation of the contralateral hand muscles is localised over the scalp using the magnetic coil. It is recommended to place the magnetic coil over the vertex (Cz) of the subject's head, and then slowly move the coil over the individual "motor hot spot" (Conforto, Z'Graggen, Kohl, Rosler, & Kaelin-Lang, 2004; Reid, 2003). The "motor hot spot" is the area of the magnetic coil that produces maximal MEP amplitude with minimal MEP threshold (Wassermann et al., 2008).

The resting motor threshold is obtained at the beginning of the MEP recording, as a baseline for the stimulus intensity. The RMT is defined as the lowest stimulus intensity to produce minimum 50% MEP of at least 50 μ V in 10 successive trials (Rossini et al., 1994). The stimulation is initially started below the expected threshold intensity. The lowest motor threshold is determined by reducing the stimulus intensity in 1% increments until all ten consecutive stimuli fail to produce MEP. Next, the upper threshold is determined by increasing the stimulus intensity in 1% increments until all ten stimuli induce MEP (Rossini et al., 1994). The MEP amplitude is measured either peak-to-peak (Rossini et al., 1994) or baseline-to-peak (Triggs, Kiers, Cros, Fang, & Chiappa, 1993). The amplitude of MEP recorded from a peripheral muscle represents an indirect index of motor neuron and corticospinal activation by magnetic stimulation

(Chen, 2000; Rothwell et al., 1999). Increased amplitude of MEP signifies higher cortical stimulation intensity by TMS (Chen, 2000; Rothwell et al., 1999).

In the present experiments, MEPs were recorded from the right thenar eminence (TE) muscle with Silver/Silver Chloride (Ag/AgCl) surface electrodes fixed to the skin with a belly-tendon montage. The amplified, bandpass-filtered (50Hz to 5KHz) EMG signal was fed into a Basic EMG Machine (Esaote Biomedica, Florence, Italy). The optimal position for activation of the right TE is determined by moving the coil in 0.5cm steps around the presumed motor hand area of the left motor cortex. The site where stimuli of slightly suprathreshold intensity consistently produced the largest MEP with the steepest negative slope in the target muscle was marked as the “motor hot spot”. The RMT intensity was approached from the individual suprathreshold levels by reducing the stimulus intensity in 1% steps. The MEPs recorded from the right TE were computed as the amplitude between the two largest peaks of opposite polarity after 20ms from the TMS pulse. The intensity of single-pulse TMS was set to 120% of individual RMT.

3.5 EEG data acquisition

This section will present the methods involved to acquire EEG data from the human scalp. It introduces the basic EEG recording systems, and the standard electrode placements of the International Federation of Societies for Electroencephalography and Clinical Neurophysiology (IFSECN) as used in the present thesis. It also explains the referencing and bipolar recordings, and the TMS artifacts removal.

The EEG signal is relatively simple to record. The method is non-invasive and painless. Recordings are made using small metal plate electrodes fixed to standard positions on the human scalp. The EEG recording system is comprised of Ag/AgCl disc electrodes with conductive paste to ensure low-resistance connection; amplifiers with filters to record voltage changes; an analog-to-digital (AD) converter to digitise the signals at 12 or more bits of precision with accuracy lower than the overall noise; and a computer for storage, processing and presentation of data (Smith, Gevins, Brown, Karnik, & Du, 2001). The electrical activity of the cortex is recorded in voltages, of the order of microvolts. In the present research, continuous EEG was recorded using a TMS-compatible EEG system (Micromed, Treviso, Italy).

The EEG electrodes with conductive paste are attached to the human scalp to detect the brain electrical activity. Conductive paste or gel provides a good electrical contact by ensuring low-resistance connection. In experiments using high-density EEG or large multi-channel montages, an electrode cap is used for faster set-up of EEG recordings. In the present experiments, an Ag/AgCl electrode cap filled with conductive paste was used to ensure good contact.

The EEG electrodes are placed according to the standard methodology of IFSECN adopted from the 10-20 EEG electrode systems by Jasper (1958), which has now been accepted worldwide as the international standard of the 10-20 EEG electrode system (Jasper & Radmussen, 1958; Niedermeyer, 2003). In this system, the head is divided into four proportions from the prominent skull

landmarks of nasion, inion, mastoid, and preauricular. The 10-20 label represents the percentage of proportional distances between the nasion and inion in the anterior-posterior plane and between the mastoids in the dorsal-ventral plane. The placements of electrodes are labelled representing the brain areas: F (frontal), C (central), P (parietal), T (temporal), O (occipital). Odd numbers for electrodes represent the letters on the left (ventral) side of the brain hemisphere and even numbers represent electrodes on the right (dorsal) side. The letter “z” represents the midline electrodes. Left and right side is from the point of view of the subject (Freeman, 2004a; Herwig, Satrapi, & Schonfeldt-Lecuona, 2003). The EEG electrode placement of 10-10 and 10-5 systems were introduced later as another standard system for high-density EEG studies (Herwig et al., 2003; Jurcak, Tsuzuki, & Dan, 2007).

The EEG recordings consist of electrically “neutral” electrodes as a reference montage, and “active” electrodes placed over different scalp regions known as the bipolar montage. The reference electrodes can be attached to the parts of the body where the electrical potential remains constant such as the vertex (Cz), ear lobes, linked-mastoids (bones behind the ear), FPz, AFz, and the nose (Herwig et al., 2003; Jurcak et al., 2007). The scalp-to-scalp bipolar recordings measure the potential difference between successive pairs of electrodes that are closely linked. A third type of electrode known as the ground electrode is needed by the amplifiers to obtain a differential voltage of the active and reference leads. The ground location includes FCz, ear lobe, wrist, or leg (Herwig et al., 2003; Jurcak et al., 2007). The high-density recordings are

usually made using standardise EEG-recording caps with removable Ag/AgCl electrodes designed for either 10-20 or 10-10 systems. Figure 3-1 illustrates the EEG-recording cap with removable electrodes arranged according to international 10-20 or 10-10 systems.

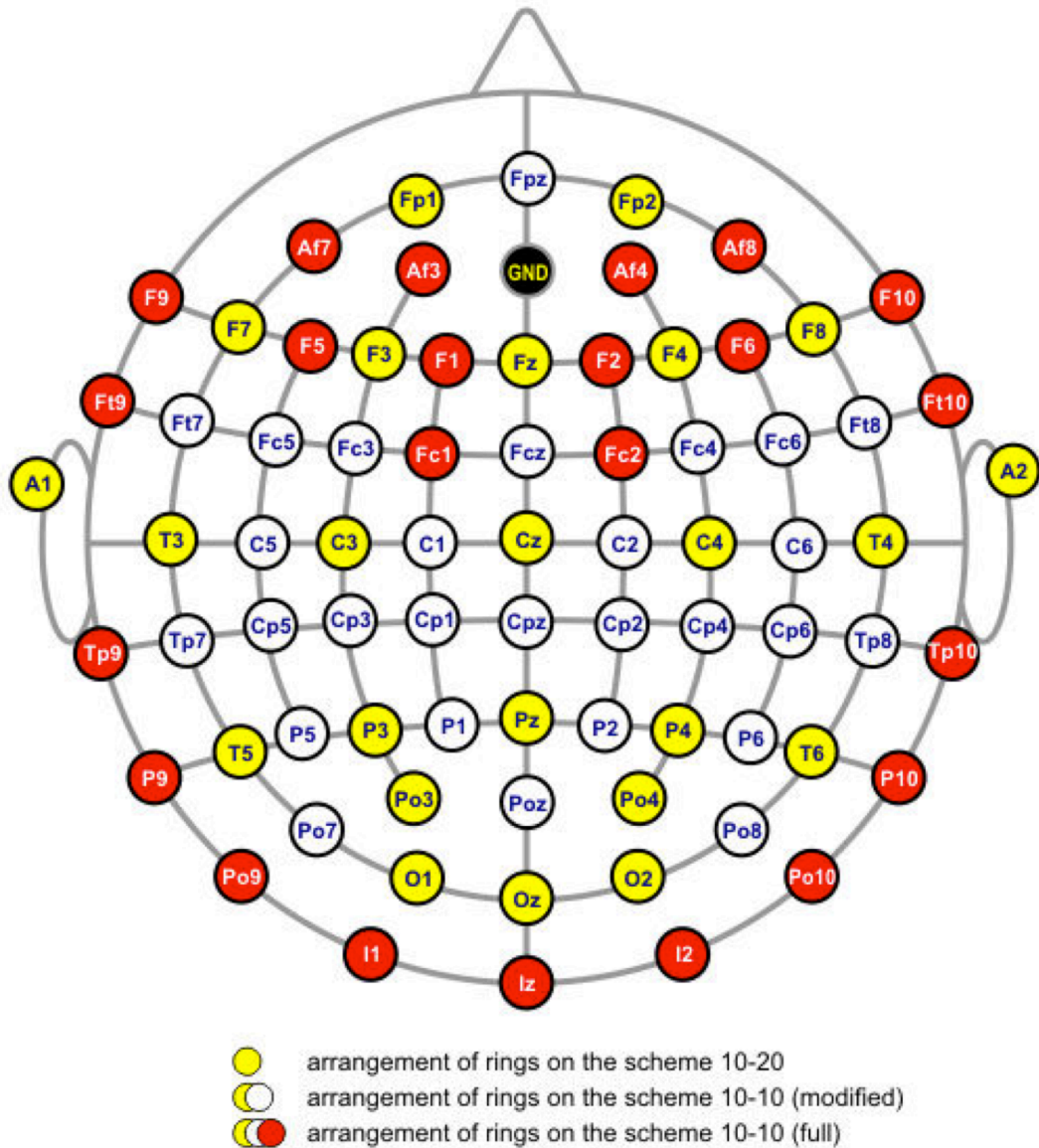


Figure 3-1 EEG-recording cap with removable Ag/AgCl electrodes for international 10-20, 10-10 (full), and 10-10 (modified) systems.

In the present thesis, the EEG signal was continuously recorded from 30 Ag/AgCl electrodes sites (Fp1, AF3, AF4, F7, F3, Fz, F4, F8, FC5, FC1, FC2, FC6, T3, C3, Cz, C4, T4, CP5, CP1, CP2, CP6, T5, P3, Pz, P4, T6, PO3, PO4, O1, O2) according to the international 10-10 (modified) EEG electrode system (Figure 3-1). The reference electrode was placed at AFz site, whereas the

ground electrode was at FCz site and has been used in previous studies using the same system (Formaggio et al., 2008; Fuggetta et al., 2008).

In order to get “clean” data for analysis, the EEG signals have to be filtered and the artifacts removed. Artifacts are unwanted electrical potentials that do not originate from the brain, which may contribute to inaccurate interpretations of the EEG signals (Niedermeyer, 2003). The EEG artifacts can be grouped into technical artifacts and physiological artifacts. The technical artifacts include power supply interference (50/60 Hz) due to high electrode impedance at contact, and the fluctuations of electrode impedance due to loose wire contacts or less application of electrode conductive paste resulting in dried leads. The technical artifacts can be avoided by proper equipment set up before the experiments and continuous monitoring during the EEG recording (Freeman, 2004b).

The physiological artifacts include body activities such as movements; bioelectrical potentials such as those generated by the eye, heart, and pharyngeal muscle; skin resistance fluctuations such as perspiration, vasomotor, and sweat gland activities (Freeman, Holmes, Burke, & Vanhatalo, 2003). The physiological artifacts can be detected using electrooculography (EOG) for eye activity such as blinking and eye movements, EMG for muscle activity, and electrocardiography (ECG) for heart activity. Unlike technical artifacts, physiological artifacts are more difficult to avoid because these bodily activities are ongoing during EEG recordings (Freeman et al., 2003). The EOG activity is the most important artifact that must be eliminated from the raw EEG

signals (Freeman et al., 2003). This is because eye blinks are approximately 100ms in duration and emulate brain rhythms at around 10Hz, the α frequency band. However, their frontal distribution, symmetry, and the amplitude of eye blinks that decreases in successive channels from anterior to posterior can distinguish eye movement artifacts from α rhythm in EEG (Niedermeyer, 2003).

One way of removing the artifacts from the EEG trace is through filtering. The filter coefficients are derived from the artifact properties such as line interference at 50Hz or from processing of the physiological bioelectrical artifacts recordings such as EOG, EMG, and ECG. This can be done using a conventional low-pass, high-pass, band-pass and notch filter (Freeman, 2004a; Freeman et al., 2003). The artifact rejection involves the identification and removal of the artifact segments from the EEG trace. Previously, EEG experts manually removed the artifacts segments by visually scoring the EEG data or the physiological artifacts. However, recent advances in digital signal processing makes it possible to remove the EEG artifacts automatically, such as by using the threshold-based rejection methods (Smith et al., 2001). Although labour- and cost-effective, this automated approach in artifact removal may results in under- or over-rejection of EEG data (Smith et al., 2001).

In the present thesis, careful EEG set-up and continuous monitoring of electrode impedance that was kept below 10k Ω minimised the technical artifacts. In order to ensure the subjects' safety, the wires were carefully arranged to avoid loops and physical contact with the subject. The EEG amplifier had a resolution of 22 bits with a range of ± 25.6 mV to avoid electrical

saturation of EEG channels induced by TMS. An anti-aliasing hardware band-pass filter was applied with a bandwidth between 0.15 and 269.5Hz. EEG data were sampled at a frequency of 1024Hz using the software package SystemPlus (Micromed, Treviso, Italy). EEG signals were filtered (1-40Hz, slope 24dB/octave) and a notch filter (50Hz) applied to all channels. A semi-automatic epoch inspection-rejection procedure was applied to remove the physiological artifacts of muscle and eye movements. Segments with values outside the range of $\pm 70\mu\text{V}$ were rejected for semiautomatic epoch rejection criterion.

3.6 EEG spectral analysis

This section present the EEG analysis of the frequency domain performed in the present research. The subsection presents the basic concepts on EEG Event-related synchronisation/desynchronisation (ERD/ERS), which form the basis of the EEG spectral analysis of event-related power (ERPow) and event-related coherence (ERCoh) in quantifying the TMS effects on brain oscillatory activity.

3.6.1 Event-related desynchronisation/synchronisation

The neuronal networks consist of populations of neurons that tend to work in synchrony. The synchronous phenomenon of neuronal elements is usually associated with oscillatory behaviour (Basar, Basar-Eroglu, et al., 1999; Basar, Demiralp, et al., 1999; Buzsaki & Draguhn, 2004). This is because there is a tendency for populations of neurons to display oscillatory dynamics when

synchronously active (Basar, Basar-Eroglu, et al., 1999; Basar, Demiralp, et al., 1999; Buzsaki & Draguhn, 2004).

There are two types of EEG signal characteristics that may occur after sensory or motor stimulations. One is known as “evoked” or event-related potentials that are time-locked and phase-locked, and can be extracted by a simple, linear method of averaging across the EEG epochs (2.3.2 Event-related potential). The other EEG signal property is time-locked but not phase-locked (induced) and can only be elicited by a non-linear method of spectral analysis (Pfurtscheller & Lopes da Silva, 1999). The synchronisation within neuronal networks can be quantified from the power spectrum of the EEG, by the magnitude and the bandwidth of the spectral peak (Pfurtscheller & Lopes da Silva, 1999). ERS represents an increase in synchrony, whereas ERD reflects desynchronised rhythmic activity (Pfurtscheller & Lopes da Silva, 1999).

3.6.2 Event-related power

The modulation of the cortical oscillatory activity by rTMS may reflect both the regional cortical activity as well as the interregional functional coupling in large-scale neuronal networks (Ilmoniemi et al., 1999; Rogasch & Fitzgerald, 2012). In the EEG spectral analysis, ERPow reflects the regional oscillatory activity of neural assemblies, and ERCoh reflects the interregional functional coupling of oscillatory neural activity (Andrew & Pfurtscheller, 1996; Pfurtscheller & Andrew, 1999). In order to characterise how rTMS induced oscillations, the EEG data were analysed with commercial software (Vision Analyser, BrainVision, Munich, Germany) then were computed for ERPow and ERCoh. A discrete Fast Fourier

Transform (FFT) of 4 epochs of 2048 data points (2 seconds) each was computed for all electrodes and then averaged under the same conditions. Power was calculated by selecting 9 electrodes: F3, Fz, F4, C3, Cz, C4, P3, Pz, and P4 from the FFT power spectrum. Power spectra were estimated for all frequency bins between 0.5 and 40Hz (0.5Hz of maximum bin width). Recordings were Hamming-windowed to control spectral leakage. Broadband power changes were obtained by averaging the power values for the frequency ranges chosen for the analysis (δ , θ , α , and β frequency bands). The output data were imported into Microsoft Excel to calculate ERPow.

In order to reduce the effects of inter-subject and inter-electrode variation in absolute spectral power values and to quantify the event-related relative changes of EEG power at an electrode x (ERPow _{x}), an accepted event-related desynchronisation/ synchronisation (ERD/ERS) procedure was used (Leocani, Toro, Manganotti, Zhuang, & Hallett, 1997b; Pfurtscheller & Aranibar, 1977), according to equation (1).

$$\text{ERPow}_x = \frac{(\text{Pow}_{x \text{ event}} - \text{Pow}_{x \text{ reference}})}{\text{Pow}_{x \text{ reference}}} \times 100 \quad (1)$$

The ERPow (or ERD/ERS) transformation was defined as the percentage decrease/increase of instant power density at the 'event' compared to a 'pre-event' baseline. Therefore, ERPow decreases imply a decrease in synchrony of the underlying neuronal populations, which are expressed as negative values, while ERPow increases are expressed as positive values.

3.6.3 Event-related coherence

Coherence was calculated by selecting a combination of the C3 electrode (the nearest channel to the TMS coil position) with 9 electrodes, creating the following pairs of electrodes: C3-F3, C3-Fz, C3-F4, C3-C3, C3-Cz, C3-C4, C3-P3, C3-Pz, and C3-P4 from the FFT power spectrum. The coherence values were calculated for each frequency bin (λ) from 0.5 to 40 Hz (0.5Hz of maximum bin width) according to equation (2) using commercial software (Vision Analyser, BrainVision, Munich, Germany).

$$\text{Coh}_{xy}(\lambda) = |R_{xy}(\lambda)|^2 = \frac{|f_{xy}|^2}{(|f_{xx}(\lambda)| |f_{yy}(\lambda)|)} \quad (2)$$

Equation (2) is the extension of the Pearson's correlation coefficient to complex number pairs. In this equation, f denotes the spectral estimate of two EEG signals x and y for a given frequency bin (λ). The numerator contains the cross-spectrum for x and y (f_{xy}), and the denominator the respective auto spectra for x (f_{xx}) and y (f_{yy}). For the frequency λ , the coherence value (Coh_{xy}) is obtained by squaring the magnitude of the complex correlation coefficient R , and is a real number between 0 and 1. Because coherence is the cross-correlation of two power spectra divided by the respective powers, it is already normalized by power within each subject. In order to reduce the effect of inter-subject and inter-electrode pair variations in absolute coherence values introduced by the reference electrodes (Fein, Raz, Brown, & Merrin, 1988; Rappelsberger & Petsche, 1988), event-related relative coherence (ERCoH_{xy}) was obtained by

subtracting the baseline value ($\text{Coh}_{xy \text{ reference}}$) from the corresponding event conditions ($\text{Coh}_{xy \text{ event}}$), according to equation (3).

$$\text{ERCoh}_{xy} = \text{Coh}_{xy \text{ event}} - \text{Coh}_{xy \text{ reference}} \quad (3)$$

Therefore, coherence magnitude increments were expressed as positive values and coherence decrements were expressed as negative values (Manganotti et al., 1998b). Broadband ERCoh changes were obtained by averaging the coherence values for the frequency ranges chosen for analysis (δ , θ , α and β frequency bands). The output data were imported into Microsoft Excel to calculate ERCoh.

3.7 Statistical analysis

Data were analysed using SPSS for Windows version 18. Repeated measures analyses of variance (ANOVA) were used to compare variables. For each ANOVA, the sphericity assumption was assessed with Mauchly's test. Greenhouse-Geisser epsilon adjustments for non-sphericity were applied where appropriate. Post-hoc paired t-tests adjusted for Bonferroni corrections were used for multiple comparisons. For all statistical tests, $p < .05$ was considered significant.

3.8 Summary

The purpose of the current chapter was to describe the general methods used in all experiments of the present thesis. The subsections present the participants, experimental paradigms, MEP recording, EEG data acquisition,

and EEG analysis as a basis for the subsequent results chapters. The purpose of this chapter was to make the reader familiar of the general methodology that was employed in this research. More detailed descriptions of materials and design employed in each of the experiments will be presented in the methodology section of the respective experiments.

4. The number of rTMS pulses and cortical oscillations

This chapter presents an rTMS-EEG experiment investigating the changes in EEG oscillatory activity after high frequency (~11Hz) rTMS relative to the number of magnetic pulses. It begins with a brief introduction on the importance of the current experiment, and explicitly outlines its aims and predictions. The next section presents the methods specific to the experiment. Following this, the chapter outlines a summary of the results consisting of the behavioural MEPs and EEG spectral power and coherence of the frequency ranges analysed in the experiment. The chapter concludes with a discussion of the results and highlights some interesting findings that emphasise the crucial role of high-density EEG in future rTMS study of brain organisation.

4.1 Introduction

There are many studies exploring the effects of the number of magnetic pulses on motor cortical excitability after simple or conventional rTMS protocols of high frequency magnetic stimulation (Fitzgerald et al., 2006; Hoogendam et al., 2010). The conventional protocol of high frequency rTMS refers to trains of repetitive stimuli delivered at a fixed frequency, usually in the range of 5-20Hz. However, studies on rTMS-induced aftereffects using varying numbers of magnetic pulses tended to use MEP as the index of cortical excitability with

contradictory outcomes (Fitzgerald et al., 2006). Several studies demonstrated increased MEP size after high frequency magnetic stimulation linear to the number of TMS pulses; the higher the number of applied magnetic pulses, the higher the MEP amplitudes (Maeda et al., 2000b; Modugno et al., 2001; Peinemann et al., 2004). However, other studies showed no effects on MEP size irrespective of the total number of applied pulses (Daskalakis et al., 2006; Quartarone et al., 2005; Suppa, Bologna, et al., 2008). On the other hand, a study of 10Hz rTMS on 20 healthy subjects by Jung et al. (2008) demonstrated an increase in MEP after application of 300 magnetic pulses (trains of 1.5s) up to 120-min, but a decrease in MEP size after 1000 pulses (trains of 5s) for 90-min (Jung et al., 2008).

These contradictory results of behavioural correlates suggest the importance of assessing the modulation of cortical excitability after rTMS using a potentially more sensitive electrophysiological technique such as EEG (Thut & Pascual-Leone, 2010b). Several studies that have used both behavioural and EEG measurements as the index of rTMS aftereffects showed the presence of EEG signals despite the absence of behavioural correlates (Holler, Siebner, Cunnington, & Gerschlagel, 2006; Rossi et al., 2000). These findings suggest that EEG may be a more sensitive and robust electrophysiological index of motor cortical excitability post rTMS than the behavioural index (Thut & Pascual-Leone, 2010b).

Although the combination of rTMS and EEG may provide a more accurate cortical read-out than MEPs, there are only a limited number of studies

examining the association between the number of rTMS pulses and the effects of EEG oscillatory activity at rest (Miniussi & Thut, 2010; Shafi et al., 2012). A meta-analysis of rTMS-EEG studies by Thut and Pascual-Leone (2010) demonstrated linear correlations between the EEG aftereffects size and the total number of rTMS pulses in high-frequency protocols (5-20 Hz rTMS) (Thut & Pascual-Leone, 2010b). However, these studies using conventional, high frequency rTMS protocols (5-20 Hz) differed in the total number of pulses, duration of magnetic trains, intensity of stimulation, and the intertrain interval (Thut & Pascual-Leone, 2010b).

To date, there is no study of high frequency magnetic stimulation that has investigated the human EEG oscillatory activity at rest by manipulating the number of magnetic pulses within a train of stimulation, while holding other TMS parameters constant. Brignani *et al.* (2008) examined the effects of the duration of magnetic stimulation on human EEG oscillatory activity after a conventional, low frequency of 1Hz rTMS (Brignani et al., 2008). In that study, they divided 600 pulses of continuous 1Hz rTMS into three blocks of time, each containing 200 pulses (block 1: 0-3.33-min; block 2: 3.34-6.66-min; block 3: 6.67-10-min), and compared the cortical oscillatory activity among the three stimulation blocks (Brignani et al., 2008). They demonstrated that the EEG power modulations of motor cortical oscillatory activity increased linearly with the duration of stimulation; synchronisation was higher in α (8-12Hz) than β (12-30Hz) frequency rhythms (Brignani et al., 2008).

4.2 Aims

The first aim of the present experiment was to investigate the EEG motor cortical oscillatory activity of θ , μ , and β frequency bands in the healthy human brain at “rest”, induced by high frequency rTMS trains of varying numbers of pulses. The rTMS was manipulated along one dimension: the number of applied magnetic pulses for each short train of rTMS—twenty intermittent trains of 20 rTMS pulses (rTMS 20; 400 pulses) versus twenty intermittent trains of 60 rTMS pulses (rTMS 60; 1200 pulses). The other rTMS parameters were constant across all experimental conditions (the frequency of rTMS was tuned to each participant’s Rolandic μ rhythm, i.e., the natural frequency of the resting motor cortex; stimulus intensity was 100% RMT).

The second aim was to look at the presence of cumulative effects—the condition at which later part of an experimental session may show different effects from the early part of the experiments (Hamidi, Johson, Feredoes, & Postle, 2011) within the different rTMS trains. In order to address this problem, the short trains of 20 intermittent trains of magnetic stimulation were divided into two parts (part A consisted of the first ten intermittent trains of magnetic stimulation, and part B consisted of the following ten intermittent trains) for both rTMS 20 and rTMS 60 protocols. EEG data were analysed in terms of the immediate responses up to 60s after each magnetic train. EEG responses were evaluated using spectral analysis of ERPow and ERCoh, which reflect the regional neural activity and the interregional functional coupling among cortical

areas, respectively. MEPs were recorded at the beginning and at the end of each experimental condition.

We predicted that trains with a relatively higher number of applied pulses (rTMS 60; 1200 pulses) would generate a higher EEG power modulation compared with trains of fewer pulses (rTMS 20; 400 pulses) after high frequency rTMS. Since the stimulation was applied over the left M1 at rest and tuned to each subject's Rolandic μ rhythm, we expected μ (10-12 Hz) rhythm would be the dominant frequency after the magnetic stimulation. A previous study by Rosanova *et al.* (2009) showed that each cortical area tended to preserve its own natural frequency after magnetic stimulation; TMS constantly evoked dominant α oscillations in the occipital cortex, β oscillations in the parietal cortex and fast β / γ oscillations in the frontal cortex (Rosanova et al., 2009). As for the cumulative effects, we predicted that the trains of rTMS 60 pulses would be more effective than the trains of rTMS 20 pulses in producing pronounced cumulative effects during high frequency magnetic stimulation.

4.3 Methods

This section describes the specific methods employed in the present experiment to investigate the modulation of motor cortical oscillatory activity after a varying number of magnetic pulses. The subsections present the participants, experimental paradigms, the procedural steps of TMS recording, EEG data acquisition, and the EEG spectral analysis applied in the present experiment.

4.3.1 Participants

Twelve healthy volunteers (six males, six females; mean age 22.18 ± 1.07 years) with no previous history of neurological disorder or head trauma took part in the study.

4.3.2 Experimental design

Each subject sat in a comfortable armchair with elbows flexed at 90° , hands in a relaxed position, eyes opened, watching a computer screen. The subjects were asked not to move and to try not to blink throughout the experimental session in order to minimise physiological artifacts, such as EMG and EOG artifacts. Three minutes of resting EEG activity was recorded at the start of the experimental session.

In order to make sure that the frequency of magnetic stimulation was constant across all subjects, the trains of rTMS were delivered at the frequency of individual μ rhythm. The μ rhythm is the natural frequency over the central rolandic or sensorimotor area during a relaxed state (Niedermeyer et al., 2004; Pfurtscheller et al., 2006; Pineda, 2005). The spectral distribution of the μ rhythm has an average peak of 10–11Hz in normal, healthy adults, however this frequency differs among individuals (Pineda, 2005; Sauseng et al., 2009). By delivering rTMS at the individual μ peak and keeping other parameters of stimulation constant, the interpretation of the alteration in EEG oscillatory activity is related only to the manipulation of the number of applied rTMS pulses. In the present experiment, we applied high frequency rTMS at the frequency of an individual's μ peak (mean $11.05\text{Hz} \pm 0.56$) over the left M1 at

the stimulus intensity of 100% RMT concurrently with high-density multichannel EEG recording. To our knowledge, this is the first rTMS-EEG study of the motor cortex that delivered rTMS at the frequency of the individual's μ peak.

Each subject participated in all three experimental conditions—twenty intermittent trains of 20 pulses (400 stimuli, rTMS 20), twenty intermittent trains of 60 pulses (1200 stimuli, rTMS 60), and sham rTMS with 20 trains of 20 pulses (400 stimuli) as a control condition. In order to avoid order effects, the order of the three experimental conditions was counterbalanced across all participants. The intertrain interval was set to 68s across all experimental conditions because the event-related changes in continuous EEG need time to develop and to recover. Baseline MEPs were also recorded before and after each experimental protocol to evaluate the conditioning effects of rTMS. Figure 4-1 presents the experimental paradigm

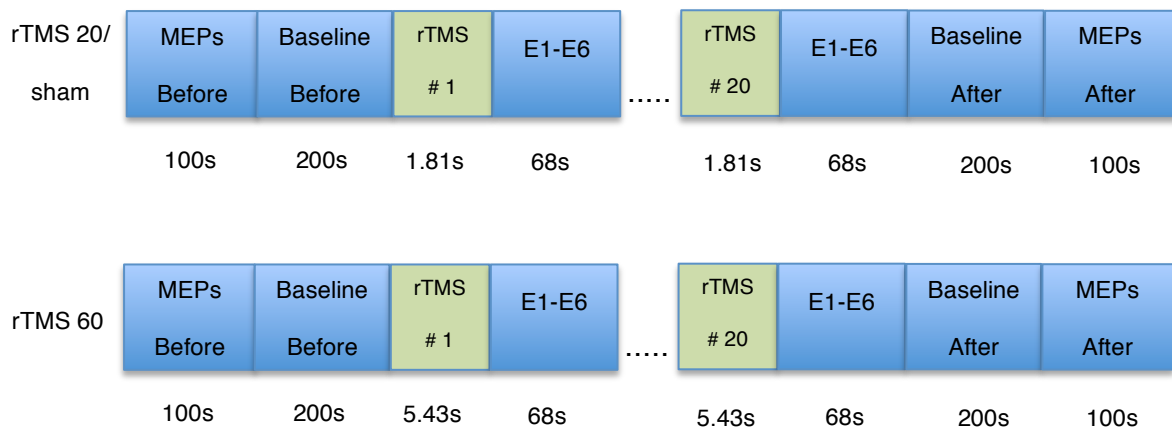


Figure 4-1 Experimental paradigm. The study design consisted of three experimental conditions of twenty intermittent trains of 20 or 60 high frequency (~11 Hz) rTMS pulses delivered over the human primary motor cortex at rest (rTMS 20, rTMS 60 and sham rTMS 20). It comprised epochs of EEG recorded continuously before, during, and after the trains of stimulation (Baseline Before, E1, E2, E3, E4, E5, E6 and Baseline After respectively). MEPs were also recorded at the beginning and at the end of each experimental condition.

The subjects rested for 20-min in-between experimental conditions in order to minimise fatigue and avoid carry-over effects from one experimental condition to the next. A study by Fitzgerald *et al.* (2007) showed the absence of carry-over effects in terms of the modulation of cortical excitability after 15-min of multiple short-trains of high frequency rTMS (Fitzgerald *et al.*, 2007). However, Thut and Pascual-Leone (2010) in a review of TMS-EEG co-registration studies revealed a lasting effect of several high frequency rTMS protocols on EEG activity (Thut & Pascual-Leone, 2010b). Therefore, in order to make sure there was no carry-over effect in the experimental conditions and there is no effect of fatigue as a confound factor, we compared the different baseline periods in-between the experimental paradigms across the three frequency bands analysed.

4.3.3 TMS-EEG recording

TMS was performed using a high-power Magstim-Rapid stimulator (Magstim, Whitland, UK) and the magnetic stimulator was connected to a TMS-compatible EMG machine to synchronise the recording of the MEP from the right TE muscle with the TMS pulse. The MEPs recorded from the right TE were computed as the amplitude between the two largest peaks of opposite polarity after 20ms from the TMS pulse. The intensity of the single-pulse TMS was fixed at 120% of individual RMT. In order to assess the conditioning effects of rTMS, ten single-pulse TMS was delivered within 100s at the start and at the end of each of the three experimental paradigms. Mean MEP peak-to-peak amplitudes (mV) and latencies (ms) were normalized with the baseline before and analysed

with repeated measures ANOVAs with the factor of “condition” (rTMS 20 pulses, rTMS 60 pulses, sham rTMS 20 pulses).

The EEG data were simultaneously recorded using a TMS compatible EEG amplifier (SD MRI 32, Micromed, Treviso, Italy) and an electrode cap of 30 Ag/AgCl electrodes placed according to a 10/10 (modified) system as previously described in Chapter 3 Methods.

4.3.4 EEG spectral analysis

EEG data were analysed with commercial software (Vision Analyser, BrainVision) to quantify the rTMS-induced aftereffects. The EEG analysis began one second after rTMS in order to eliminate large TMS artifacts contaminating the EEG signal. The EEG data were segmented into temporal windows of identical length (1000ms containing 1024 data points) for eight time intervals. The time intervals were as follows: Baseline before trains of rTMS (200s), first epoch (1-5s), second epoch (6-10s), third epoch (11-15s), fourth epoch (16-20 s), fifth epoch (36-40s), sixth epoch (56-60s), and baseline after rTMS (200s). Each epoch comprised of 80 trials for the three experimental conditions (rTMS 20, rTMS 60 and sham rTMS 20).

EEG signals were filtered (1-40Hz, slope 24 dB/octave) and a notch filter (50Hz) was applied to all channels. A semi-automatic epoch inspection-rejection procedure was applied in order to remove the physiological TMS artifacts such as muscle movements and eye blinks. Segments with values outside the range of $\pm 70\mu\text{V}$ were rejected during the semi-automatic epoch

rejection procedure. A mean of 51.0 ± 17.8 of clean data out of 80 trials for each epoch were extracted from the three experimental conditions.

EEG spectral analyses were evaluated using FFT for all frequency bins between 1 and 40Hz (1Hz of maximum bin width). Recordings were Hamming-windowed to control spectral leakage. Broadband power changes were acquired by averaging the power values of θ (4-7Hz), μ (10-12Hz), and β (13-30Hz) frequency bands. The output data were imported into Microsoft Excel, to calculate ERPow and ERCoh. The baseline power before stimulation was used as a reference.

4.3.5 Statistical analysis

To address the problem of any carry-over effects in the experimental conditions, we compared the different baseline values in-between protocols of the three frequency bands analysed. Repeated measures ANOVAs were applied for ERPow θ , μ , and β frequency ranges. Two within-subjects factors were tested: *time* (three levels: baseline before the first rTMS conditions, baseline before the second rTMS condition, and baseline before the third rTMS condition) and *electrode* (nine levels: F3, Fz, F4, C3, Cz, C4, P3, Pz, P4).

In order to investigate the rTMS aftereffects of motor cortical oscillations after varying number of magnetic pulses, repeated measures ANOVAs for both ERPow and ERCoh were performed for the three frequency bands of θ , μ , and β . Four within-subjects factors were tested: *condition* (three levels: rTMS 20 pulses, rTMS 60 pulses, sham rTMS 20 pulses); *epoch* (six levels: epoch one, 1-5s; epoch two, 6-10s; epoch three, 11-15s; epoch four, 16-20s; epoch five,

36-40s; epoch six, 56-60s); *part* (two levels: part A, during the first ten trains of stimulation; part B, during the subsequent ten trains of stimulation) and *electrode* (nine levels: F3, Fz, F4, C3, Cz, C4, P3, Pz, P4) for ERPow or *pair of electrodes* (nine levels: C3-F3, C3-Fz, C3-F4, C3-C3, C3-Cz, C3-C4, C3-P3, C3-Pz, C3-P4) for ERCoh. We assessed the cumulative effects produced by rTMS by looking at the difference in EEG oscillations between part A and part B of the different rTMS protocols (rTMS 20 part A, 200 stimuli; rTMS 20 part B, 400 stimuli; rTMS 60 part A, 600 stimuli; rTMS 60 part B, 1200 stimuli).

4.4 Results

The initial sample was comprised of twelve adult, healthy participants of whom eleven subjects' data were suitable for reliable EEG analysis. We removed one subject's data because of excessive eye blinks and muscle activities that significantly decreased the quantity of clean data required to produce a reliable spectral estimate. There was no report of any adverse side effects during or immediately after the experiment. The subjects' RMT ranged from 65 to 89% with a mean motor threshold of $77.3\% \pm 8.5$.

The statistical analyses did not indicate any carry-over effects in-between the three rTMS conditions (rTMS 20, rTMS 60 and sham rTMS 20). There was no significant main effect of *time* nor a significant two-way interaction of *time x electrode* for the three frequency bands of θ , μ , and β . [θ : *time* ($F_{2,20} = 1.23$; $p = .32$, $\eta_p^2 = .1$), *time x electrode* ($F_{16,160} = .18$; $p = 1.0$, $\eta_p^2 = .02$); μ : *time* ($F_{1.16,11.6} = 1.74$; $p = .22$, $\eta_p^2 = .15$), *time x electrode* ($F_{16,160} = 1.67$; $p = .06$, $\eta_p^2 = .1$); β :

time ($F_{2,20} = .36$; $p = .703$, $\eta_p^2 = .04$), time x electrode ($F_{16,160} = 1.09$; $p = .37$, $\eta_p^2 = .1$)].

4.4.1 EEG Event-related power

This subsection presents the results of ERPow of 11 subjects. For each of the three frequency bands of interest (θ , μ , β), four factors were tested within subjects using ANOVAs: *condition*, *electrode*, *epoch*, and *part*. This subsection focuses on the main experimental findings, which are discussed in Section 4.5.1 rTMS and regional oscillatory activity. The remaining findings are presented in the subsequent tables.

4.4.1.1 ERPow θ

Table 4-1 summarises the ANOVAs of the main effects and interactions for ERPow θ .

Table 4-1 ERPow θ

Factors	ERPow θ
Condition***	$F_{2,20} = 12.67$; $p < .001$; $\eta_p^2 = .56$
Electrode**	$F_{2,1,20,8} = 10.32$; $p < .01$; $\eta_p^2 = .51$
Epoch***	$F_{1.5,14,8} = 50.18$; $p < .001$; $\eta_p^2 = .83$
Part	$F_{1,10} = 3.45$; $p = .09$; $\eta_p^2 = .26$
Condition x Electrode***	$F_{16,160} = 3.1$; $p < .001$; $\eta_p^2 = .24$
Condition x Epoch***	$F_{2.4,24,4} = 10.4$; $p < .001$; $\eta_p^2 = .51$
Condition x Part**	$F_{2,20} = 6.95$; $p < .01$; $\eta_p^2 = .41$
Condition x Electrode x Epoch***	$F_{80,800} = 3.16$; $p < .001$; $\eta_p^2 = .24$
Condition x Electrode x Part	$F_{16,160} = 0.786$; $p = .70$; $\eta_p^2 = .07$
Condition x Epoch x Part	$F_{10,100} = 1.76$; $p = .07$; $\eta_p^2 = .15$

* $p < .05$; ** $p < .01$; *** $p < .001$

The post-hoc comparisons for the significant two-way interaction of *condition x epoch* showed increased ERPow θ for the experimental condition of rTMS 60 compared to sham until epoch four (20s after the trains of magnetic

stimulation). The experimental condition of rTMS 20 demonstrated increased ERPow synchronisation compared to sham only in epoch one (5s after the trains of magnetic stimulation). The highest synchronisation was during epoch one for rTMS 60 (120.0%) versus rTMS 20 (76.9%) and sham (17.8%). Figure 4-2 illustrates the percentage of ERPow modulation of *condition x epoch* for θ rhythm.

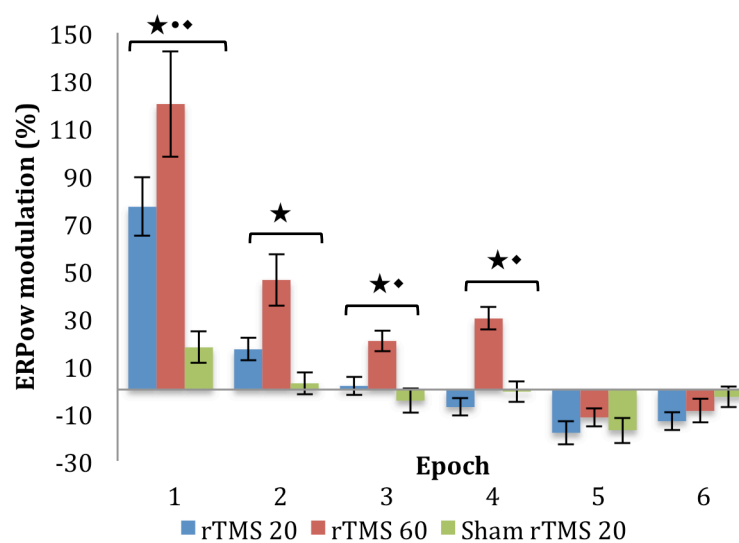


Figure 4-2 ERPow θ as a function of *Condition* and *Epoch*. The figure illustrates EEG synchronisation for rTMS 60 pulses for 20s after magnetic stimulation.
 ★significant rTMS 60 vs. sham; ♦significant rTMS 20 vs. sham
 ♦significant rTMS 60 vs. rTMS 20; ($p < .05$; Bonferroni corrected; $n=11$)

The post-hoc comparisons for the two-way interaction of *condition x electrode* showed increased ERPow θ for rTMS 60 compared to sham across all electrodes. ERPow θ for rTMS 20 compared to sham revealed significant synchronisation in electrodes Fz and C3 only. C3 was the most dominant electrode exhibiting EEG cortical oscillations for both conditions of rTMS 60

(62.6%) and rTMS 20 (33.7%) versus sham (10.4%). Figure 4-3 illustrates the percentage of ERPow modulation of *condition x electrode* for θ rhythm.

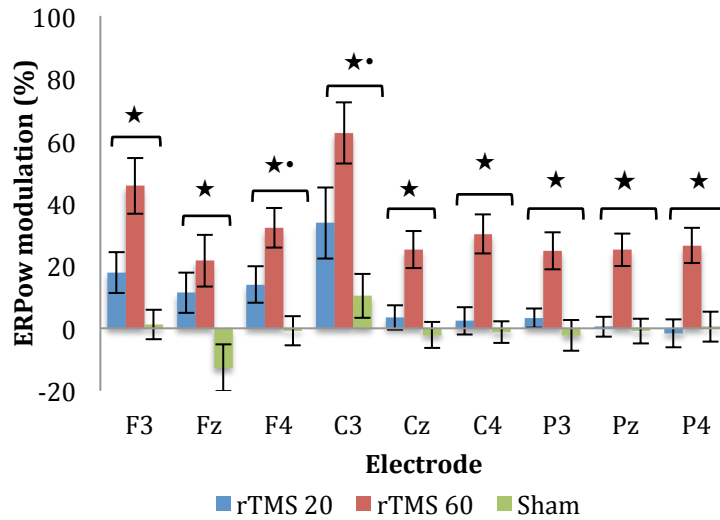


Figure 4-3 ERPow θ as a function of *Condition* and *Electrode*. The figure illustrates EEG synchronisation for rTMS 60 pulses across all electrodes. C3 is the most dominant electrode after magnetic stimulation.
 *significant rTMS 60 vs. sham; •significant rTMS 20 vs. sham
 ($p < .05$; Bonferroni corrected; $n=11$)

The post-hoc comparisons for *condition x epoch x electrode* revealed that rTMS 60 induced more EEG synchronisation than rTMS 20 and sham across all electrodes for 20s after magnetic stimulation. The most sensitive electrode in epoch one was C3, which showed higher ERPow modulations in rTMS 60 (287.9%) and rTMS 20 (223.2%) versus sham (74.6%). Figure 4-4 illustrates the percentage of ERPow modulation of *condition x epoch x electrode* for θ rhythm.

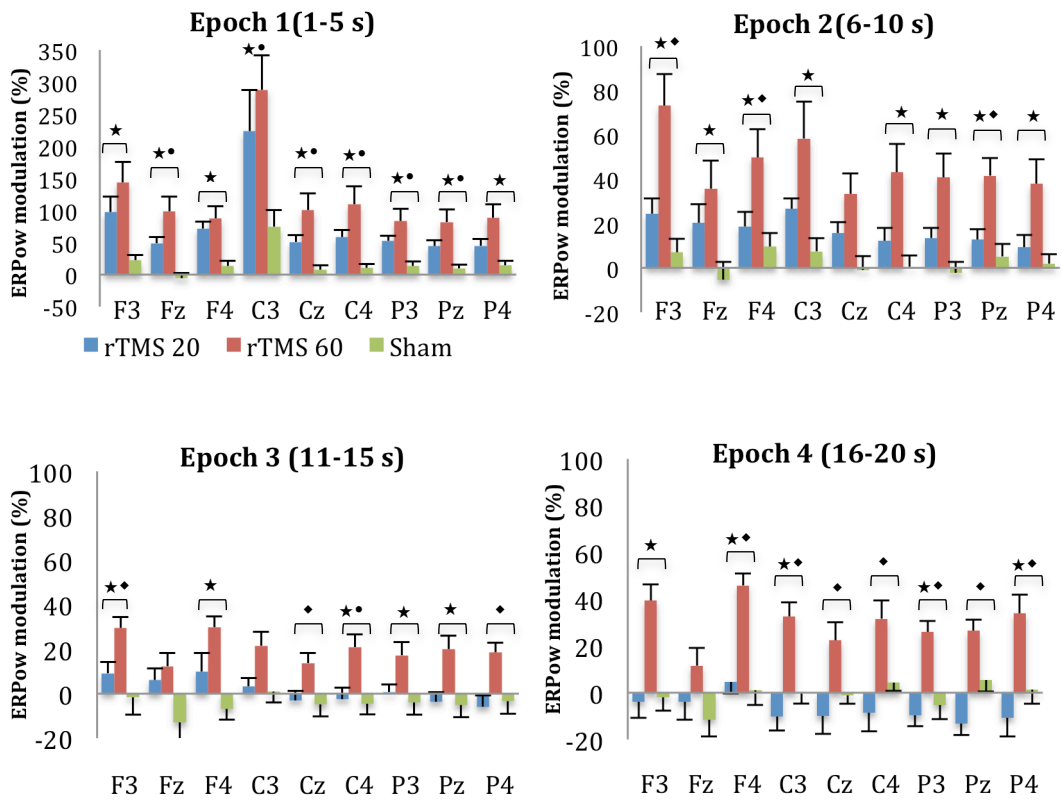


Figure 4-4 ERPow θ as a function of *Condition*, *Electrode*, and *Epoch*. The figure illustrates EEG synchronisation for rTMS 60 pulses across all electrodes for 20s after magnetic stimulation. C3 is the most dominant electrode at epoch one.
 *significant rTMS 60 vs. sham; •significant rTMS 20 vs. sham;
 ♦significant rTMS 60 vs. rTMS 20; ($p < .05$; Bonferroni corrected; $n=11$)

The post-hoc comparisons for *condition* \times *part* did not reveal significant interactions for either rTMS 20 or rTMS 60.

4.4.1.2 ERPow μ

Table 4-2 summarises the ANOVAs of the significant main effects and interactions for ERPow μ .

Table 4-2 ERPow μ

Factors	ERPow μ
Condition	$F_{2,20} = 1.78; p = .19; \eta_p^2 = .15$
Electrode**	$F_{2,9,29,4} = 6.11; p < .01; \eta_p^2 = .38$
Epoch***	$F_{5,50} = 15.22; p < .001; \eta_p^2 = .6$
Part**	$F_{1,10} = 13.75; p < .01; \eta_p^2 = .58$
Condition x Electrode*	$F_{16,160} = 1.85; p < .05; \eta_p^2 = .16$
Condition x Epoch***	$F_{10,100} = 7.06; p < .001; \eta_p^2 = .41$
Condition x Part	$F_{2,20} = 0.17; p = .85; \eta_p^2 = .02$
Condition x Electrode x Epoch***	$F_{80,800} = 1.77; p < .001; \eta_p^2 = .15$
Condition x Electrode x Part***	$F_{16,160} = 3.16; p < .001; \eta_p^2 = .24$
Condition x Epoch x Part*	$F_{10,100} = 2.46; p < .05; \eta_p^2 = .2$

* $p < .05$; ** $p < .01$; *** $p < .001$

The post-hoc comparisons for the significant two-way interaction of *condition x epoch* showed an increase in ERPow μ for the experimental condition of rTMS 20 (32.8%) and rTMS 60 (18.6%) compared to sham (2.1%) only in epoch one for 5s after the trains of magnetic stimulation. Figure 4-5 illustrates the percentage of ERPow modulation of *condition x epoch* for μ rhythm.

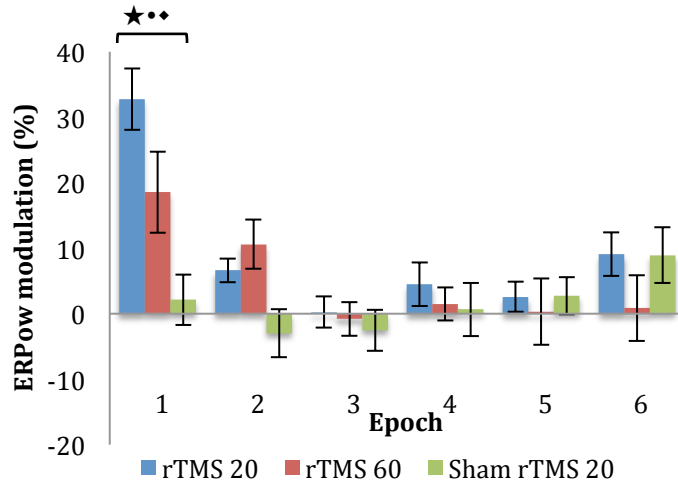


Figure 4-5 ERPow μ as a function of *Condition* and *Epoch*. The figure illustrates EEG synchronisation for rTMS 20 pulses for 5s after magnetic stimulation.
 ★significant rTMS 60 vs. sham; ★significant rTMS 20 vs. sham;
 ♦significant rTMS 60 vs. rTMS 20; ($p < .05$; Bonferroni corrected; $n=11$)

The post-hoc comparisons for *condition x epoch x electrode* revealed that short trains of rTMS 20 induced EEG synchronisation compared to sham in F3, Fz, C3, P3, and P4 electrodes for approximately 5s after trains of magnetic stimulation. At epoch one, C3 demonstrated increased ERPow modulation for rTMS 20 (80.2%) and rTMS 60 (64.0%) compared to sham (21.5%). At epoch two, rTMS 60 had a significant higher EEG oscillation versus sham rTMS for F3, Fz, and P3 electrodes. Figure 4-6 illustrates the percentage of ERPow modulation of *condition x epoch x electrode* for μ rhythm.

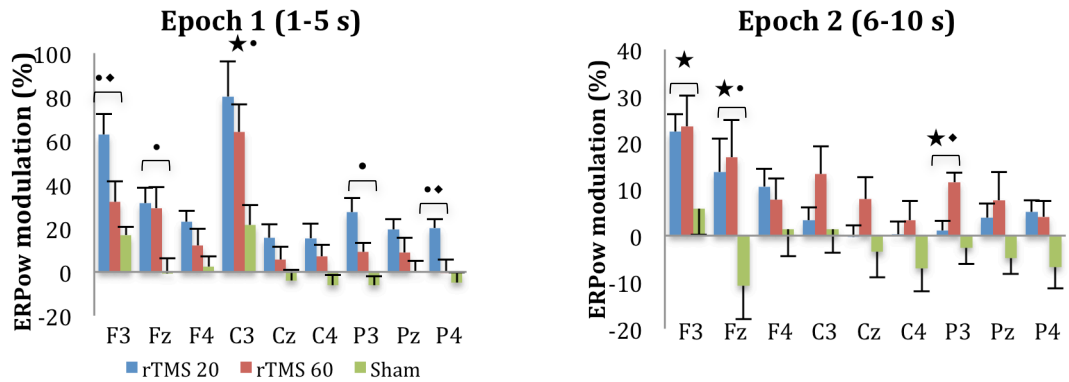


Figure 4-6 ERPow μ as a function of *Condition*, *Epoch*, and *Electrode*. The figure illustrates EEG synchronisation for rTMS 20 pulses and rTMS 60 pulses at selected electrodes for 10s after magnetic stimulation.

★significant rTMS 60 vs. sham; •significant rTMS 20 vs. sham;
 ♦significant rTMS 60 vs. rTMS 20; ($p < .05$; Bonferroni corrected; $n=11$)

The post-hoc comparisons for *condition x epoch x part* showed increased EEG synchronisation for rTMS 20 in epoch one (part A 25.28%, part B 40.23%), and epoch two (part A 3.63%, part B 9.64%). The experimental condition of rTMS 60 showed a significant increase in EEG synchronisation from part A to part B at epoch two only (part A 4.67%, part B 16.53%). Figure 4-7 illustrates the percentage of ERPow modulation of *condition x epoch x part* for μ rhythm.

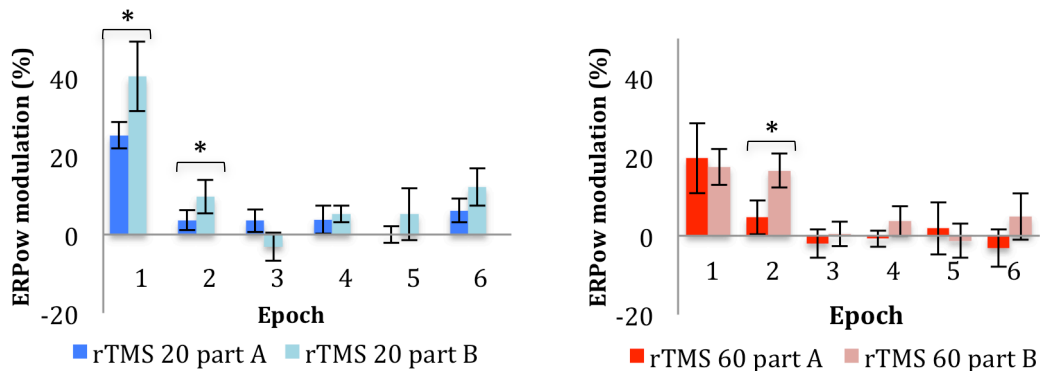


Figure 4-7 ERPow μ as a function of *Condition*, *Epoch*, and *Part*. The figure illustrates cumulative effects of EEG synchronisation for rTMS 20 pulses for 10s after magnetic stimulation.
 *significant part A vs. part B of rTMS 20/rTMS 60; ($p < .05$; Bonferroni corrected; $n=11$)

The post-hoc comparisons for *condition x electrode* did not reveal significant interactions for either rTMS 20 or rTMS 60 across all electrodes.

4.4.1.3 ERPow β

Table 4-3 summarises the ANOVAs of the main effects and interactions for ERPow β .

Table 4-3 ERPow β

Factors	ERPow β
Condition	$F_{2,20} = 2.78$; $p = .09$; $\eta_p^2 = .22$
Electrode*	$F_{2,7,27} = 4.56$; $p < .05$; $\eta_p^2 = .31$
Epoch***	$F_{5,50} = 20.49$; $p < .001$; $\eta_p^2 = .67$
Part	$F_{1,10} = 0.05$; $p = .83$; $\eta_p^2 = .01$
Condition x Electrode**	$F_{16,160} = 2.79$; $p < .01$; $\eta_p^2 = .22$
Condition x Epoch***	$F_{10,100} = 4.23$; $p < .001$; $\eta_p^2 = .3$
Condition x Part***	$F_{2,20} = 20.53$; $p < .001$; $\eta_p^2 = .67$
Condition x Electrode x Epoch***	$F_{80,800} = 2.14$; $p < .001$; $\eta_p^2 = .18$
Condition x Electrode x Part***	$F_{16,160} = 4.15$; $p < .001$; $\eta_p^2 = .29$
Condition x Epoch x Part	$F_{10,100} = 1.6$; $p = .12$; $\eta_p^2 = .14$

* $p < .05$; ** $p < .01$; *** $p < .001$

The post-hoc comparisons for the significant two-way interaction of *condition x epoch* showed higher EEG oscillations for rTMS 20 (15.1%) versus rTMS 60 (3.7%) and sham (2.3%) at epoch one only. Figure 4-8 illustrates the percentage of ERPow modulation of *condition x epoch* for β rhythm.

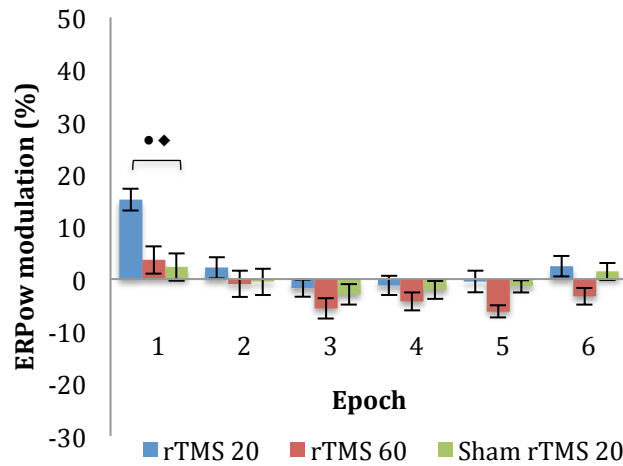


Figure 4-8 ERPow β as a function of *Condition* and *Epoch*. The figure illustrates EEG synchronisation for rTMS 20 pulses for 5s after magnetic stimulation.
 •significant rTMS 20 vs. sham; ♦significant rTMS 60 vs. rTMS 20
 ($p < .05$; Bonferroni corrected; $n=11$)

The post-hoc comparisons for *condition x epoch x electrode* revealed a higher power modulation for rTMS 20 mainly in epoch one compared to sham for C3, Cz, P3, and Pz, and rTMS 60 compared to sham for F4 and C3 electrodes. C3 was the most sensitive electrode at epoch one for rTMS 20 (40.3%) and rTMS 60 (36.7%) compared to sham (10.0%). Figure 4-9 illustrates the percentage of ERPow modulation of *condition x epoch x electrode* for β rhythm.

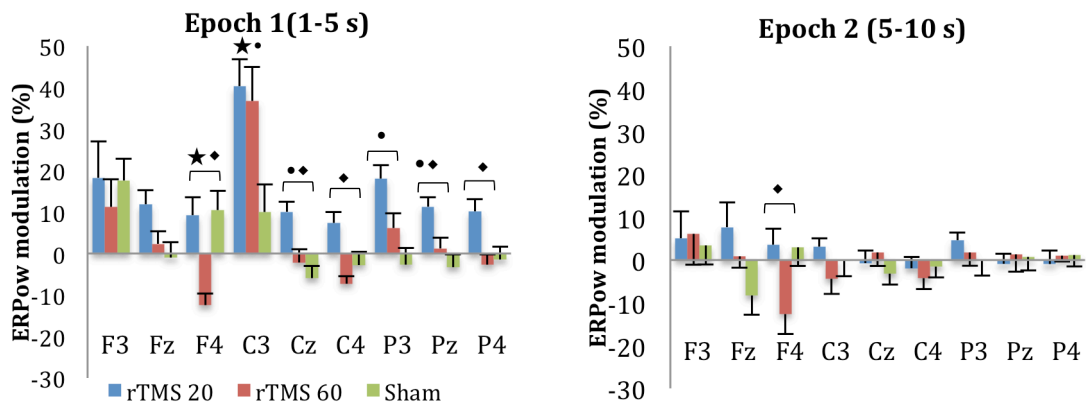


Figure 4-9 ERPow β as a function of *Condition*, *Electrode*, and *Epoch*. The figure illustrates EEG synchronisation for rTMS 20 pulses at mainly central-parietal electrodes for 5s after magnetic stimulation.
 *significant rTMS 60 vs. sham; •significant rTMS 20 vs. sham;
 ♦significant rTMS 60 vs. rTMS 20; ($p < .05$; Bonferroni corrected; $n=11$)

4.4.2 EEG Event-related coherence

This subsection presents the results of ERCoh of 11 subjects for θ , μ , and β of the following nine pairs of electrodes: C3-F3, C3-Fz, C3-F4, C3-C3, C3-Cz, C3-C4, C3-P3, C3-Pz, and C3-P4, referenced to the C3 electrode (the nearest channel to the TMS coil position over M1). This subsection focuses on the main experimental findings, which are discussed in Section 4.5.2 rTMS and interregional functional connectivity. The remaining findings are presented in the subsequent tables.

4.4.2.1 ERCoh θ

Table 4-4 summarises the ANOVAs of the main effects and interactions for ERCoh θ .

Table 4-4 ERCoh θ

Factors	ERCoh θ
Condition	$F_{2,20} = 1.29; p = .3; \eta_p^2 = .12$
Pairs of Electrodes ***	$F_{8,80} = 21.98; p < .001; \eta_p^2 = .69$
Epoch***	$F_{1.7,17.5} = 14.95; p < .001; \eta_p^2 = .6$
Part	$F_{1,10} = 3.59; p = .09; \eta_p^2 = .26$
Condition x Pairs of Electrodes ***	$F_{16,160} = 3.27; p < .001; \eta_p^2 = .25$
Condition x Epoch	$F_{4.3,43} = 2.05; p = .1; \eta_p^2 = .17$
Condition x Part	$F_{2,20} = 2.93; p = .08; \eta_p^2 = .23$
Condition x Pairs of Electrodes x Epoch**	$F_{80,800} = 1.56; p < .01; \eta_p^2 = .13$
Condition x Pairs of Electrodes x Part	$F_{16,160} = 0.97; p = .49; \eta_p^2 = .09$
Condition x Epoch x Part	$F_{10,100} = 0.99; p = .46; \eta_p^2 = .09$

* $p < .05$; ** $p < .01$; *** $p < .001$

At epoch one, the post-hoc comparisons of *condition x epoch x electrode* initially showed a decrease in functional coupling of the C3-F3 pair of electrodes for rTMS 60 (-0.18%), and rTMS 20 (-0.1%) versus sham (-0.07%). However, the subsequent epochs showed an increase in functional coupling for rTMS 60 compared to sham rTMS (epoch two C3-Fz; epoch three C3-Fz, C3-F4; epoch four C3-Cz, C3-C4). Figure 4-10 illustrates the percentage of ERCoh modulation of *condition x epoch x electrode* for θ .

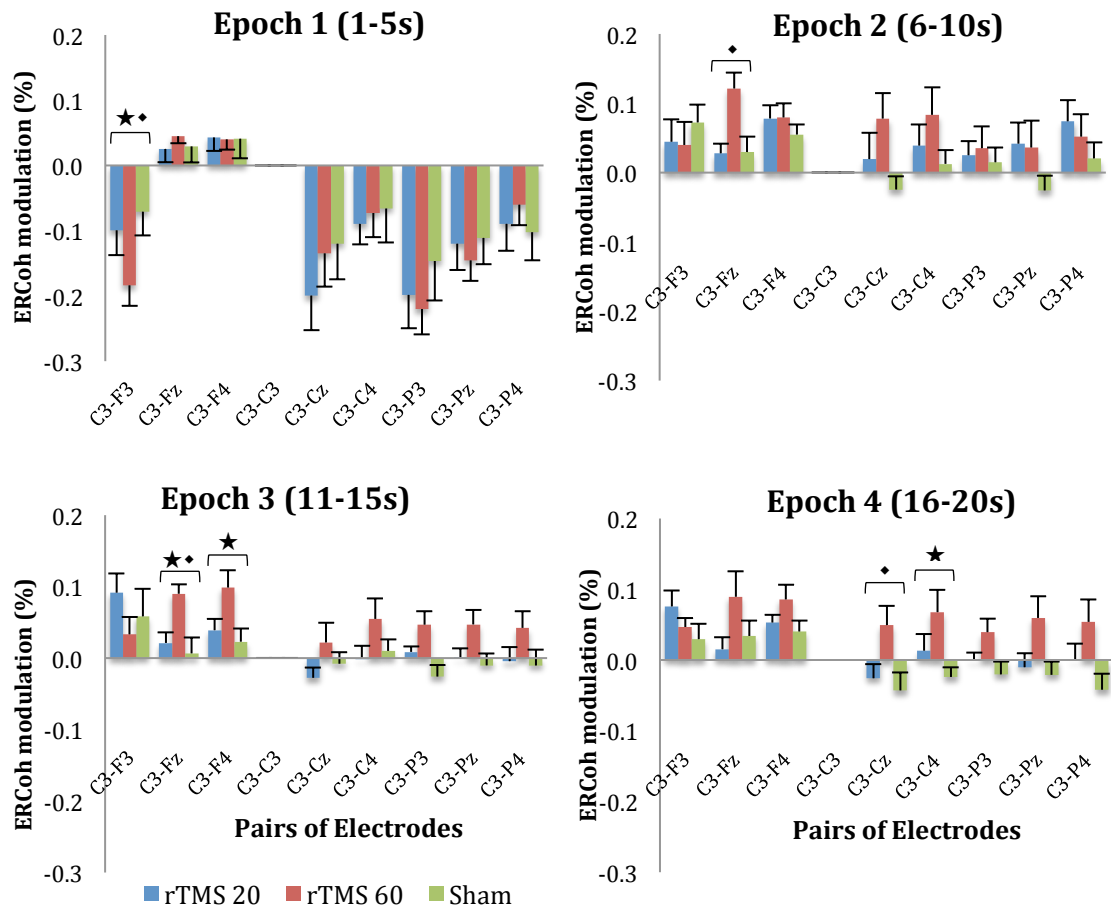


Figure 4-10 ERCoh θ as a function of *Condition*, *Epoch* and *Pairs of electrodes*. The figure illustrates an initial decrease in ERCoh for rTMS 60 pulses for 5s followed by an increase of ERCoh for 15s after magnetic stimulation mainly in the frontal electrodes referenced to C3.
 ★significant rTMS 60 vs. sham; ◆significant rTMS 60 vs. rTMS 20
 ($p < .05$; Bonferroni corrected; $n=11$)

4.4.2.2 ERCoh μ

Table 4-5 summarises the ANOVAs of the main effects and interactions for ERCoh μ . The post-hoc comparisons do not show any significant interactions for any conditions.

Table 4-5 ERCoh μ

Factors	ERCoh μ
Condition	$F_{2,20} = 1.19; p = .33; \eta_p^2 = .11$
Pairs of Electrodes ***	$F_{3,7,36,8} = 9.37; p < .001; \eta_p^2 = .48$
Epoch*	$F_{5,50} = 3.15; p < .05; \eta_p^2 = .24$
Part	$F_{1,10} = 4.77; p = .06; \eta_p^2 = .32$
Condition x Pairs of Electrodes	$F_{16,160} = 1.58; p = .08; \eta_p^2 = .14$
Condition x Epoch*	$F_{10,100} = 2.3; p < .05; \eta_p^2 = .19$
Condition x Part	$F_{2,20} = 0.6; p = .56; \eta_p^2 = .06$
Condition x Pairs of Electrodes x Epoch*	$F_{80,800} = 1.89; p < .05; \eta_p^2 = .16$
Condition x Pairs of Electrodes x Part*	$F_{16,160} = 2.81; p < .05; \eta_p^2 = .22$
Condition x Epoch x Part	$F_{10,100} = 1.04; p = .41; \eta_p^2 = .09$

* $p < .05$; ** $p < .01$; *** $p < .001$

4.4.2.3 ERCoh β

Table 4-6 summarises the ANOVAs of the main effects and interactions for ERCoh β . None of the post-hoc comparisons showed any significant interactions for any conditions.

Table 4-6 ERCoh β

Factors	ERCoh β
Condition	$F_{2,20} = 0.04; p = .96; \eta_p^2 = .004$
Pairs of Electrodes ***	$F_{3,1,30,9} = 17.91; p < .001; \eta_p^2 = .64$
Epoch***	$F_{5,50} = 8.49; p < .001; \eta_p^2 = .46$
Part	$F_{1,10} = 0.12; p = .74; \eta_p^2 = .01$
Condition x Pairs of Electrodes	$F_{16,160} = 1.89; p = .06; \eta_p^2 = .16$
Condition x Epoch	$F_{10,100} = 1.37; p = .21; \eta_p^2 = .12$
Condition x Part	$F_{2,20} = 1.02; p = .38; \eta_p^2 = .09$
Condition x Pairs of Electrodes x Epoch	$F_{80,800} = 1.13; p = .21; \eta_p^2 = .1$
Condition x Pairs of Electrodes x Part*	$F_{16,160} = 3.7; p < .05; \eta_p^2 = .27$
Condition x Epoch x Part	$F_{4,6,45,7} = 0.96; p = .48; \eta_p^2 = .09$

* $p < .05$; ** $p < .01$; *** $p < .001$

4.4.3 MEPs

The ANOVA for MEPs with normalised amplitude showed no significant main effect of *condition* ($F_{2,30} = 2.9$; $p = .07$, $\eta_p^2 = .16$). The MEPs with normalised latency also did not show significant a main effect of *condition* ($F_{2,30} = .03$; $p = .97$, $\eta_p^2 = .002$).

4.5 Discussion

The present experiment was designed to investigate the modulation of motor cortical oscillatory activity in the θ , μ , and β brain rhythms after high frequency rTMS ($\sim 11\text{Hz}$) of varying number of pulses. The main finding of this experiment was the greater EEG power modulation in θ compared to μ and β during short trains of rTMS 60 pulses for 20s post magnetic stimulation. The results indicated that the topography and the temporal dynamics of θ and μ modulations were not identical. The θ rhythm displayed a global topography, whereas μ had a more focal topography. Moreover, the focal μ enhancement dominated earlier after the train of high frequency rTMS for approximately 5s, whilst the global θ enhancement had a relatively longer temporal dynamics of 20s post rTMS.

4.5.1 rTMS and regional oscillatory activity

In this experiment, the spectral analysis of ERPow quantified the modulation of the regional or local oscillatory activity of the motor cortical area after high frequency rTMS of varying pulses. The results confirmed our hypothesis that the trains with relatively higher numbers of pulses (rTMS 60) produced greater

ERPow modulation, with slightly longer duration of EEG aftereffects (20s) than shorter trains of rTMS 20. However, contrary to our earlier prediction that μ rhythm—a variant of α rhythm and the natural frequency of the sensorimotor cortex—would be the dominant frequency after rTMS over M1, it was θ band that showed the highest EEG aftereffects of ERPow modulations followed by α and β brain rhythms.

Previous TMS-EEG co-registration studies showed that magnetic stimulation applied over the sensory or motor cortical area primarily triggered the α and β brain oscillations (Thut & Miniussi, 2009). TMS transiently altered EEG oscillatory activity in the α band (Brignani et al., 2008; Jing & Takigawa, 2000; Oliviero et al., 2003; Sauseng et al., 2009; Veniero et al., 2011; Zarkowski, Shin, Dang, Russo, & Avery, 2006), produced higher EEG power modulation in the β frequency rhythm (Paus et al., 2001; Van Der Werf & Paus, 2006); or triggered EEG synchronisation in α more than β (Fuggetta et al., 2005; Fuggetta et al., 2008; Veniero et al., 2011). However, none of these authors analysed low frequency EEG oscillations such as θ after rTMS over the resting motor cortex.

The rTMS aftereffects in low frequency oscillations of θ and δ were associated more often with magnetic stimulation over the dorsolateral prefrontal cortex (DLPFC) than the sensory or motor cortical areas (Thut & Miniussi, 2009). Schutter *et al.* (2001) applied low frequency 1Hz rTMS at suprathreshold intensities to the right DLPFC for 20 minutes to investigate the rTMS residual effects on mood (Schutter, van Honk, d'Alfonso, Postma, & de Haan, 2001).

They observed an increase in the θ oscillatory activity in the left hemisphere at 25-35 and 55-65 minutes after rTMS associated with reduced anxiety (Schutter et al., 2001). However, the neurophysiologic basis of the rTMS-induced θ oscillations was not explored in their study (Schutter et al., 2001).

Although θ rhythm is conventionally associated with the hippocampus, high-density intracranial EEG (iEEG) recordings have revealed the presence of θ oscillations over widespread regions in the resting human cortex (Cantero et al., 2003; Kahana et al., 2001; Raghavachari et al., 2001; Raghavachari et al., 2006). High-density iEEG recordings of epileptic patients showed θ oscillations scattered across multiple locations in the brain of the same subject in quiet wakefulness, and the absence of functional coupling between the hippocampus and the cerebral cortex during the occurrence of θ oscillations (Cantero et al., 2003). The observations provide evidence that human θ is not confined to the hippocampus, but may also appear in various regions of the cerebral cortex (Cantero et al., 2003; Jacobs et al., 2006; Klimesch, 1999; Mitchell et al., 2008; Rizzuto et al., 2006). Animal studies have also demonstrated that θ oscillations were not restricted to the rodent hippocampus, but could also appear in many regions of the sensorimotor cortex (Basar & Guntekin, 2008; Buzsaki, 2005; Leung & Borst, 1987; Silva, Amitai, & Connors, 1991). The cortical θ rhythms as opposed to the hippocampal θ suggest the presence of independent generators of θ near the surface of the human brain (Caplan et al., 2003; Kahana, Sekuler, Caplan, Kirschen, & Madsen, 1999; Rizzuto et al., 2006). Therefore, the increase in EEG ERPow modulation of θ rhythms after magnetic stimulation

observed in the present study might reflect the presence of independent cortical θ generators over the motor network.

Moreover, in the present experiment, the topography and the temporal dynamics of θ and μ rhythms are distinctly different. The μ rhythm was focally distributed and dominated early for about 5s, whereas the θ oscillations displayed global distribution across multiple locations of the EEG electrodes for 20s after rTMS. The distinct topography and temporal dynamics of θ and μ frequency bands suggest the presence of independent θ and μ generators over the motor network with different reactivity to rTMS. Furthermore, the θ and α brain rhythms have primarily diverse functional and behavioural significance, thus may indicate the difference in their origins (Basar & Guntekin, 2008; Sauseng & Klimesch, 2008).

Nevertheless, the θ oscillations seen in the present study might originate from the thalamus through vast neuronal networks between the cortex and the thalamus (Buzsaki & Draguhn, 2004; Steriade, 2006). Hughes et al. (2004) investigated the cellular mechanisms of θ and α oscillations of the cat lateral geniculate nucleus (LGN) of the thalamus (Hughes et al., 2004). They observed a similar intrinsic neuronal behaviour exhibited by both the α and θ waves at the thalamus (Hughes et al., 2004). High stimulation of mGluR would strongly depolarise the TC neurons, and resulted in α oscillations (Hughes et al., 2004). On the other hand, low stimulation intensity of mGluR with less depolarisation of the TC neurons triggered θ oscillations (Hughes & Crunelli, 2005, 2007; Hughes et al., 2004).

However, the limitation of EEG is that it only allows the investigation of the network properties on a macro-level through the synchronicity of a large population of neurons in the cortex (Komssi & Kahkonen, 2006; Rogasch & Fitzgerald, 2012). It is not possible to explore the network properties on a cellular or micro-level using EEG (Huerta & Volpe, 2009). Therefore, we are unable to establish whether the interactions of rTMS with the cortical θ generators are in parallel with the thalamocortical loops eliciting θ and μ oscillations over the motor cortex.

In the present experiment, the μ rhythm was more synchronised compared to the β frequency band. This result was in line with a previous rTMS/EEG study by Fuggetta *et al.* (2008) who observed higher synchronisation in α (10-12Hz) compared to β (18-22Hz) after short intermittent trains of 5Hz rTMS over the M1 (Fuggetta *et al.*, 2008). The TMS-induced α oscillations during quiet wakefulness might be due to the resetting of the stimulated neurons by TMS to oscillate at the natural frequencies of the motor cortex (Fuggetta *et al.*, 2005; Manganotti *et al.*, 2012; Paus, Sipila, *et al.*, 2001; Rosanova *et al.*, 2009). It may be speculated that the resetting phenomena by rTMS produced synchronous cortical oscillatory brain rhythms generated by the vast recursive loops of cortex-thalamus-cortex pathways (Fuggetta *et al.*, 2005; Manganotti *et al.*, 2012; Paus, Sipila, *et al.*, 2001; Rosanova *et al.*, 2009).

The other aim of the present experiment was to investigate the presence of the cumulative effect between the 20 intermittent trains of rTMS 20 and rTMS 60. In order to address the problem we analysed the difference in the EEG

activity between the first ten trains (part A), and the subsequent ten trains of magnetic stimulations (part B). We predicted that a relatively longer train of rTMS 60 (1200 pulses) would produce a stronger cumulative effect than shorter trains of stimulation. Instead, the relatively shorter train of rTMS 20 (400 pulses) induced a higher cumulative effect in μ rhythm for 5 s after the magnetic stimulation. This result implied that the EEG synchronisation was reached earlier with relatively fewer numbers of pulses during high-frequency rTMS.

This observation was in line with the findings of Aydin-Abidin *et al.* (2006) that shorter high-frequency rTMS trains (10Hz, 600 pulses) were more efficient than longer rTMS trains (10Hz, 1200 pulses) to stimulate the visual cortex of anaesthetised cats (Aydin-Abidin, Moliadze, Eysel, & Funke, 2006). A TMS/PET study by Paus *et al.* (2001) over the DLPFC revealed that 300 pulses of 10Hz rTMS were enough to increase the cortico-cortical connectivity of the stimulated hemisphere (Paus, Castro-Alamancos, & Petrides, 2001). The reason that high frequency rTMS with a large number of pulses did not produce pronounced cumulative effects could be due to the compensatory homeostatic mechanisms of the brain. The homeostatic mechanisms will preserve the safety and the normal functioning of the brain despite internal stimuli or external artificial perturbation (Nelson, Sjostrom, & Turrigiano, 2002; Turrigiano & Nelson, 2000, 2004). Moreover, the local inhibitory interneuronal network involving the complex interplay of ionotropic GABA_A receptors and the metabotropic GABA_B receptors might also play a role in limiting the aftereffects of high-frequency

rTMS with longer trains of magnetic stimulation (Manganotti et al., 2012; McDonnell, Orekhov, & Ziemann, 2007; Thickbroom, 2007; Ziemann, 2004b).

4.5.2 rTMS and interregional functional connectivity

The spectral analysis of EEG coherence represents the physiological changes of the interregional neuronal networks of the cortex (Leocani, Toro, Manganotti, Zhuang, & Hallett, 1997a; Pfurtscheller & Andrew, 1999). It detects small oscillatory activity in shared variance of signals of the frequency domains and measures the spatio-temporal correlation between a pair of signals (Leocani et al., 1997a; Pfurtscheller & Andrew, 1999). The coherence normalises the cross spectrum of two electrodes by the power spectrum of each channel (Nunez & Srinivasan, 2006; Srinivasan, Winter, & Nunez, 2006). The EEG power and coherence of closely spaced electrodes can be correlated due to the effect of volume conduction (Nunez & Srinivasan, 2006). In the present study, the alteration in the functional connectivity between the cortico-cortical areas induced by rTMS was quantified by the spectral analysis of ERCoh.

The ERCoh results showed statistically significant interactions only in the θ band. Initially, we observed a decrease of ERCoh θ of mainly rTMS 60 in the frontal region (C3-F3 pair) ipsilateral to the stimulation site. However, the decrease in functional coupling only lasted for 5s after magnetic stimulation. It was subsequently followed by higher ERCoh modulation of rTMS 60 up to 20 s post stimulation in the frontal and central pairs of electrodes (C3-Fz, C3-F4, C3-Cz, and C3-C4). These results suggested a rebound phenomenon for rTMS 60 during high-frequency magnetic stimulation. In line with the result of the

cumulative effects, the rebound phenomenon observed in ERCoh of rTMS 60 suggested the influence of a cortical compensatory mechanism to ensure the safety of the brain after high frequency artificial stimulation (Ortu, Ruge, Deriu, & Rothwell, 2009; Thickbroom, 2007; Turrigiano & Nelson, 2004). The rebound phenomenon also indicates the effects of robust cortical inhibition after magnetic stimulation (Reis et al., 2008). Previous TMS-EEG investigations observed modulation in EEG coherence either in the α or β frequency rhythms (Fuggetta et al., 2008; Jing & Takigawa, 2000; Oliviero et al., 2003; Strens et al., 2002). The differences in ERCoh results in the present study reflect the different sensitivities, origins, and functional roles of various brain oscillations in response to high frequency rTMS.

4.5.3 MEPs and cortical excitability

The present experiment demonstrated that both short and long trains of high frequency rTMS stimulation modulated the regional and interregional functional connectivity of oscillatory neural activity despite the absence of MEP changes. Maeda et al. (2000) described that 10Hz rTMS had no lasting effect on MEP size after administration of 240 pulses (Maeda et al., 2000b). Several TMS investigations that used MEP as the indirect index of cortical excitability have not found any changes in MEP sizes despite high frequency magnetic stimulations (Daskalakis et al., 2006; Romeo et al., 2000), whereas studies of combined TMS-EEG have demonstrated the ability of EEG to record cortical output even when there is no apparent muscular activity (Thut & Pascual-Leone, 2010b). These observations illustrates that high density EEG is probably

a more sensitive and robust method of measuring cortical activity than MEPs after magnetic stimulation (Thut & Pascual-Leone, 2010b).

Moreover, a combined TMS/EEG study by Mäki and Ilmoniemi (2010) found that the amplitudes of MEP and EEG oscillations were not strongly correlated (Maki & Ilmoniemi, 2010). The authors argued that the cortical excitability component of MEP amplitude fluctuations were specific to the neurons controlling the target muscle, while the EEG signal reflects the sum of activity from a large neuronal population of cortical areas including those that control different muscles (Maki & Ilmoniemi, 2010). Furthermore, MEP, which is commonly used in TMS experiments as an indicator of cortical excitability is relatively far from the TMS source, separated by at least three synapses from TMS (Huerta & Volpe, 2009; Siebner & Rothwell, 2003). In contrast, the scalp EEG signal is nearer to TMS source, and represents the brain's own electrical activity through the synchronous excitatory and inhibitory input of pyramidal dendrites, making it a powerful tool to provide accurate interpretation of cortical output (Rogasch & Fitzgerald, 2012; Taylor et al., 2008; Thut & Pascual-Leone, 2010a).

4.6 Summary

Overall, the present study has offered a new insight into the possible manifestation of the independent human motor cortical θ generators after high-frequency rTMS via non-invasive electrophysiological measurement. Animal studies have also demonstrated that θ oscillations were not restricted to the rodent hippocampus, but could also appear in many regions of the sensorimotor

cortex. On the other hand, clinical studies using intracranial EEG demonstrated the presence of independent cortical θ generators as opposed to the hippocampal θ . Therefore, the increase in EEG ERPow modulation of θ rhythms after magnetic stimulation observed in the present study might reflect the presence of independent cortical θ generators over the motor network. Our study provides an important bridge between animal θ studies and the direct evidence for cortical oscillatory generators using invasive human intracranial recordings. More rTMS/EEG investigations are required to explore the functional significance of rTMS-induced θ oscillations and other brain rhythms in order to understand the dynamics of brain organisation. The subsequent chapter presents our attempt to demonstrate the dichotomy of low versus high frequency magnetic stimulation with low frequency EEG oscillations of δ and θ rhythms.

5. The frequencies of rTMS and cortical oscillations

This chapter continues our investigations of the short-term modulation of motor cortical oscillatory activity after rTMS. The goal of the present experiment was to explore the differential effects of low versus high frequency magnetic stimulation in the modulation of the low frequency δ and θ oscillations. The chapter begins with a brief introduction on the importance of the current experiment, and explicitly outlines the aim of the study. The next section presents the methods specific to the experiment. Next, the chapter outlines a summary of the results consisting of the EEG spectral power and coherence of the frequency ranges analysed in the experiment. Finally, the chapter concludes with a discussion of the main findings, and emphasises the contribution of the present thesis in understanding short-term plasticity-like mechanisms induced by short trains of conventional rTMS protocols.

5.1 Introduction

In humans, low and high stimulation frequencies often result in opposite physiological effects. In particular, studies on the human motor cortex using MEPs as an index of cortical excitability have mainly showed that high frequencies of rTMS, especially at high intensities of stimulation, lead to facilitatory aftereffects on corticospinal excitability, and low frequency rTMS

usually results in suppression of corticospinal excitability (Di Lazzaro et al., 2011; Di Lazzaro et al., 2008; Fitzgerald et al., 2002; Fitzgerald et al., 2006; Khedr, Gilio, & Rothwell, 2004; Maeda et al., 2000b; O'Shea & Walsh, 2007).

However, studies of combined rTMS and EEG over the human motor cortex using low frequency rTMS 1Hz (Brignani et al., 2008) and high frequency rTMS 5Hz (Fuggetta et al., 2008) showed a linear increase of EEG power modulation for the frequency bands of α and β brain rhythms. A recent rTMS-EEG study by Veniero *et al.* (2011) attempted to emulate the classical dichotomy between low versus high frequency rTMS of MEP measurements (Veniero et al., 2011). They explored the modulations of the ongoing oscillatory activity of M1 at rest after high frequency 20Hz rTMS (Veniero et al., 2011), and quantified the EEG oscillatory activity using the same analysis method of ERPow with previous studies (Brignani et al., 2008; Fuggetta et al., 2008). The main reason they chose rTMS 20Hz as the high frequency protocol was because they speculated that the rTMS 5Hz chosen in Fuggetta *et al* (2008) was not high enough to show the difference in EEG activity between high and low frequency of magnetic stimulation (Veniero et al., 2011). However, they also observed increased EEG synchronisation in α (8-12Hz) more than β (13-30Hz) after high frequency 20Hz rTMS, and the α oscillations lasted for 5 minutes (Veniero et al., 2011). Consequently, the three previous rTMS-EEG studies on the motor cortex using different frequencies of magnetic stimulation (Brignani et al., 2008; Fuggetta et al., 2008; Veniero et al., 2011) did not emulate the

classical dichotomy between low versus high frequency rTMS as observed by behavioural measures such as MEPs.

The inability of rTMS-EEG to distinguish the opposite effect of low versus high frequency of magnetic stimulation at the cortical level might be because α and β oscillations are not the best indices to reflect the dichotomy between low versus high frequency (Veniero et al., 2011). A differential effect of low-high frequency rTMS might be better demonstrated by the modulation of other brain rhythms such as θ or γ (Veniero et al., 2011). Therefore, it is important to explore these dichotomy effects by applying various frequencies of rTMS and exploring the modulation of EEG oscillatory properties in low frequency oscillations (LFO) such as δ and θ as well as α and β brain rhythms.

5.2 Aim

The aim of the present experiment was to investigate whether the various frequencies of magnetic stimulation would induce different effects in EEG oscillatory activity at rest, particularly in LFO. To address this question, we applied low frequency 1Hz rTMS, and high frequency 5Hz and 10Hz rTMS over M1 in normal, healthy individuals. The other parameters of stimulation (20 intermittent trains of 20 rTMS pulses at 100% RMT) were held constant across the three experimental protocols. The rTMS-induced oscillations were analysed using spectral analysis of ERPow and ERCoh for the frequency ranges of δ , θ , α and β .

5.3 Methods

This section describes the specific methods employed in the present experiment to explore the possible dichotomy in the modulation of motor cortical oscillatory activity between low and high frequency rTMS protocols. The subsections present the participants, experimental paradigms, the procedural steps of TMS recording, EEG data acquisition and the EEG spectral analysis applied in the present experiment.

5.3.1 Participants

Forty-four healthy volunteers (18 males, mean age 23.73 ± 2.5 years) participated in the study. None of the subjects had a medical history of neurological disorder, head injury or were on medications.

5.3.2 Experimental design

The experiment was designed to look at the modulation of low frequency 1Hz rTMS, and high frequency 5Hz and 10Hz rTMS on cortical oscillations. Forty-four healthy volunteers were randomly divided into four experimental groups with eleven subjects in each group. The between-subject groups received one of the four experimental conditions (rTMS 1Hz, rTMS 5Hz, rTMS 10Hz, or sham rTMS 10Hz). Active rTMS and sham rTMS were applied over the left M1 simultaneously with online EEG data recordings. A total number of 400 stimuli (20 trains of 20 magnetic pulses) were applied for each of the three frequencies of stimulation. The duration of each train for 1Hz rTMS was 20s, the intertrain interval was 30s, and the rTMS was applied for 16-min 40s. As for 5Hz rTMS,

the duration of each train was 4s, the intertrain interval was 30s, and the rTMS was applied for 11-min 20s. For 10Hz rTMS the duration of each train was 2s, the intertrain interval was 30s and the rTMS was applied for 10-min and 40s.

Figure 5-1 presents the experimental paradigm.

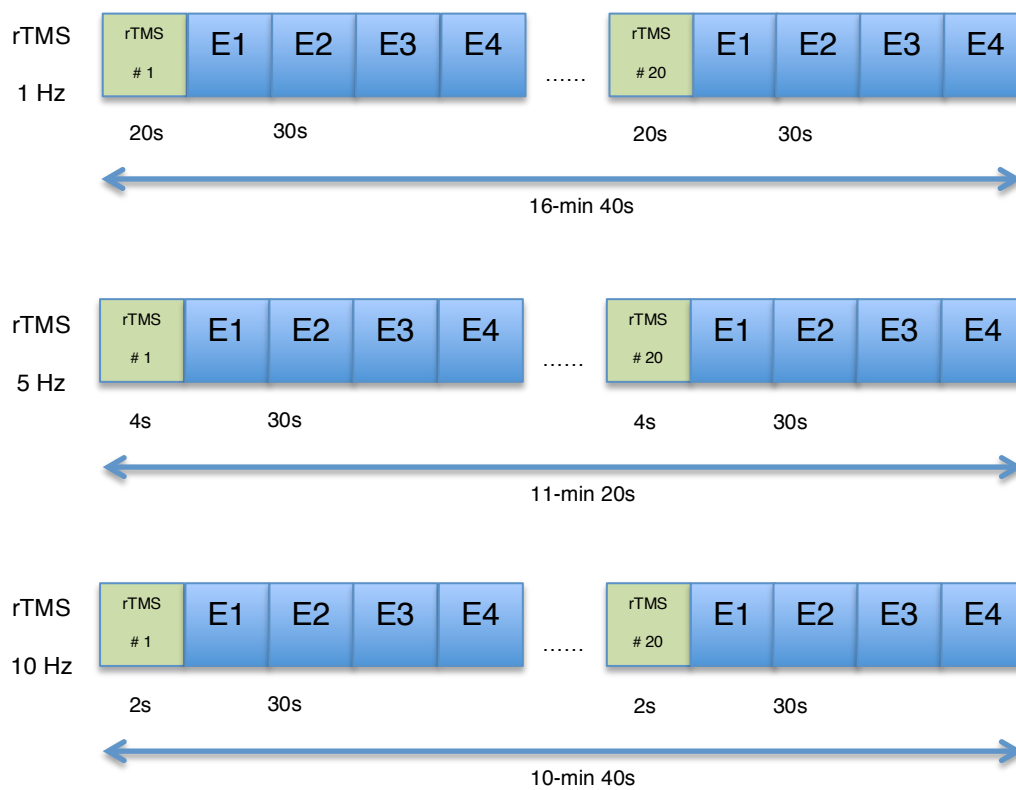


Figure 5.1 Experimental paradigm of 20 trains of 20 magnetic pulses of rTMS 1Hz, 5Hz and 10Hz.

5.3.3 TMS-EEG recording

TMS was carried out with a high-power Magstim-Rapid stimulator (Magstim, Whitland, Dyfed, UK). The EEG data were acquired using a MR compatible EEG amplifier (SD MRI 32, Micromed, Treviso, Italy) and an electrode cap of 30 Ag/AgCl electrodes placed according to a 10/10 (modified) system.

5.3.4 EEG spectral analysis

EEG data were analysed with commercial software (Vision Analyser, Brain Vision, Munich, Germany). The EEG analysis began one second after rTMS in order to eliminate large TMS artifacts contaminating the EEG signal. The EEG data were segmented into temporal windows of identical length (2s containing 2048 data points) for four time intervals. The time intervals were as follows: first epoch (1-5s), second epoch (6-10s), third epoch (11-15s), and fourth epoch (16-20s) as reference epoch. Each epoch was comprised of 40 trials for the four groups of stimulation (rTMS 1Hz, rTMS 5Hz, rTMS 10Hz, and sham rTMS 10Hz). EEG signals were filtered (1-40Hz, slope 24 dB/octave) and a notch filter (50Hz) applied to all channels. Segments with values outside the range of ± 70 μV were rejected during the semi-automatic epoch rejection procedure. A mean of 25.0 ± 6.1 of clean data out of 40 trials for each epoch were extracted from the four experimental groups.

Nine electrodes (F3, Fz, F4, C3, Cz, C4, P3, Pz, and P4) were chosen for EEG analysis because of their proximity to the motor cortex. For each subject, epoch and frequency of stimulation, a discrete FFT of the segments was computed for the nine electrodes, and then averaged. Recordings were non-overlapping Hamming-windowed to control spectral leakage. Broadband power changes were acquired by averaging the power values of δ (1-3Hz), θ (4-7Hz), μ (10-12Hz) and β (13-30Hz) frequency bands. The output data were imported into Microsoft Excel, to calculate ERPow and ERCoh in order to

reduce the effects of inter-subject and inter-electrode variations. The baseline power before stimulation was used as a reference.

5.3.5 Statistical analysis

Spectral analysis of ERPow and ERCoh was submitted to repeated measures ANOVAs for δ , θ , μ , and β frequency bands. Three-way ANOVAs were applied with the factors: *rTMS frequency* (1Hz, 5Hz, 10Hz, and sham 10Hz); *epoch* (first epoch, 1-5s; second epoch, 6-10s; third epoch, 11-15s); and *electrode* (F3, Fz, F4, C3, Cz, C4, P3, Pz and P4) for ERPow analyses or *pair of electrodes* (C3-F3, C3-Fz, C3-F4, C3-C3, C3-Cz, C3-C4, C3-P3, C3-Pz, and C3-P4) for ERCoh analyses.

5.4 Results

This section presents the experimental findings of the current experiment. The results of ERPow and ERCoh of the four frequency ranges (δ , θ , μ , and β) will be presented in the respective subsections and will be discussed in greater detail in the subsequent discussion section. No adverse side effects were reported by any of the participants during all levels of the experiment.

5.4.1 EEG Event-related power

The perturbation of brain rhythms was present in the participants at the frequencies of rTMS delivered over the left M1. This was determined by evaluating the individual EEG responses using spectral analysis of ERPow transformation, which reflected the regional oscillatory activity of neural assemblies for the frequency bands from 1-30Hz. The differences between

rTMS 1Hz, rTMS 5Hz, rTMS 10Hz, and sham rTMS 10Hz experimental groups are clearly seen in Figure 5.2 where the mean ERPow for all the four groups is superimposed.

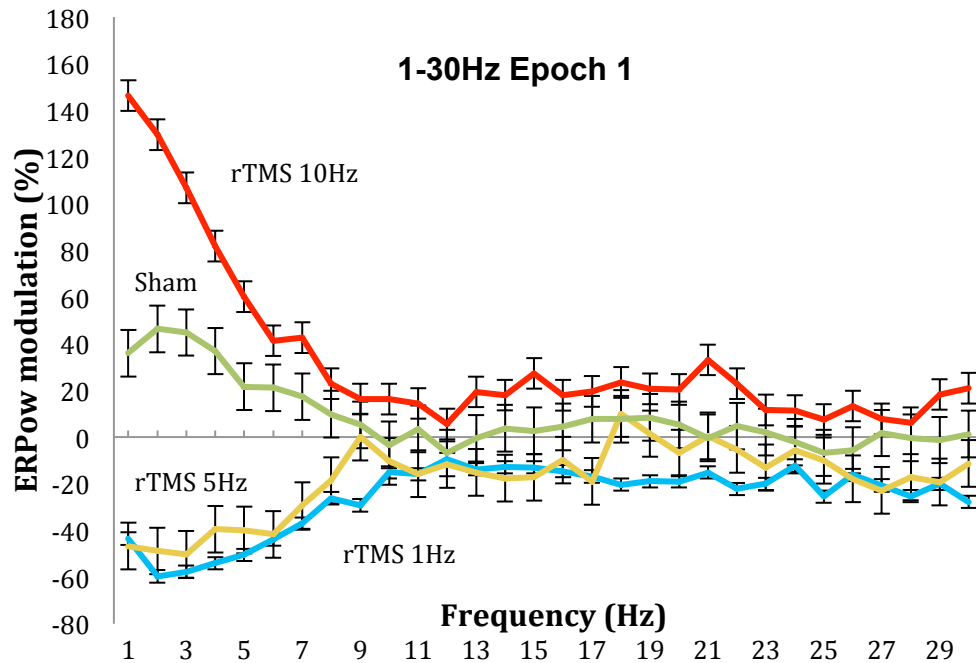


Figure 5-2 ERPow transformation from 1 to 30Hz, for all the electrodes analysed and the four groups of rTMS Frequency: rTMS 1Hz (n=11), rTMS 5Hz (n=11), rTMS 10Hz (n=11), and sham rTMS 10Hz (n=11). The figure shows the frequency-dependant effect of rTMS on modulation of neural oscillations mostly in the δ (1-3Hz) and θ (4-7Hz) frequency ranges.

Our prediction that rTMS modulates low frequency oscillations of δ and θ more than μ and β was verified by the results presented in Figure 5.2. The dichotomy between low and high frequency rTMS is clearly seen in the frequency bands of 1-7Hz. The group receiving active rTMS 10Hz shows an enhancement of EEG ERPow modulation in the frequency ranges of 1-7Hz, whereas groups of active rTMS 1Hz and active rTMS 5Hz exhibit decrease of ERPow in the same low frequency rhythms.

In order to summarise the data, and because spectra from all electrodes have similar shapes, we averaged the ERPow transformation of the EEG electrodes for four frequency bands of δ , θ , μ and β . The subsection on ERPow focuses on the main experimental findings, which will be discussed in Section 5.5.1 rTMS and regional oscillatory activity. The rest of the other findings are presented in the subsequent tables.

5.4.1.1 ERPow δ

Table 5-1 summarises the ANOVAs of the main effects and interactions for ERPow δ .

Table 5-1 ERPow δ

Factors	ERPow δ
rTMS Frequency***	$F_{3,40} = 45.05; p < .001; \eta_p^2 = .77$
Epoch***	$F_{1,6,63.7} = 29.6; p < .001; \eta_p^2 = .43$
Electrode***	$F_{4,5,179} = 12.07; p < .001; \eta_p^2 = .23$
rTMS Frequency x Epoch***	$F_{4,8,63.7} = 60.33; p < .001; \eta_p^2 = .82$
rTMS Frequency x Electrode***	$F_{13,4,179} = 10.32; p < .001; \eta_p^2 = .4$
rTMS Frequency x Epoch x Electrode***	$F_{16,3,217} = 9.05; p < .001; \eta_p^2 = .4$

* $p < .05$; ** $p < .01$; *** $p < .001$

The post-hoc comparisons for the significant interaction of *rTMS frequency x epoch* showed that there was a significant EEG synchronisation of ERPow modulation for rTMS 10Hz compared with sham for 10s after magnetic stimulation [epoch one: rTMS 10Hz (127.5%) vs. sham (42.3%); epoch 2: rTMS 10Hz (53.6%) vs. sham (7.7%)]. In contrast, there was an opposite decrease of ERPow modulation (desynchronisation) for rTMS 1Hz and rTMS 5Hz compared with sham for 10s post rTMS [epoch one: rTMS 1Hz (-53.7%), rTMS 5Hz (-48.6%) vs. sham (42.3%), epoch two: rTMS 1Hz (-52.6%), rTMS 5Hz (-48.7%)

vs. sham (7.7%]). Figure 5-3 illustrates the percentage of ERPow modulation of *rTMS frequency x epoch* for δ rhythm.

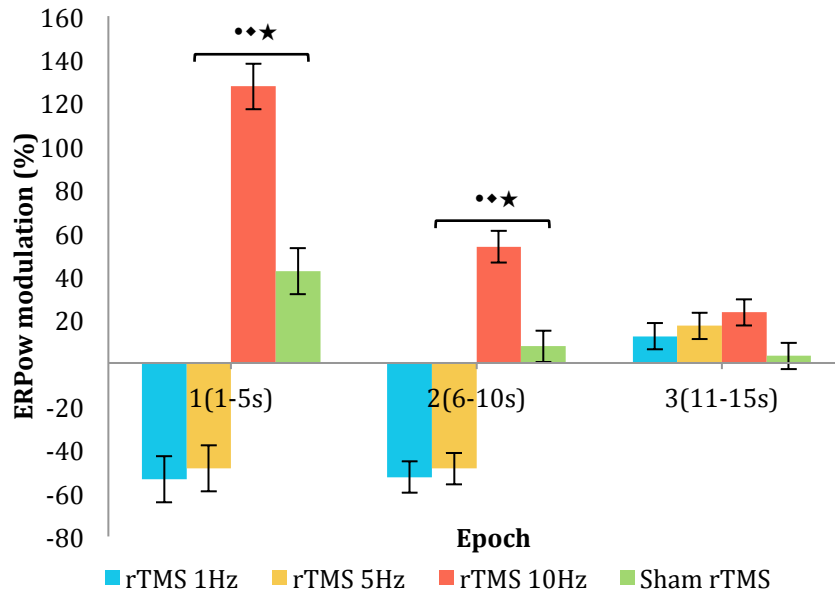


Figure 5-3 ERPow δ as a function of *rTMS Frequency* and *Epoch of time*. The figure illustrates EEG synchronisation for rTMS 10Hz and desynchronisation for rTMS 1Hz and 5Hz compared to sham for 10s after magnetic stimulation.

- significant rTMS 1Hz vs. sham; ♦ significant rTMS 5Hz vs. sham;
- ★ significant rTMS 10Hz vs. sham ($p < .05$; Bonferroni corrected; $n = 44$)

The post-hoc comparisons for the significant interaction of *rTMS frequency x electrode* showed increased ERPow δ for rTMS 10Hz and decreased ERPow δ for rTMS 1Hz and 5Hz versus sham across all electrodes. C3 was the most dominant electrode exhibiting EEG synchronisation for rTMS 10Hz (125%), and desynchronisation for rTMS 1Hz (-39%) and rTMS 5Hz (-21%) versus sham (30%). Figure 5-4 illustrates the percentage of ERPow modulation of *rTMS frequency x electrode* for δ rhythm.

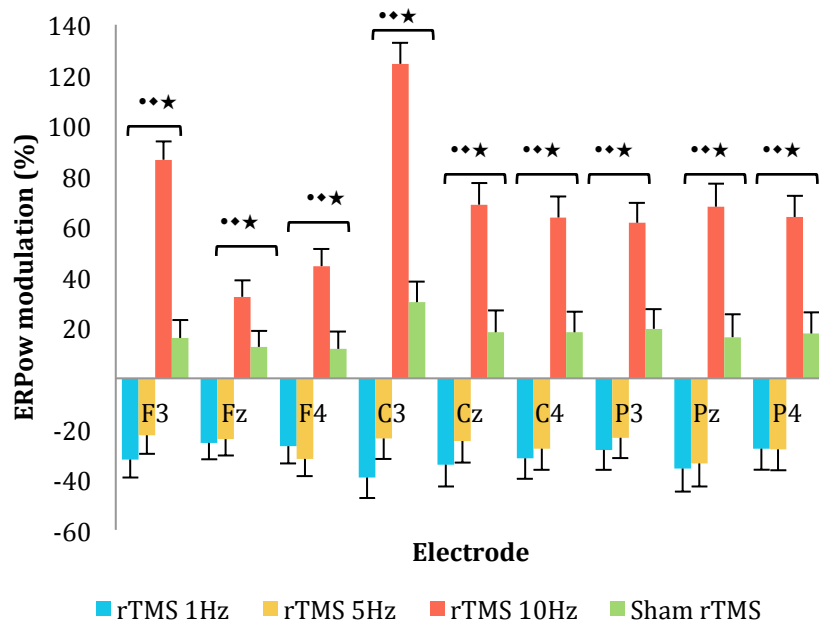


Figure 5-4 ERPow δ as a function of *rTMS Frequency* and *Electrode*. The figure illustrates EEG synchronisation for rTMS 10Hz and desynchronisation for rTMS 1Hz and 5Hz compared to sham across all electrodes after magnetic stimulation. C3 is the most sensitive electrode.
 •significant rTMS 1Hz vs. sham; ♦significant rTMS 5Hz vs. sham;
 ★significant rTMS 10Hz vs. sham ($p < .05$; Bonferroni corrected; $n = 44$)

The post-hoc comparisons for the significant interaction of *rTMS frequency x epoch x electrode* showed EEG synchronisation in rTMS 10Hz and desynchronisation in rTMS 1Hz and rTMS 5Hz versus sham across all electrodes for 10s after magnetic stimulation. C3 was the most sensitive electrode affected by the experimental manipulations [epoch one: rTMS 10Hz (270.9%), rTMS 1Hz (-63.3%), rTMS 5Hz (-51.7%), sham (73.9%); epoch two: rTMS 10Hz (73.1%), rTMS 1Hz (-63.7%), rTMS 5Hz (-47.5%), sham (11.3%)]. Figure 5-5 illustrates the percentage of ERPow modulation of *rTMS frequency x epoch x electrode* for δ rhythm. Figure 5-6 illustrates the topographic brain maps of ERPow for δ frequency range.

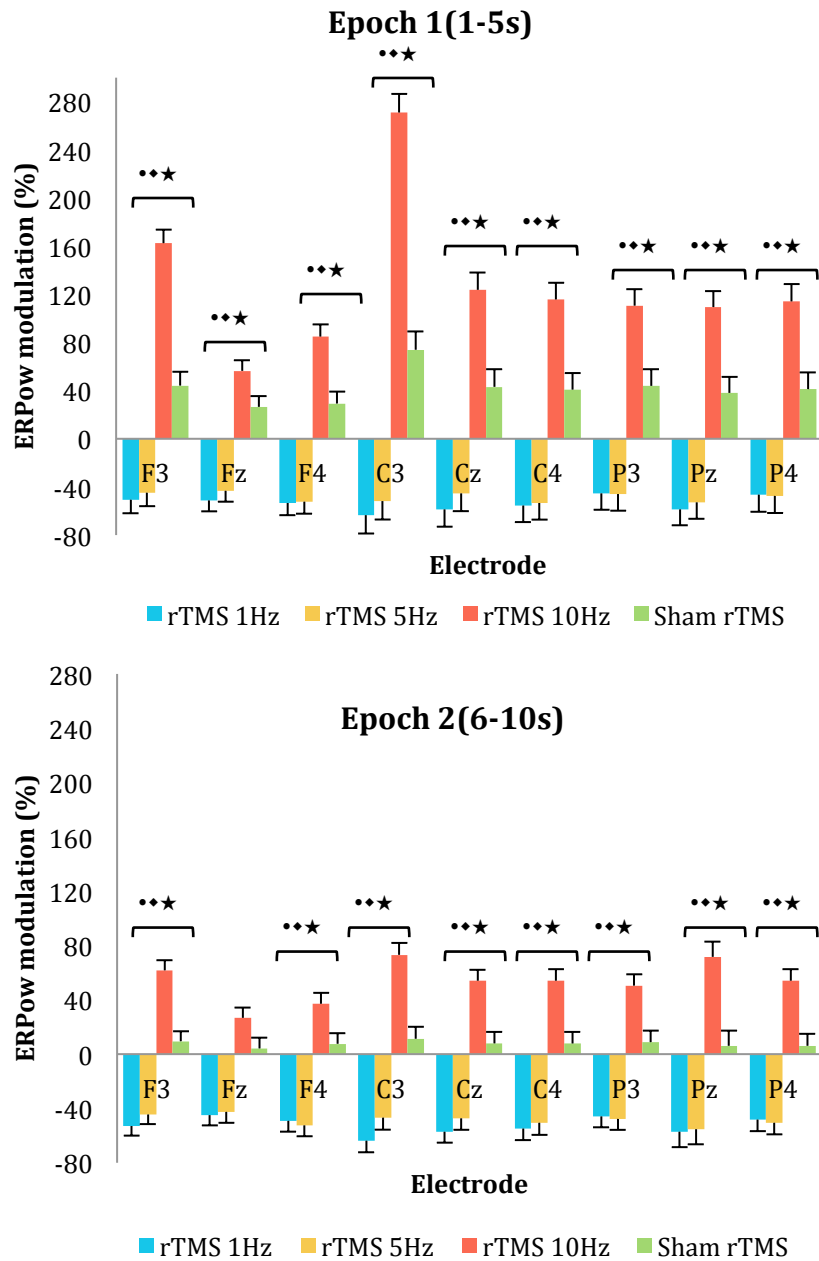


Figure 5-5 ERPow δ as a function of *rTMS Frequency*, *Epoch of time*, and *Electrode*. The figure illustrates EEG synchronisation for rTMS 10Hz and desynchronisation for rTMS 1Hz and 5Hz compared to sham across all electrodes for 10s after magnetic stimulation. C3 is the most sensitive electrode in epoch 1.

- significant rTMS 1Hz vs. sham; ♦significant rTMS 5Hz vs. sham;
- ★significant rTMS 10Hz vs. sham ($p < .05$; Bonferroni corrected; $n = 44$)

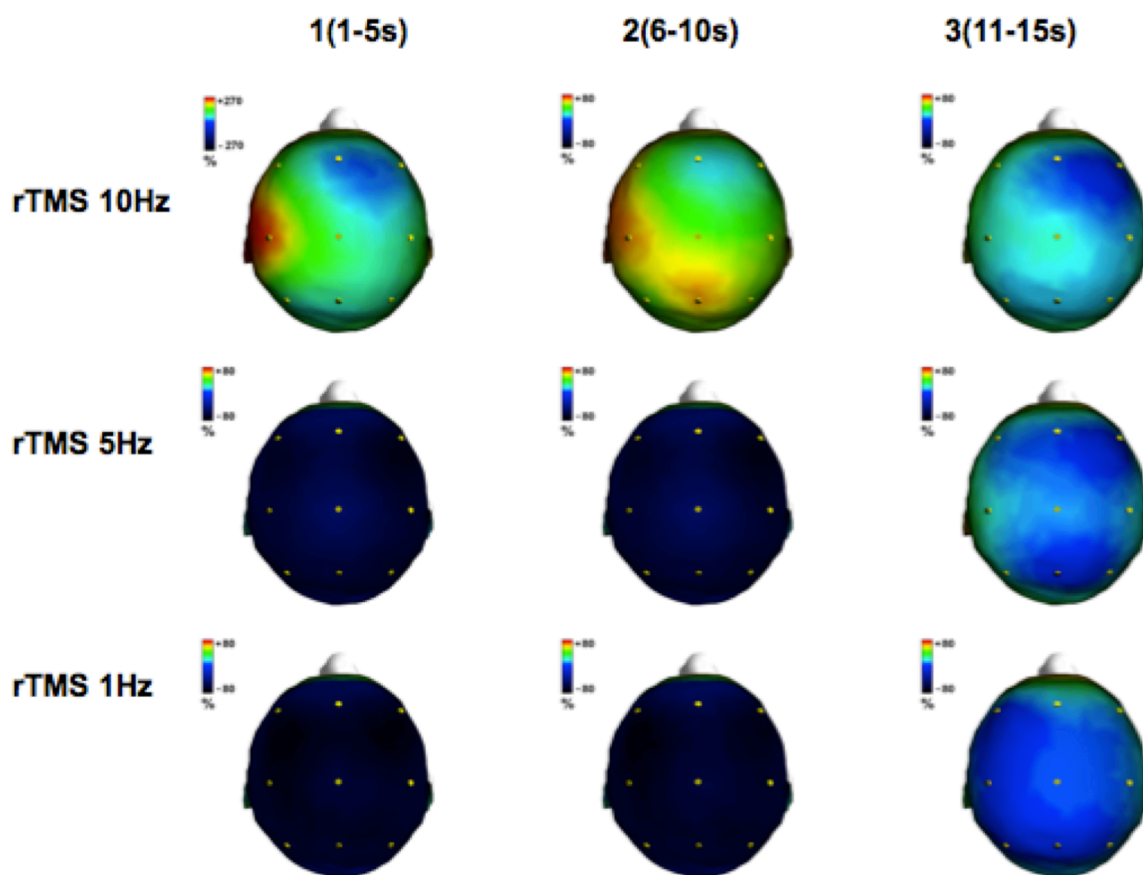


Figure 5-6 Topographic brain maps of ERPow δ . The figure illustrates EEG synchronisation for rTMS 10Hz and desynchronisation for rTMS 1Hz and 5Hz compared to sham across all electrodes for 10s after magnetic stimulation.

5.4.1.2 ERPow θ

Table 5-2 summarises the ANOVAs of the main effects and interactions for ERPow θ .

Table 5-2 ERPow θ

Factors	ERPow θ
rTMS Frequency***	$F_{3,40} = 33.36; p < .001; \eta_p^2 = .71$
Epoch***	$F_{2,80} = 21.61; p < .001; \eta_p^2 = .35$
Electrode**	$F_{4,9,194.4} = 3.76; p < .01; \eta_p^2 = .09$
rTMS Frequency x Epoch***	$F_{6,80} = 49.25; p < .001; \eta_p^2 = .79$
rTMS Frequency x Electrode***	$F_{14,6,194.4} = 5.62; p < .001; \eta_p^2 = .3$
rTMS Frequency x Epoch x Electrode***	$F_{21,7,289.6} = 4.7; p < .001; \eta_p^2 = .26$

* $p < .05$; ** $p < .01$; *** $p < .001$

The post-hoc comparisons for the significant interaction of *rTMS frequency x epoch* showed that there was a significant EEG synchronisation for rTMS 10Hz (56.5%) for 5s after magnetic stimulation. In contrast, there was a desynchronisation of EEG oscillations for rTMS 1Hz and 5Hz for 10s after magnetic stimulation [epoch one: rTMS 1Hz (-46.4%), rTMS 5Hz (-37.6 %) vs. sham (24.2%); epoch two: rTMS 1Hz (-38.7%), rTMS 5Hz (-32.5%) vs. sham (5.1%)]. Figure 5-7 illustrates the percentage of ERPow modulation of *rTMS frequency x epoch* for θ rhythm.

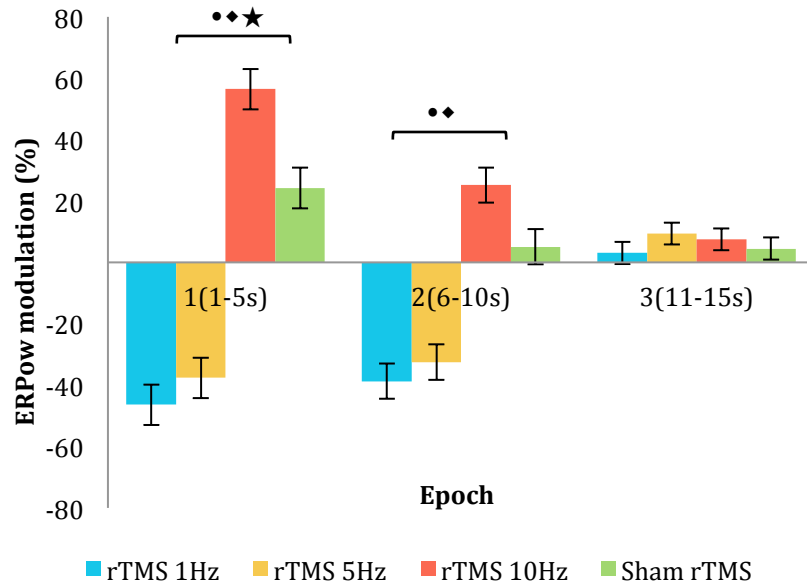


Figure 5-7 ERPow θ as a function of *rTMS Frequency* and *Epoch of time*. The figure illustrates EEG synchronisation for rTMS 10Hz and desynchronisation for rTMS 1Hz and 5Hz compared to sham for 10s after magnetic stimulation.
 •significant rTMS 1Hz vs. sham; ♦significant rTMS 5Hz vs. sham;
 ★significant rTMS 10Hz vs. sham ($p < .05$; Bonferroni corrected; $n = 44$)

The post-hoc comparisons for the significant interaction of *rTMS frequency* \times *electrode* showed a similar synchronisation effect for rTMS 10Hz and desynchronisation for rTMS 1Hz and 5Hz compared with sham across all electrodes after magnetic stimulation. C3 was the most dominant electrode exhibiting EEG synchronisation for rTMS 10Hz (53%), and EEG desynchronisation for rTMS 1Hz (-36%) and rTMS 5Hz (-22%) versus sham (17%). Figure 5-8 illustrates the percentage of ERPow modulation of *rTMS frequency* \times *electrode* for θ rhythm.

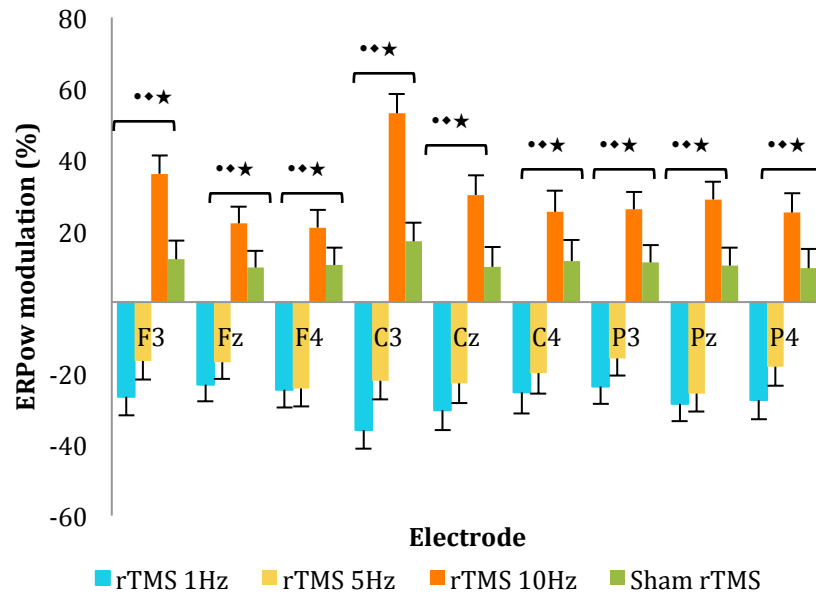


Figure 5-8 ERPow θ as a function of *rTMS Frequency* and *Electrode*. The figure illustrates EEG synchronisation for rTMS 10Hz and desynchronisation for rTMS 1Hz and 5Hz compared to sham across all electrodes after magnetic stimulation. C3 is the most sensitive electrode.
 • significant rTMS 1Hz vs. sham; ♦ significant rTMS 5Hz vs. sham;
 ★ significant rTMS 10Hz vs. sham ($p < .05$; Bonferroni corrected; $n = 44$)

The post-hoc comparisons for the significant interaction of *rTMS frequency* \times *epoch* \times *electrode* showed EEG synchronisation in rTMS 10Hz and desynchronisation in rTMS 1Hz and rTMS 5Hz versus sham across all electrodes for 10s after magnetic stimulation. C3 was the most sensitive electrode affected by the experimental manipulations [epoch one: rTMS 10Hz (115.9%), rTMS 1Hz (-55.3%), rTMS 5Hz (-38.4%), sham (39.8%); epoch two: rTMS 10Hz (32.9%), rTMS 1Hz (-49.3%), rTMS 5Hz (-33.7%), sham (5.2%)]. Figure 5-9 illustrates the percentage of ERPow modulation of *rTMS frequency* \times *epoch* \times *electrode* for θ rhythm. Figure 5-10 illustrates the topographic brain maps of ERPow for θ frequency range.

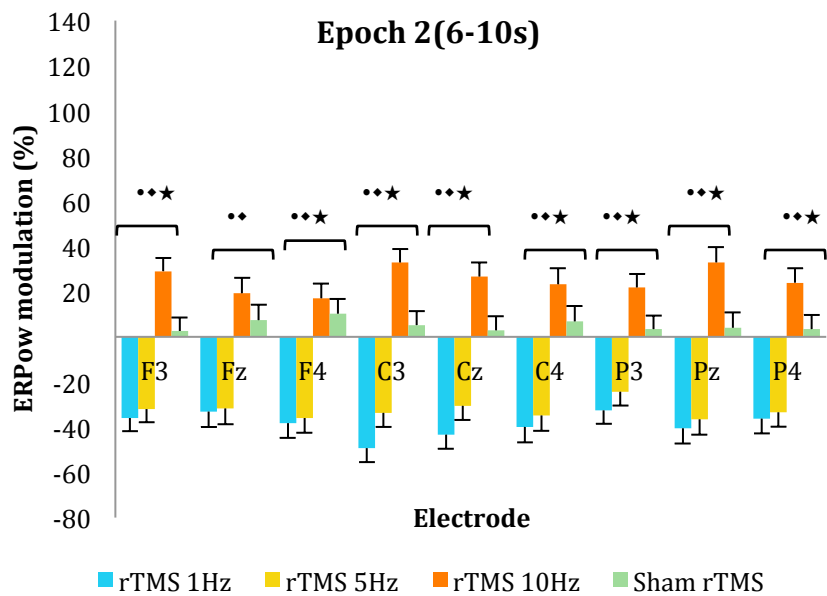
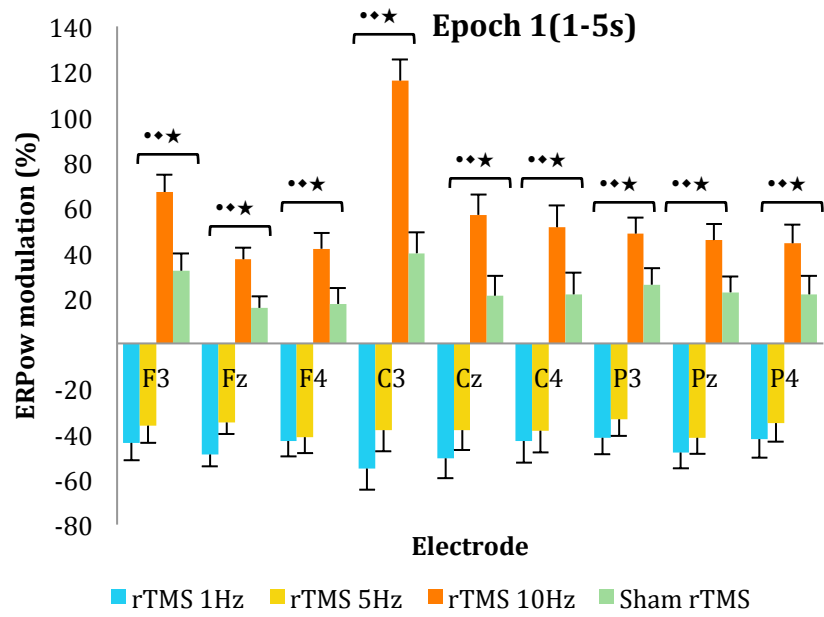


Figure 5-9 ERPow θ as a function of *rTMS Frequency*, *Epoch of time*, and *Electrode*. The figure illustrates EEG synchronisation for rTMS 10Hz and desynchronisation for rTMS 1Hz and 5Hz compared to sham across all electrodes for 10s after magnetic stimulation. C3 is the most sensitive electrode in epoch 1.

- significant rTMS 1Hz vs. sham; ◆ significant rTMS 5Hz vs. sham;
- ★ significant rTMS 10Hz vs. sham ($p < .05$; Bonferroni corrected; $n = 44$)

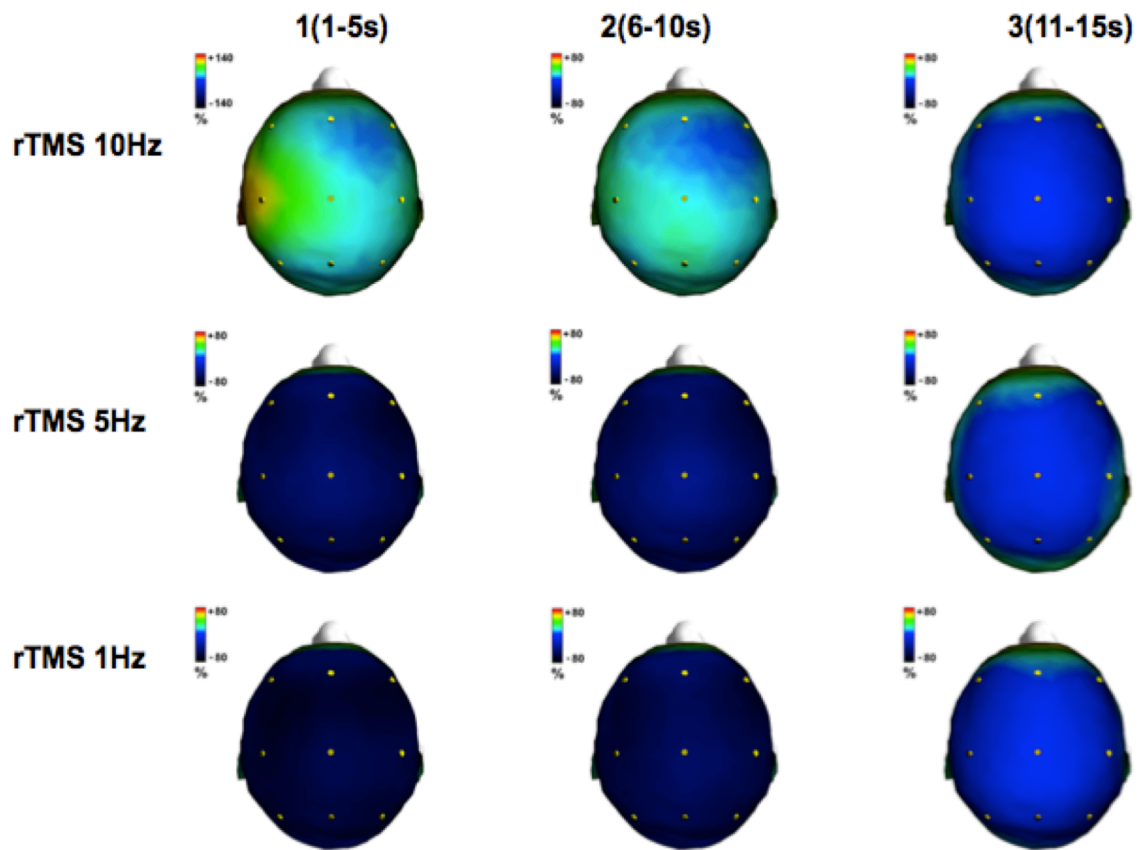


Figure 5-10 Topographic brain maps ERPow θ . The figure illustrates EEG synchronisation for rTMS 10Hz and desynchronisation for rTMS 1Hz and 5Hz compared to sham for 10s after magnetic stimulation.

5.4.1.3 ERPow μ

Table 5-3 summarises the ANOVAs of the main effects and interactions for ERPow μ .

Table 5-3 ERPow μ

Factors	ERPow μ
rTMS frequency***	$F_{3,40} = 9.56; p < .001; \eta_p^2 = .42$
Epoch*	$F_{1,64.4} = 3.71; p < .05; \eta_p^2 = .09$
Electrode*	$F_{4,7,187.4} = 2.54; p < .05; \eta_p^2 = .06$
rTMS frequency x Epoch***	$F_{4,8,64.4} = 11.09; p < .001; \eta_p^2 = .45$
rTMS frequency x Electrode***	$F_{14,1,187.4} = 3.38; p < .001; \eta_p^2 = .2$
rTMS frequency x Epoch x Electrode***	$F_{26,5,353.2} = 2.74; p < .001; \eta_p^2 = .17$

* $p < .05$; ** $p < .01$; *** $p < .001$

The post-hoc comparisons for the significant interaction of *rTMS frequency x epoch* showed that there was a significant EEG desynchronisation for rTMS 1Hz compared with sham for 10s after magnetic stimulation [epoch one: rTMS 1Hz (-20.7) vs. sham (2.6%); epoch two: rTMS 1Hz (-20.0%) vs. sham (1.8%)]. Figure 5-11 illustrates the percentage of ERPow modulation of *rTMS frequency x epoch* for μ rhythm. None of the other post-hoc interactions are significant.

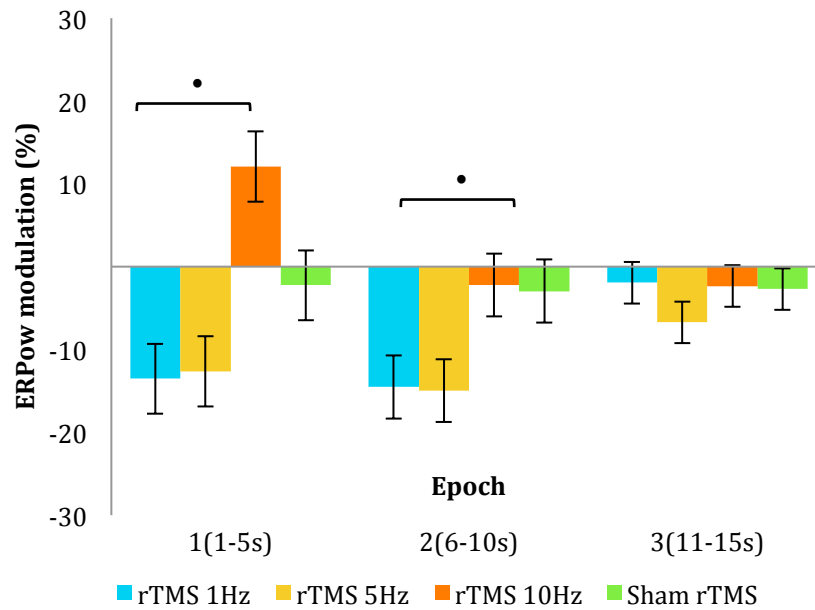


Figure 5-11 ERPow μ as a function of rTMS Frequency and Epoch of time. The figure illustrates EEG desynchronisation for rTMS 1Hz compared to sham for 10s after magnetic stimulation.
 •significant rTMS 1Hz vs. sham; ($p < .05$; Bonferroni corrected; $n = 44$)

5.4.1.4 ERPow β

Table 5-4 summarises the ANOVAs of the main effects and interactions for ERPow β .

Table 5-4 ERPow β

Factors	ERPow β
rTMS Frequency***	$F_{3,40} = 27.53; p < .001; \eta_p^2 = .67$
Epoch*	$F_{1,7,66.8} = 3.51; p < .05; \eta_p^2 = .08$
Electrode*	$F_{4,7,188} = 3.67; p < .05; \eta_p^2 = .08$
rTMS Frequency x Epoch***	$F_{5,66.8} = 19.81; p < .001; \eta_p^2 = .6$
rTMS Frequency x Electrode***	$F_{14,1,188} = 3.65; p < .001; \eta_p^2 = .22$
rTMS Frequency x Epoch x Electrode***	$F_{22,1,294.1} = 4.38; p < .001; \eta_p^2 = .25$

* $p < .05$; ** $p < .01$; *** $p < .001$

The post-hoc comparisons for the significant interaction of *rTMS frequency x epoch* showed that there was a significant EEG synchronisation for rTMS 10Hz for 5s after magnetic stimulation [epoch one: rTMS 10Hz (17.1%) vs. sham (1.8%)]. However, there was a significance desynchronisation for rTMS 1Hz and rTMS 5Hz for 10s post magnetic stimulation [epoch one: rTMS 1Hz (-18.6%), rTMS 5Hz (-10.9%) vs. sham (1.8%), epoch two: rTMS 1Hz (-15.8%), rTMS 5Hz (-12.1%) vs. sham (2.0%)]. Figure 5-12 illustrates the percentage of ERPow modulation of *rTMS frequency x epoch* for β rhythm. None of the other post-hoc comparisons show significant interactions.

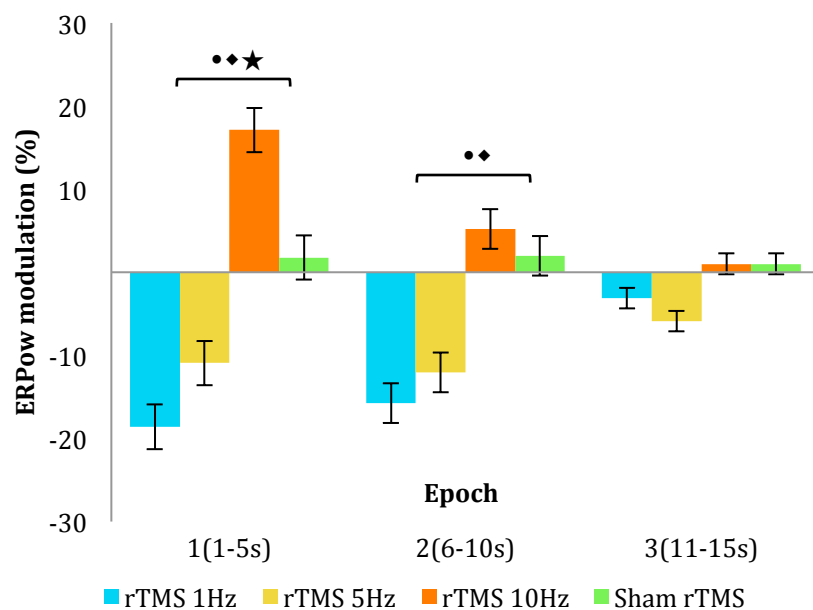


Figure 5-12 ERPow β as a function of *rTMS Frequency* and *Epoch of time*. The figure illustrates EEG synchronisation for rTMS 10Hz and desynchronisation for rTMS 1Hz and 5Hz compared to sham for 10s after magnetic stimulation.

•significant rTMS 1Hz vs. sham; ♦significant rTMS 5Hz vs. sham;
 ★significant rTMS 10Hz vs. sham ($p < .05$; Bonferroni corrected; $n = 44$)

5.4.2 EEG Event-related coherence

This subsection presents the results of ERCoh for δ , θ , μ , and β of the following nine pairs of electrodes: C3-F3, C3-Fz, C3-F4, C3-C3, C3-Cz, C3-C4, C3-P3, C3-Pz, and C3-P4, referenced to C3 electrode (the nearest channel to the TMS coil position over M1). This subsection focuses on the main experimental findings, which are discussed in Section 5.5.2 rTMS and interregional functional connectivity. The remaining findings are presented in the subsequent tables.

5.4.2.1 ERCoh δ

Table 5-5 summarises the ANOVAs of the main effects and interactions for ERCoh δ . The post-hoc comparisons do not show any significant interactions.

Table 5-5 ERCoh δ

Factors	ERCoh δ
rTMS Frequency	$F_{3,40} = 3.71; p = .1; \eta_p^2 = .19$
Epoch	$F_{2,80} = 2.31; p = .1; \eta_p^2 = .14$
Pair of Electrodes*	$F_{8,320} = 0.28; p < .05; \eta_p^2 = .07$
rTMS Frequency x Epoch	$F_{6,80} = 1.07; p = .38; \eta_p^2 = .03$
rTMS Frequency x Pairs of Electrodes	$F_{24,320} = 1.61; p = .09; \eta_p^2 = .04$
rTMS Frequency x Epoch x Pairs of Electrodes	$F_{48,640} = 1.99; p = .12; \eta_p^2 = .13$

* $p < .05$; ** $p < .01$; *** $p < .001$

5.4.2.2 ERCoh θ

Table 5-6 summarises the ANOVAs of the main effects and interactions for ERCoh θ .

Table 5-6 ERCoh θ

Factors	ERCoh θ
rTMS Frequency	$F_{3,40} = 2.36; p = .09; \eta_p^2 = .15$
Epoch***	$F_{2,80} = 20.43; p < .001; \eta_p^2 = .34$
Pairs of Electrodes***	$F_{5,7,227.8} = 4.73; p < .001; \eta_p^2 = .11$
rTMS Frequency x Epoch*	$F_{6,80} = 4.38; p < .05; \eta_p^2 = .25$
rTMS Frequency x Pairs of Electrodes*	$F_{17,1,227.8} = 1.76; p < .05; \eta_p^2 = .12$
rTMS Frequency x Epoch x Pair of Electrodes**	$F_{24,6,328.1} = 2.02; p < .01; \eta_p^2 = .13$

* $p < .05$; ** $p < .01$; *** $p < .001$

The post-hoc comparisons of *rTMS frequency x epoch x pair of electrodes* showed a significant decrease in functional coupling for rTMS 1Hz, 5Hz, and 10Hz versus sham for 5s after magnetic stimulation in C3-Cz, C3-P3, and C3-Pz pairs of electrodes. A significant decrease in functional coupling for rTMS 1Hz, and 5Hz was observed at epoch two post stimulation in C3-Fz, C3-Cz, C3-C4, C3-P3, C3-Pz, and C3-P4) (see Figure 5-13).

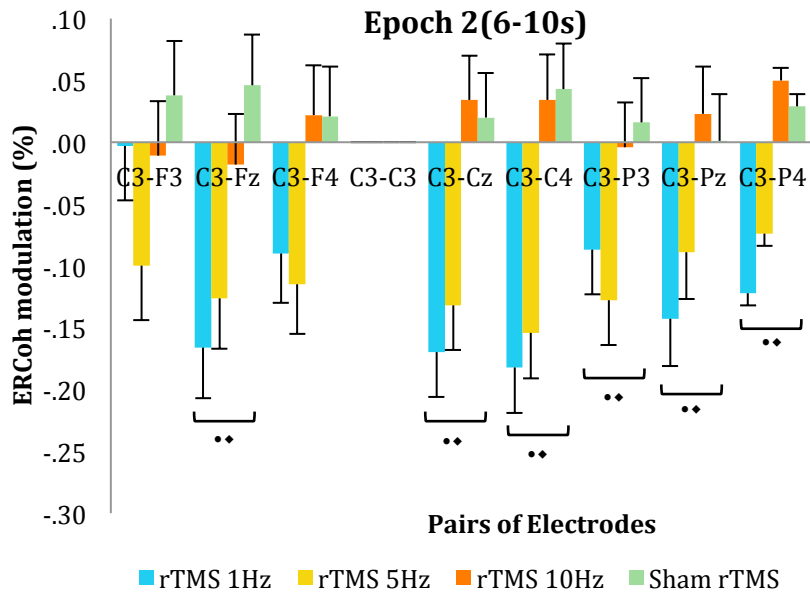
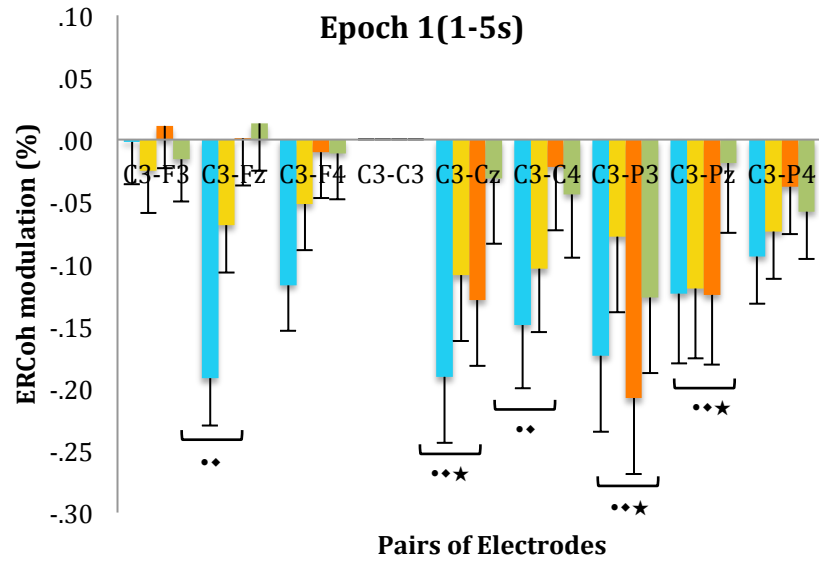


Figure 5-13 ERCoh θ transformation of nine pairs of electrodes referenced to C3 electrode (C3-F3, C3-Fz, C3-F4, C3-C3, C3-Cz, C3-C4, C3-P3, C3-Pz, C3-P4), as a function of *rTMS Frequency*, *Epoch of time*, and *Electrode*. The figure illustrates decrease in functional coupling for rTMS 1Hz and 5Hz for 10s and rTMS 10Hz for 5s after magnetic stimulation.

♦significant rTMS 1Hz vs. sham; ◆significant rTMS 5Hz vs. sham;
 ★significant rTMS 10Hz vs. sham ($p < .05$; Bonferroni corrected; $n = 44$)

5.4.2.3 ERCoh μ

Table 5-7 summarises the ANOVAs of the main effects and interactions for ERCoh μ .

Table 5-7 ERCoh μ

Factors	ERCoh μ
rTMS Frequency*	$F_{3,40} = 3.25; p < .05; \eta_p^2 = .2$
Epoch	$F_{2,80} = 2.16; p = .12; \eta_p^2 = .05$
Pairs of Electrodes *	$F_{6,240.4} = 2.43; p < .05; \eta_p^2 = .06$
rTMS Frequency x Epoch	$F_{6,80} = 2.06; p = .07; \eta_p^2 = .13$
rTMS Frequency x Pairs of Electrodes **	$F_{18,240.4} = 2.14; p < .01; \eta_p^2 = .14$
rTMS Frequency x Epoch x Pair of Electrodes **	$F_{25.8,344.5} = 1.91; p < .01; \eta_p^2 = .13$

* $p < .05$; ** $p < .01$; *** $p < .001$

The post-hoc comparisons of *rTMS frequency x epoch x pair of electrodes* showed a significant decrease in functional coupling for rTMS 10Hz versus sham in epoch one for C3-Cz pair of electrodes. However, a rebound increase in functional coupling was observed in epoch two for rTMS 10Hz versus sham in C3-Cz, C3-C4, and C3-P4 pairs of electrodes. A significant decrease in ERCoh of rTMS 1Hz versus sham is observed in epoch two of C3-Fz, C3-Pz, and C3-P4 pairs of electrodes (see Figure 5-14).

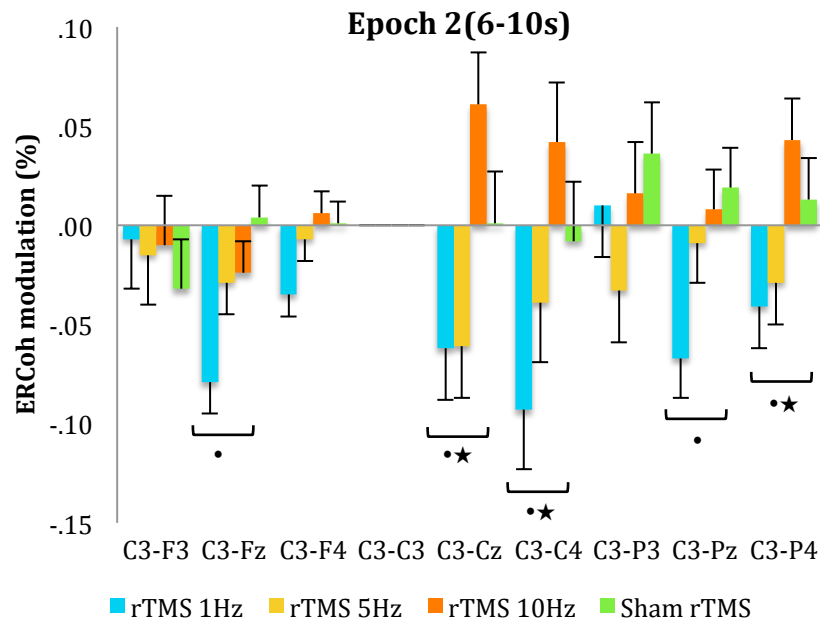
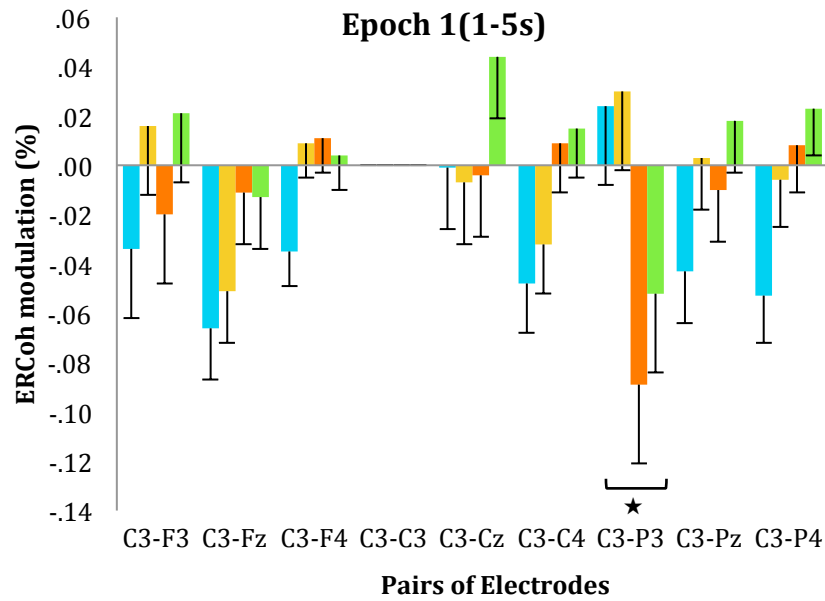


Figure 5-14 ERCoh μ transformation of nine pairs of electrodes referenced to C3 electrode (C3-F3, C3-Fz, C3-F4, C3-C3, C3-Cz, C3-C4, C3-P3, C3-Pz, C3-P4), as a function of *rTMS Frequency*, *Epoch of time*, and *Electrode*. The figure illustrates decrease in functional coupling for rTMS 1Hz and 10Hz compared to sham for 10s after magnetic stimulation.
 •significant rTMS 1Hz vs. sham; ★significant rTMS 10Hz vs. sham
 ($p < .05$; Bonferroni corrected; $n = 44$)

5.4.2.4 ERCoh β

Table 5-8 summarises the ANOVAs of the main effects and interactions for ERCoh β . The post-hoc comparisons do not show any significant interactions.

Table 5-8 ERCoh β

Factors	ERCoh β
rTMS Frequency	$F_{3,40} = 0.85; p = .48; \eta_p^2 = .05$
Epoch*	$F_{1,7,69.2} = 3.3; p < .05; \eta_p^2 = .08$
Pairs of Electrodes*	$F_{4,8,192.7} = 2.49; p < .05; \eta_p^2 = .06$
rTMS Frequency x Epoch*	$F_{5,2,69.2} = 2.7; p < .05; \eta_p^2 = .17$
rTMS Frequency x Pairs of Electrodes *	$F_{14,5,192.7} = 3.21; p < .05; \eta_p^2 = .19$
rTMS Frequency x Epoch x Pairs of Electrodes*	$F_{16,7,222.4} = 1.92; p < .05; \eta_p^2 = .13$

* $p < .05$; ** $p < .01$; *** $p < .001$

5.5 Discussion

The present experiment was designed as an attempt to demonstrate the dichotomy of low versus high frequency rTMS in the modulation of LFO such as δ and θ . The main finding of this experiment was the acute short-lasting (10 seconds) rTMS frequency-dependent synchronisation effect on LFO after short trains of magnetic stimulation. In particular, rTMS 10Hz increased the EEG power (neural synchronisation) for δ and θ bands; in contrast, rTMS 1Hz and 5Hz decreased the EEG power (neural desynchronisation) on the same LFO. To our knowledge, this is the first study that shows the dichotomy of low versus high frequency of magnetic stimulation on EEG oscillatory activity at rest.

5.5.1 rTMS and regional oscillatory activity

In this experiment, the spectral analysis of ERPow computed the regional oscillatory activity of the motor cortical area after low and high frequency magnetic stimulation. The results confirmed the prediction that LFO such as δ and θ are the best indices in reflecting the dichotomy between low versus high frequency of magnetic stimulation instead of α and β oscillations. However, contrary to our earlier prediction that the effects of EEG synchronisation would be linear in rTMS 5Hz and rTMS 10Hz, instead we observed a linear EEG desynchronisation of LFO in rTMS 5Hz and rTMS 1Hz.

Although the distinction between high and low frequency ranges has not been clearly defined, the current convention distinguishing low and high frequency rTMS by the cut-off of 1Hz was agreed at the International rTMS Safety Conference in Bethesda, MD (Wassermann et al., 1996). Low frequency TMS is defined as the application of magnetic stimulation at one stimulus every second or less ($\leq 1\text{Hz}$), whilst high frequency is the application of TMS $> 1\text{Hz}$ (Wassermann et al., 1996). The agreement of using 1Hz as the cut-off frequency is because TMS can have excitatory as well as inhibitory effects, depending on the stimulation frequencies used (Fitzgerald et al., 2006; Rothwell, 1997). Generally, rTMS with low frequency stimulation of 1Hz or less decreased the excitability of the motor cortex and resulted in a long-lasting depression of MEPs (Fitzgerald et al., 2002; Fitzgerald et al., 2006; Maeda et al., 2000b). Conversely, stimulation with high frequency rTMS of 5Hz or more

led to increases in cortical excitability (Maeda et al., 2000b; Pascual-Leone et al., 1994; Peinemann et al., 2004).

However, rTMS-EEG studies of the human motor cortex using low frequency rTMS 1Hz (Brignani et al., 2008) and high frequency rTMS 5Hz (Fuggetta et al., 2008) showed linear synchronisation of α and β brain rhythms. The reason why the effects of rTMS 5Hz are linear with low frequency rTMS 1Hz could be due to the insufficient time interval between pulses in rTMS 5Hz to cause large “summation” of neural activity, which consequently resulted in lesser recruitment and activation of cortico-thalamic descending pathways (Fuggetta et al., 2008; Veniero et al., 2011).

In a groundbreaking study by Allen *et al.* (2007) published in the journal *Science* on the physiology of rTMS, the authors demonstrated a tight coupling between the TMS-evoked neural responses and the changes in cerebral haemodynamics across various stimulation frequencies (Allen et al., 2007). In the study, they explored the effects of short rTMS trains (1-4s) at stimulation frequencies of 1-8 Hz on neural processing and neurovascular coupling in the cat visual cortex by using single unit, local field potentials, tissue oxygenation and haemodynamic recordings (Allen et al., 2007). They found that the effects of the neural oscillations and haemodynamic signals were dose dependent, scaling linearly with low and high stimulation frequencies and duration (Allen et al., 2007). Their findings are in contrast with the differential rTMS aftereffects of low and high frequency stimulation in humans. Allen *et al.* (2007) argued that their divergent findings from human TMS studies were because the non-

invasive behavioural recordings in human are not highly sensitive to quantifying neuronal excitability. In contrast, direct neural recordings in animal studies provide a higher sensitivity in quantifying the time course of TMS-evoked neural and haemodynamic changes (Allen et al., 2007).

In the same study of Allen *et al.* (2007), the authors also measured the degree of phase locking from the distribution of local field potential for spontaneous and evoked activity across the frequency bands of δ , θ , α , β , and γ oscillations. Interestingly, the authors observed that θ oscillation was strongly desynchronised along with the other brain rhythms, relative to spike timing for 30s after rTMS, and a similar trend of desynchronisation was also observed in the δ band after evoked activity (Allen et al., 2007). Their findings verified that the rTMS-induced modulations of neural activity could be readily observed in LFO such as δ and θ (Allen et al., 2007). Therefore, in the present study we tried to extend the findings in animal studies to humans by quantifying the rTMS aftereffects on low frequency oscillatory activity of δ and θ as well as α and β after varying frequencies of magnetic stimulation. Our results of EEG desynchronisation of δ and θ after short trains of rTMS 1Hz and rTMS 5Hz were in line with the results of Allen *et al.* (2007).

However, in our study we also observed an opposite EEG synchronisation of δ and θ after short trains of rTMS 10Hz lasting for 10s. This result is consistent with a recent rTMS-EEG study by Manganotti *et al.* (2012), who explored the modulation of cortical oscillatory activity after different types of TMS on both M1 regions of the healthy brain (Manganotti et al., 2012). During

the same experimental session, the participants underwent three types of TMS: single-pulse TMS over the left M1; paired-pulse with an ISI of 3ms over the left M1; transcallosal rTMS with an ISI of 10ms over both the left and right M1 (Manganotti et al., 2012). Time-frequency wavelet analysis was used to quantify the dynamic modulation of rTMS-induced oscillations (Manganotti et al., 2012). The authors observed that the single-pulse, paired-pulse, and transcallosal TMS induced acute short-lasting synchronisation in δ mainly in central and parietal electrodes, and global synchronisation of θ for approximately 1s (Manganotti et al., 2012). As for the frequency bands of α and β , they observed short-lasting desynchronisation followed by a rebound of synchronisation over the frontal, central and parietal electrodes for about 5s (Manganotti et al., 2012).

The synchronised LFO and the rebound synchronisation of α and β suggest the involvement of inhibitory GABA neurotransmission after TMS perturbation of the motor cortex (Manganotti et al., 2012). The insight into the cellular mechanisms of repeated stimulation could be derived from animal studies investigating thalamic short-term plasticity (Grenier et al., 2003; Steriade & Timofeev, 2003; Timofeev et al., 2002). The rhythmic stimulation with pulse-trains at 10Hz on anaesthetised cats with dual EEG intracellular recordings from the TC and cortical neurons demonstrated that the TC neurons remained hyperpolarised during repeated stimulations due to the influence of GABAergic thalamic reticular (RE) neurons (Steriade & Timofeev, 2003; Timofeev et al., 2002). The hyperpolarisation of TC neurons results in the generation of oscillatory activity at about 2Hz (the frequency range of δ), lasting for 8s after

the cessation of repetitive stimulations (Timofeev et al., 2002). Hence, does the EEG synchronisation of LFO seen in our present experiment of rTMS 10Hz reflect the perturbation of TMS on the GABAergic inhibitory interneurons? To address this problem, it is important to perform a study preferably on animals, investigating both the rTMS-induced oscillations, and the modulation of neurotransmitters after magnetic stimulation.

5.5.2 rTMS and interregional functional connectivity

In order to determine whether rTMS of varying frequencies modulates oscillatory activity of remote cortical regions we performed ERCoh analysis, reflecting the spatial-temporal relationship between two oscillatory signals, referenced to C3 (the nearest channel to the stimulation site). Our data showed a decrease in functional coupling of rTMS 5Hz and rTMS 10Hz compared to sham for θ frequency band, especially in central-parietal electrodes. This finding is consistent with the results of Oliviero *et al.* (2003), who applied intermittent short trains of high frequency 5Hz rTMS over M1 (Oliviero et al., 2003). They observed a significant decrease in the cortico-cortical interhemispheric coherence in the upper α frequency band (10.7-13.6Hz) between motor and premotor cortex for a few minutes after magnetic stimulation (Oliviero et al., 2003). In another online rTMS-EEG study of short trains of high frequency 5Hz rTMS over M1 by Fuggetta *et al.* (2008), the authors observed a short-lasting increase in functional coupling for subthreshold rTMS in α and threshold rTMS for β band (Fuggetta et al., 2008). Nevertheless, the increased ERCoh in their

experiment was only confined to 500ms after the magnetic stimulation (Fuggetta et al., 2008).

However, our results also showed a decrease in functional coupling of rTMS 1Hz for θ and μ frequency bands. This result is in contrast with the findings of Strens *et al.* (2002), who demonstrated an increase in coherence of α band after low frequency stimulation of rTMS 1Hz (Strens et al., 2002). Nevertheless, Strens *et al.* (2002) applied one long train of 1500 stimuli at subthreshold intensity (90% AMT) to the left M1, whereas we applied repetitive twenty short trains of twenty pulses at 100% RMT to the left M1. Moreover, the cortico-cortical coherence of α band observed in the study of Strens *et al.* (2002) were after active muscular contractions of the distal upper limb muscles as opposed to resting state (Strens et al., 2002).

One possible explanation for the modulation of ERCoh in our study is that short train rTMS may induce an acute alteration of interregional cortical oscillations with a functional disconnection between distant brain areas of the motor cortical network. The alterations of functional coupling by TMS might be due to its effects on GABAergic inhibitory interneurons (McDonnell et al., 2007; Thickbroom, 2007; Ziemann, 2011). Alternatively, rTMS might indirectly modify the subcortical structures through corticothalamic networks (Bestmann, 2008), hence causing secondary changes in cortico-cortical coupling (Oliviero et al., 2003). Changes in interregional functional coupling following short trains of rTMS over motor cortex as measured by ERCoh suggest that cortico-cortical coherence may provide a sensitive measure of motor network connectivity

following rTMS (Fuggetta et al., 2008; Rogasch & Fitzgerald, 2012; Strens et al., 2002).

The present experiment exhibits prominent sham effects after magnetic stimulation. The reason is because the sham condition was performed with an intensity of 100% RMT with the real TMS coil tilted at 90° to the skull; therefore there may be currents that still penetrate the skull and stimulate the cortical tissue. Moreover, the effects of coil click may also play a role in triggering the sham response (Rossi et al., 2009). Unfortunately, better devices that can provide sensory artifacts by electrical stimulation and can emulate the effects of magnetic stimulation are not yet available (Rossi et al., 2009). However using “real” TMS coil with a modified stimulation condition such as angling and dislocating the coil and reducing the stimulation intensity has been shown to be reliable sham condition in randomised rTMS trials (Herwig et al., 2010).

5.6 Summary

Overall, the chapter highlights that extracting meaning from the on-going brain oscillations in the intact human brain is possible using rTMS-EEG coregistration studies. In particular, the present experiment demonstrated the ability of EEG δ and θ oscillations to show the dichotomy of low versus high frequency rTMS. The results emphasised that far from being epiphenomena, spontaneous brain rhythms may have an important role in short-term plasticity-like mechanisms induced by rTMS. In the two experiments described in Chapter 4 and 5, we demonstrated acute, short-lasting modulation of EEG oscillatory activity after short trains of simple rTMS protocols. The following chapter presents our

experiment investigating rTMS-induced oscillatory activity after continuous theta-burst stimulation, a pattern rTMS protocol in humans associated with long-term synaptic plasticity mechanisms of LTD.

6. Theta-burst stimulation and cortical oscillations

This chapter presents a combined rTMS-EEG study involving pattern rTMS protocol of continuous theta-burst stimulation. The goal of this experiment was to explore the long-lasting modulation of EEG oscillatory activity along with behavioural MEPs and reaction times after cTBS at rest and during the execution of a motor task. This chapter begins with a brief introduction as to the importance of the current experiment in filling the gap of knowledge of the cTBS effects on the macro cellular level of network oscillations. The next section presents the cTBS-EEG and behavioural methods specific to the present experiment. Next, the chapter outlines a summary of the results consisting of the behavioural MEPs and RT, and the EEG spectral power and coherence of the frequency ranges analysed in the experiment. Finally, the chapter concludes with a discussion of the main findings and highlights the important contribution of the present study in understanding cTBS-induced EEG oscillations and the plasticity-like mechanisms of LTD.

6.1 Introduction

Theta-burst stimulation is a variant of high frequency rTMS that is able to prolong the aftereffects of the induced plastic changes for up to an hour despite its lower stimulus intensity and shorter duration of stimulation (Huang et al., 2005; Paulus, 2005). Studies exploring the residual effects of TBS mainly rely

on peripheral muscular responses of MEPs to indirectly measure cortical excitability post TBS. The protocol of cTBS suppresses MEPs amplitude, and iTBS enhances MEPs sizes for 20 to 60 minutes (Di Lazzaro, Pilato, Dileone, Profice, Oliviero, Mazzone, Insola, Ranieri, Meglio, et al., 2008; Huang et al., 2011; Ishikawa et al., 2007; Suppa, Ortu, et al., 2008; Trippe et al., 2009). These long-term residual effects of TBS emulate the pattern of plasticity—LTP and LTD—of the hippocampus (Cardenas-Morales et al., 2011; Di Lazzaro et al., 2008; Paulus, 2005).

The mechanisms of cortical plasticity induced by TBS are largely unknown (Cardenas-Morales et al., 2010; Hoogendam et al., 2010). Several researchers highlighted the involvement of NMDA receptors, as demonstrated by clinical studies in humans (Huang et al., 2007; Huang, Rothwell, Edwards, & Chen, 2008; Teo et al., 2007). Others proposed the involvement of inhibitory GABA neurotransmission after TBS perturbation of the motor cortex (Thickbroom, 2007; Trippe et al., 2009). Alternative mechanisms include TBS modulation on gene expression and protein levels (Aydin-Abidin et al., 2008; Cheeran et al., 2008). Although the mechanisms of TBS on the micro- or synaptic level are well understood, it remains unclear how TBS modulates the macro-level neuronal network, such as cortical oscillations (Cardenas-Morales et al., 2010; Hoogendam et al., 2010; Huerta & Volpe, 2009).

A cTBS-EEG study by Schindler et al. (2008) investigated the alteration of network oscillations post-cTBS of 600 pulses on the frontal eye field of four healthy subjects (Schindler et al., 2008). The authors demonstrated enhanced

neuronal synchronisation of the cerebral hemisphere ipsilateral to the stimulation site relative to the non-stimulated hemisphere for up to one hour in δ , θ , α , β , and γ brain rhythms (Schindler et al., 2008). The authors suggested that cTBS might interfere with cortical information transfer through its effect on neuronal synchronisation (Schindler et al., 2008). However, in their study, the authors modified the TBS paradigm (30 Hz bursts repeated at 6 Hz) and used higher stimulation intensity (80% RMT), making direct comparison with the original protocol (Huang et al., 2005) problematic.

A recent study by McAllister et al. (2011) explored the modulation of cortical oscillations and the cortical plasticity induced by cTBS in M1 (McAllister et al., 2011). They investigated the modulation of cortical oscillatory activity by cTBS of 600 pulses after a visuomotor training task using both MEP and EEG measurements (McAllister et al., 2011). The authors did not observe any significant synchronisation of the baseline EEG power spectra of δ , θ , α , and β after the visuomotor training task, as compared to a decrease in MEPs sizes (McAllister et al., 2011). They concluded that EEG was not a sensitive index of cortical output to plasticity-inducing paradigms of cTBS (McAllister et al., 2011). However, instead of using multichannel EEG that would provide a comprehensive cortical read-out post cTBS, the power spectra in the study of McAllister et al. (2011) was derived from only a single electrode of C3 (McAllister et al., 2011).

6.2 Aims

In the present study, we address the limited knowledge of cTBS-induced effects on motor cortical oscillations. The first aim of this experiment was to compare the temporal dynamics of human cortical excitability post-cTBS using both behavioural and EEG measurements. Thus, we delivered sub-threshold high-frequency cTBS over the left M1 in healthy participants and measured the cortical readouts via behavioural measurements of MEPs and a motor choice RT task, with simultaneous EEG recording. Our second aim was to investigate how preconditioning the motor cortex with high-frequency cTBS affects the subsequent patterns of oscillatory activity in the motor cortex and the cortico-cortical areas. The cTBS-induced cortical oscillations for both regional and interregional connectivity were quantified by EEG spectral analysis of ERPow and ERCoh.

6.3 Methods

6.3.1 Participants

Twenty-six healthy volunteers (13 males, 13 females; mean age, 26.7 years \pm 5.8 years) with no history of neurological disorder or medical conditions were randomly divided into two groups receiving either real magnetic stimulation or sham as control.

6.3.2 Experimental design

The experiment was designed to look at the modulation of EEG cortical oscillations as well as MEPs and RT indices after cTBS. Subjects were tested in

a quiet room, seated in a comfortable armchair with eyes open, facing a computer screen. Each subject undertook a 40-min recording session consisting of four blocks of 9'40" duration each. Block 0 (i.e. baseline) preceded the application of cTBS; the remaining three blocks followed the cTBS. Each block was comprised of five events: 1) a pause of 1'10", 2) MEPs recording for 1'10", 3) EEG recording at rest for 3'00", where a stationary black fixation cross symbol (0.8° of visual angle) on a grey background was presented at the centre of the screen, 4) a brief pause of 20", and 5) EEG recording during the execution of a choice RT task of 4'00" duration. Figure 6-1 shows the experimental paradigm.

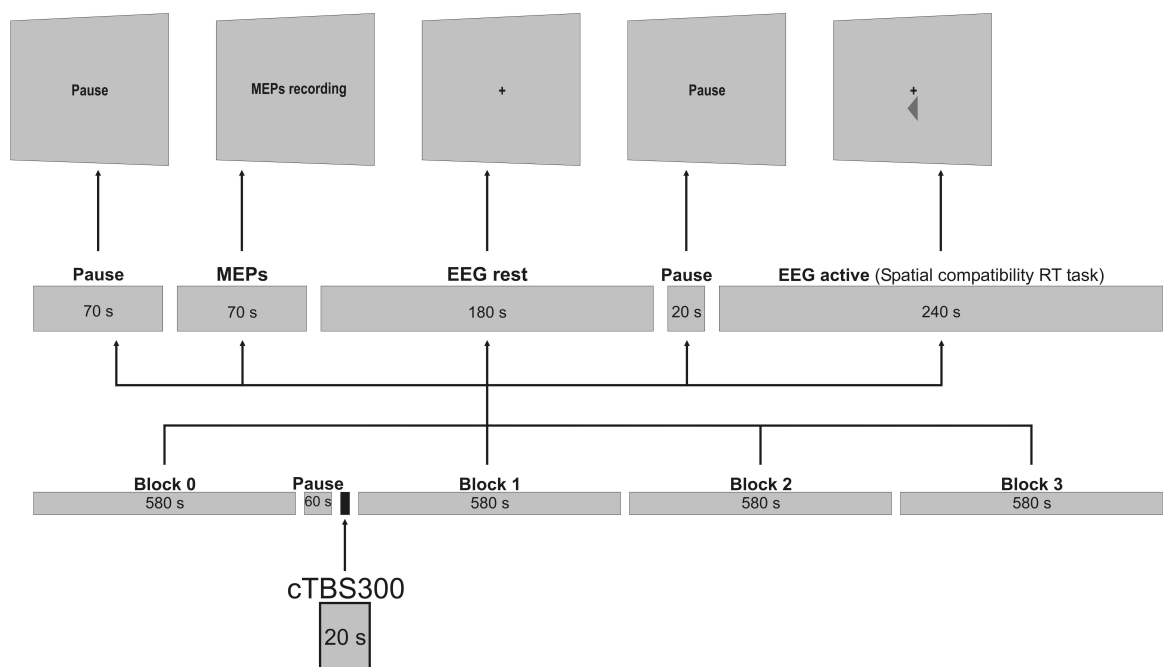


Figure 6-1 cTBS-EEG experimental paradigm.

6.3.3 TBS procedure and MEP recording

TMS was carried out with a high-power Magstim-Rapid stimulator (Magstim, Whitland, Dyfed, UK), as already explained in Chapter 3 Methods. The pattern of cTBS comprised of a 20s train of uninterrupted TBS with bursts of 3 pulses at 50Hz repeated every 200ms (i.e. 5Hz) for a total of 300 pulses as originally proposed by Huang et al. (2005). We applied cTBS over the left M1 and the stimulus intensity was at 80% of individual AMT.

A TMS-compatible EMG machine recorded the MEP in the resting right TE muscle at a stimulus intensity of 120% of the motor threshold. A total of ten TMS pulses were delivered in 1'10" in each of the four blocks of the entire experimental session. We measured MEPs at block 0 (baseline) from 9'30" to 8'20" before cTBS, block one from 1'10" to 2'20", block two from 10'50" to 12'00", and block three from 20'30" to 21'40" after cTBS (Figure 6.1 Experimental paradigm).

6.3.4 Reaction time task

In order to investigate the effects of cTBS on the execution of an active motor task, the participants were asked to perform a motor choice RT task. On each RT trial, a target stimulus of an arrowhead—pointing either to the left or right—was presented in the centre of the computer screen. The colour of the central arrow was isoluminant, either cyan or magenta. If the cyan arrow appeared on the screen, the participants were requested to press the response key on the same side of the arrowhead (compatible condition). However, if the magenta arrow appeared, a response against the direction of the arrowhead was

required (incompatible condition). Two keyboard keys were used for response execution, the “C” key by the left index finger and the “M” key by the right index finger. The visual display included a white fixation cross continuously present throughout the experimental blocks (0.5° of visual angle), whereas the arrowhead (1.5° of visual angle) was displayed for 300ms. The participants were given 1500ms to respond, and were asked to respond as quickly and as accurately as possible. Visual feedback, with the duration of 300ms, was subsequently provided indicating whether the participants had achieved a correct response.

There were a total of 96 trials in each block of the experiment. Half of the trials displayed a “compatible condition” (cyan arrowhead) and another half presented an “incompatible condition” (magenta arrowhead). In order for the participants to become familiar with the task, a practice block of 24 trials preceded the experiment. The time interval between the successive trials was randomised between 2100 and 3100ms (mean $2600\text{ms} \pm 343\text{ms}$). The duration of the RT was 4’00” in each of the four experimental blocks. The RT performance was measured at block 0 (baseline) from 6’40” to 1’00” before cTBS, block one from 5’40” to 9’40”, block two from 15’20” to 19’20”, and block three from 25’00” to 29’00” after cTBS (Figure 6.1 Experimental paradigm). Correct responses were divided from errors and subjected to an absolute filtering criterion to remove anticipatory or overly delayed responses (RTs < 150 ms and RTs > 1300 ms). Figure 6-2 presents the spatial compatibility RT task.

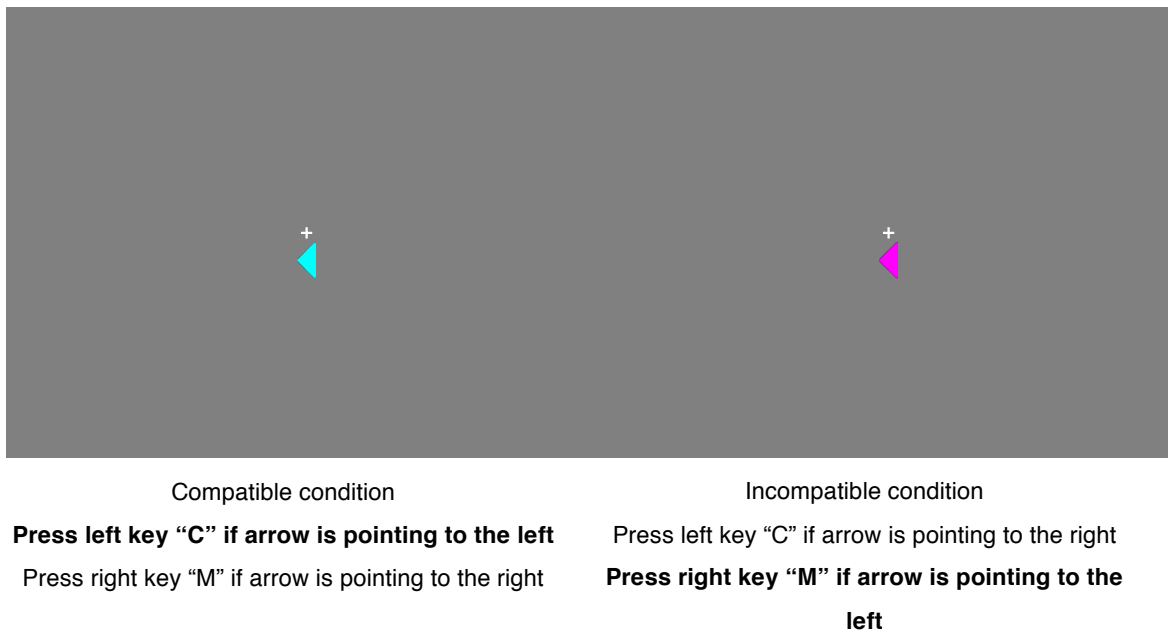


Figure 6-2. Spatial compatibility RT task: illustrating the arrowheads for the compatible and the incompatible conditions.

6.3.5 EEG recording and spectral analysis

The EEG data were acquired using a MR compatible EEG amplifier (SD MRI 32, Micromed, Treviso, Italy) and electrode cap of 30 Ag/AgCl electrodes placed according to a 10/10 (modified) system. Recordings were Hamming-windowed to control spectral leakage. EEG data were filtered (0.1-50Hz, slope 24 dB/octave), and EMG signals were bandpass-filtered (30-300Hz, slope 48 dB/octave). The following channels were selected for inspection: F3, Fz, F4, C3, Cz, C4, P3, Pz, and P4. A notch filter (50Hz) was applied to all channels. After division into segments of 2 seconds, a semi-automatic segment inspection-rejection procedure was applied to avoid muscle or EOG activity. Epochs with eye blinks and muscular movement artifacts (as indicated by activity at the

electrodes exceeding $\pm 70\mu\text{V}$) were excluded from the EEG analysis. Overall, the number of accepted segments for each block was 47 to 81 out of 96 trials.

To demonstrate the cTBS-induced oscillations, EEG data were analysed with commercial software (Vision Analyser, Brain Vision, Munich, Germany) followed by computation of ERPow and ERCoh. A discrete FFT of blocks of 2048 data points (2s) each was computed for all electrodes and then averaged under the same conditions. Power spectra were estimated for all frequency bins between 0.5 and 40Hz (0.5Hz of maximum bin width). The ERPow and ERCoh transformations were submitted to repeated measures ANOVAs for θ (4.0–7.5Hz), μ (10.0-12.5Hz), low β (13.0-19.5Hz) and high β (20.0-30.0 Hz) frequency ranges. Event-related transformations were computed for the four blocks of EEG at “rest” and “active” (during the motor RT task). EEG at “rest” consisted of a baseline from 8’20” to 5’20” before cTBS, block one from 2’20” to 5’20”, block two from 12’00” to 15’00”, and block three from 21’40” to 24’40” after cTBS. EEG “active” comprised of a reference block from 5’00” to 1’00” before cTBS, 5’40” to 9’40”, 15’20” to 19’20”, and 25’00” to 29’00” for the three blocks after cTBS (Figure 6.1 Experimental paradigm).

6.3.6 Statistical analysis

Repeated measures ANOVAs were used to compare variables before and after cTBS. Statistical analyses were performed on normalised values of MEP amplitudes and latencies for both real and sham cTBS. The normalisation was with the MEP values recorded at block 0, “pre-event” baseline. The peak-to-peak mean amplitudes or latencies of MEPs at rest were submitted to a two-

way ANOVA with factors *block* (three levels – block 1, 2, 3) and *group* (two levels - real cTBS and sham cTBS). In order to determine the correlation between the modulation of MEPs and the oscillatory indices after cTBS, a Pearson's correlation ($p < .05$; two-tailed) coefficient was calculated between the changes of MEPs amplitude and ERPow for the three blocks of time (block 1, 2, 3) in all frequency bands over C3 electrodes. C3 was selected due to its proximity to the motor cortex.

Statistical analyses on mean normalised correct trial scores (accuracy error rates) and mean normalised motor response onset latencies (RT) were performed using ANOVAs of within-subjects factors: *block* (three levels – block 1, 2, 3); *direction of the arrowhead* (two levels - left and right); *response position* (two levels - left and right); *colour of the arrowhead* (two levels – cyan and magenta); and between-subject factor of *group* (two levels – real cTBS and sham cTBS). The normalisation of mean RTs and accuracy were recorded at block 0, a “pre-event” baseline.

For “rest” and “active” event-related transformations, three-way ANOVAs of within-subject factors were performed: *block* (three levels – block 1, 2, 3); *electrode* (nine levels – F3, Fz, F4, C3, Cz, C4, P3, Pz, P4) for ERPow and *pair of electrodes* for ERCoh (nine levels – C3-F3, C3-Fz, C3-F4, C3-C3, C3-Cz, C3-C4, C3-P3, C3-Pz, C3-P4); and the between-subject factor of *group* (two levels – real cTBS and sham cTBS).

6.4 Results

This section presents the experimental findings of the current experiment. The following subsections present the results of behavioural MEPs and RT, and EEG oscillations of θ , μ , low β , and high β after cTBS for “rest” and “active” conditions. The main experimental findings are discussed in greater detail in the discussion subsection. No adverse side effects were reported by any of the participants during all levels of the experiment.

6.4.1 MEPs

The statistical analysis revealed a significant interaction for normalised amplitude of MEPs for the factors *group x block* ($F_{2,48} = 3.1$, $p < .05$, $\eta_p^2 = .01$). Post-hoc comparisons for *group x block* demonstrated a significant decrease in MEP size for real cTBS compared to sham cTBS for 20-min post magnetic stimulation (block one: 0.63 vs. 1.16; block two: 0.56 vs. 1.15). Figure 6-3 displays the cTBS-induced aftereffects on the mean normalised MEPs amplitude at rest across blocks of the two experimental groups.

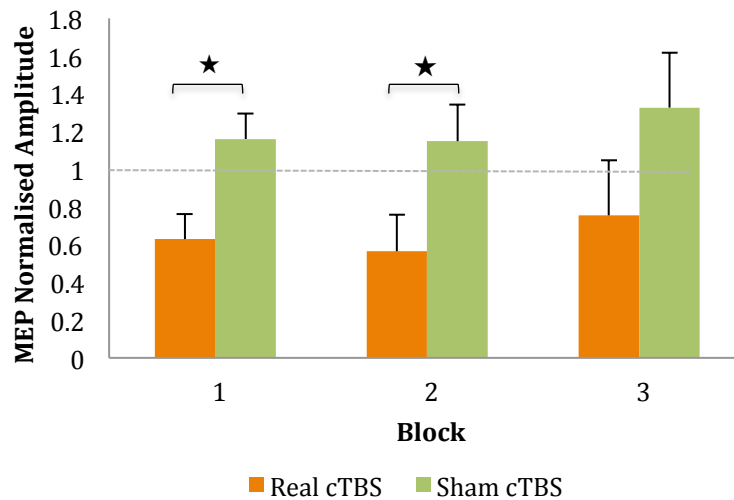


Figure 6-3 MEPs normalised amplitude. The figure illustrates the long-lasting conditioning effect of MEPs amplitude at rest for up to 20-min after cTBS 300 pulses. ★significant real cTBS vs. sham ($p < .05$; Bonferroni corrected; $n = 26$)

No other main factors or interactions were significant for MEP normalised latency; factor: *latency* ($F_{2,48} = .17$, $p = 0.13$, $\eta_p^2 = .007$), *group x latency* ($F_{2,48} = 1.37$, $p = 1.1$, $\eta_p^2 = .054$). Moreover, none of the correlation analyses between the modulation of MEP amplitude and the ERPow of C3 across the three blocks of time were significant.

6.4.2 Motor RT

The only significant main factor for normalised RT was *block* ($F_{2,48} = 7.7$, $p < .005$, $\eta_p^2 = .24$). Post-hoc comparisons for *block* revealed a decreasing trend of RT from block one (0.95) to block two (0.92) and block three (0.91). No other main factors or interactions were significant for normalised RT and accuracy. Figure 6-4 illustrates the normalised RT across blocks of the two groups of participants.

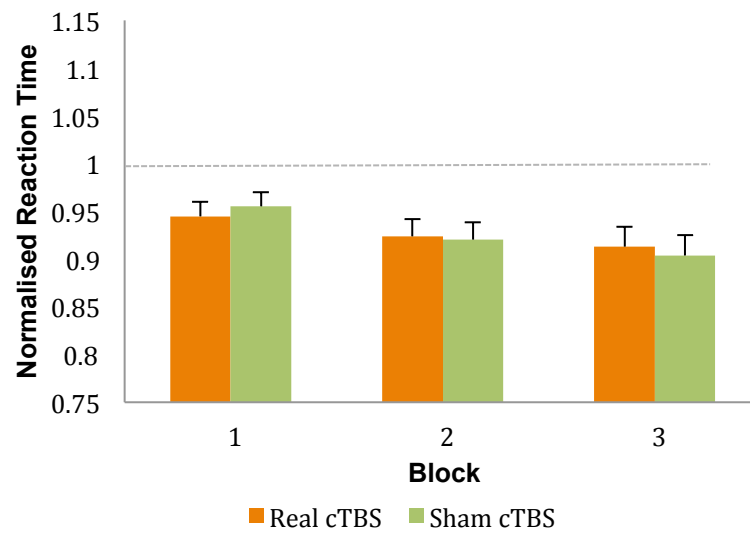


Figure 6-4 Normalised reaction time. The figure illustrates an absence of a long-lasting conditioning effect of cTBS 300 pulses on RT task performance. ($p < .05$; Bonferroni corrected; $n = 26$)

6.4.3 EEG Event-related power

The following subsections present the results of the ERPow transformation of θ , μ , low β , and high β oscillations. The subsection focuses on the main experimental findings, which will be discussed in Section 6.5.3 cTBS and regional oscillatory activity. The remaining findings are presented in the subsequent tables.

6.4.3.1 ERPow θ

Table 6-1 summarises the ANOVAs of the main effects and interactions for ERPow θ at rest.

Table 6-1 ERPow θ rest

Factors	ERPow θ rest
Group	$F_{1,24} = 4.26; p = .06; \eta_p^2 = .17$
Block	$F_{1,6,38.3} = 0.92; p = .39; \eta_p^2 = .04$
Electrode	$F_{4,9,116.9} = 1.88; p = .11; \eta_p^2 = .07$
Group x Block	$F_{1,6,38.3} = 0.06; p = .91; \eta_p^2 = .003$
Group x Electrode	$F_{4,9,116.9} = 1.75; p = .13; \eta_p^2 = .07$
Group x Block x Electrode*	$F_{16,384} = 1.81; p < .05; \eta_p^2 = .07$

* $p < .05$; ** $p < .01$; *** $p < .001$

The post-hoc comparisons for the significant interaction of *Group x Block x Electrode* for θ at rest showed a significant increase in cortical oscillations, mainly at central-parietal electrodes, for real cTBS compared to sham cTBS across the three blocks of time [block 1: C3 (38.4 vs. -12.5%), C4 (28.5 vs. -4.3%) and P3 (28.7 vs. -5.6%); block 2: Fz (24.6 vs. -15.7%), C3 (30.5 vs. -2.2%), C4 (29.2 vs. -3.1%); block 3: C3 (33.6 vs. -1.6%), P3 (29.9 vs. -10.3%) and Pz (42.0 vs. 0.3%)]. Figure 6-5 illustrates the percentage of ERPow modulation of *Group x Block x Electrode* for θ at rest.

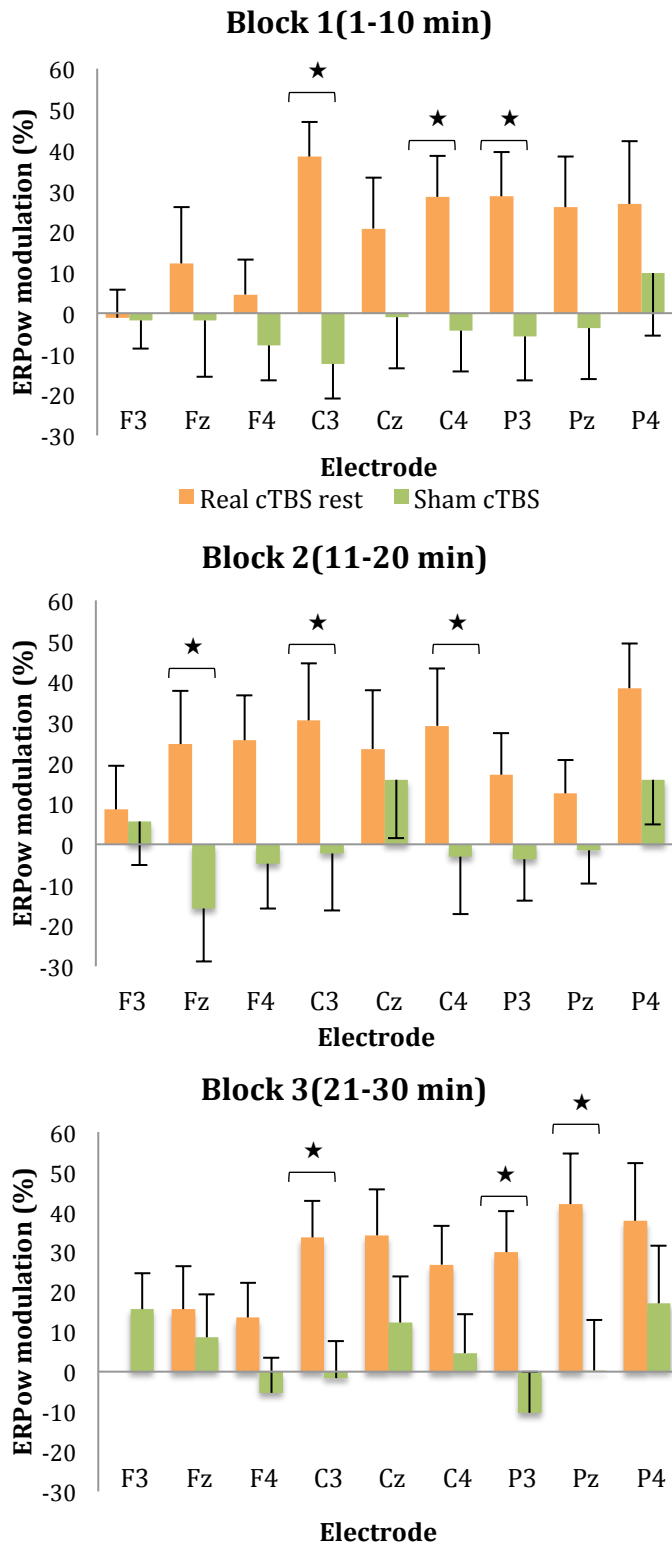


Figure 6-5 ERPow θ as a function of *Group*, *Block of time*, and *Electrode*. The figure illustrates EEG synchronisation for real cTBS θ at rest compared to sham at central-parietal electrodes for 30-min after magnetic stimulation. ★significant real cTBS rest vs. sham ($p < .05$; Bonferroni corrected; $n = 26$)

Table 6-2 summarises the ANOVAs of the main effects and interactions for ERPow θ during the active motor task. The post-hoc comparisons did not show any significant interactions.

Table 6-2 ERPow θ active

Factors	ERPow θ active
Group	$F_{1,24} = 0.45; p = .51; \eta_p^2 = .02$
Block*	$F_{2,48} = 5.11; p < .05; \eta_p^2 = .18$
Electrode	$F_{5,2,123.7} = 1.31; p = .26; \eta_p^2 = .05$
Group x Block*	$F_{2,48} = 12.61; p < .001; \eta_p^2 = .35$
Group x Electrode*	$F_{5,2,123.7} = 5.84; p < .001; \eta_p^2 = .2$
Group x Block x Electrode	$F_{8,4,201.7} = 1.67; p = .1; \eta_p^2 = .07$

* $p < .05$; ** $p < .01$; *** $p < .001$

6.4.3.2 ERPow μ

Table 6-3 summarises the ANOVAs of the main effects and interactions for ERPow μ at rest. None of the interactions were significant.

Table 6-3 ERPow μ rest

Factors	ERPow μ rest
Group*	$F_{1,24} = 5.11; p < .05; \eta_p^2 = .18$
Block	$F_{2,48} = 1.53; p = .23; \eta_p^2 = .06$
Electrode*	$F_{4,9,116.7} = 3.16; p < .05; \eta_p^2 = .12$
Group x Block	$F_{2,48} = 0.01; p = .99; \eta_p^2 = 0$
Group x Electrode	$F_{4,9,116.7} = 1.55; p = .18; \eta_p^2 = .06$
Group x Block x Electrode	$F_{6,8,163.3} = 1.67; p = .12; \eta_p^2 = .07$

* $p < .05$; ** $p < .01$; *** $p < .001$

Table 6-4 summarises the ANOVAs of the main effects and interactions for ERPow μ during the active motor task.

Table 6-4 ERPow μ active

Factors	ERPow μ active
Group	$F_{1,24} = 0.3; p = .59; \eta_p^2 = .01$
Block	$F_{2,48} = 2.95; p = .06; \eta_p^2 = .11$
Electrode*	$F_{4,6,111.1} = 4.75; p < .01; \eta_p^2 = .17$
Group x Block*	$F_{2,48} = 3.6; p < .05; \eta_p^2 = .13$
Group x Electrode*	$F_{4,6,111.1} = 3.76; p < .05; \eta_p^2 = .14$
Group x Block x Electrode	$F_{16,384} = 1.59; p = .07; \eta_p^2 = .06$

* $p < .05$; ** $p < .01$; *** $p < .001$

The post-hoc comparisons for the significant interaction of *Group x Electrode* showed higher EEG synchronisation for real cTBS compared to sham cTBS of C3 (78.1 vs. 32.4%) and Cz (70.6 vs. 41.1%) electrodes during the active motor task. Figure 6-6 illustrates the percentage of ERPow modulation of *Group x Electrode* for μ rhythm at active state.

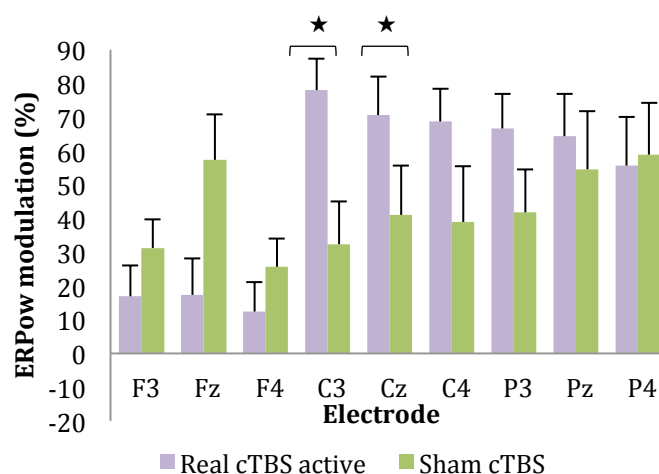


Figure 6-6 ERPow μ as a function of *Group* and *Electrode*. The figure illustrates EEG synchronisation of C3 and Cz electrodes for real cTBS μ compared to sham during the active motor task.

★significant real cTBS active vs. sham ($p < .05$; Bonferroni corrected; $n = 26$)

6.4.3.3 ERPow low β

Table 6-5 summarises the ANOVAs of the main effects and interactions for ERPow low β at rest.

Table 6-5 ERPow low β rest

Factors	ERPow low β rest
Group**	$F_{1,24} = 9.09; p < .01; \eta_p^2 = .28$
Block*	$F_{2,48} = 4.52; p < .05; \eta_p^2 = .16$
Electrode***	$F_{4,9,118.6} = 5.46; p < .001; \eta_p^2 = .19$
Group x Block	$F_{2,48} = 2.12; p = .13; \eta_p^2 = .08$
Group x Electrode***	$F_{4,9,118.6} = 4.78; p < .001; \eta_p^2 = .17$
Group x Block x Electrode	$F_{16,384} = 1.24; p = .24; \eta_p^2 = .05$

* $p < .05$; ** $p < .01$; *** $p < .001$

The post-hoc two-way interaction *Group x Electrode* showed a higher EEG power modulation for real cTBS at rest compared to sham for the electrodes F4 (37.6 vs. -3.5%), C3 (16.4 vs. -2.4%), C4 (15.1 vs. -0.2%) and P3 (13.1 vs. -7.9%). Figure 6.7 illustrates the percentage of ERPow modulation of *Group x Electrode* for low β at rest.

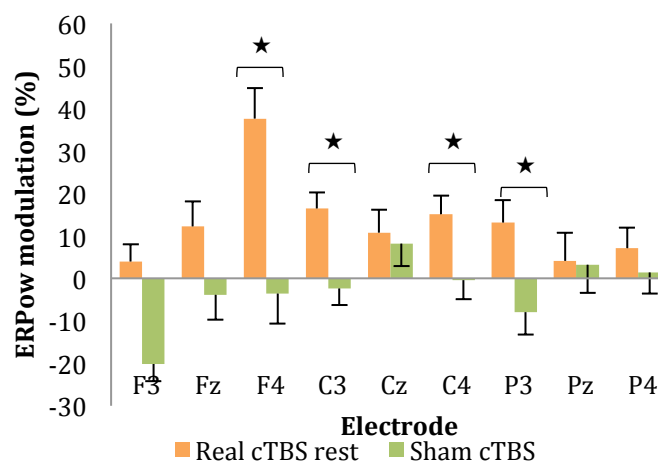


Figure 6-7 ERPow low β as a function of *Group* and *Electrode*. The figure illustrates illustrating EEG synchronisation of F4, C3, C4, and P3 electrodes for real cTBS compared to sham at rest. ★significant real cTBS rest vs. sham ($p < .05$; Bonferroni corrected; $n = 26$)

Table 6-6 summarises the ANOVAs of the main effects and interactions for ERPow low β during the active motor task.

Table 6-6 ERPow low β active

Factors	ERPow low β active
Group	$F_{1,24} = 2.52; p = .13; \eta_p^2 = .1$
Block*	$F_{2,48} = 8.81; p < .01; \eta_p^2 = .27$
Electrode*	$F_{5,120.8} = 4.34; p < .01; \eta_p^2 = .15$
Group x Block	$F_{2,48} = 1.61; p = .21; \eta_p^2 = .06$
Group x Electrode*	$F_{5,120.8} = 2.92; p < .05; \eta_p^2 = .11$
Group x Block x Electrode	$F_{8.5,204.2} = 1.82; p = .07; \eta_p^2 = .07$

* $p < .05$; ** $p < .01$; *** $p < .001$

The post-hoc comparison of the significant two-way interaction *Group x Electrode* showed higher EEG synchronisation for real cTBS compared to sham in Cz (45.5 vs. 18.5%) and C4 (36.5 vs. 15%). Figure 6-8 illustrates the percentage of ERPow modulation of *Group x Electrode* for low β during the active motor task.

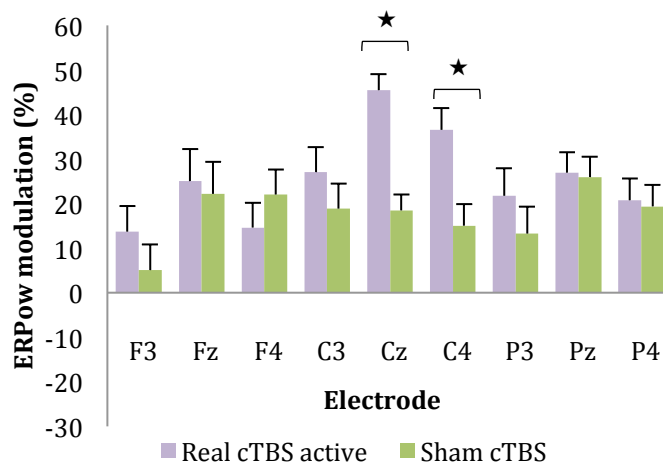


Figure 6-8 ERPow low β as a function of *Group* and *Electrode*. The figure illustrates EEG synchronisation of Cz and C4 electrodes for real cTBS compared to sham during the active motor task.
 ★significant real cTBS active vs. sham ($p < .05$; Bonferroni corrected; $n = 26$)

6.4.3.4 ERPow high β

Table 6-7 summarises the ANOVAs of the main effects and interactions for ERPow high β at rest.

Table 6-7 ERPow high β rest

Factors	ERPow high β rest
Group*	$F_{1,24} = 4.35; p < .05; \eta_p^2 = .15$
Block	$F_{2,48} = 2.3; p = .11; \eta_p^2 = .09$
Electrode	$F_{3,7,88.7} = 1.36; p = .26; \eta_p^2 = .05$
Group x Block	$F_{2,48} = 2.67; p = .08; \eta_p^2 = .1$
Group x Electrode*	$F_{3,7,88.7} = 3.66; p < .05; \eta_p^2 = .13$
Group x Block x Electrode*	$F_{6,7,159.7} = 2.6; p < .05; \eta_p^2 = .1$

* $p < .05$; ** $p < .01$; *** $p < .001$

The post-hoc interaction *Group x Electrode* indicated higher synchronisation for real cTBS versus sham for the frontal electrodes: F3 (9.7 vs. -6.9%), Fz (19.9 vs. -10.7%) and F4 (25.1 vs. -8.9%). Figure 6-9 illustrates the percentage of ERPow modulation of *Group x Electrode* for high β at rest.

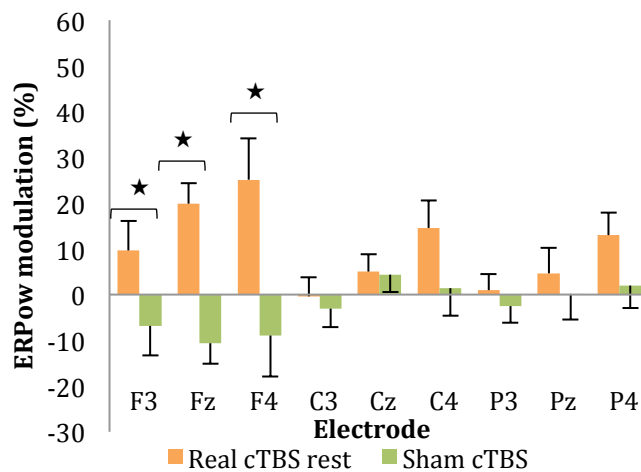


Figure 6-9 ERPow high β as a function of *Group* and *Electrode*. The figure illustrates EEG synchronisation of F3, Fz and F4 electrodes for real cTBS compared to sham at rest.
 ★significant real cTBS rest vs. sham ($p < .05$; Bonferroni corrected; $n = 26$)

The post-hoc comparisons for the significant interaction of *Group x Block x Electrode* for high β at rest showed a significant increase in cortical oscillations for real cTBS compared to sham cTBS in the frontal electrodes across the three blocks of time [block 1: F3 (12.8 vs. -3.9%), Fz (17.9 vs. -16.9%); block 2: F4 (42.2 vs. -21.2%); block 3: Fz (22.7 vs. -11.9%) and F4 (36.3 vs. -5.6%)]. Figure 6-10 illustrates the percentage of ERPow modulation of *Group x Block x Electrode* for high β at rest.

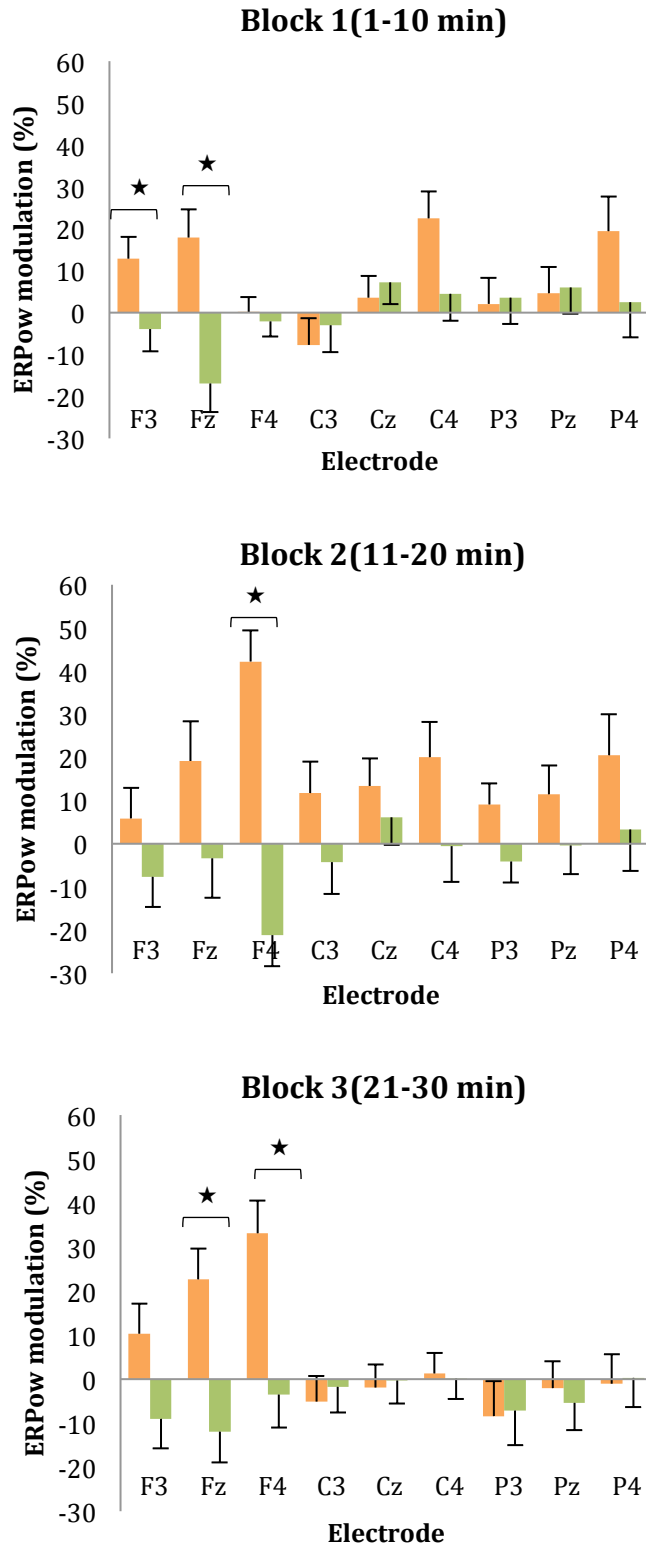


Figure 6-10 ERPow high β as a function of *Group*, *Block*, and *Electrode*. The figure illustrates EEG synchronisation of the frontal electrodes for real cTBS compared to sham across the three blocks of time at rest. ★significant real cTBS rest vs. sham ($p < .05$; Bonferroni corrected; $n = 26$)

Table 6-8 summarises the ANOVAs of the main effects and interactions for ERPow high β during the active motor task. The post-hoc comparisons did not show any significant interactions.

Table 6-8 ERPow high β active

Factors	ERPow high β active
Group	$F_{1,24} = 1.81; p = .19; \eta_p^2 = .07$
Block*	$F_{2,48} = 3.29; p < .05; \eta_p^2 = .12$
Electrode**	$F_{3,7,88.7} = 3.96; p < .01; \eta_p^2 = .14$
Group x Block*	$F_{2,48} = 5.1; p < .05; \eta_p^2 = .18$
Group x Electrode	$F_{3,7,88.7} = 2.42; p = .06; \eta_p^2 = .09$
Group x Block x Electrode	$F_{8,1,194.3} = 0.85; p = .56; \eta_p^2 = .03$

* $p < .05$; ** $p < .01$; *** $p < .001$

6.4.4 EEG Event-related coherence

This subsection presents the results of ERCoh for θ , μ , low β , and high β brain rhythms of the following nine pairs of electrodes: C3-F3, C3-Fz, C3-F4, C3-C3, C3-Cz, C3-C4, C3-P3, C3-Pz, and C3-P4, referenced to C3 electrode. This subsection focuses on the main experimental findings, which will be discussed in Section 6.5.4 cTBS and interregional functional connectivity. The remaining findings are presented in the subsequent tables.

6.4.4.1 ERCoh θ

No significant main effects and interactions were found either for ERCoh θ at rest or during the active motor task. Table 6-9 and 6-10 summarise the ANOVAs of the main effects and interactions for ERCoh θ at rest and active, respectively.

Table 6-9 ERCoh θ rest

Factors	ERCoh θ rest
Group**	$F_{1,24} = 12.28; p < .01; \eta_p^2 = .34$
Block	$F_{2,48} = 1.67; p = .2; \eta_p^2 = .07$
Pairs of Electrodes*	$F_{4,2,100.4} = 2.75; p < .05; \eta_p^2 = .1$
Group x Block	$F_{2,48} = 0.81; p = .45; \eta_p^2 = .03$
Group x Pairs of Electrodes	$F_{4,2,100.4} = 1.73; p = .15; \eta_p^2 = .07$
Group x Block x Pairs of Electrodes	$F_{7,8,186.3} = 1.84; p = .07; \eta_p^2 = .07$

* $p < .05$; ** $p < .01$; *** $p < .001$

Table 6-10 ERCoh θ active

Factors	ERCoh θ active
Group	$F_{1,24} = 1.17; p = .29; \eta_p^2 = .05$
Block	$F_{2,48} = 2.92; p = .06; \eta_p^2 = .11$
Pairs of Electrodes*	$F_{4,7,113.4} = 3.21; p < .05; \eta_p^2 = .12$
Group x Block	$F_{2,48} = 2.06; p = .14; \eta_p^2 = .08$
Group x Pairs of Electrodes	$F_{4,7,113.4} = 1.08; p = .38; \eta_p^2 = .04$
Group x Block x Pairs of Electrodes	$F_{7,6,182.1} = 1.34; p = .23; \eta_p^2 = .05$

* $p < .05$; ** $p < .01$; *** $p < .001$

6.4.4.2 ERCoh μ

No significant main effects and interactions were found either for ERCoh μ at rest or during the active motor task. Table 6-11 and 6-12 summarise the ANOVAs of the main effects and interactions for ERCoh μ at rest and active, respectively.

Table 6-11 ERCoh μ rest

Factors	ERCoh μ rest
Group	$F_{1,24} = 0.003; p = .96; \eta_p^2 = 0$
Block	$F_{2,48} = 1.37; p = .26; \eta_p^2 = .05$
Pair of Electrodes	$F_{3,8,91.6} = 2.3; p = .07; \eta_p^2 = .09$
Group x Block*	$F_{2,48} = 3.37; p < .05; \eta_p^2 = .12$
Group x Pairs of Electrodes*	$F_{3,8,91.6} = 3.02; p < .05; \eta_p^2 = .11$
Group x Block x Pairs of Electrodes	$F_{7,8,187} = 1.38; p = .21; \eta_p^2 = .05$

* $p < .05$; ** $p < .01$; *** $p < .001$

Table 6-12 ERCoh μ active

Factors	ERCoh μ active
Group	$F_{1,24} = 0.59; p = .45; \eta_p^2 = .02$
Block*	$F_{2,48} = 3.45; p < .05; \eta_p^2 = .13$
Pairs of Electrodes	$F_{4,2,101.6} = 0.36; p = .94; \eta_p^2 = .02$
Group x Block	$F_{2,48} = 0.3; p = .67; \eta_p^2 = .02$
Group x Pairs of Electrodes *	$F_{4,2,101.6} = 3.0; p < .05; \eta_p^2 = .11$
Group x Block x Pairs of Electrodes	$F_{6,3,150.4} = 1.17; p = .32; \eta_p^2 = .05$

* $p < .05$; ** $p < .01$; *** $p < .001$

6.4.4.3 ERCoh low β

Table 6-13 summarises the ANOVAs of the main effects and interactions for ERCoh low β at rest.

Table 6-13 ERCoh low β rest

Factors	ERCoh low β rest
Group**	$F_{1,24} = 14.45; p < .01; \eta_p^2 = .38$
Block*	$F_{2,48} = 5.1; p < .05; \eta_p^2 = .18$
Pairs of Electrodes	$F_{4,6,109.9} = 1.25; p = .29; \eta_p^2 = .05$
Group x Block	$F_{2,48} = 1.5; p = .23; \eta_p^2 = .06$
Group x Pairs of Electrodes **	$F_{4,6,109.9} = 4.88; p < .01; \eta_p^2 = .17$
Group x Block x Pairs of Electrodes **	$F_{7,2,173.5} = 3.06; p < .01; \eta_p^2 = .11$

* $p < .05$; ** $p < .01$; *** $p < .001$

Post-hoc comparisons of the two-way interaction *Group x Pair of Electrodes* showed a decrease in functional coupling for real cTBS versus sham in C3-Fz (-0.015 vs. 0.004%), C3-Cz (-0.006 vs. 0.016%), C3-P3 (-0.021 vs. 0.019%), C3-Pz (-0.011 vs. 0.02%) and C3-P4 (-0.011 vs. 0.004%) pairs of electrodes. Figure 6-11 illustrates the percentage of ERCoh modulation of *Group x Pair of Electrodes* for low β at rest.

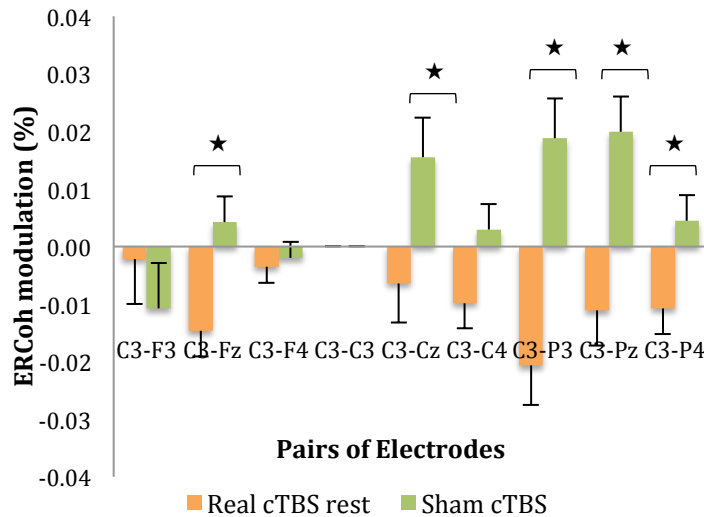


Figure 6-11 ERCoh low β as a function of *Group* and *Pairs of Electrodes*. The figure illustrates EEG synchronisation of C3-Fz, C3-Cz, C3-P3, C3-Pz, and C3-P4 pairs of electrodes for real cTBS compared to sham at rest.

★significant real cTBS rest vs. sham ($p < .05$; Bonferroni corrected; $n = 26$)

Post-hoc comparisons for the three-way interactions *Group* \times *Block* \times *Pairs of Electrodes* demonstrated a decrease in functional coupling for real cTBS compared to sham cTBS at rest across all blocks of time [block one: C3-Fz (-0.017 vs. 0.008%), C3-Cz (-0.033 vs. 0.019%), C3-P3 (-0.036 vs. 0.015%), C3-Pz (-0.024 vs. 0.017%) and C3-P4 (-0.024 vs. 0.007%); block two: C3-C4 (-0.012 vs. 0.009%), C3-P3 (-0.011 vs. 0.022%); block three: C3-Fz (-0.019 vs. 0.009%), C3-P3 (-0.017 vs. 0.022%), C3-Pz (-0.015 vs. 0.014%)]. Figure 6-12 illustrates the percentage of ERCoh modulation of *Group* \times *Block* \times *Pairs of Electrodes* for low β at rest.

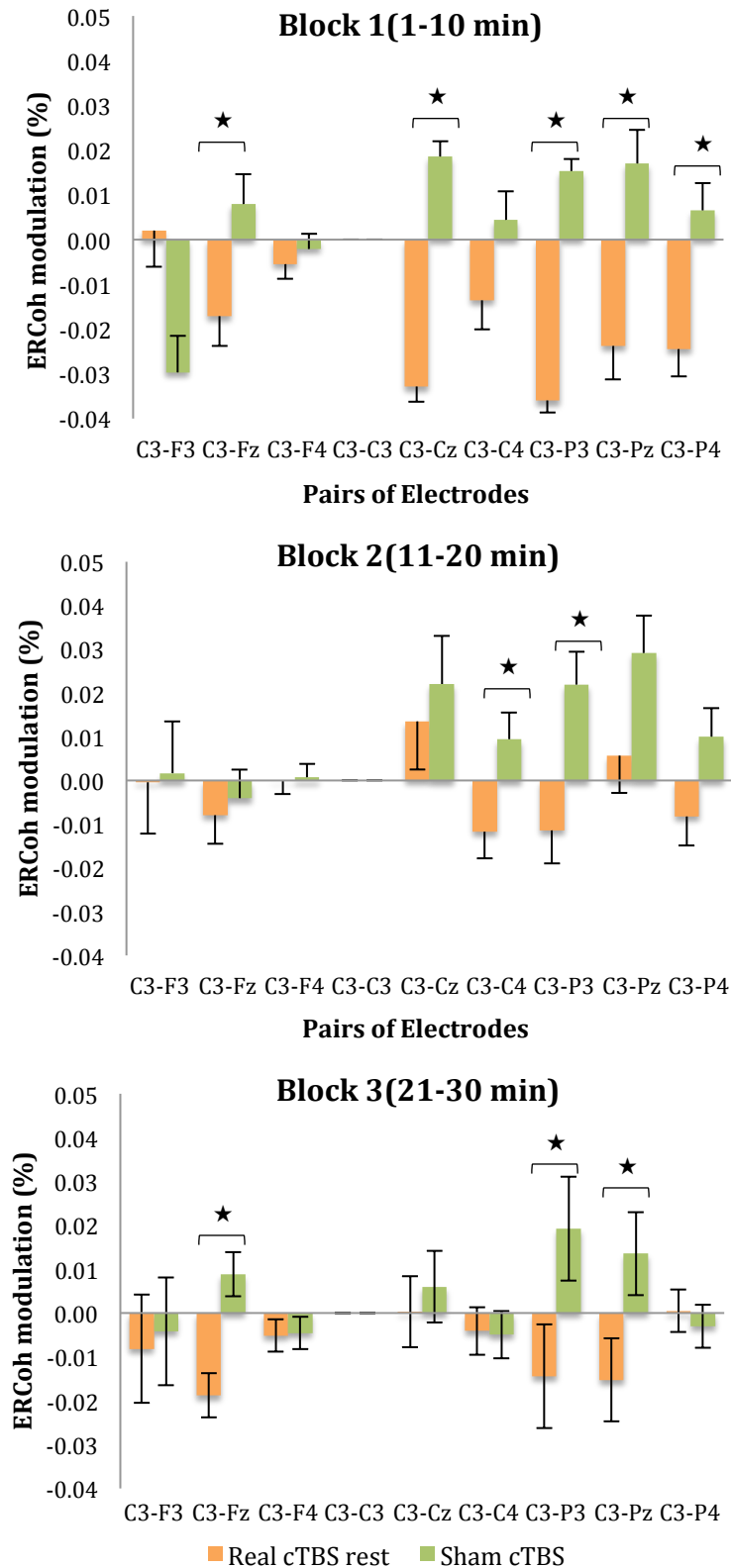


Figure 6-12 ERCoh low β as a function of *Group*, *Block* and *Pairs of Electrodes*. The figure illustrates EEG synchronisation of several frontal-central-parietal pairs of electrodes for real cTBS compared to sham at rest across the three blocks of time. ★significant real cTBS rest vs. sham ($p < .05$; Bonferroni corrected; $n = 26$)

Table 6-14 summarises the ANOVAs of the main effects and interactions for ERCoh low β during the active motor task. There were no significant effects or interactions.

Table 6-14 ERCoh low β active

Factors	ERCoh low β active
Group	$F_{1,24} = 1.2; p = .29; \eta_p^2 = .05$
Block	$F_{2,48} = 0.62; p = .54; \eta_p^2 = .03$
Pairs of Electrodes	$F_{3,4,82.7} = 2.27; p = .08; \eta_p^2 = .09$
Group x Block	$F_{2,48} = 0.77; p = .47; \eta_p^2 = .03$
Group x Pairs of Electrodes	$F_{3,4,82.7} = 0.76; p = .54; \eta_p^2 = .03$
Group x Block x Pairs of Electrodes	$F_{6,6,157.4} = 0.42; p = .88; \eta_p^2 = .02$

* $p < .05$; ** $p < .01$; *** $p < .001$

6.4.4.5 ERCoh high β

Table 6-15 summarises the ANOVAs of the main effects and interactions for ERCoh high β at rest. Post-hoc comparisons did not show any significant interactions.

Table 6-15 ERCoh high β rest

Factors	ERCoh high β rest
Group	$F_{1,24} = 1.45; p = .24; \eta_p^2 = .06$
Block	$F_{2,48} = 0.69; p = .51; \eta_p^2 = .03$
Pairs of Electrodes**	$F_{3,2,76.2} = 4.07; p < .01; \eta_p^2 = .15$
Group x Block*	$F_{2,48} = 5.22; p < .05; \eta_p^2 = .18$
Group x Pairs of Electrodes*	$F_{3,2,76.2} = 4.07; p < .05; \eta_p^2 = .1$
Group x Block x Pairs of Electrodes	$F_{6,3,151.4} = 1.54; p = .17; \eta_p^2 = .06$

* $p < .05$; ** $p < .01$; *** $p < .001$

Table 6-16 summarises the ANOVAs of the main effects and interactions for ERCoh high β during the active motor task.

Table 6-16 ERCoh high β active

Factors	ERCoh high β active
Group***	$F_{1,24} = 21.4$; $p < .001$; $\eta_p^2 = .47$
Block	$F_{2,48} = 0.73$; $p = .49$; $\eta_p^2 = .03$
Pairs of Electrodes	$F_{3,4,82.5} = 1.56$; $p = .2$; $\eta_p^2 = .06$
Group x Block*	$F_{2,48} = 3.64$; $p < .05$; $\eta_p^2 = .13$
Group x Pairs of Electrodes***	$F_{3,4,82.5} = 9.88$; $p < .001$; $\eta_p^2 = .29$
Group x Block x Pairs of Electrodes*	$F_{5,2,125.4} = 2.37$; $p < .05$; $\eta_p^2 = .09$

* $p < .05$; ** $p < .01$; *** $p < .001$

Post-hoc comparisons of the two-way interaction *Group x Pair of Electrodes* showed a decrease in functional coupling for real cTBS versus sham in C3-Cz (-0.018 vs. 0.041%), C3-C4 (-0.009 vs. 0.029%), C3-P3 (-0.018 vs. 0.056%), C3-Pz (-0.029 vs. 0.04%) and C3-P4 (-0.02 vs. 0.034%) pairs of electrodes. Figure 6-13 illustrates the percentage of ERCoh modulation of *Group x Pair of Electrodes* for high β during the active motor task.

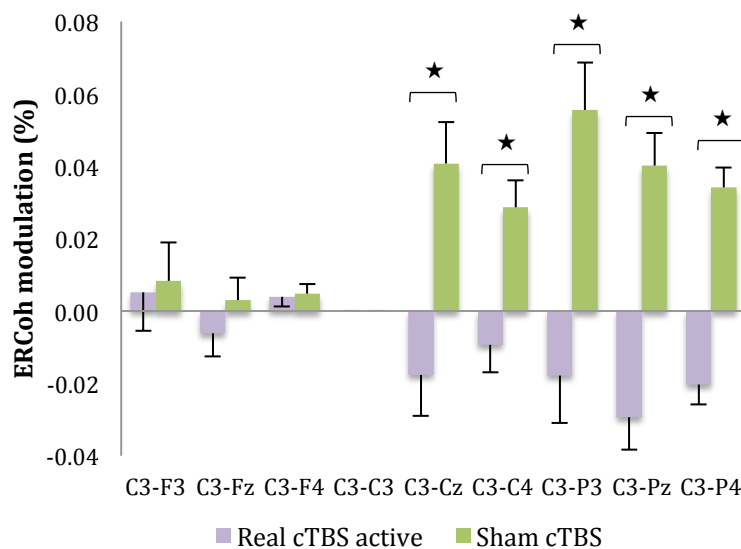


Figure 6-13 ERCoh high β as a function of *Group* and *Pairs of Electrodes*. The figure illustrates EEG synchronisation of C3-Cz, C3-C4, C3-P3, C3-Pz, and C3-P4 pairs of electrodes for real cTBS compared to sham during the active motor task. ★significant real cTBS rest vs. sham ($p < .05$; Bonferroni corrected; $n = 26$)

Post-hoc analyses for the significant three-way interaction *Group x Block x Pair of Electrodes* demonstrated a decrease in functional coupling in real cTBS compared to sham across the three blocks in the central-parietal pairs of electrodes: [block one: C3-Cz (-0.036 vs. 0.059%), C3-C4 (-0.03 vs. 0.03%), C3-P3 (-0.027 vs. 0.062%), C3-Pz (-0.041 vs. 0.051%) and C3-P4 (-0.033 vs. 0.043%); block two: C3-C4 (0.004 vs. 0.038%), C3-P3 (-0.016 vs. 0.037%), C3-Pz (-0.01 vs. 0.027%) and C3-P4 (-0.002 vs. 0.027%); block three: C3-Cz (-0.023 vs. 0.038%), C3-P3 (-0.011 vs. 0.068%), C3-Pz (-0.037 vs. 0.043%) and C3-P4 (-0.026 vs. 0.032%)]. Figure 6-14 illustrates the percentage of ERCoh modulation of *Group x Block x Pair of Electrodes* for high β during active motor task.

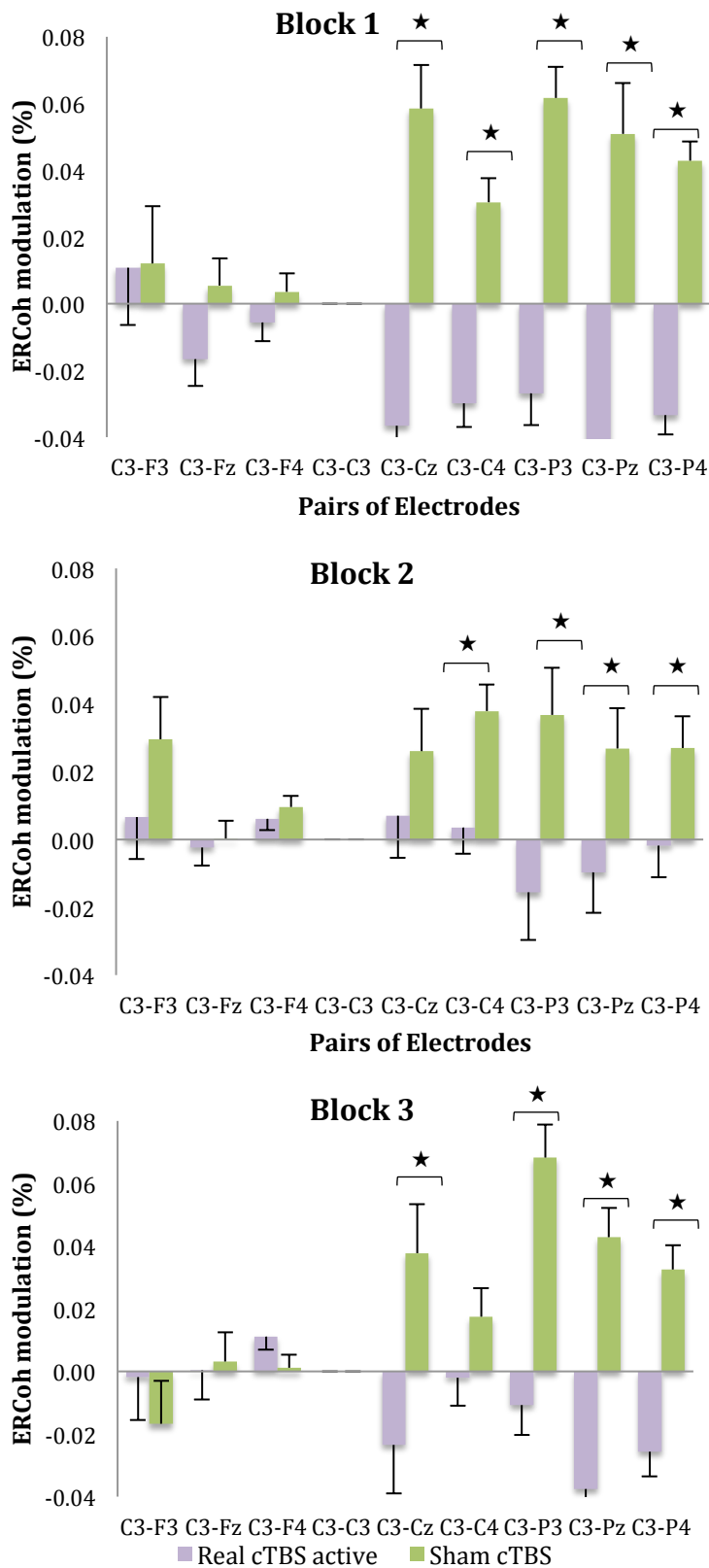


Figure 6-14 ERCoh high β as a function of *Group*, *Block* and *Pairs of Electrodes*. The figure illustrates EEG synchronisation of the central-parietal pairs of electrodes for real cTBS compared to sham across the three blocks during the active motor task. ★significant real cTBS rest vs. sham ($p < .05$; Bonferroni corrected; $n = 26$)

6.5 Discussion

The present experiment was designed as an attempt to compare the temporal dynamics of cortical excitability induced by cTBS using both behavioural and EEG measurements. The other goal was to investigate how preconditioning the motor cortex with high frequency cTBS altered the patterns of cortical synchronisation. In order to address these aims, we measured behavioural indices (MEPs and RTs) and EEG oscillatory phenomena (ERPow and ERCoh) induced by cTBS both at rest and during an active motor task. We quantified the mean normalised EEG responses to high-frequency rTMS for 30-min after magnetic stimulation.

Our main finding was a lengthier increase in cortical synchronisation for at least 30-min compared to a relatively shorter (20-min) suppression of MEP amplitude. This finding indicates that EEG has the potential to be a sensitive index of cortical plasticity induced by theta burst magnetic stimulation. We found β to be the most sensitive brain rhythm modulated by cTBS. Since β oscillations are dominant at the cortical level during awake and alert states (Salenius & Hari, 2003; Sauseng & Klimesch, 2008), our finding reinforced the hypothesis that TBS acts on the cortical level instead of the subcortical regions (Cardenas-Morales et al., 2010; Di Lazzaro, Ziemann, et al., 2008; Huang et al., 2005; Paulus, 2005). However, there was no significant change in reaction time induced by cTBS. This result suggests that a healthy motor system is able to maintain normal brain functioning despite transient perturbation by cTBS (Ortu et al., 2009).

6.5.1 cTBS and MEPs

In the present experiment, we measured MEPs at rest as the indirect index of motor cortical excitability after cTBS. We observed a 20-min long-lasting suppression of MEPs normalised amplitude after 300 pulses of high-frequency cTBS compared to sham cTBS. This finding is in line with several cTBS-MEPs studies, which showed suppression of MEP amplitude after a low-intensity conditioning train of cTBS, emulating LTD mechanisms of synaptic plasticity (Huang et al., 2005; Stefan et al., 2008; Suppa, Ortu, et al., 2008; Zafar et al., 2008).

At present, the mechanisms responsible for the suppression of MEP amplitude after high frequency but low intensity cTBS remain elusive (Cardenas-Morales et al., 2011; Hoogendam et al., 2010). The suppression of MEPs after cTBS is indeed puzzling, since we would expect enhancement in MEPs sizes after high frequency magnetic stimulation (Cardenas-Morales et al., 2011; Hoogendam et al., 2010). Instead, cTBS mimicked the conventional protocol of low frequency 1Hz rTMS. It has been suggested that MEP suppression may be due to inhibitory responses being built up slower but saturated later than facilitation after cTBS (Huang et al., 2005).

6.5.2 cTBS and reaction time

In the present study, RT was used as the behavioural index to quantify the cTBS-induced modulation of cortical excitability during an active motor task. We did not find any significant interactions for motor latency responses in the correct trials across blocks of time for either real cTBS or sham cTBS. This

finding contradicted our earlier hypothesis that cTBS would increase RT in the contralateral right hand to the site of magnetic stimulation. Nevertheless, we observed that the two groups of participants had shorter RTs for successive blocks of time. The improved RT suggests a possible “practice effect”, where mean RTs consistently decrease when the participants perform the same cognitive task repeatedly (Dutilh, Vandekerckhove, Tuerlinckx, & Wagenmakers, 2009). The improved performance due to the “practice effect” may involve the modifications of response strategy (Dutilh et al., 2009).

Contrary to our findings, previous investigations have demonstrated that conditioning the left motor cortex with cTBS resulted in prolonged RT in the right conditioned hand for up to 10-min, and a decrease in RT in the left unconditioned hand for approximately 30-min after cTBS (Mochizuki, Franca, Huang, & Rothwell, 2005). Moreover, after the application of cTBS over either the left or right PMd, the response latency in a choice RT task was delayed in both hands (Mochizuki et al., 2005). Their findings indicate that cTBS leads to widespread long-lasting interference on motor behaviour (Mochizuki et al., 2005).

However, the absence of a significant effect on choice RT after cTBS in our study might be due to the application of cTBS over the M1 instead of the PMd. The M1 is primarily involved in the motor execution of simple RT protocol (Muellbacher et al., 2002; Porter & Sakamoto, 1988), whereas the premotor cortex is the cortical region responsible for motor preparation during a choice RT task (Perfetti et al., 2011). Therefore, we should probably apply the cTBS

over the PMd instead of M1 to quantify the choice RT task, or simply use a simple RT protocol. However, there are studies that have demonstrated MEP suppression after magnetic stimulation but without any significant outcome on simple RT performances (Iyer, Schleper, & Wassermann, 2003; Stinear et al., 2009). The fact that movement was not compromised in their studies and ours suggests that a healthy motor system is able to functionally compensate for transient perturbation of motor cortical excitability induced by artificial magnetic stimulation (Iyer et al., 2003; Ortu et al., 2009; Stinear et al., 2009).

6.5.3 cTBS and regional oscillatory activity

In the present study, we computed ERPow in order to quantify the cTBS-induced modulation of cortical oscillations. We observed that cTBS induced a general increase in cortical oscillations mainly in the β brain rhythms for at least 30-min after cTBS. Our findings indicate longer-lasting EEG changes than behavioural MEPs after cTBS. The discrepancy between MEPs and EEG findings in our study could be due to the fact that cTBS affects MEPs and EEG oscillatory activities through different mechanisms (Maki & Ilmoniemi, 2010). MEP amplitudes reflect the neuronal excitability of the target muscle and are influenced by corticospinal excitability, whilst EEG oscillations are the total activity of the synchronous excitatory and inhibitory input of pyramidal dendrites (Maki & Ilmoniemi, 2010). Moreover, the EEG signal is nearer to the site of magnetic stimulation, linked monosynaptically to TMS from the pyramidal neurons of the cortex (Huerta & Volpe, 2009; Siebner & Rothwell, 2003). However, the MEP that is commonly used in rTMS experiments as an index of

cortical excitability is further from the TMS source, linked polysynaptically to TMS by at least three synapses (corticospinal neurons, motor neurons of the spinal cord, and the neuromuscular synapses) (Huerta & Volpe, 2009; Siebner & Rothwell, 2003). It is important to point out that LTP and LTD of synaptic plasticity are monosynaptic events (Malenka & Bear, 2004). Therefore, EEG that is able to provide monosynaptic cortical readout is probably a more sensitive index of cortical plasticity-inducing paradigms of TBS than behavioural MEPs (Huerta & Volpe, 2009; Rogasch & Fitzgerald, 2012; Thut & Pascual-Leone, 2010b).

In the present experiment, we found that β was the most sensitive frequency band modulated by cTBS both during rest and active states. Physiologically, β oscillations are associated with motor activity and are cortically generated (Salenius & Hari, 2003; Sauseng & Klimesch, 2008). Our findings support the hypothesis that TBS would mainly interfere with cortical activity rather than the subcortical structures (Cardenas-Morales et al., 2010; Huang et al., 2011; Paulus, 2005). The stimulus intensity of cTBS in the present experiment is subthreshold (80% AMT), and this stimulus is not enough to activate the descending pathways (Cardenas-Morales et al., 2010; Huang et al., 2011; Paulus, 2005). Moreover, our results demonstrated a focal enhancement of β oscillations in the frontal region of the cortex (see Figure 6-9 and 6-10). A focal synchrony suggests a cortical origin, whilst a global synchrony indicates the involvement of deeper structures, such as the thalamus, through the thalamocortical networks (Pell et al., 2011; Shafi et al., 2012). Our findings are

in line with the study of Rosanova *et al.* (2009), who observed enhancement of β oscillations in the frontal region, indicating β as the natural frequency of the frontal cortex (Rosanova *et al.*, 2009). However, EEG reflects the activity of a large population of neurons (Komssi & Kahkonen, 2006), therefore we cannot exclude the influence of the thalamocortical network in generating β oscillations over the motor cortex. Moreover, basal ganglia have also been implicated in the generation of β oscillations as shown in several TMS studies on Parkinson's disease (Brown, 2003; Jenkinson & Brown, 2011; Moran *et al.*, 2011)

EEG analyses post-cTBS also revealed enhanced EEG synchronisation for θ band at rest. This finding is in line with our previous experiments that showed a short-lasting enhancement of θ oscillatory activity after short-trains of high-frequency rTMS protocols of 10Hz and 11Hz. The increased synchrony of θ oscillations may be due to the presence of independent θ generators over the motor network as discovered from animal studies (Leung & Borst, 1987; Silva *et al.*, 1991) and human intracranial EEG recordings (Cantero *et al.*, 2003; Caplan *et al.*, 2003; Raghavachari *et al.*, 2006). However, the global topography of θ changes observed in the present experiment suggests the probable involvement of the thalamocortical network in generating θ oscillations over the cerebral cortex (R. Llinas & Ribary, 2001; Timofeev, 2011). Studies using invasive intracranial EEG electrodes on patients or animals will give a more accurate interpretation of the origin of the brain rhythms than non-invasive surface EEG.

We also observed enhance synchrony of μ rhythm mainly in the C3 and Cz—the EEG electrodes closest to the left M1 (Jurcak et al., 2007; Okamoto et al., 2004)—after the active motor task. The increased synchronisation of Rolandic μ rhythm—a variant α rhythm—in the “active” state rather than at “rest” is rather surprising because μ is dominant during quiet wakefulness and is attenuated by motor movements or somatosensory stimuli (Niedermeyer et al., 2004; Pineda, 2005). Although μ rhythm was formerly thought as merely epiphenomena without any functional significance, recent studies indicate that μ is more than an idling state of the sensorimotor cortex and instead reflects the integration of sensory and motor neurons important for cortical information processes (Niedermeyer et al., 2004; Pineda, 2005).

6.5.4 cTBS and interregional functional connectivity

In order to determine whether cTBS might have remote or global effects besides local modulations, we quantified the interregional coupling of remote brain regions using ERCoh, which reflects the spatial-temporal connection between two oscillatory signals (Andrew & Pfurtscheller, 1996; Leocani et al., 1997a; Pfurtscheller & Andrew, 1999). The electrodes are referenced to C3 (the closest electrode to the left M1) in order to investigate how cTBS modulates the cortico-cortical coherence of the motor network. Our results showed long lasting 30-min intrahemispheric and interhemispheric connectivity changes after cTBS. In particular, we found a decrease in functional connectivity for real cTBS between the pre-conditioned left M1 and the distant areas of the motor network in the β brain rhythm for 30-min after the magnetic stimulation. This functional

disconnection was mainly in the central-parietal electrodes of the low β rhythm at “rest”—during a no-task condition, and high β rhythm at “active” state—during the execution of a choice motor task.

It is interesting to note that the decreased cortico-cortical coherence induced by cTBS seen in the present experiment was similar to the results of high frequency rTMS (5Hz), which is commonly used to increase cortical excitability (Fuggetta et al., 2008; Oliviero et al., 2003). Since the cTBS paradigm mimics the effects of the conventional low frequency 1Hz rTMS, we expected that the coherence results would be consistent with the findings of Strens *et al.* (2002), who demonstrated a focal increase in coherence during an active task compared to a resting condition after 1Hz rTMS of subthreshold intensity over M1 (Strens et al., 2002). However, in principle, TBS is a high frequency magnetic stimulation, therefore the decrease in functional coupling might not be so surprising after all. Moreover, the interregional decrease in connectivity may be mainly because of the suppression of the left M1 (area C3) by cTBS, but not at the other regions of the brain.

In the case of sham cTBS, we have found a synchronisation of cortico-cortical connectivity between M1 and central-parietal cortex for high β band during the execution of a motor RT task. This was in opposition to the decreasing coherence between the same cortical regions after the perturbation produced by real cTBS. This result suggests that in a perfectly functioning brain, the execution of a complex motor task induced increased connectivity between functionally connected cortical areas. Previous investigations, which analysed

the interregional coherence to assess the neurophysiological processes underlying the performance during higher task demands, such as skilled or sequential finger movements, have found an increase in functional coupling mainly in the β frequency range (13-20Hz) (Calmels et al., 2006; Jancke, Steinmetz, Benilow, & Ziemann, 2004; Manganotti et al., 1998a). The increased coherence oscillations suggest the involvement of a global scale sensorimotor network in encoding information processing during motor tasks (Shafi et al., 2012). Here we show that cTBS is able to modulate the cortico-cortical oscillatory activity, attesting that TBS-EEG combined methods have the potential to uncover the mechanism of TBS-induced cortical plasticity (Cardenas-Morales et al., 2011; Cardenas-Morales et al., 2010).

6.6 Summary

Overall, our present work suggests a probable link between motor cortical network oscillations and the neuroplastic alterations in the human brain after cTBS. Although it was tempting to associate increased neuronal synchronisation after cTBS with mechanisms of LTD, the limitation of inferences of EEG at micro-level make us cautious to do so. Surface EEG will only record neural activity if there is large-scale synchronicity underlying the electrode. Therefore, our result can be interpreted on a macroscopic scale but not at the micro-level, which cannot be computed with scalp EEG. Nevertheless, due to the rise of therapeutic protocols using plasticity-induced paradigms such as TBS to treat symptoms of neuropsychiatric disorders, it is thus important to understand the mechanisms of cTBS-induced cortical plasticity in terms of the

alterations in brain oscillations. This knowledge may contribute to the therapeutic strategy of reversing the altered brain oscillations in neuropsychiatric disorders using non-invasive transcranial magnetic stimulation.

7. Conclusion

This final chapter begins with a summary of the main findings obtained from the three rTMS-EEG co-registration experiments reported in the present thesis. The subsection highlights the importance of exploring the oscillatory activity of low frequency brain rhythms such as θ besides μ and β oscillations in rTMS studies involving the human motor cortex. Next, the chapter suggests some future work following the findings of the current thesis. Finally, the conclusion of the contribution of the present work wraps up the thesis.

7.1 Summary of the main experimental findings

Experiment 1 was designed to investigate the short-term modulation of cortical oscillations after high frequency rTMS by manipulating the different number of magnetic pulses. We compared the cortical readout of direct electrophysiological EEG after high frequency rTMS ($\sim 11\text{Hz}$) of 20 trains of 20 pulses (400 magnetic pulses; rTMS 20) versus 20 trains of 60 pulses (1600 magnetic pulses; rTMS 60) over the left M1 at rest. Our main finding was the distinctly different topography and temporal dynamics of θ and μ rhythms. The θ synchronisation was globally distributed across multiple locations of the EEG electrodes for 20s after rTMS 60 pulses. On the other hand, the μ rhythm was focally distributed and dominated early for 5s after rTMS 20 pulses. These findings point to the probable presence of independent θ and μ generators over the human motor network with different reactivity to rTMS. However, we could

not rule out the contribution of the thalamocortical network in generating θ and μ rhythms in the cerebral cortex.

Experiment 2 was our attempt to investigate whether low frequency brain rhythms such as δ and θ oscillations could be used to exhibit the dichotomy between the simple protocols of low and high frequency magnetic stimulation. To address this question, we applied short trains of low frequency 1Hz rTMS versus high frequency 5Hz and 10Hz rTMS over M1 at rest with simultaneous EEG recordings. Here, we show for the first time the ability of low frequency EEG oscillations of δ and θ brain rhythms to contrast the modulatory effects of low and high frequency rTMS. However, in this experiment, the results of high frequency 5Hz rTMS mimicked the effects of low frequency 1Hz rTMS. The findings of the two experiments on the short-lasting modulation of low frequency oscillations after rTMS suggest that rTMS can be used to explore the functional significance of δ and θ as well as μ and β cortical rhythms. Moreover, we also demonstrated that short trains of rTMS were able to induce short-term plasticity-like mechanisms over the motor cortex. Although the rTMS-induced short-term plasticity-like mechanisms are enough for basic neuroscience research, the short-lasting effects are not sufficient for clinical intervention.

In experiment 3, we examined whether a pattern rTMS protocol of cTBS—which is able to induce longer-lasting behavioural effects after magnetic stimulation—could modulate EEG oscillatory activity for relatively longer periods of time. In this experiment, we applied 300 pulses of short intensity but high frequency cTBS over the left M1 and measured the EEG oscillatory activity both

at rest and during an active motor task. We also compared the direct EEG cortical output with the indirect behavioural MEPs at rest and RTs during active conditions. Our results showed that cTBS could modulate the cortical brain rhythms, particularly β oscillations, for at least 30-min compared to the 20-min MEPs suppression. This finding suggests that EEG is probably a more sensitive index of cortical output after cTBS compared to MEPs. Therefore, EEG can be used to explore the long-term plasticity-like LTD mechanisms induced by cTBS over the M1. Moreover, the dominant β synchronisation seen in the study supports the hypothesis that cTBS mainly acts at the cortical level rather than in the subcortical structures due to its low intensity of stimulation.

The three experiments considered together show that by combining rTMS with EEG we could investigate the underlying plasticity-like mechanisms induced by magnetic stimulation at a global or macro level of cortical and network oscillations. Our findings that rTMS can modulate low frequency oscillations could be extended to clinical studies investigating the disturbance of brain rhythms in various neuropsychiatric disorders.

7.2 Future directions

There are several limitations of the present work. In the cTBS-EEG experiment the induced oscillatory activity was for at least 30-min after cTBS. Unfortunately, we did not wait for the EEG oscillations to return to the baseline. Future studies should investigate the time course of cortical oscillations by cTBS beyond the 30-min temporal window. Another limitation of the study is the non-correlation between the behavioural MEPs and the EEG changes, despite both

measurements been determined by the same cTBS manipulation. Although in the discussion in chapter 6, the different underlying mechanisms of MEPs and EEG are suggested as the probable reason, a simpler explanation could be the cause. The total of ten TMS pulses delivered to measure the MEPs on each of the four experimental blocks (block 0, 1, 2, 3) might not be sufficient to obtain a good signal to noise ratio. Moreover, MEP amplitudes are known to have high inter-trial variability among subjects (Maeda, Keenan, Tormos, Topka, & Pascual-Leone, 2000a; Roy Choudhury et al., 2011), so more trials may be needed to get a reliable measure. Future work should take into account the sufficient number of stimulation trials for both MEP and EEG in order to obtain a good signal to noise ratio before comparing the two cortical indices.

Although rTMS-induced modulatory aftereffects share many similarities with the mechanisms of synaptic plasticity, the evidence for such associations is, however, indirect (Hoogendam et al., 2010; Pell et al., 2011). Studies of combined rTMS or neuroimaging techniques such as PET and fMRI, and electrophysiological techniques such as EEG and MEG, have found strong indirect links between rTMS and plasticity, but direct evidence is still lacking (Hallett & Rothwell, 2011; Hoogendam et al., 2010; Pell et al., 2011). Animal studies can offer better flexibility in order to establish a direct link between rTMS and plasticity (Hoogendam et al., 2010).

Moreover, synaptic plasticity is probably not the only mechanism underlying the residual effects of magnetic stimulation (Hoogendam et al., 2010; Pell et al., 2011). This has been demonstrated in our studies of short trains

rTMS, where the EEG oscillatory activity is not correlated with MEPs amplitude. Although rTMS and plasticity share many characteristics such as rTMS has effects that outlast the experimental manipulation, the temporal pattern of rTMS—the frequency dependency effects—is similar to LTP/LTD, rTMS plays a role in learning, rTMS directly impairs or facilitates LTP in rats (Hoogendaam et al., 2011), however there is no causal proof that the underlying mechanisms of LTP/LTD and rTMS are identical (Hoogendaam et al., 2011). It is more likely that there is a multiplicity of mechanisms driving the sustained rTMS aftereffects (Pell et al., 2011). Alternative mechanisms driving the modulatory aftereffects of rTMS are altered membrane excitability due to the influence of membrane potentials (RMP and MT) and ion channels (Hallett, 2000; Pell et al., 2011). The membrane potential is an important determinant of excitability. The response of a nerve to sequences of impulses at sub- or supra-threshold levels results in a time dependent pattern of excitability changes, which follows changing levels of depolarization and hyperpolarization at the axonal membrane (Pell et al., 2011). Other alternative mechanisms include reduced cortical excitability in the resting states (Touge et al., 2001), increased excitability at the spinal cord (Quartarone et al., 2005), and breakdown of cortical inhibition (Pascual-Leone et al., 2000). Future studies should address the multiplicity of mechanisms that drive the rTMS aftereffects besides LTP-/LTD-like mechanisms.

The ability of rTMS to modulate low frequency brain rhythms such as θ oscillations is an exciting phenomenon. Evidence from EEG and MEG studies demonstrate that the common link among a wide range of neuropsychiatric

disorders is the perturbation of the thalamocortical resonance known as Thalamocortical dysrhythmia (Henning Proske, Jeanmonod, & Verschure, 2011; Jeanmonod et al., 2003; Llinas et al., 1999; Schulman et al., 2011). The idea behind TCD is that persistent, abnormal, internally generated δ or θ oscillations in the thalamic neurons disrupt the normal, state-dependent, flow of information within the thalamo-cortico-thalamic network (Llinas et al., 1999). Although the occurrence of low frequency oscillations is normal during slow-wave sleep, during awake periods, and at rest, prolonged δ and θ rhythms may lead to the disturbances of sensation, motor performance and cognition observed in a number of disorders including Parkinson's disease, schizophrenia, epilepsy, neuropathic pain, tinnitus, major depression, and obsessive-compulsive disorder (Henning Proske et al., 2011; Jeanmonod et al., 2003; Jones, 2010; Llinas et al., 1999; Schulman et al., 2011; Walton & Llinas, 2010; Whitwell et al., 2011). In parallel, several rTMS protocols have been shown to be able to improve symptoms of various neuropsychiatric disorders (Chen, 2010, 2012; Hallett & Rothwell, 2011; Kleinjung et al., 2011; Langguth et al., 2010; Miniussi & Rossini, 2011; Ziemann, 2011) although the optimal parameters of magnetic stimulation remain elusive (Hallett & Rothwell, 2011; Wassermann & Zimmermann, 2012). In our study, the increase in delta and theta power accords with the presence of low-threshold spike (LTS) bursting activity, with delta and theta rhythmicity in the medial thalamus of patients with TCD, as demonstrated by MEG and single-unit recordings during stereotactic surgery (Jeanmonod et al., 2003). These results support the hypothesis that electrical

brain stimulation like TMS can trigger an oscillation, or reset the ongoing rhythmic activity, of a local thalamic pacemaker (Fuggetta et al., 2005; Van Der Werf et al., 2006). The EEG de-synchronisation observed in rTMS 1Hz and 5Hz point to the potential of rTMS to reverse the overly rhythmic LFOs. These findings may provide an insight into the electrophysiological mechanisms underlying the improvement of many neuropsychiatric symptoms regardless of using different rTMS protocols of either low frequency (1Hz) or high frequency (5Hz) (Feinsod et al., 1998; Mally and Stone, 1999; Siebner, 2000).

However, to our knowledge, there is no study that investigates the probable link between rTMS aftereffects and the TCD phenomenon in clinical populations. Can rTMS reverse TCD, thus alleviating the numerous symptoms in neuropsychiatric disorders? Future clinical trials can exploit the ability of combined rTMS-EEG to modulate and measure the dysrhythmic thalamocortical oscillatory activity in neuropsychiatric disorders.

Concluding remarks...

Overall, the present thesis provides new insights into the ability of rTMS to induce low frequency brain rhythms besides μ and β oscillations, such as θ and δ , over the motor network. We applied rTMS over the healthy motor cortex, and investigated the propagation of induced EEG oscillatory activity in the regional and long-range interregional connections of cortical areas. Thus, by quantifying the modulation of motor cortical oscillations in healthy subjects after rTMS, we have contributed to the understanding of the oscillatory dynamics and the

connectivity patterns induced by rTMS. By inferring the cortical oscillatory dynamics in the healthy brain, we provide the baseline for researchers and clinicians to distinguish the oscillatory patterns that may be disrupted in patients of various neuropsychiatric disorders. The combined rTMS-EEG could have wide applicability in clinical research for characterising disturbances in oscillatory patterns and the altered functional connectivity in neuropsychiatric illnesses (Hampson & Hoffman, 2010; Miniussi & Rossini, 2011; Rogasch & Fitzgerald, 2012). By directly entrain the oscillatory brain rhythms in a control manner, the rTMS-EEG can indeed offer exciting possibilities as a diagnostic and therapeutic tool (Thut, Schyns, & Gross, 2011). Hence, the author concludes her work in this thesis with an optimistic hope that one day non-invasive brain stimulation will be the treatment of choice for neuropsychiatric diseases.

References

- Agostino, R., Iezzi, E., Dinapoli, L., Suppa, A., Conte, A., & Berardelli, A. (2008). Effects of intermittent theta-burst stimulation on practice-related changes in fast finger movements in healthy subjects. *Eur J Neurosci*, *28*(4), 822-828.
- Allen, E. A., Pasley, B. N., Duong, T., & Freeman, R. D. (2007). Transcranial magnetic stimulation elicits coupled neural and hemodynamic consequences. *Science*, *317*(5846), 1918-1921.
- Amassian, V. E., Cracco, R. Q., & Maccabee, P. J. (1989). Focal stimulation of human cerebral cortex with the magnetic coil: a comparison with electrical stimulation. *Electroencephalogr Clin Neurophysiol*, *74*(6), 401-416.
- Amassian, V. E., Cracco, R. Q., Maccabee, P. J., & Cracco, J. B. (1992). Cerebello-frontal cortical projections in humans studied with the magnetic coil. *Electroencephalogr Clin Neurophysiol*, *85*(4), 265-272.
- Anand, S., & Hotson, J. (2002). Transcranial magnetic stimulation: neurophysiological applications and safety. *Brain Cogn*, *50*(3), 366-386.
- Andrew, C., & Pfurtscheller, G. (1996). Event-related coherence as a tool for studying dynamic interaction of brain regions. *Electroencephalogr Clin Neurophysiol*, *98*(2), 144-148.
- Arana, A. B., Borckardt, J. J., Ricci, R., Anderson, B., Li, X., Linder, K. J., et al. (2008). Focal electrical stimulation as a sham control for repetitive transcranial magnetic stimulation: Does it truly mimic the cutaneous sensation and pain of active prefrontal repetitive transcranial magnetic stimulation? *Brain Stimul*, *1*(1), 44-51.
- Aydin-Abidin, S., Moliadze, V., Eysel, U. T., & Funke, K. (2006). Effects of repetitive TMS on visually evoked potentials and EEG in the anaesthetized cat: dependence on stimulus frequency and train duration. *J Physiol*, *574*(Pt 2), 443-455.
- Aydin-Abidin, S., Trippe, J., Funke, K., Eysel, U. T., & Benali, A. (2008). High- and low-frequency repetitive transcranial magnetic stimulation differentially activates c-Fos and zif268 protein expression in the rat brain. *Exp Brain Res*, *188*(2), 249-261.
- Babiloni, C., Frisoni, G., Steriade, M., Bresciani, L., Binetti, G., Del Percio, C., et al. (2006). Frontal white matter volume and delta EEG sources negatively correlate in awake subjects with mild cognitive impairment and Alzheimer's disease. *Clin Neurophysiol*, *117*(5), 1113-1129.
- Baillieux, H., De Smet, H. J., Dobbeleir, A., Paquier, P. F., De Deyn, P. P., & Marien, P. (2010). Cognitive and affective disturbances following focal cerebellar damage in adults: a neuropsychological and SPECT study. *Cortex*, *46*(7), 869-879.

- Baillieux, H., De Smet, H. J., Paquier, P. F., De Deyn, P. P., & Marien, P. (2008). Cerebellar neurocognition: insights into the bottom of the brain. *Clin Neurol Neurosurg*, *110*(8), 763-773.
- Barker, R. A., Barasi, S., & Neal, M. J. (2008). *Neuroscience at a glance*: Blackwell Publishing.
- Barker, A. T., Jalinous, R., & Freeston, I. L. (1985). Non-invasive magnetic stimulation of human motor cortex. *Lancet*, *1*(8437), 1106-1107.
- Basar, E., Basar-Eroglu, C., Karakas, S., & Schurmann, M. (1999). Oscillatory brain theory: a new trend in neuroscience. *IEEE Eng Med Biol Mag*, *18*(3), 56-66.
- Basar, E., Demiralp, T., Schurmann, M., Basar-Eroglu, C., & Ademoglu, A. (1999). Oscillatory brain dynamics, wavelet analysis, and cognition. *Brain Lang*, *66*(1), 146-183.
- Basar, E., & Guntekin, B. (2008). A review of brain oscillations in cognitive disorders and the role of neurotransmitters. *Brain Res*, *1235*, 172-193.
- Bear, M. F., & Malenka, R. C. (1994). Synaptic plasticity: LTP and LTD. *Curr Opin Neurobiol*, *4*(3), 389-399.
- Belluscio, M. A., Mizuseki, K., Schmidt, R., Kempster, R., & Buzsaki, G. (2012). Cross-frequency phase-phase coupling between theta and gamma oscillations in the hippocampus. *J Neurosci*, *32*(2), 423-435.
- Berger, H. (1969). On the electroencephalogram of man. *Electroencephalogr Clin Neurophysiol*, Suppl 28:37+.
- Bestmann, S. (2008). The physiological basis of transcranial magnetic stimulation. *Trends Cogn Sci*, *12*(3), 81-83.
- Bestmann, S., Baudewig, J., Siebner, H. R., Rothwell, J. C., & Frahm, J. (2003). Is functional magnetic resonance imaging capable of mapping transcranial magnetic cortex stimulation? *Suppl Clin Neurophysiol*, *56*, 55-62.
- Bohning, D. E., Shastri, A., McConnell, K. A., Nahas, Z., Lorberbaum, J. P., Roberts, D. R., et al. (1999). A combined TMS/fMRI study of intensity-dependent TMS over motor cortex. *Biol Psychiatry*, *45*(4), 385-394.
- Borojerdi, B., Ziemann, U., Chen, R., Butefisch, C. M., & Cohen, L. G. (2001). Mechanisms underlying human motor system plasticity. *Muscle Nerve*, *24*(5), 602-613.
- Brasil-Neto, J. P., Cohen, L. G., Panizza, M., Nilsson, J., Roth, B. J., & Hallett, M. (1992). Optimal focal transcranial magnetic activation of the human motor cortex: effects of coil orientation, shape of the induced current pulse, and stimulus intensity. *J Clin Neurophysiol*, *9*(1), 132-136.
- Brignani, D., Manganotti, P., Rossini, P. M., & Miniussi, C. (2008). Modulation of cortical oscillatory activity during transcranial magnetic stimulation. *Human brain mapping*, *29*(5), 603-612.
- Brown, P. (2003). Oscillatory nature of human basal ganglia activity: relationship to the pathophysiology of Parkinson's disease. *Mov Disord*, *18*(4), 357-63.
- Buzsaki, G. (2002). Theta oscillations in the hippocampus. *Neuron*, *33*(3), 325-340.

- Buzsaki, G. (2005). Theta rhythm of navigation: link between path integration and landmark navigation, episodic and semantic memory. *Hippocampus*, 15(7), 827-840.
- Buzsaki, G., & Draguhn, A. (2004). Neuronal oscillations in cortical networks. *Science (New York, N Y)*, 304(5679), 1926-1929.
- Calmels, C., Holmes, P., Jarry, G., Hars, M., Lopez, E., Paillard, A., et al. (2006). Variability of EEG synchronization prior to and during observation and execution of a sequential finger movement. *Hum Brain Mapp*, 27(3), 251-266.
- Canedo, A. (1997). Primary motor cortex influences on the descending and ascending systems. *Prog Neurobiol*, 51(3), 287-335.
- Cantero, J. L., Atienza, M., Stickgold, R., Kahana, M. J., Madsen, J. R., & Kocsis, B. (2003). Sleep-dependent theta oscillations in the human hippocampus and neocortex. *J Neurosci*, 23(34), 10897-10903.
- Caplan, J. B., Madsen, J. R., Schulze-Bonhage, A., Aschenbrenner-Scheibe, R., Newman, E. L., & Kahana, M. J. (2003). Human theta oscillations related to sensorimotor integration and spatial learning. *J Neurosci*, 23(11), 4726-4736.
- Cardenas-Morales, L., Gron, G., & Kammer, T. (2011). Exploring the aftereffects of theta burst magnetic stimulation on the human motor cortex: A functional imaging study. *Hum Brain Mapp*, 32(11), 1948-1960.
- Cardenas-Morales, L., Nowak, D. A., Kammer, T., Wolf, R. C., & Schonfeldt-Lecuona, C. (2010). Mechanisms and applications of theta-burst rTMS on the human motor cortex. *Brain Topogr*, 22(4), 294-306.
- Cheeran, B., Talelli, P., Mori, F., Koch, G., Suppa, A., Edwards, M., et al. (2008). A common polymorphism in the brain-derived neurotrophic factor gene (BDNF) modulates human cortical plasticity and the response to rTMS. *J Physiol*, 586(Pt 23), 5717-5725.
- Chen, R. (2000). Studies of human motor physiology with transcranial magnetic stimulation. *Muscle Nerve Suppl*, 9, S26-32.
- Chen, R. (2010). Repetitive transcranial magnetic stimulation as treatment for depression in Parkinson's disease. *Mov Disord*, 25(14), 2272-2273.
- Chen, R. (2012). Repetitive transcranial magnetic stimulation as a treatment for essential tremor? *Clin Neurophysiol*, 123(5), 850-851.
- Chen, R., Classen, J., Gerloff, C., Celnik, P., Wassermann, E. M., Hallett, M., et al. (1997). Depression of motor cortex excitability by low-frequency transcranial magnetic stimulation. *Neurology*, 48(5), 1398-1403.
- Chen, R., Cros, D., Curra, A., Di Lazzaro, V., Lefaucheur, J. P., Magistris, M. R., et al. (2008). The clinical diagnostic utility of transcranial magnetic stimulation: report of an IFCN committee. *Clin Neurophysiol*, 119(3), 504-532.
- Chen, R., & Udupa, K. (2009). Measurement and modulation of plasticity of the motor system in humans using transcranial magnetic stimulation. *Motor Control*, 13(4), 442-453.
- Chouinard, P. A., & Paus, T. (2006). The primary motor and premotor areas of the human cerebral cortex. *Neuroscientist*, 12(2), 143-152.

- Chouinard, P. A., Van Der Werf, Y. D., Leonard, G., & Paus, T. (2003). Modulating neural networks with transcranial magnetic stimulation applied over the dorsal premotor and primary motor cortices. *J Neurophysiol*, *90*(2), 1071-1083.
- Cohen, L. G., Ziemann, U., Chen, R., Classen, J., Hallett, M., Gerloff, C., et al. (1998). Studies of neuroplasticity with transcranial magnetic stimulation. *J Clin Neurophysiol*, *15*(4), 305-324.
- Conforto, A. B., Z'Graggen, W. J., Kohl, A. S., Rosler, K. M., & Kaelin-Lang, A. (2004). Impact of coil position and electrophysiological monitoring on determination of motor thresholds to transcranial magnetic stimulation. *Clin Neurophysiol*, *115*(4), 812-819.
- Cooke, S. F., & Bliss, T. V. (2006). Plasticity in the human central nervous system. *Brain*, *129*(Pt 7), 1659-1673.
- Cracco, R. Q., Amassian, V. E., Maccabee, P. J., & Cracco, J. B. (1989). Comparison of human transcallosal responses evoked by magnetic coil and electrical stimulation. *Electroencephalogr Clin Neurophysiol*, *74*(6), 417-424.
- Crochet, S., Fuentealba, P., Cisse, Y., Timofeev, I., & Steriade, M. (2006). Synaptic plasticity in local cortical network in vivo and its modulation by the level of neuronal activity. *Cereb Cortex*, *16*(5), 618-631.
- da Silva, F. H., Gomez, J. P., Velis, D. N., & Kalitzin, S. (2005). Phase clustering of high frequency EEG: MEG components. *Clin EEG Neurosci*, *36*(4), 306-310.
- Danos, P., Guich, S., Abel, L., & Buchsbaum, M. S. (2001). Eeg alpha rhythm and glucose metabolic rate in the thalamus in schizophrenia. *Neuropsychobiology*, *43*(4), 265-272.
- Daskalakis, Z. J., Moller, B., Christensen, B. K., Fitzgerald, P. B., Gunraj, C., & Chen, R. (2006). The effects of repetitive transcranial magnetic stimulation on cortical inhibition in healthy human subjects. *Exp Brain Res*, *174*(3), 403-412.
- Davies, C. H., Starkey, S. J., Pozza, M. F., & Collingridge, G. L. (1991). GABA autoreceptors regulate the induction of LTP. *Nature*, *349*(6310), 609-611.
- de Lange, F. P., Jensen, O., Bauer, M., & Toni, I. (2008). Interactions between posterior gamma and frontal alpha/beta oscillations during imagined actions. *Front Hum Neurosci*, *2*, 7.
- Destexhe, A., Contreras, D., & Steriade, M. (1999). Cortically-induced coherence of a thalamic-generated oscillation. *Neuroscience*, *92*(2), 427-443.
- Di Lazzaro, V., Dileone, M., Pilato, F., Capone, F., Musumeci, G., Ranieri, F., et al. (2011). Modulation of motor cortex neuronal networks by rTMS: comparison of local and remote effects of six different protocols of stimulation. *J Neurophysiol*, *105*(5), 2150-2156.
- Di Lazzaro, V., Oliviero, A., Profice, P., Insola, A., Mazzone, P., Tonali, P., et al. (1999). Direct recordings of descending volleys after transcranial magnetic and electric motor cortex stimulation in conscious humans. *Electroencephalogr Clin Neurophysiol Suppl*, *51*, 120-126.

- Di Lazzaro, V., Pilato, F., Dileone, M., Profice, P., Oliviero, A., Mazzone, P., et al. (2008). The physiological basis of the effects of intermittent theta burst stimulation of the human motor cortex. *J Physiol*, *586*(16), 3871-3879.
- Di Lazzaro, V., Pilato, F., Dileone, M., Profice, P., Oliviero, A., Mazzone, P., et al. (2008). Low-frequency repetitive transcranial magnetic stimulation suppresses specific excitatory circuits in the human motor cortex. *J Physiol*, *586*(Pt 18), 4481-4487.
- Di Lazzaro, V., Pilato, F., Saturno, E., Oliviero, A., Dileone, M., Mazzone, P., et al. (2005). Theta-burst repetitive transcranial magnetic stimulation suppresses specific excitatory circuits in the human motor cortex. *J Physiol*, *565*(Pt 3), 945-950.
- Di Lazzaro, V., Profice, P., Pilato, F., Dileone, M., Oliviero, A., & Ziemann, U. (2010). The effects of motor cortex rTMS on corticospinal descending activity. *Clin Neurophysiol*, *121*(4), 464-473.
- Di Lazzaro, V., Ziemann, U., & Lemon, R. N. (2008). State of the art: Physiology of transcranial motor cortex stimulation. *Brain Stimul*, *1*(4), 345-362.
- Duffau, H. (2006). Brain plasticity: from pathophysiological mechanisms to therapeutic applications. *J Clin Neurosci*, *13*(9), 885-897.
- Dutilh, G., Vandekerckhove, J., Tuerlinckx, F., & Wagenmakers, E. J. (2009). A diffusion model decomposition of the practice effect. *Psychon Bull Rev*, *16*(6), 1026-1036.
- Epstein, C. M. (2008). A six-pound battery-powered portable transcranial magnetic stimulator. *Brain Stimul*, *1*(2), 128-130.
- Fein, G., Raz, J., Brown, F. F., & Merrin, E. L. (1988). Common reference coherence data are confounded by power and phase effects. *Electroencephalogr. Clin. Neurophysiol.*, *69*(6), 581.
- Feinsod, M., Kreinin, B., Chistyakov, A., & Klein, E. (1998). Preliminary evidence for a beneficial effect of low-frequency, repetitive transcranial magnetic stimulation in patients with major depression and schizophrenia. *Depression and anxiety*, *7*(2), 65-68.
- Fitzgerald, P. B., Brown, T. L., Daskalakis, Z. J., Chen, R., & Kulkarni, J. (2002). Intensity-dependent effects of 1 Hz rTMS on human corticospinal excitability. *Clin Neurophysiol*, *113*(7), 1136-1141.
- Fitzgerald, P. B., Fountain, S., & Daskalakis, Z. J. (2006). A comprehensive review of the effects of rTMS on motor cortical excitability and inhibition. *Clin Neurophysiol*, *117*(12), 2584-2596.
- Fitzgerald, P. B., Fountain, S., Hoy, K., Maller, J., Enticott, P., Laycock, R., et al. (2007). A comparative study of the effects of repetitive paired transcranial magnetic stimulation on motor cortical excitability. *J Neurosci Methods*, *165*(2), 265-269.
- Fitzpatrick, S. M., & Rothman, D. L. (2000). Meeting report: transcranial magnetic stimulation and studies of human cognition. *J Cogn Neurosci*, *12*(4), 704-709.
- Formaggio, E., Storti, S. F., Avesani, M., Cerini, R., Milanese, F., Gasparini, A., et al. (2008). EEG and fMRI coregistration to investigate the cortical

- oscillatory activities during finger movement. *Brain Topogr*, 21(2), 100-111.
- Freeman, W. J. (2004a). Origin, structure, and role of background EEG activity. Part 1. Analytic amplitude. *Clin Neurophysiol*, 115(9), 2077-2088.
- Freeman, W. J. (2004b). Origin, structure, and role of background EEG activity. Part 2. Analytic phase. *Clin Neurophysiol*, 115(9), 2089-2107.
- Freeman, W. J. (2005). Origin, structure, and role of background EEG activity. Part 3. Neural frame classification. *Clin Neurophysiol*, 116(5), 1118-1129.
- Freeman, W. J. (2006). Origin, structure, and role of background EEG activity. Part 4: Neural frame simulation. *Clin Neurophysiol*, 117(3), 572-589.
- Freeman, W. J., Holmes, M. D., Burke, B. C., & Vanhatalo, S. (2003). Spatial spectra of scalp EEG and EMG from awake humans. *Clin Neurophysiol*, 114(6), 1053-1068.
- Fuggetta, G., Fiaschi, A., & Manganotti, P. (2005). Modulation of cortical oscillatory activities induced by varying single-pulse transcranial magnetic stimulation intensity over the left primary motor area: a combined EEG and TMS study. *Neuroimage*, 27(4), 896-908.
- Fuggetta, G., Pavone, E. F., Fiaschi, A., & Manganotti, P. (2008). Acute modulation of cortical oscillatory activities during short trains of high-frequency repetitive transcranial magnetic stimulation of the human motor cortex: a combined EEG and TMS study. *Hum Brain Mapp*, 29(1), 1-13.
- Fuggetta, G., Pavone, E. F., Walsh, V., Kiss, M., & Eimer, M. (2006). Cortico-cortical interactions in spatial attention: A combined ERP/TMS study. *J Neurophysiol*, 95(5), 3277-3280.
- Fuggetta, G., Rizzo, S., Pobric, G., Lavidor, M., & Walsh, V. (2009). Functional representation of living and nonliving domains across the cerebral hemispheres: a combined event-related potential/transcranial magnetic stimulation study. *J Cogn Neurosci*, 21(2), 403-414.
- Gevins, A. S., Morgan, N. H., Bressler, S. L., Doyle, J. C., & Cuttillo, B. A. (1986). Improved event-related potential estimation using statistical pattern classification. *Electroencephalogr Clin Neurophysiol*, 64(2), 177-186.
- Goldman, R. I., Stern, J. M., Engel, J., Jr., & Cohen, M. S. (2002). Simultaneous EEG and fMRI of the alpha rhythm. *Neuroreport*, 13(18), 2487-2492.
- Gray, C. M., & Singer, W. (1989). Stimulus-specific neuronal oscillations in orientation columns of cat visual cortex. *Proc Natl Acad Sci U S A*, 86(5), 1698-1702.
- Grenier, F., Timofeev, I., Crochet, S., & Steriade, M. (2003). Spontaneous field potentials influence the activity of neocortical neurons during paroxysmal activities in vivo. *Neuroscience*, 119(1), 277-291.
- Grossheinrich, N., Rau, A., Pogarell, O., Hennig-Fast, K., Reinl, M., Karch, S., et al. (2009). Theta burst stimulation of the prefrontal cortex: safety and impact on cognition, mood, and resting electroencephalogram. *Biol Psychiatry*, 65(9), 778-784.

- Guillery, R. W., & Sherman, S. M. (2002). The thalamus as a monitor of motor outputs. *Philos Trans R Soc Lond B Biol Sci*, 357(1428), 1809-1821.
- Haber, S. N., & Calzavara, R. (2009). The cortico-basal ganglia integrative network: the role of the thalamus. *Brain Res Bull*, 78(2-3), 69-74.
- Hallett, M. (2000). Transcranial magnetic stimulation and the human brain. *Nature*, 406(6792), 147-150.
- Hallett, M. (2007). Transcranial magnetic stimulation: a primer. *Neuron*, 55(2), 187-199.
- Hallett, M., & Rothwell, J. (2011). Milestones in clinical neurophysiology. *Mov Disord*, 26(6), 958-967.
- Hamidi, M., Johson, J. S., Feredoes, E., & Postle, B. R. (2011). Does high-frequency repetitive transcranial magnetic stimulation produce residual and/or cumulative effects within an experimental session? *Brain Topogr*, 23(4), 355-367.
- Hampson, M., & Hoffman, R. E. (2010). Transcranial magnetic stimulation and connectivity mapping: tools for studying the neural bases of brain disorders. *Front Syst Neurosci*, 4.
- Hari, R., Forss, N., Avikainen, S., Kirveskari, E., Salenius, S., & Rizzolatti, G. (1998). Activation of human primary motor cortex during action observation: a neuromagnetic study. *Proc Natl Acad Sci U S A*, 95(25), 15061-15065.
- Hari, R., & Salmelin, R. (1997). Human cortical oscillations: a neuromagnetic view through the skull. *Trends Neurosci*, 20(1), 44-49.
- Harmony, T., Fernandez, T., Silva, J., Bernal, J., Diaz-Comas, L., Reyes, A., et al. (1996). EEG delta activity: an indicator of attention to internal processing during performance of mental tasks. *Int J Psychophysiol*, 24(1-2), 161-171.
- Harmony, T., Fernandez, T., Silva, J., Bosch, J., Valdes, P., Fernandez-Bouzas, A., et al. (1999). Do specific EEG frequencies indicate different processes during mental calculation? *Neurosci Lett*, 266(1), 25-28.
- Heide, G., Witte, O. W., & Ziemann, U. (2006). Physiology of modulation of motor cortex excitability by low-frequency suprathreshold repetitive transcranial magnetic stimulation. *Exp Brain Res*, 171(1), 26-34.
- Henning Proske, J., Jeanmonod, D., & Verschure, P. F. M. J. (2011). A computational model of thalamocortical dysrhythmia. *The European journal of neuroscience*, 33(7), 1281-1290.
- Herwig, U., Cardenas-Morales, L., Connemann, B. J., Kammer, T., & Schonfeldt-Lecuona, C. (2010). Sham or real--post hoc estimation of stimulation condition in a randomized transcranial magnetic stimulation trial. *Neurosci Lett*, 471(1), 30-33.
- Herwig, U., Satrapi, P., & Schonfeldt-Lecuona, C. (2003). Using the international 10-20 EEG system for positioning of transcranial magnetic stimulation. *Brain Topogr*, 16(2), 95-99.
- Hess, G. (2004). Synaptic plasticity of local connections in rat motor cortex. *Acta Neurobiol Exp (Wars)*, 64(2), 271-276.

- Holler, I., Siebner, H. R., Cunnington, R., & Gerschlagel, W. (2006). 5 Hz repetitive TMS increases anticipatory motor activity in the human cortex. *Neurosci Lett*, *392*(3), 221-225.
- Hoogendam, J. M., Ramakers, G. M., & Di Lazzaro, V. (2010). Physiology of repetitive transcranial magnetic stimulation of the human brain. *Brain Stimul*, *3*(2), 95-118.
- Houweling, S., van Dijk, B. W., Beek, P. J., & Daffertshofer, A. (2010). Cortico-spinal synchronization reflects changes in performance when learning a complex bimanual task. *Neuroimage*, *49*(4), 3269-3275.
- Huang, Y. Z., Chen, R. S., Rothwell, J. C., & Wen, H. Y. (2007). The aftereffect of human theta burst stimulation is NMDA receptor dependent. *Clin Neurophysiol*, *118*(5), 1028-1032.
- Huang, Y. Z., Edwards, M. J., Rounis, E., Bhatia, K. P., & Rothwell, J. C. (2005). Theta burst stimulation of the human motor cortex. *Neuron*, *45*(2), 201-206.
- Huang, Y. Z., Rothwell, J. C., Chen, R. S., Lu, C. S., & Chuang, W. L. (2011). The theoretical model of theta burst form of repetitive transcranial magnetic stimulation. *Clin Neurophysiol*, *122*(5), 1011-1018.
- Huang, Y. Z., Rothwell, J. C., Edwards, M. J., & Chen, R. S. (2008). Effect of physiological activity on an NMDA-dependent form of cortical plasticity in human. *Cereb Cortex*, *18*(3), 563-570.
- Hubl, D., Nyffeler, T., Wurtz, P., Chaves, S., Pflugshaupt, T., Luthi, M., et al. (2008). Time course of blood oxygenation level-dependent signal response after theta burst transcranial magnetic stimulation of the frontal eye field. *Neuroscience*, *151*(3), 921-928.
- Huerta, P. T., & Volpe, B. T. (2009). Transcranial magnetic stimulation, synaptic plasticity and network oscillations. *J Neuroeng Rehabil*, *6*, 7.
- Hughes, S. W., & Crunelli, V. (2005). Thalamic mechanisms of EEG alpha rhythms and their pathological implications. *Neuroscientist*, *11*(4), 357-372.
- Hughes, S. W., & Crunelli, V. (2007). Just a phase they're going through: the complex interaction of intrinsic high-threshold bursting and gap junctions in the generation of thalamic alpha and theta rhythms. *Int J Psychophysiol*, *64*(1), 3-17.
- Hughes, S. W., Lorincz, M., Cope, D. W., Blethyn, K. L., Kekesi, K. A., Parri, H. R., et al. (2004). Synchronized oscillations at alpha and theta frequencies in the lateral geniculate nucleus. *Neuron*, *42*(2), 253-268.
- Iezzi, E., Conte, A., Suppa, A., Agostino, R., Dinapoli, L., Scontrini, A., et al. (2008). Phasic voluntary movements reverse the aftereffects of subsequent theta-burst stimulation in humans. *J Neurophysiol*, *100*(4), 2070-2076.
- Ilmoniemi, R. J., Ruohonen, J., Virtanen, J., Aronen, H. J., & Karhu, J. (1999). EEG responses evoked by transcranial magnetic stimulation. *Electroencephalogr Clin Neurophysiol Suppl*, *51*, 22-29.

- Ilmoniemi, R. J., Virtanen, J., Ruohonen, J., Karhu, J., Aronen, H. J., Naatanen, R., et al. (1997). Neuronal responses to magnetic stimulation reveal cortical reactivity and connectivity. *Neuroreport*, *8*(16), 3537-3540.
- Ishikawa, S., Matsunaga, K., Nakanishi, R., Kawahira, K., Murayama, N., Tsuji, S., et al. (2007). Effect of theta burst stimulation over the human sensorimotor cortex on motor and somatosensory evoked potentials. *Clin Neurophysiol*, *118*(5), 1033-1043.
- Iyer, M. B., Schleper, N., & Wassermann, E. M. (2003). Priming stimulation enhances the depressant effect of low-frequency repetitive transcranial magnetic stimulation. *J Neurosci*, *23*(34), 10867-10872.
- Jacobs, J., Hwang, G., Curran, T., & Kahana, M. J. (2006). EEG oscillations and recognition memory: theta correlates of memory retrieval and decision making. *Neuroimage*, *32*(2), 978-987.
- Jancke, L., Steinmetz, H., Benilow, S., & Ziemann, U. (2004). Slowing fastest finger movements of the dominant hand with low-frequency rTMS of the hand area of the primary motor cortex. *Exp Brain Res*, *155*(2), 196-203.
- Jasper, H. H., & Radmussen, T. (1958). Studies of clinical and electrical responses to deep temporal stimulation in men with some considerations of functional anatomy. *Res Publ Assoc Res Nerv Ment Dis*, *36*, 316-334.
- Jeanmonod, D., Schulman, J., Ramirez, R., Cancro, R., Lanz, M., Morel, A., et al. (2003). Neuropsychiatric thalamocortical dysrhythmia: surgical implications. *Neurosurgery clinics of North America*, *14*(2), 251-265.
- Jenkinsen, N., & Brown, P. (2011). New insights into the relationship between dopamine, beta oscillations and motor function. *Trends Neurosci*, *34*(12), 611-8.
- Jensen, O., Kaiser, J., & Lachaux, J. P. (2007). Human gamma-frequency oscillations associated with attention and memory. *Trends Neurosci*, *30*(7), 317-324.
- Jing, H., & Takigawa, M. (2000). Observation of EEG coherence after repetitive transcranial magnetic stimulation. *Clin Neurophysiol*, *111*(9), 1620-1631.
- Jones, E. G. (2002). Thalamic circuitry and thalamocortical synchrony. *Philos Trans R Soc Lond B Biol Sci*, *357*(1428), 1659-1673.
- Jones, E. G. (2010). Thalamocortical dysrhythmia and chronic pain. *Pain*, *150*(1), 4-5.
- Joundi, R. N., Jenkinson, N., Brittain, J. S., Aziz, T. Z., & Brown, P. (2012). Driving oscillatory activity in the human cortex enhances motor performance. *Curr Biol*, *22*(5), 403-7.
- Jung, S. H., Shin, J. E., Jeong, Y. S., & Shin, H. I. (2008). Changes in motor cortical excitability induced by high-frequency repetitive transcranial magnetic stimulation of different stimulation durations. *Clin Neurophysiol*, *119*(1), 71-79.
- Jurcak, V., Tsuzuki, D., & Dan, I. (2007). 10/20, 10/10, and 10/5 systems revisited: their validity as relative head-surface-based positioning systems. *Neuroimage*, *34*(4), 1600-1611.
- Kahana, M. J., Seelig, D., & Madsen, J. R. (2001). Theta returns. *Curr Opin Neurobiol*, *11*(6), 739-744.

- Kahana, M. J., Sekuler, R., Caplan, J. B., Kirschen, M., & Madsen, J. R. (1999). Human theta oscillations exhibit task dependence during virtual maze navigation. *Nature*, *399*(6738), 781-784.
- Khedr, E. M., Gilio, F., & Rothwell, J. (2004). Effects of low frequency and low intensity repetitive paired pulse stimulation of the primary motor cortex. *Clin Neurophysiol*, *115*(6), 1259-1263.
- Khedr, E. M., Rothwell, J. C., Shawky, O. A., Ahmed, M. A., Foly, N., & Hamdy, A. (2007). Dopamine levels after repetitive transcranial magnetic stimulation of motor cortex in patients with Parkinson's disease: preliminary results. *Mov Disord*, *22*(7), 1046-1050.
- Kleinjung, T., Steffens, T., Landgrebe, M., Vielsmeier, V., Frank, E., Burger, J., et al. (2011). Repetitive transcranial magnetic stimulation for tinnitus treatment: no enhancement by the dopamine and noradrenaline reuptake inhibitor bupropion. *Brain Stimul*, *4*(2), 65-70.
- Klimesch, W. (1999). EEG alpha and theta oscillations reflect cognitive and memory performance: a review and analysis. *Brain Res Brain Res Rev*, *29*(2-3), 169-195.
- Kobayashi, M., & Pascual-Leone, A. (2003). Transcranial magnetic stimulation in neurology. *Lancet Neurol*, *2*(3), 145-156.
- Komssi, S., & Kahkonen, S. (2006). The novelty value of the combined use of electroencephalography and transcranial magnetic stimulation for neuroscience research. *Brain Res Rev*, *52*(1), 183-192.
- Komssi, S., Kahkonen, S., & Ilmoniemi, R. J. (2004). The effect of stimulus intensity on brain responses evoked by transcranial magnetic stimulation. *Hum Brain Mapp*, *21*(3), 154-164.
- Kujirai, T., Sato, M., Rothwell, J. C., & Cohen, L. G. (1993). The effect of transcranial magnetic stimulation on median nerve somatosensory evoked potentials. *Electroencephalogr Clin Neurophysiol*, *89*(4), 227-234.
- Lang, N., Nitsche, M. A., Paulus, W., Rothwell, J. C., & Lemon, R. N. (2004). Effects of transcranial direct current stimulation over the human motor cortex on corticospinal and transcallosal excitability. *Exp Brain Res*, *156*(4), 439-443.
- Langguth, B., Kleinjung, T., Landgrebe, M., de Ridder, D., & Hajak, G. (2010). rTMS for the treatment of tinnitus: the role of neuronavigation for coil positioning. *Neurophysiol Clin*, *40*(1), 45-58.
- Larson, J., Wong, D., & Lynch, G. (1986). Patterned stimulation at the theta frequency is optimal for the induction of hippocampal long-term potentiation. *Brain Res*, *368*(2), 347-350.
- Lee, L., Siebner, H. R., Rowe, J. B., Rizzo, V., Rothwell, J. C., Frackowiak, R. S., et al. (2003). Acute remapping within the motor system induced by low-frequency repetitive transcranial magnetic stimulation. *J Neurosci*, *23*(12), 5308-5318.
- Lefaucheur, J. P., Antal, A., Ahdab, R., Ciampi de Andrade, D., Fregni, F., Khedr, E. M., et al. (2008). The use of repetitive transcranial magnetic

- stimulation (rTMS) and transcranial direct current stimulation (tDCS) to relieve pain. *Brain Stimul*, 1(4), 337-344.
- Leocani, L., Toro, C., Manganotti, P., Zhuang, P., & Hallett, M. (1997a). Event-related coherence and event-related desynchronization/synchronization in the 10 Hz and 20 Hz EEG during self-paced movements. *Electroencephalogr Clin Neurophysiol*, 104(3), 199-206.
- Leocani, L., Toro, C., Manganotti, P., Zhuang, P., & Hallett, M. (1997b). Event-related coherence and event-related desynchronization/synchronization in the 10 Hz and 20 Hz EEG during self-paced movements. *Electroencephalogr. Clin. Neurophysiol.*, 104(3), 199.
- Leung, L. W., & Borst, J. G. (1987). Electrical activity of the cingulate cortex. I. Generating mechanisms and relations to behavior. *Brain Res*, 407(1), 68-80.
- Levy, R., Hazrati, L. N., Herrero, M. T., Vila, M., Hassani, O. K., Mouroux, M., et al. (1997). Re-evaluation of the functional anatomy of the basal ganglia in normal and Parkinsonian states. *Neuroscience*, 76(2), 335-343.
- Light, G. A., Williams, L. E., Minow, F., Sprock, J., Risling, A., Sharp, R., et al. (2010). Electroencephalography (EEG) and event-related potentials (ERPs) with human participants. *Curr Protoc Neurosci, Chapter 6*, Unit 6 25 21-24.
- Llinas, R., & Ribary, U. (2001). Consciousness and the brain. The thalamocortical dialogue in health and disease. *Ann N Y Acad Sci*, 929, 166-175.
- Llinas, R. R., Ribary, U., Jeanmonod, D., Kronberg, E., & Mitra, P. P. (1999). Thalamocortical dysrhythmia: A neurological and neuropsychiatric syndrome characterized by magnetoencephalography. *Proc Natl Acad Sci U S A*, 96(26), 15222-15227.
- Llinas, R. R., & Steriade, M. (2006). Bursting of thalamic neurons and states of vigilance. *J Neurophysiol*, 95(6), 3297-3308.
- Londero, A., Lefaucheur, J. P., Malinvaud, D., Brugieres, P., Peignard, P., Nguyen, J. P., et al. (2006). [Magnetic stimulation of the auditory cortex for disabling tinnitus: preliminary results]. *Presse Med*, 35(2 Pt 1), 200-206.
- Maeda, F., Keenan, J. P., Tormos, J. M., Topka, H., & Pascual-Leone, A. (2000a). Interindividual variability of the modulatory effects of repetitive transcranial magnetic stimulation on cortical excitability. *Exp Brain Res*, 133(4), 425-430.
- Maeda, F., Keenan, J. P., Tormos, J. M., Topka, H., & Pascual-Leone, A. (2000b). Modulation of corticospinal excitability by repetitive transcranial magnetic stimulation. *Clin Neurophysiol*, 111(5), 800-805.
- Maki, H., & Ilmoniemi, R. J. (2010). EEG oscillations and magnetically evoked motor potentials reflect motor system excitability in overlapping neuronal populations. *Clin Neurophysiol*, 121(4), 492-501.
- Malenka, R. C. (1994). Synaptic plasticity in the hippocampus: LTP and LTD. *Cell*, 78(4), 535-538.

- Malenka, R. C. (2003). Synaptic plasticity and AMPA receptor trafficking. *Ann N Y Acad Sci*, 1003, 1-11.
- Malenka, R. C., & Bear, M. F. (2004). LTP and LTD: an embarrassment of riches. *Neuron*, 44(1), 5-21.
- Mally, J., & Stone, T. W. (1999). Improvement in Parkinsonian symptoms after repetitive transcranial magnetic stimulation. *Journal of the neurological sciences*, 162(2), 179-184.
- Manganotti, P., Formaggio, E., Storti, S. F., De Massari, D., Zamboni, A., Bertoldo, A., et al. (2012). Time-frequency analysis of short-lasting modulation of EEG induced by intracortical and transcallosal paired TMS over motor areas. *J Neurophysiol*.
- Manganotti, P., Gerloff, C., Toro, C., Katsuta, H., Sadato, N., Zhuang, P., et al. (1998a). Task-related coherence and task-related spectral power changes during sequential finger movements. *Electroencephalogr Clin Neurophysiol*, 109(1), 50-62.
- Manganotti, P., Gerloff, C., Toro, C., Katsuta, H., Sadato, N., Zhuang, P., et al. (1998b). Task-related coherence and task-related spectral power changes during sequential finger movements. *Electroencephalogr. Clin. Neurophysiol.*, 109(1), 50.
- Martinez, L., Lamas, J. A., & Canedo, A. (1995). Pyramidal tract and corticospinal neurons with branching axons to the dorsal column nuclei of the cat. *Neuroscience*, 68(1), 195-206.
- McAllister, S. M., Rothwell, J. C., & Ridding, M. C. (2011). Cortical oscillatory activity and the induction of plasticity in the human motor cortex. *Eur J Neurosci*, 33(10), 1916-1924.
- McClintock, S. M., Freitas, C., Oberman, L., Lisanby, S. H., & Pascual-Leone, A. (2011). Transcranial magnetic stimulation: a neuroscientific probe of cortical function in schizophrenia. *Biol Psychiatry*, 70(1), 19-27.
- McDonnell, M. N., Orekhov, Y., & Ziemann, U. (2007). Suppression of LTP-like plasticity in human motor cortex by the GABAB receptor agonist baclofen. *Exp Brain Res*, 180(1), 181-186.
- Merton, P. A., Hill, D. K., Morton, H. B., & Marsden, C. D. (1982). Scope of a technique for electrical stimulation of human brain, spinal cord, and muscle. *Lancet*, 2(8298), 597-600.
- Merton, P. A., & Morton, H. B. (1980). Stimulation of the cerebral cortex in the intact human subject. *Nature*, 285(5762), 227.
- Meyer, G. (1987). Forms and spatial arrangement of neurons in the primary motor cortex of man. *J Comp Neurol*, 262(3), 402-428.
- Middleton, F. A., & Strick, P. L. (2000). Basal ganglia and cerebellar loops: motor and cognitive circuits. *Brain Res Brain Res Rev*, 31(2-3), 236-250.
- Miniussi, C., & Rossini, P. M. (2011). Transcranial magnetic stimulation in cognitive rehabilitation. *Neuropsychol Rehabil*, 1-23.
- Miniussi, C., & Thut, G. (2010). Combining TMS and EEG offers new prospects in cognitive neuroscience. *Brain Topogr*, 22(4), 249-256.

- Mitchell, D. J., McNaughton, N., Flanagan, D., & Kirk, I. J. (2008). Frontal-midline theta from the perspective of hippocampal "theta". *Prog Neurobiol*, *86*(3), 156-185.
- Mochizuki, H., Franca, M., Huang, Y. Z., & Rothwell, J. C. (2005). The role of dorsal premotor area in reaction task: comparing the "virtual lesion" effect of paired pulse or theta burst transcranial magnetic stimulation. *Exp Brain Res*, *167*(3), 414-421.
- Modugno, N., Nakamura, Y., MacKinnon, C. D., Filipovic, S. R., Bestmann, S., Berardelli, A., et al. (2001). Motor cortex excitability following short trains of repetitive magnetic stimuli. *Exp Brain Res*, *140*(4), 453-459.
- Moran, R. J., Mallet, N., Litvak, V., Dolan, R. J., Magill, P. J., Friston, K. J., & Brown, P. (2011). *PLoS Comput Biol*, *7*(8), e1002124.
- Muellbacher, W., Ziemann, U., Boroojerdi, B., & Hallett, M. (2000). Effects of low-frequency transcranial magnetic stimulation on motor excitability and basic motor behavior. *Clin Neurophysiol*, *111*(6), 1002-1007.
- Muellbacher, W., Ziemann, U., Wissel, J., Dang, N., Kofler, M., Facchini, S., et al. (2002). Early consolidation in human primary motor cortex. *Nature*, *415*(6872), 640-644.
- Nahas, Z., Lomarev, M., Roberts, D. R., Shastri, A., Lorberbaum, J. P., Teneback, C., et al. (2001). Unilateral left prefrontal transcranial magnetic stimulation (TMS) produces intensity-dependent bilateral effects as measured by interleaved BOLD fMRI. *Biol Psychiatry*, *50*(9), 712-720.
- Nathan, P. W. (1990). Touch and surgical division of the anterior quadrant of the spinal cord. *J Neurol Neurosurg Psychiatry*, *53*(11), 935-939.
- Nelson, S. B., Sjostrom, P. J., & Turrigiano, G. G. (2002). Rate and timing in cortical synaptic plasticity. *Philos Trans R Soc Lond B Biol Sci*, *357*(1428), 1851-1857.
- Niedermeyer, E. (2003). The clinical relevance of EEG interpretation. *Clin Electroencephalogr*, *34*(3), 93-98.
- Niedermeyer, E., Goldszmidt, A., & Ryan, D. (2004). "Mu rhythm status" and clinical correlates. *Clin EEG Neurosci*, *35*(2), 84-87.
- Nitsche, M. A., & Paulus, W. (2000). Excitability changes induced in the human motor cortex by weak transcranial direct current stimulation. *J Physiol*, *527 Pt 3*, 633-639.
- Nitsche, M. A., & Paulus, W. (2011). Transcranial direct current stimulation--update 2011. *Restor Neurol Neurosci*, *29*(6), 463-492.
- Nunez, P. L. (1989). Generation of human EEG by a combination of long and short range neocortical interactions. *Brain Topogr*, *1*(3), 199-215.
- Nunez, P. L. (1996). Spatial analysis of EEG. *Electroencephalogr Clin Neurophysiol Suppl*, *45*, 37-38.
- Nunez, P. L., & Srinivasan, R. (2006). A theoretical basis for standing and traveling brain waves measured with human EEG with implications for an integrated consciousness. *Clin Neurophysiol*, *117*(11), 2424-2435.
- Nunez, P. L., & Srinivasan, R. (2006). *Electric fields of the brain: The Neurophysics of EEG*: Oxford University Press.

- Nyffeler, T., Wurtz, P., Luscher, H. R., Hess, C. W., Senn, W., Pflugshaupt, T., et al. (2006). Repetitive TMS over the human oculomotor cortex: comparison of 1-Hz and theta burst stimulation. *Neurosci Lett*, *409*(1), 57-60.
- O'Halloran, C. J., Kinsella, G. J., & Storey, E. (2012). The cerebellum and neuropsychological functioning: a critical review. *J Clin Exp Neuropsychol*, *34*(1), 35-56.
- O'Shea, J., & Walsh, V. (2007). Transcranial magnetic stimulation. *Curr Biol*, *17*(6), R196-199.
- Oberman, L. M., Edwards, D., Eldaief, M., & Pascual-Leone, A. (2011). Safety of theta burst transcranial magnetic stimulation: a systematic review of the literature. *J Clin Neurophysiol*, *28*(1), 67-74.
- Oberman, L. M., & Pascual-Leone, A. (2009). Report of seizure induced by continuous theta burst stimulation. *Brain Stimul*, *2*(4), 246-247.
- Ogiue-Ikeda, M., Kawato, S., & Ueno, S. (2003). The effect of repetitive transcranial magnetic stimulation on long-term potentiation in rat hippocampus depends on stimulus intensity. *Brain Res*, *993*(1-2), 222-226.
- Okamoto, M., Dan, H., Sakamoto, K., Takeo, K., Shimizu, K., Kohno, S., et al. (2004). Three-dimensional probabilistic anatomical cranio-cerebral correlation via the international 10-20 system oriented for transcranial functional brain mapping. *Neuroimage*, *21*(1), 99-111.
- Oldfield, R. C. (1971). The assessment and analysis of handedness: the Edinburgh inventory. *Neuropsychologia*, *9*(1), 97-113.
- Oliviero, A., Strens, L. H., Di Lazzaro, V., Tonali, P. A., & Brown, P. (2003). Persistent effects of high frequency repetitive TMS on the coupling between motor areas in the human. *Exp Brain Res*, *149*(1), 107-113.
- Ortu, E., Ruge, D., Deriu, F., & Rothwell, J. C. (2009). Theta Burst Stimulation over the human primary motor cortex modulates neural processes involved in movement preparation. *Clin Neurophysiol*, *120*(6), 1195-1203.
- Osipova, D., Takashima, A., Oostenveld, R., Fernandez, G., Maris, E., & Jensen, O. (2006). Theta and gamma oscillations predict encoding and retrieval of declarative memory. *J Neurosci*, *26*(28), 7523-7531.
- Parent, A., & Hazrati, L. N. (1995a). Functional anatomy of the basal ganglia. I. The cortico-basal ganglia-thalamo-cortical loop. *Brain Res Brain Res Rev*, *20*(1), 91-127.
- Parent, A., & Hazrati, L. N. (1995b). Functional anatomy of the basal ganglia. II. The place of subthalamic nucleus and external pallidum in basal ganglia circuitry. *Brain Res Brain Res Rev*, *20*(1), 128-154.
- Pareti, G., & De Palma, A. (2004). Does the brain oscillate? The dispute on neuronal synchronization. *Neurol Sci*, *25*(2), 41-47.
- Pascual-Leone, A., Freitas, C., Oberman, L., Horvath, J. C., Halko, M., Eldaief, M., et al. (2011). Characterizing brain cortical plasticity and network dynamics across the age-span in health and disease with TMS-EEG and TMS-fMRI. *Brain Topogr*, *24*(3-4), 302-315.

- Pascual-Leone, A., Valls-Sole, J., Wassermann, E. M., & Hallett, M. (1994). Responses to rapid-rate transcranial magnetic stimulation of the human motor cortex. *Brain*, *117* (Pt 4), 847-858.
- Pascual-Leone, A., Walsh, V., & Rothwell, J. (2000). Transcranial magnetic stimulation in cognitive neuroscience--virtual lesion, chronometry, and functional connectivity. *Curr Opin Neurobiol*, *10*(2), 232-237.
- Passingham, R. E. (1988). Premotor cortex and preparation for movement. *Exp Brain Res*, *70*(3), 590-596.
- Passingham, R. E. (1989). Premotor cortex and the retrieval of movement. *Brain Behav Evol*, *33*(2-3), 189-192.
- Paulus, W. (2005). Toward establishing a therapeutic window for rTMS by theta burst stimulation. *Neuron*, *45*(2), 181-183.
- Paus, T., Castro-Alamancos, M. A., & Petrides, M. (2001). Cortico-cortical connectivity of the human mid-dorsolateral frontal cortex and its modulation by repetitive transcranial magnetic stimulation. *Eur J Neurosci*, *14*(8), 1405-1411.
- Paus, T., Sipila, P. K., & Strafella, A. P. (2001). Synchronization of neuronal activity in the human primary motor cortex by transcranial magnetic stimulation: an EEG study. *J Neurophysiol*, *86*(4), 1983-1990.
- Paus, T., & Wolforth, M. (1998). Transcranial magnetic stimulation during PET: reaching and verifying the target site. *Hum Brain Mapp*, *6*(5-6), 399-402.
- Peinemann, A., Lehner, C., Mentschel, C., Munchau, A., Conrad, B., & Siebner, H. R. (2000). Subthreshold 5-Hz repetitive transcranial magnetic stimulation of the human primary motor cortex reduces intracortical paired-pulse inhibition. *Neuroscience letters*, *296*(1), 21-24.
- Peinemann, A., Reimer, B., Loer, C., Quartarone, A., Munchau, A., Conrad, B., et al. (2004). Long-lasting increase in corticospinal excitability after 1800 pulses of subthreshold 5 Hz repetitive TMS to the primary motor cortex. *Clin Neurophysiol*, *115*(7), 1519-1526.
- Pell, G. S., Roth, Y., & Zangen, A. (2011). Modulation of cortical excitability induced by repetitive transcranial magnetic stimulation: influence of timing and geometrical parameters and underlying mechanisms. *Prog Neurobiol*, *93*(1), 59-98.
- Penfield, W., & Welch, K. (1951). The supplementary motor area of the cerebral cortex; a clinical and experimental study. *AMA Arch Neurol Psychiatry*, *66*(3), 289-317.
- Perfetti, B., Moisello, C., Landsness, E. C., Kvint, S., Pruski, A., Onofrij, M., et al. (2011). Temporal evolution of oscillatory activity predicts performance in a choice-reaction time reaching task. *J Neurophysiol*, *105*(1), 18-27.
- Pfurtscheller, G., & Andrew, C. (1999). Event-Related changes of band power and coherence: methodology and interpretation. *J Clin Neurophysiol*, *16*(6), 512-519.
- Pfurtscheller, G., & Aranibar, A. (1977). Event-related cortical desynchronization detected by power measurements of scalp EEG. *Electroencephalogr.Clin.Neurophysiol.*, *42*(6), 817.

- Pfurtscheller, G., Brunner, C., Schlogl, A., & Lopes da Silva, F. H. (2006). Mu rhythm (de)synchronization and EEG single-trial classification of different motor imagery tasks. *Neuroimage*, *31*(1), 153-159.
- Pfurtscheller, G., & Lopes da Silva, F. H. (1999). Event-related EEG/MEG synchronization and desynchronization: basic principles. *Clinical neurophysiology : official journal of the International Federation of Clinical Neurophysiology*, *110*(11), 1842-1857.
- Pfurtscheller, G., Stancak, A., Jr., & Neuper, C. (1996a). Event-related synchronization (ERS) in the alpha band--an electrophysiological correlate of cortical idling: a review. *Int J Psychophysiol*, *24*(1-2), 39-46.
- Pfurtscheller, G., Stancak, A., Jr., & Neuper, C. (1996b). Post-movement beta synchronization. A correlate of an idling motor area? *Electroencephalogr Clin Neurophysiol*, *98*(4), 281-293.
- Picard, N., & Strick, P. L. (2001). Imaging the premotor areas. *Curr Opin Neurobiol*, *11*(6), 663-672.
- Pineda, J. A. (2005). The functional significance of mu rhythms: translating "seeing" and "hearing" into "doing". *Brain Res Brain Res Rev*, *50*(1), 57-68.
- Porter, L. L., & Sakamoto, K. (1988). Organization and synaptic relationships of the projection from the primary sensory to the primary motor cortex in the cat. *J Comp Neurol*, *271*(3), 387-396.
- Quartarone, A., Bagnato, S., Rizzo, V., Morgante, F., Sant'angelo, A., Battaglia, F., et al. (2005). Distinct changes in cortical and spinal excitability following high-frequency repetitive TMS to the human motor cortex. *Exp Brain Res*, *161*(1), 114-124.
- Raghavachari, S., Kahana, M. J., Rizzuto, D. S., Caplan, J. B., Kirschen, M. P., Bourgeois, B., et al. (2001). Gating of human theta oscillations by a working memory task. *J Neurosci*, *21*(9), 3175-3183.
- Raghavachari, S., Lisman, J. E., Tully, M., Madsen, J. R., Bromfield, E. B., & Kahana, M. J. (2006). Theta oscillations in human cortex during a working-memory task: evidence for local generators. *J Neurophysiol*, *95*(3), 1630-1638.
- Rappelsberger, P., & Petsche, H. (1988). Probability mapping: power and coherence analyses of cognitive processes. *Brain Topogr.*, *1*(1), 46.
- Reid, V. (2003). Transcranial magnetic stimulation. *Phys Med Rehabil Clin N Am*, *14*(2), 307-325, ix.
- Reis, J., Robertson, E. M., Krakauer, J. W., Rothwell, J., Marshall, L., Gerloff, C., et al. (2008). Consensus: Can transcranial direct current stimulation and transcranial magnetic stimulation enhance motor learning and memory formation? *Brain Stimul*, *1*(4), 363-369.
- Ridding, M. C., & Rothwell, J. C. (1999). Afferent input and cortical organisation: a study with magnetic stimulation. *Exp Brain Res*, *126*(4), 536-544.
- Ridding, M. C., & Rothwell, J. C. (2007). Is there a future for therapeutic use of transcranial magnetic stimulation? *Nat Rev Neurosci*, *8*(7), 559-567.

- Ridding, M. C., & Ziemann, U. (2010). Determinants of the induction of cortical plasticity by non-invasive brain stimulation in healthy subjects. *J Physiol*, *588*(Pt 13), 2291-2304.
- Rizzuto, D. S., Madsen, J. R., Bromfield, E. B., Schulze-Bonhage, A., & Kahana, M. J. (2006). Human neocortical oscillations exhibit theta phase differences between encoding and retrieval. *Neuroimage*, *31*(3), 1352-1358.
- Rogasch, N. C., & Fitzgerald, P. B. (2012). Assessing cortical network properties using TMS-EEG. *Hum Brain Mapp*.
- Romeo, S., Gilio, F., Pedace, F., Ozkaynak, S., Inghilleri, M., Manfredi, M., et al. (2000). Changes in the cortical silent period after repetitive magnetic stimulation of cortical motor areas. *Exp Brain Res*, *135*(4), 504-510.
- Romero, J. R., Anshel, D., Sparing, R., Gangitano, M., & Pascual-Leone, A. (2002). Subthreshold low frequency repetitive transcranial magnetic stimulation selectively decreases facilitation in the motor cortex. *Clin Neurophysiol*, *113*(1), 101-107.
- Rosanova, M., Casali, A., Bellina, V., Resta, F., Mariotti, M., & Massimini, M. (2009). Natural frequencies of human corticothalamic circuits. *J Neurosci*, *29*(24), 7679-7685.
- Rossi, S., Hallett, M., Rossini, P. M., & Pascual-Leone, A. (2009). Safety, ethical considerations, and application guidelines for the use of transcranial magnetic stimulation in clinical practice and research. *Clin Neurophysiol*, *120*(12), 2008-2039.
- Rossi, S., Pasqualetti, P., Rossini, P. M., Feige, B., Ulivelli, M., Glocker, F. X., et al. (2000). Effects of repetitive transcranial magnetic stimulation on movement-related cortical activity in humans. *Cereb Cortex*, *10*(8), 802-808.
- Rossini, P. M., Barker, A. T., Berardelli, A., Caramia, M. D., Caruso, G., Cracco, R. Q., et al. (1994). Non-invasive electrical and magnetic stimulation of the brain, spinal cord and roots: basic principles and procedures for routine clinical application. Report of an IFCN committee. *Electroencephalogr Clin Neurophysiol*, *91*(2), 79-92.
- Rothwell, J. C. (1991). Physiological studies of electric and magnetic stimulation of the human brain. *Electroencephalogr Clin Neurophysiol Suppl*, *43*, 29-35.
- Rothwell, J. C. (1997). Techniques and mechanisms of action of transcranial stimulation of the human motor cortex. *J Neurosci Methods*, *74*(2), 113-122.
- Rothwell, J. C., Hallett, M., Berardelli, A., Eisen, A., Rossini, P., & Paulus, W. (1999). Magnetic stimulation: motor evoked potentials. The International Federation of Clinical Neurophysiology. *Electroencephalogr Clin Neurophysiol Suppl*, *52*, 97-103.
- Roy Choudhury, K., Boyle, L., Burke, M., Lombard, W., Ryan, S., & McNamara, B. (2011). Intra subject variation and correlation of motor potentials evoked by transcranial magnetic stimulation. *Ir J Med Sci*, *180*(4), 873-880.

- Sack, A. T. (2006). Transcranial magnetic stimulation, causal structure-function mapping and networks of functional relevance. *Curr Opin Neurobiol*, 16(5), 593-599.
- Sack, A. T., & Linden, D. E. (2003). Combining transcranial magnetic stimulation and functional imaging in cognitive brain research: possibilities and limitations. *Brain Res Brain Res Rev*, 43(1), 41-56.
- Sadato, N., Ibanez, V., Deiber, M. P., & Hallett, M. (2000). Gender difference in premotor activity during active tactile discrimination. *Neuroimage*, 11(5 Pt 1), 532-540.
- Salenius, S., & Hari, R. (2003). Synchronous cortical oscillatory activity during motor action. *Curr Opin Neurobiol*, 13(6), 678-684.
- Sauseng, P., & Klimesch, W. (2008). What does phase information of oscillatory brain activity tell us about cognitive processes? *Neurosci Biobehav Rev*, 32(5), 1001-1013.
- Sauseng, P., Klimesch, W., Gerloff, C., & Hummel, F. C. (2009). Spontaneous locally restricted EEG alpha activity determines cortical excitability in the motor cortex. *Neuropsychologia*, 47(1), 284-288.
- Schindler, K., Nyffeler, T., Wiest, R., Hauf, M., Mathis, J., Hess Ch, W., et al. (2008). Theta burst transcranial magnetic stimulation is associated with increased EEG synchronization in the stimulated relative to unstimulated cerebral hemisphere. *Neurosci Lett*, 436(1), 31-34.
- Schoffelen, J. M., & Gross, J. (2009). Source connectivity analysis with MEG and EEG. *Hum Brain Mapp*, 30(6), 1857-1865.
- Schreckenberger, M., Lange-Asschenfeldt, C., Lochmann, M., Mann, K., Siessmeier, T., Buchholz, H. G., et al. (2004). The thalamus as the generator and modulator of EEG alpha rhythm: a combined PET/EEG study with lorazepam challenge in humans. *Neuroimage*, 22(2), 637-644.
- Schulman, J. J., Cancro, R., Lowe, S., Lu, F., Walton, K. D., & Llinas, R. R. (2011). Imaging of thalamocortical dysrhythmia in neuropsychiatry. *Frontiers in human neuroscience*, 5, 69.
- Schutter, D. J., van Honk, J., d'Alfonso, A. A., Postma, A., & de Haan, E. H. (2001). Effects of slow rTMS at the right dorsolateral prefrontal cortex on EEG asymmetry and mood. *Neuroreport*, 12(3), 445-447.
- Shafi, M. M., Westover, M. B., Fox, M. D., & Pascual-Leone, A. (2012). Exploration and modulation of brain network interactions with noninvasive brain stimulation in combination with neuroimaging. *Eur J Neurosci*, 35(6), 805-825.
- Schyns, P. G., Thut, G., & Gross, J. (2011). Cracking the code of oscillatory activity. *PLoS Biol*, 9(5), e1001064.
- Sherman, S. M. (2001). A wake-up call from the thalamus. *Nat Neurosci*, 4(4), 344-346.
- Sherman, S. M. (2007). The thalamus is more than just a relay. *Curr Opin Neurobiol*, 17(4), 417-422.
- Sherman, S. M., & Guillery, R. W. (2002). The role of the thalamus in the flow of information to the cortex. *Philos Trans R Soc Lond B Biol Sci*, 357(1428), 1695-1708.

- Siebner, H. R. (2000). Simultaneous repetitive transcranial magnetic stimulation does not speed fine movement in PD. *Neurology*, *54*(1), 272; author reply 273.
- Siebner, H. R., Bergmann, T. O., Bestmann, S., Massimini, M., Johansen-Berg, H., Mochizuki, H., et al. (2009). Consensus paper: combining transcranial stimulation with neuroimaging. *Brain Stimul*, *2*(2), 58-80.
- Siebner, H. R., Hartwigsen, G., Kassuba, T., & Rothwell, J. C. (2009). How does transcranial magnetic stimulation modify neuronal activity in the brain? Implications for studies of cognition. *Cortex*, *45*(9), 1035-1042.
- Siebner, H. R., Lang, N., Rizzo, V., Nitsche, M. A., Paulus, W., Lemon, R. N., et al. (2004). Preconditioning of low-frequency repetitive transcranial magnetic stimulation with transcranial direct current stimulation: evidence for homeostatic plasticity in the human motor cortex. *J Neurosci*, *24*(13), 3379-3385.
- Siebner, H. R., & Rothwell, J. (2003). Transcranial magnetic stimulation: new insights into representational cortical plasticity. *Exp Brain Res*, *148*(1), 1-16.
- Silva, L. R., Amitai, Y., & Connors, B. W. (1991). Intrinsic oscillations of neocortex generated by layer 5 pyramidal neurons. *Science*, *251*(4992), 432-435.
- Smith, M. E., Gevins, A., Brown, H., Karnik, A., & Du, R. (2001). Monitoring task loading with multivariate EEG measures during complex forms of human-computer interaction. *Hum Factors*, *43*(3), 366-380.
- Srinivasan, R., Winter, W. R., & Nunez, P. L. (2006). Source analysis of EEG oscillations using high-resolution EEG and MEG. *Prog Brain Res*, *159*, 29-42.
- Stamoulis, C., Oberman, L. M., Praeg, E., Bashir, S., & Pascual-Leone, A. (2011). Single pulse TMS-induced modulations of resting brain neurodynamics encoded in EEG phase. *Brain Topogr*, *24*(2), 105-113.
- Stefan, K., Gentner, R., Zeller, D., Dang, S., & Classen, J. (2008). Theta-burst stimulation: remote physiological and local behavioral aftereffects. *Neuroimage*, *40*(1), 265-274.
- Steriade, M. (2001). Impact of network activities on neuronal properties in corticothalamic systems. *J Neurophysiol*, *86*(1), 1-39.
- Steriade, M. (2006). Grouping of brain rhythms in corticothalamic systems. *Neuroscience*, *137*(4), 1087-1106.
- Steriade, M., & Timofeev, I. (2003). Neuronal plasticity in thalamocortical networks during sleep and waking oscillations. *Neuron*, *37*(4), 563-576.
- Steriade, M., Timofeev, I., & Grenier, F. (2001). Natural waking and sleep states: a view from inside neocortical neurons. *J Neurophysiol*, *85*(5), 1969-1985.
- Stinear, C. M., Barber, P. A., Coxon, J. P., Verryt, T. S., Acharya, P. P., & Byblow, W. D. (2009). Repetitive stimulation of premotor cortex affects primary motor cortex excitability and movement preparation. *Brain Stimul*, *2*(3), 152-162.

- Strafella, A. P., Paus, T., Fraraccio, M., & Dagher, A. (2003). Striatal dopamine release induced by repetitive transcranial magnetic stimulation of the human motor cortex. *Brain*, *126*(Pt 12), 2609-2615.
- Strens, L. H., Oliviero, A., Bloem, B. R., Gerschlager, W., Rothwell, J. C., & Brown, P. (2002). The effects of subthreshold 1 Hz repetitive TMS on cortico-cortical and interhemispheric coherence. *Clin Neurophysiol*, *113*(8), 1279-1285.
- Suppa, A., Bologna, M., Gilio, F., Lorenzano, C., Rothwell, J. C., & Berardelli, A. (2008). Preconditioning repetitive transcranial magnetic stimulation of premotor cortex can reduce but not enhance short-term facilitation of primary motor cortex. *J Neurophysiol*, *99*(2), 564-570.
- Suppa, A., Ortu, E., Zafar, N., Deriu, F., Paulus, W., Berardelli, A., et al. (2008). Theta burst stimulation induces aftereffects on contralateral primary motor cortex excitability in humans. *J Physiol*, *586*(Pt 18), 4489-4500.
- Talelli, P., Greenwood, R. J., & Rothwell, J. C. (2007). Exploring Theta Burst Stimulation as an intervention to improve motor recovery in chronic stroke. *Clin Neurophysiol*, *118*(2), 333-342.
- Taylor, P. C., Walsh, V., & Eimer, M. (2008). Combining TMS and EEG to study cognitive function and cortico-cortico interactions. *Behav Brain Res*, *191*(2), 141-147.
- Teo, J. T., Swayne, O. B., & Rothwell, J. C. (2007). Further evidence for NMDA-dependence of the aftereffects of human theta burst stimulation. *Clin Neurophysiol*, *118*(7), 1649-1651.
- Thaler, D., Chen, Y. C., Nixon, P. D., Stern, C. E., & Passingham, R. E. (1995). The functions of the medial premotor cortex. I. Simple learned movements. *Exp Brain Res*, *102*(3), 445-460.
- Thickbroom, G. W. (2007). Transcranial magnetic stimulation and synaptic plasticity: experimental framework and human models. *Exp Brain Res*, *180*(4), 583-593.
- Thut, G., Ives, J. R., Kampmann, F., Pastor, M. A., & Pascual-Leone, A. (2005). A new device and protocol for combining TMS and online recordings of EEG and evoked potentials. *J Neurosci Methods*, *141*(2), 207-217.
- Thut, G., & Miniussi, C. (2009). New insights into rhythmic brain activity from TMS-EEG studies. *Trends Cogn Sci*, *13*(4), 182-189.
- Thut, G., & Pascual-Leone, A. (2010a). Integrating TMS with EEG: How and what for? *Brain Topogr*, *22*(4), 215-218.
- Thut, G., & Pascual-Leone, A. (2010b). A review of combined TMS-EEG studies to characterize lasting effects of repetitive TMS and assess their usefulness in cognitive and clinical neuroscience. *Brain Topogr*, *22*(4), 219-232.
- Thut, G., Veniero, D., Romei, V., Miniussi, C., Schyns, P., & Gross, J. (2011). Rhythmic TMS causes local entrainment of natural oscillatory signatures. *Curr Biol*, *21*(14), 1176-1185.
- Thut, G., Schyns, P. G., & Gross, J. (2011). Entrainment of perceptually relevant brain oscillations by non-invasive rhythmic stimulation of the human brain. *Front Psychol*, *2*, 170.

- Timofeev, I. (2011). Neuronal plasticity and thalamocortical sleep and waking oscillations. *Prog Brain Res*, 193, 121-144.
- Timofeev, I., Grenier, F., Bazhenov, M., Houweling, A. R., Sejnowski, T. J., & Steriade, M. (2002). Short- and medium-term plasticity associated with augmenting responses in cortical slabs and spindles in intact cortex of cats in vivo. *J Physiol*, 542(Pt 2), 583-598.
- Todd, G., Flavel, S. C., & Ridding, M. C. (2006). Low-intensity repetitive transcranial magnetic stimulation decreases motor cortical excitability in humans. *J Appl Physiol*, 101(2), 500-505.
- Touge, T., Gerschlager, W., Brown, P., & Rothwell, J. C. (2001). Are the aftereffects of low-frequency rTMS on motor cortex excitability due to changes in the efficacy of cortical synapses? *Clin Neurophysiol*, 112(11), 2138-2145.
- Triggs, W. J., Kiers, L., Cros, D., Fang, J., & Chiappa, K. H. (1993). Facilitation of magnetic motor evoked potentials during the cortical stimulation silent period. *Neurology*, 43(12), 2615-2620.
- Trippe, J., Mix, A., Aydin-Abidin, S., Funke, K., & Benali, A. (2009). Theta burst and conventional low-frequency rTMS differentially affect GABAergic neurotransmission in the rat cortex. *Exp Brain Res*, 199(3-4), 411-421.
- Turrigiano, G. G., & Nelson, S. B. (2000). Hebb and homeostasis in neuronal plasticity. *Curr Opin Neurobiol*, 10(3), 358-364.
- Turrigiano, G. G., & Nelson, S. B. (2004). Homeostatic plasticity in the developing nervous system. *Nat Rev Neurosci*, 5(2), 97-107.
- Uhlhaas, P. J., Haenschel, C., Nikolic, D., & Singer, W. (2008). The role of oscillations and synchrony in cortical networks and their putative relevance for the pathophysiology of schizophrenia. *Schizophr Bull*, 34(5), 927-943.
- Uhlhaas, P. J., & Singer, W. (2010). Abnormal neural oscillations and synchrony in schizophrenia. *Nat Rev Neurosci*, 11(2), 100-113.
- Van Der Werf, Y. D., & Paus, T. (2006). The neural response to transcranial magnetic stimulation of the human motor cortex. I. Intracortical and cortico-cortical contributions. *Exp Brain Res*, 175(2), 231-245.
- Van Der Werf, Y. D., Sadikot, A. F., Strafella, A. P., & Paus, T. (2006). The neural response to transcranial magnetic stimulation of the human motor cortex. II. Thalamocortical contributions. *Experimental brain research Experimentelle Hirnforschung Experimentation cerebrale*, 175(2), 246-255.
- Veniero, D., Brignani, D., Thut, G., & Miniussi, C. (2011). Alpha-generation as basic response-signature to transcranial magnetic stimulation (TMS) targeting the human resting motor cortex: A TMS/EEG co-registration study. *Psychophysiology*, 48(10), 1381-1389.
- Virtanen, J., Ruohonen, J., Naatanen, R., & Ilmoniemi, R. J. (1999). Instrumentation for the measurement of electric brain responses to transcranial magnetic stimulation. *Med Biol Eng Comput*, 37(3), 322-326.
- Walsh, V., & Cowey, A. (2000). Transcranial magnetic stimulation and cognitive neuroscience. *Nat Rev Neurosci*, 1(1), 73-79.

- Walsh, V., & Pascual-Leone, A. (2003). *TMS: A Neurochronometrics of Mind*. Cambridge, MA: MIT Press.
- Walsh, V., & Rushworth, M. (1999). A primer of magnetic stimulation as a tool for neuropsychology. *Neuropsychologia*, *37*(2), 125-135.
- Walton, K. D., Dubois, M., & Llinas, R. R. (2010). Abnormal thalamocortical activity in patients with Complex Regional Pain Syndrome (CRPS) type I. *Pain*, *150*(1), 41-51.
- Walton, K. D., & Llinas, R. R. (2010). Central Pain as a Thalamocortical Dysrhythmia: A Thalamic Efference Disconnection? In L. Kruger & A. R. Light (Eds.), *Translational Pain Research: From Mouse to Man*. Boca Raton, FL.
- Wang, H. Y., Crupi, D., Liu, J., Stucky, A., Cruciata, G., Di Rocco, A., et al. (2011). Repetitive transcranial magnetic stimulation enhances BDNF-TrkB signaling in both brain and lymphocyte. *J Neurosci*, *31*(30), 11044-11054.
- Wassermann, E. M., Epstein, C., Ziemann, U., Walsh, V., Paus, T., Lisanby, S. (2008). *Oxford Handbook of Transcranial Stimulation: Oxford Library of Psychology*.
- Wassermann, E. M., Grafman, J., Berry, C., Hollnagel, C., Wild, K., Clark, K., et al. (1996). Use and safety of a new repetitive transcranial magnetic stimulator. *Electroencephalogr Clin Neurophysiol*, *101*(5), 412-417.
- Wassermann, E. M., & Zimmermann, T. (2012). Transcranial magnetic brain stimulation: therapeutic promises and scientific gaps. *Pharmacol Ther*, *133*(1), 98-107.
- Whitwell, J. L., Avula, R., Master, A., Vemuri, P., Senjem, M. L., Jones, D. T., et al. (2011). Disrupted thalamocortical connectivity in PSP: A resting-state fMRI, DTI, and VBM study. *Parkinsonism Relat Disord*, *17*(8), 599-605.
- Wu, S. W., Shahana, N., Huddleston, D. A., Lewis, A. N., & Gilbert, D. L. (2012). Safety and tolerability of theta-burst transcranial magnetic stimulation in children. *Dev Med Child Neurol*.
- Zafar, N., Paulus, W., & Sommer, M. (2008). Comparative assessment of best conventional with best theta burst repetitive transcranial magnetic stimulation protocols on human motor cortex excitability. *Clin Neurophysiol*, *119*(6), 1393-1399.
- Zarkowski, P., Shin, C. J., Dang, T., Russo, J., & Avery, D. (2006). EEG and the variance of motor evoked potential amplitude. *Clin EEG Neurosci*, *37*(3), 247-251.
- Zhang, Y., Llinas, R. R., & Lisman, J. E. (2009). Inhibition of NMDARs in the Nucleus Reticularis of the Thalamus Produces Delta Frequency Bursting. *Front Neural Circuits*, *3*, 20.
- Ziemann, U. (2004a). LTP-like plasticity in human motor cortex. *Suppl Clin Neurophysiol*, *57*, 702-707.
- Ziemann, U. (2004b). TMS induced plasticity in human cortex. *Rev Neurosci*, *15*(4), 253-266.

- Ziemann, U. (2011). Transcranial magnetic stimulation at the interface with other techniques: a powerful tool for studying the human cortex. *Neuroscientist*, 17(4), 368-381.
- Ziemann, U., Bruns, D., & Paulus, W. (1996). Enhancement of human motor cortex inhibition by the dopamine receptor agonist pergolide: evidence from transcranial magnetic stimulation. *Neurosci Lett*, 208(3), 187-190.
- Ziemann, U., Hallett, M., & Cohen, L. G. (1998). Mechanisms of deafferentation-induced plasticity in human motor cortex. *J Neurosci*, 18(17), 7000-7007.
- Ziemann, U., Ilic, T. V., & Jung, P. (2006). Long-term potentiation (LTP)-like plasticity and learning in human motor cortex--investigations with transcranial magnetic stimulation (TMS). *Suppl Clin Neurophysiol*, 59, 19-25.
- Ziemann, U., Paulus, W., Nitsche, M. A., Pascual-Leone, A., Byblow, W. D., Berardelli, A., et al. (2008). Consensus: Motor cortex plasticity protocols. *Brain Stimul*, 1(3), 164-182.
- Ziemann, U., Wittenberg, G. F., & Cohen, L. G. (2002). Stimulation-induced within-representation and across-representation plasticity in human motor cortex. *J Neurosci*, 22(13), 5563-5571.